LEABHARLANN CHOLÁISTE NA TRÍONÓIDE, BAILE ÁTHA CLIATH | TRINITY COLLEGE LIBRARY DUBLIN
Ollscoil Átha Cliath | The University of Dublin

Terms and Conditions of Use of Digitised Theses from Trinity College Library Dublin

Copyright statement

All material supplied by Trinity College Library is protected by copyright (under the Copyright and Related Rights Act, 2000 as amended) and other relevant Intellectual Property Rights. By accessing and using a Digitised Thesis from Trinity College Library you acknowledge that all Intellectual Property Rights in any Works supplied are the sole and exclusive property of the copyright and/or other IPR holder. Specific copyright holders may not be explicitly identified. Use of materials from other sources within a thesis should not be construed as a claim over them.

A non-exclusive, non-transferable licence is hereby granted to those using or reproducing, in whole or in part, the material for valid purposes, providing the copyright owners are acknowledged using the normal conventions. Where specific permission to use material is required, this is identified and such permission must be sought from the copyright holder or agency cited.

Liability statement

By using a Digitised Thesis, I accept that Trinity College Dublin bears no legal responsibility for the accuracy, legality or comprehensiveness of materials contained within the thesis, and that Trinity College Dublin accepts no liability for indirect, consequential, or incidental, damages or losses arising from use of the thesis for whatever reason. Information located in a thesis may be subject to specific use constraints, details of which may not be explicitly described. It is the responsibility of potential and actual users to be aware of such constraints and to abide by them. By making use of material from a digitised thesis, you accept these copyright and disclaimer provisions. Where it is brought to the attention of Trinity College Library that there may be a breach of copyright or other restraint, it is the policy to withdraw or take down access to a thesis while the issue is being resolved.

Access Agreement

By using a Digitised Thesis from Trinity College Library you are bound by the following Terms & Conditions. Please read them carefully.

I have read and I understand the following statement: All material supplied via a Digitised Thesis from Trinity College Library is protected by copyright and other intellectual property rights, and duplication or sale of all or part of any of a thesis is not permitted, except that material may be duplicated by you for your research use or for educational purposes in electronic or print form providing the copyright owners are acknowledged using the normal conventions. You must obtain permission for any other use. Electronic or print copies may not be offered, whether for sale or otherwise to anyone. This copy has been supplied on the understanding that it is copyright material and that no quotation from the thesis may be published without proper acknowledgement.

Modulation of TRAF6 function by the vaccinia virus protein A52

Submitted to the
University of Dublin

For the degree of
Doctor of Philosophy

By
Tara Hurst

School of Biochemistry and Immunology
Trinity College Dublin
Dublin 2
Ireland

2008

TRINITY COLLEGE
0 8 JAN 2009
LIBRARY DUBLIN
THESIS
8670

Declaration

This thesis is submitted by the undersigned to the University of Dublin for the examination of Doctorate in Philosophy. The work herein is my own and has not been submitted as an exercise for a degree to any other university. The library at Trinity College Dublin may lend or copy this thesis upon request.

Tara Hurst

Large DNA viruses, like Vaccinia virus (VACV), encode numerous proteins that are not essential for viral replication but which modulate the antiviral immune response. A number of VACV immunomodulatory proteins have been found to target different components of the innate immune response, including interleukin-1 receptor/ Toll-like receptor (IL-1R/TLR) signalling pathways. The VACV protein A52 has previously been shown to interact with two members of the IL-1R/TLR signalling pathways, TRAF6 and IRAK2. Further, A52 is a potent inhibitor of IL-1R/TLR-induced NF-κB activation, likely by inhibiting the function of IRAK2. Interestingly, A52 was also found to activate p38 MAP kinase (MAPK), enhancing TLR-dependent IL-10 induction. The interaction between A52 and TRAF6 was found to be crucial for A52-induced MAPK activation.

In the present study, the molecular mechanism of A52-TRAF6 binding and subsequent MAPK activation was investigated. Several proteins that interact with TRAF6 have been shown to contain a consensus sequence of amino acids (P-X-E-X-X-Acidic/Aromatic), known as the TRAF6 binding motif. A putative TRAF6 interaction motif in A52 was identified at residues 149-154 (RNEKLF), which is located in the C-terminal region of A52 previously found to be required for binding to TRAF6. Compellingly, mutation of a single residue within this motif (F154A) abrogated the ability of A52 to activate MAPK but did not affect the ability of A52 to inhibit NF-κB nor to bind to TRAF6. Thus, the F154 residue appears to be crucial for activation of MAPK via TRAF6 rather than for binding to TRAF6. In response to ligand stimulation, TRAF6 is autoubiquitinated, a step critical to both MAPK and NF-κB activation. A52 altered the kinetics of IL-1-induced TRAF6 ubiquitination, leading to a more rapid response, which may favour MAPK activation. In addition, the ability of A52 to facilitate or hinder recruitment of other signalling molecules to TRAF6 was examined. Preliminary results suggest that A52 can recruit the MAP3K, TAK1, to TRAF6 in the absence of ligand stimulation and this might be crucial to the ligand-independent activation of MAPK by A52.

I would like to thank my supervisor, Prof. Andrew Bowie, for giving me the opportunity to work in his lab and for all of the support and guidance during the project. Andrew- thank you for helping me to persevere through a challenging project with all its ups and downs. Who knew TRAF6 ubiquitination would turn out to be such a drama? Thank you for helping me to work through the tough parts of the project and to finish the PhD at last.

I am indebted to the members of the Bowie lab for their advice, help, support, humour and commiseration over the last four years. It has been a lively and dynamic group to work in and it would be impossible for me to mention everyone to whom I owe a lot. I am grateful to Geraldine Brosnan and Sinead Keating for all of their help with learning methods and interpreting results, as well as helping me to assemble the thesis in time for the deadline. The ubiquitination assays are technically challenging and I am grateful to Sinead for working with me to optimise the methods used. Thanks for always being there for me when I needed help and advice, Dr. K! And for being a willing companion for the therapeutic trips to Kennedy's. Geraldine - I just wanted to say that I really appreciate the kindness and understanding you have shown to me since I came to the Bowie lab - you are one in a million! Thank you to Orla Mulhern for sharing the PhD experience with me and being a good friend throughout. I wish you all the best with your PhD, Mulherno! Thank you to Sinead Flannery (the Amazing Flanno, Ta-da!) for always being ready with a sympathetic ear and also a laugh. I hope you enjoy the ubiquitination studies as much as I have. To the lovely Leonie Unterholzner - thanks for the laughs, the help with methods and the career advice. Thanks to Michael Carty for the banter and the entertaining political discussions across the lab bench. You can stop humouring me now, Michael.

I would like to thank members of the School of Biochemistry and Immunology who provided invaluable assistance, advice and technical support during this project. In particular, I would like to acknowledge Mary Pat O'Sullivan and Miriam Wilson for their friendship, sense of humour and support. I would also like to thank Liam Cross and Noel Breslin for their prompt and helpful assistance with lab equipment and computer issues.

I would like to thank Andre Vogel, Nick Jagoe, Ray Chambers and Amir Khan for technical advice and assistance with the expression and purification of GST-A52. I would also like to thank Jenn Corcoran, Deniz Top and Roberto de Antueno of Dalhousie University, Halifax, Canada for technical advice. I am grateful to James Chen and

Shizuo Akira for the generous gift of the TRAF6$^{-/-}$ and IRAK2$^{-/-}$ MEFs, respectively, which were used in this project.

I would also like to thank my friends who have stuck by me during my PhD, despite my best attempts to scare them off with stories of TRAF6 ubiquitination: Erin Rushton, Jen O'Gorman, Max Treacy, and Ailbhe Daly. I am grateful for your friendship since the first day at B.U., Erin - seems like yesterday! You have always been a great inspiration to me, both intellectually and politically, and I appreciate your quiet strength. I am particularly grateful to Max for helping me keep my sense of humour intact during the hectic final year of the PhD.

I could not have done this project without the unfailing support of my parents, Paul and Grace Hurst, and I would like to dedicate this thesis to them. Thank you for the poems, stories and jokes that made my day and inspired me to keep working. More than once I thought I could not continue and you always helped me push through those times. Thank you! I would also like to thank my brother and sister-in-law, Paul and Natasha, as well as my sister Heidi.

	Page
Declaration	i
Summary	ii
Acknowledgments	iii
Table of Contents	v
List of Figures	x
List of Tables	xiv
List of Abbreviations	xv
Chapter One: Introduction	**1**
1.1 Viral infection and the innate immune response	**1**
1.2 Cytosolic PRRs	**3**
1.2.1 RIG-I-like receptors	3
1.2.2 IPS-1	5
1.2.3 Cytosolic DNA receptors	6
1.2.4 Viral immune evasion by cytosolic PRRs	6
1.3 TLRs	**7**
1.3.1 TLRs and their ligands	7
1.3.1.1 Lipid-based ligands	8
a) TLR4	
b) TLRs 1,2 and 6	
1.3.1.2 Nucleic acid-based ligands	10
a) TLR3	
b) TLRs 7 and 8	
c) TLR9	
1.3.1.3 Protein ligands	14
a) TLR5	
b) TLR11	
1.3.2 Downstream signalling pathways	15
1.3.2.1 Adaptor molecules	16
a) MyD88	
b) Mal	
c) TRIF	
d) TRAM	

e) SARM
1.3.2.2 IL-1-receptor associated kinases (IRAKs) 19
1.3.2.3 TRAFs 22
a) TRAF structure
b) TRAF6
c) TRAF6 ubiquitination
1.3.2.4 Activation of NF-κB 28
1.3.2.5 Activation of MAPK and AP-1 transcription factor 28
1.3.2.6 IRFs and induction of IFNs 29
a) IRF3
b) IRF5
c) IRF7
d) IFNs and IFN-stimulated genes (ISGs)
1.3.3 TLRs and viral immune evasion 32
1.4 Poxviruses 37
1.4.1 Poxviral structure 38
1.4.2 Summary of the poxviral lifecycle 39
1.4.3 Poxvirus virion and viral entry into host cells 40
1.4.4 Transcription and replication 41
1.4.5 Poxviral exit and cell-to-cell spread 42
1.4.6 Poxvirus detection by PRRs 43
1.4.7 Poxviral immune evasion strategies 43
1.4.7.1 Virostealth
1.4.7.2 Virotransduction
1.4.7.3 Viromimetics: virokines and viroceptors
1.4.7.4 Ubiquitin ligases
1.4.8 A52 47
1.5 Aims 48

Chapter Two: Materials and Methods 50
2.1 Materials 50
2.1.1 Reagents and Molecular Biology Kits 50
2.1.2 Antibodies 52
2.1.3 Cells 53
2.1.4 DNA expression vectors 53

2.1.5 Reporter plasmids 54
2.2 Methods 54
2.2.1 Cell culture 54
2.2.2 Site-directed mutagenesis 57
2.2.3 Cloning 58
2.2.4 Plasmid transformation 60
2.2.5 Plasmid DNA preparation 61
2.2.6 Spectrophotometry 62
2.2.7 Transfection 62
2.2.8 Immunoprecipitation 63
2.2.9 Western blotting 64
2.2.10 Assay of IκB phosphorylation and degradation 65
2.2.11 Phosphorylated p38 assay 66
2.2.11 Ubiquitination assays 66
2.2.12.1 Ubiquitination of endogenous TRAF6 in R1s and HepG2s
2.2.12.2 Ubiquitination of over-expressed TRAF6
2.2.12.3 Ubiquitination of endogenous TRAF6 in the presence of A52
2.2.12.5 Overexpression of HA-ubiquitin in R1s
2.2.12.4 Overexpressed myc-ubiquitin in R1s
2.2.13 Native PAGE 68
2.2.14 A52 and GFP-A52 dimerisation assay 69
2.2.15 Luciferase reporter gene assays 69
2.2.15.1 NF-κB Reporter Gene Assay
2.2.15.2 MAP kinase activation
2.2.16 GST-A52 Expression 71
2.2.17 VACV infection 74
2.2.17.1 Growth and purification of VACV working stocks
2.2.17.2 Plaque assay
2.2.17.3 HA-Ubiquitination of TRAF6 and VACV A52 in VACV-infected R1s or MEFs
2.2.18 Bioinformatics 77

Chapter Three: Results I - The interaction between A52 and the TRAFs
3.1 Introduction 79
3.2 Results 83
3.2.1 GST-A52 can be expressed in *E.coli* and purified

3.2.2 The antibodies produced in response to GST-A52 do not detect over-expressed A52
3.2.3 Antibodies raised against a peptide of A52 detect a protein in VACV-infected cells that is not A52
3.2.4 The FLAG-TRAFs are expressed in R1s
3.2.5 The FLAG antibody detects A52
3.2.6 Cloning of the TRAFs into the pCMV-HA vector was unsuccessful
3.2.7 A52 immunoprecipitates with endogenous TRAFs 2, 3 and 6
3.2.8 A52 interacts with TRAF6 in the absence of IRAK1 and IRAK2
3.3 Discussion 95

Chapter Four: Results II - Identification and characterisation of a non-canonical TRAF6 binding motif in A52
4.1 Introduction 101
4.2 Results 105
4.2.1 TRAF6 is needed for A52 to activate p38 and JNK MAP kinases
4.2.2 A52 has a non-canonical TRAF6 binding motif
4.2.3 Deletion of the TRAF6 binding motif of A52 abrogates the A52-TRAF6 interaction
4.2.4 The TRAF6 binding motif mutants of A52 inhibit NF-κB activation
4.2.5 The F154A and ΔT6BM mutants of A52 do not drive p38 activation
4.2.6 Secondary structure of A52
4.2.7 Mutation of the F154 residue of A52 does not alter dimerisation
4.3 Discussion 119

Chapter Five: Results III - The effect of wild-type and mutant A52 on TRAF6 auto-ubiquitination
5.1 Introduction 130
5.2 Results 133
5.2.1 Endogenous ubiquitination of TRAF6 is not detectable
5.2.2 TRAF6 ubiquitination is detected with over-expressed myc-tagged ubiquitin
5.2.3 A52 alters the kinetics of TRAF6 ubiquitination
5.2.4 The A52 mutants F154A and ΔT6BM do not alter TRAF6 ubiquitination kinetics
5.2.5 A52 is itself ubiquitinated

5.3 Discussion 145

Chapter Six: Results IV - Determining the role of TRAF6 signalling partners in A52-induced MAPK activation

6.1 Introduction 152

6.2 Results 155

6.2.1 Requirement for IRAK1 or IRAK2 required for A52-mediated p38 activation

6.2.2 An effect of A52 on TRAF6 oligomerisation could not be detected

6.2.3 TAB2 interacts with TRAF6 in the absence of ligand stimulation

6.2.4 A role for TAK1 in A52-induced p38 activation

6.2.5 The association of TRAF6 and TAK1 in the presence of A52

6.2.6 A52 interacts with TAK1 in the absence of TRAF6

6.2.7 F154A interacts weakly with TAK1 in the presence or absence of TRAF6

6.3 Discussion 166

Chapter Seven: Discussion 172

Chapter Eight: References 183

Appendix One 209

Appendix Two 210

Chapter One: Introduction

1.1 The cytosolic PRRs.

1.2 The TIR domain of IL-1R/TLRs.

1. 3 The core IL-1R/TLR signalling pathways using MyD88.

1. 4 Toll-like receptors (TLRs) response to their respective ligands is mediated by intracellular TIR adaptor proteins.

1.5 Tumour necrosis receptor factors (TRAFs) are multidomain proteins.

1.6 The ubiquitin pathway.

1. 7 MAP kinase activation by TLRs, IL-1R and TNFR.

1.8 Variola virus is the causative agent of smallpox.

Chapter Three: Results I

3.1 GST-A52 is weakly expressed in BL21 (DE3) *E. coli* cells.

3.2 GST-A52 is expressed more strongly in Rosetta-Gami 2 cells.

3.3 GST-A52 does not elute from glutathione beads with 10mM reduced glutathione.

3.4 GST-A52 is eluted from glutathione sepharose beads with 1% SDS.

3.5 GST-A52 eluted with 20mM reduced glutathione is used for antibody production.

3.6 Antibodies raised to GST-A52 in rabbit L114 may detect A52 over-expressed in R1s.

3.7 Antibodies to GST-A52 do not detect A52 over-expressed in R1s.

3.8 Antibodies raised against a peptide of A52 do not detect the over-expressed A52.

3.9 The FLAG-TRAFs are expressed and are detected with the FLAG antibody.

3.10 The FLAG antibody cross-reacts with A52R.

3.11 Sub-cloning of the TRAFs into the pCMV-HA vector.

3.12 The HA-TRAFs are not expressed.

3.13 HA-TRAF6 is myc-tagged and the other TRAFs are not expressed.

3.14 A52 interacts with endogenous TRAF2, TRAF3 and TRAF6.

3.15 A52 interacts with endogenous TRAF6 in IRAK2 knock out MEFs and IRAK1-deficient 293 HEKs.

Chapter Four: Results II

4.1 A52 can activate MAP kinases in wild-type but not in TRAF6$^{-/-}$ MEFs.

4.2 The C-terminus of A52 has a non-canonical TRAF6-binding motif.

4.3 The TRAF6 binding motif mutants are expressed and are detected by the A52 antibody.

4.4 The TRAF6 binding motif deletion construct is expressed and detected by the A52 antibody.

4.5 The TRAF6 binding motif mutants E151A and F154A bind to TRAF6.

4.6 The TRAF6 binding motif deletion construct does not co-precipitate with TRAF6.

4.7 The TRAF6 binding motif deletion construct does not interact with endogenous IRAK2.

4.8 A52 mutants F154A and ΔT6BM still inhibit IL-1-induced NF-κB.

4.9 A52 mutant F154A inhibits CD4-TLR4-induced NF-κB.

4.10 A52, F154A and ΔT6BM inhibit LPS-induced IL-8 production in TLR4 cells.

4.11 A52, F154A and ΔT6BM inhibit IL-1-induced IkB degradation.

4.12 A52 mutants F154A and ΔT6BM do not drive p38 activation.

4.13 A52 mutant F154A does not drive JNK activation.

4.14 A52, F154A and ΔT6BM do not induce phosphorylation of p38 and JNK MAPK.

4.15 A52 activates the human IL-10 promoter weakly in R1s.

4.16 Predicted secondary structure of A52.

4.17 Wild-type A52 forms a homodimer under non-denaturing conditions.

4.18 Wild-type A52 forms a dimer with GFP-A52.

4.19 A52 forms a homodimer in solution.

Chapter Five: Results III

5.1 Poly-ubiquitinated FLAG-TRAF6 is not detected in R1s following Il-1 stimulation

5.2 Endogenous TRAF6 is not ubiquitinated in HepG2 cells following Il-1 stimulation.

5.3 Ubiquitinated TRAF6 is detected when myc-ubiquitin is overexpressed.

5.4 TRAF6 ubiquitination is induced by A52 when myc-ubiquitin is overexpressed and in the absence of ligand stimulation.

5.5 Ubiquitinated TRAF6 is detected when HA-ubiquitin is over-expressed.

5.6 A52 enhances TRAF6 ubiquitination at early time-points following IL-1 stimulation.

5.7 A52 enhances TRAF6 ubiquitination at early time-points following IL-1 stimulation.

5.8 Re-titration of the HA-ubiquitin construct.

5.9 F154A and ΔT6BM do not accelerate the kinetics of TRAF6 ubiquitination.

5.10 A52 is ubiquitinated in R1s.

5.11 A52 is ubiquitinated in wild-type but not *TRAF6-/-* MEFs.

5.12 TRAF6 binding motif mutants of A52 are ubiquitinated in R1s.

Chapter Six: Results IV

6.1 A52 does not activate the p38 CHOP assay in wild-type or $IRAK2^{-/-}$ MEFs.

6.2 A52 activates p38 CHOP in IL-1R cells but not in IRAK1-deficient cells.

6.3 Endogenous TRAF6 oligomerisation is observed in the absence of IL-1 stimulation.

6.4 Oligomerisation of endogenous TRAF6 is not altered by IL-1 stimulation or A52 expression.

6.5 Oligomerisation of over-expressed TRAF6.

6.6 TAB2 and TRAF6 co-precipitate in the absence of IL-1 stimulation.

6.7. TAK1 is involved in A52-induced p38 activation.

6.8 TAK1 and TRAF6 co-precipitate in the absence of IL-1 stimulation.

6.9 A52 induces the interaction of TAK1 and TRAF6.

6.10 A52 co-precipitates with endogenous TAK1 in R1s.

6.11 A52 co-precipitates with TAK1 in TRAF6$^{-/-}$ MEFs.

6.12 A52 and F154A co-precipitate with TAK1 in TRAF6$^{-/-}$ MEFs.

Chapter Seven: Final Discussion

7.1 Model of A52-mediated MAPK activation and NF-κB inhibition.

Chapter One: Introduction

Table 1.1 Ligands of Toll-like receptors.

Chapter Two: Materials and Methods

Table 2.1 Primers used in Quik-change® site-directed mutagenesis.

Table 2.2 Table 2.2 Primers used in HA-TRAFs cloning.

Table 2.3 GeneJuice™ transfection

Chapter Three: Results

Table 3.1 There are several predicted motifs and modifications in the A52 amino acid sequence.

Appendix One: Molecular Masses of Proteins Studied

Table A1.1 The predicted molecular masses of the proteins studied in this thesis.

Appendix Two: ELISA Data for Antibodies to A52

Table A2.1 ELISA data for antiserum raised to GST-A52 protein in rabbits.

Table A2.2 ELISA data for antiserum raised to A52 peptide in rabbit SG-4607.

Table A2.3 ELISA data for antiserum raised to A52 peptide in rabbit SG-4608.

AP-1	activating protein-1
ARM	Armadillo repeat motif
CARD	caspase recruitment domain
Cardif	CARD adaptor inducing IFNβ
CEV	cell-associated enveloped virus
CMV	cytomegalovirus
DAI	DNA-dependent activator of IFN-regulatory factors
DC	dendritic cell
DMEM	Dulbecco's minimum essential medium
DNA-PK	DNA-dependent protein kinase
dsRNA	double-stranded RNA
EBV	Epstein-Barr virus
ECMV	encephalomyocarditis virus
EEV	extracellular enveloped virion
EFC	entry/fusion complex
ELISA	enzyme-linked immunosorbent assay
ER	endoplasmic reticulum
ERK	extracellular signal-regulated protein kinase
FADD	FAS-associated death-domain protein
GAAP	Golgi anti-apoptotic protein
GPI	glycosylphosphatidylinositol
HIV-1	human immunodeficiency virus 1
HSV-1	herpes simplex virus type 1
IFN	interferon
IKK	IκBα kinase
IL-1R	interleukin-1 receptor
IPS-1	IFN-β promoter stimulator

IRAK	IL-1 receptor associated kinase
IRF	Interferon regulatory factor
IV	immature virion
JEV	Japanese encephalitis virus
JNK	c-Jun N-terminal kinase
LGP2	laboratory of genetics and physiology 2
LMP1	latent membrane protein 1 (from EBV)
LPS	lipopolysaccharide
LRRs	leucine-rich repeats
MAL	MyD88 adaptor-like
MAPK	mitogen-activated protein kinase
MCMV	murine cytomegalovirus
Mda-5	melanoma differentiation-associated gene 5
MEFs	murine embryonic fibroblasts
MeV	measles virus
MMTV	mouse mammary tumour virus
MV	mature virion
MVA	Modified vaccinia virus Ankara
MyD88	myeloid differentiation factor 88
NEAA	non-essential amino acids
NEMO	NF-κB essential modulator
NF-κB	Nuclear factor κB
OAS	2'-5'-oligoadenylate synthetase
ODN	oligodeoxynucleotides
ORF	open reading frame
PAMPs	pathogen-associated molecular patterns
PKR	dsRNA-dependent protein kinase R

PRRs	pattern recognition receptors
R1 cells (R1s)	HEK 293 cells supplemented with IL-1R1
RIG-I	retinoic acid-inducible gene I
RING	really interesting new gene
RIP-1	receptor-interacting protein 1
RLR	RIG-I-like receptor
RSV	respiratory syncytial virus
SAM	sterile α motif
SARM	SAM and ARM protein
ssRNA	single-stranded RNA
TANK	TRAF-family member associated NF-κB activator
TBK-1	TRAF family member-associated NF-κB activator binding kinase
TGN	trans-Golgi network
TIR domain	TLR/IL-1R domain
TLR	Toll-like receptor
TNF	tumour necrosis factor
TRADD	TNFR-associated death domain
TRAF	tumour necrosis receptor associated factor
TRAM	Toll receptor-associated molecule
TRIF	TIR domain-containing adaptor-inducing IFN-β
VACV	vaccinia virus
vhs	virion host shutoff
VISA	virus-induced signalling adaptor
VSV	vesicular stomatitis virus
WR	Western Reserve strain of VACV
WV	wrapped virion

Chapter One: Introduction

1.1 Viral infection and the innate immune response

The innate immune response is the rapid, first-line of defence of the organism against invading pathogens (Staros, 2005). This response involves the recognition of an array of common microbial molecules by a series of germline-encoded receptors referred to as pattern recognition receptors (PRRs) (Staros, 2005). The PRRs recognise specific molecules produced by microbes, including viruses, described as pathogen-associated molecular patterns (PAMPs) (Kawai and Akira, 2007). It has been suggested that the molecular signatures of PAMPs are recognised by PRRs because they represent molecules that are essential to cell survival and thus are not subject to mutation (Rassa and Ross, 2003). In addition, it is essential that the PAMPs are distinguishable from host cell molecules in order to prevent an immune response to self (Pichlmair and Reis e Sousa, 2007).

Viral infection triggers an innate antiviral immune response. Viral PAMPs include the surface glycoproteins on virions and the nucleic acids (double-stranded RNA (dsRNA) and single-stranded RNA (ssRNA) and DNA) either released from the virus during entry or expressed during replication (Akira *et al.*, 2006). For example, dsRNA is produced in the cytosol by many viruses during replication and is detected by intracellular innate immune receptors (Kawai and Akira, 2006a). Following detection, the PRRs can initiate antiviral signalling pathways leading to the production of type I interferons (IFNs), cytokines and chemokines, leading to the establishment of an antiviral state (Kawai and Akira, 2006a).

There are two classes of PRRs involved in the antiviral response: the membrane-spanning TLRs and the cytosolic RNA and DNA sensors (see below). The division of labour between these PRRs is based on their cellular localisation and their cell-specific expression (Kato *et al.*, 2005; Melchjorsen *et al.*, 2005). TLRs are expressed at the cell

surface or in the endosome and can thus detect exogenous microbial molecules, whereas the cytosolic RNA and DNA sensors can respond to viral replication products within the cytoplasm (Kawai and Akira, 2006b).

While the innate immune system comprises complex antiviral strategies, viruses have several ingenious ways to counteract the immune response and to favour viral replication. Anti-immunology has characterised the varied methods used by different pathogens to evade, subvert or inhibit the innate immune response (Finlay and McFadden, 2006). Many anti-immune strategies have been described and there are numerous examples of how viruses employ them. One strategy is to block downstream signalling pathways from PRRs. For example, the paramyxoviruses measles virus (MeV) and respiratory syncytial virus (RSV) both inhibit TLR7- and TLR9-induced IFN production (see section 1.3.2.6; Schlender *et al.*, 2005). In addition, the V proteins of paramyxoviruses associate with the PRR melanoma differentiation-associated (MDA5) and inhibit the signalling pathways that MDA5 can normally induce (Kawai and Akira, 2006a). An important part of the innate immune response is the production of cytokines and their recognition by specific receptors. Viruses are known to encode mimics of cytokines (virokines) and of their receptors (viroceptors) in order to evade or modulate the host response (Finlay and McFadden, 2006). Alternatively, viruses can turn off transcription or translation of host genes, thereby preventing expression of pro-inflammatory cytokines. For example, Vaccinia virus (VACV) inhibits cellular protein synthesis by removing the 5' cap on cellular mRNAs (McLennan, 2007). The Bunyavirus NSs protein inhibits type I IFN expression by preventing phosphorylation of the RNA polymerase II (Thomas *et al.*, 2004). Another virus, herpes simplex virus type 1 (HSV-1) encodes a protein, virion host shutoff (vhs), that acts as an mRNA-specific RNase to globally inhibit cellular protein synthesis and thereby blocks proinflammatory cytokine production (Smiley, 2004). In addition, viruses can disrupt the normal regulation of

other cellular processes, including the induction of apoptosis (Finlay and McFadden, 2006). One of the most devious subversions involves using the PRRs to stimulate viral replication, a method employed by retroviruses such as HIV (Netea *et al.*, 2004; see below).

In addition to the role in directly sensing and responding to pathogens, the innate immune system is also crucial in activating the acquired immune response. The bridge between the two types of immune response is mediated by the TLRs and the cytosolic PRRs. For example, TLRs are known to induce the maturation and activation of dendritic cells (DCs) (Netea *et al.*, 2004). RNA from HIV-1 activates plasmacytoid DCs (pDCs) by a mechanism involving endosomal acidification and TLR7-induced IFNα (Beignon *et al.*, 2005). The role for TLRs versus the cytosolic PRRs could be cell-type specific. Whereas the cytosolic PRR retinoic acid inducible gene I (RIG-I) was expendable for the antiviral response in pDCs, the TLRs were essential (Kato *et al.*, 2005). In contrast, in myeloid DCs (mDCs), single-stranded RNA (ssRNA) is sensed by TLR7 and TLR8, as well as a cytosolic PRR (Melchjorsen *et al.*, 2005).

The antiviral immune response is complicated and involves the interplay of numerous intracellular signalling pathways. It is likely to have developed through co-evolution with viruses and thus it is not surprising to find that viruses have strategies to evade detection by the host cell. The roles of cytosolic PRRs and TLRs in responding to viral infection and the strategies used by viruses to evade detection are discussed below.

1.2 Cytosolic PRRs

1.2.1 RIG-I-like receptors (RLRs)

RIG-I and MDA5 are the RNA helicases that recognise viral RNA in the cytoplasm and lead to IFN I production (Figure 1.1; Kawai and Akira, 2006a). Both helicases contain an N-

terminal caspase recruitment domain (CARD) and a helicase homology domain (Yoneyama and Fujita, 2008). In addition, RIG-I has a C-terminal repression domain (Pichlmair and Reis e Sousa, 2007). For RIG-I, a helicase domain with intact ATPase activity is required for dsRNA-induced signalling (Yoneyama *et al.*, 2004).

Studies with *MDA5*$^{-/-}$ and *RIG-I*$^{-/-}$ mice revealed that the two receptors respond to different viruses (Kato *et al.*, 2006). *RIG-I*$^{-/-}$ mice are more susceptible to Japanese encephalitis virus (JEV) and vesicular stomatitis virus (VSV) infection than *MDA5*$^{-/-}$ mice (Kato *et al.*, 2006). In contrast, *MDA5*$^{-/-}$ but not *RIG-I*$^{-/-}$ mice are highly susceptible to infection by encephalomyocarditis virus (ECMV) (Kato *et al.*, 2006). Thus, there seems to be a clear difference in the roles of the two helicases in the response to viral infection.

The difference could be due to the ability of RIG-I but not MDA5 to detect the triphosphate at the 5'-end of single-stranded RNA (Hornung *et al.*, 2006; Pichlmair *et al.*, 2006). This also explains how RIG-I can distinguish self and non-self RNAs, since most cellular RNA is modified to mask the 5'-triphosphate group (Ishii and Akira, 2008). For example, all cellular mRNA is modified by the addition of a 7-methyl guanosine cap at the 5' end (Ishii and Akira, 2008). In addition, RIG-I is able to detect short dsRNA molecules compared to the long dsRNA molecules sensed by MDA5 (Kato *et al.*, 2008).

Expression of the related helicase, laboratory of genetics and physiology 2 (LGP2), is induced by IFN, dsRNA and viral infection (Komuro and Horvath, 2006). Although LGP2 lacks the conserved CARD domain found in RIG-I and MDA5, it has the helicase domain and repression domain required for RNA binding (Yoneyama and Fujita, 2007). LGP2 was found to act as a negative regulator of RIG-I and MDA5 function *in vitro* but not *in vivo* (Ishii and Akira, 2008).

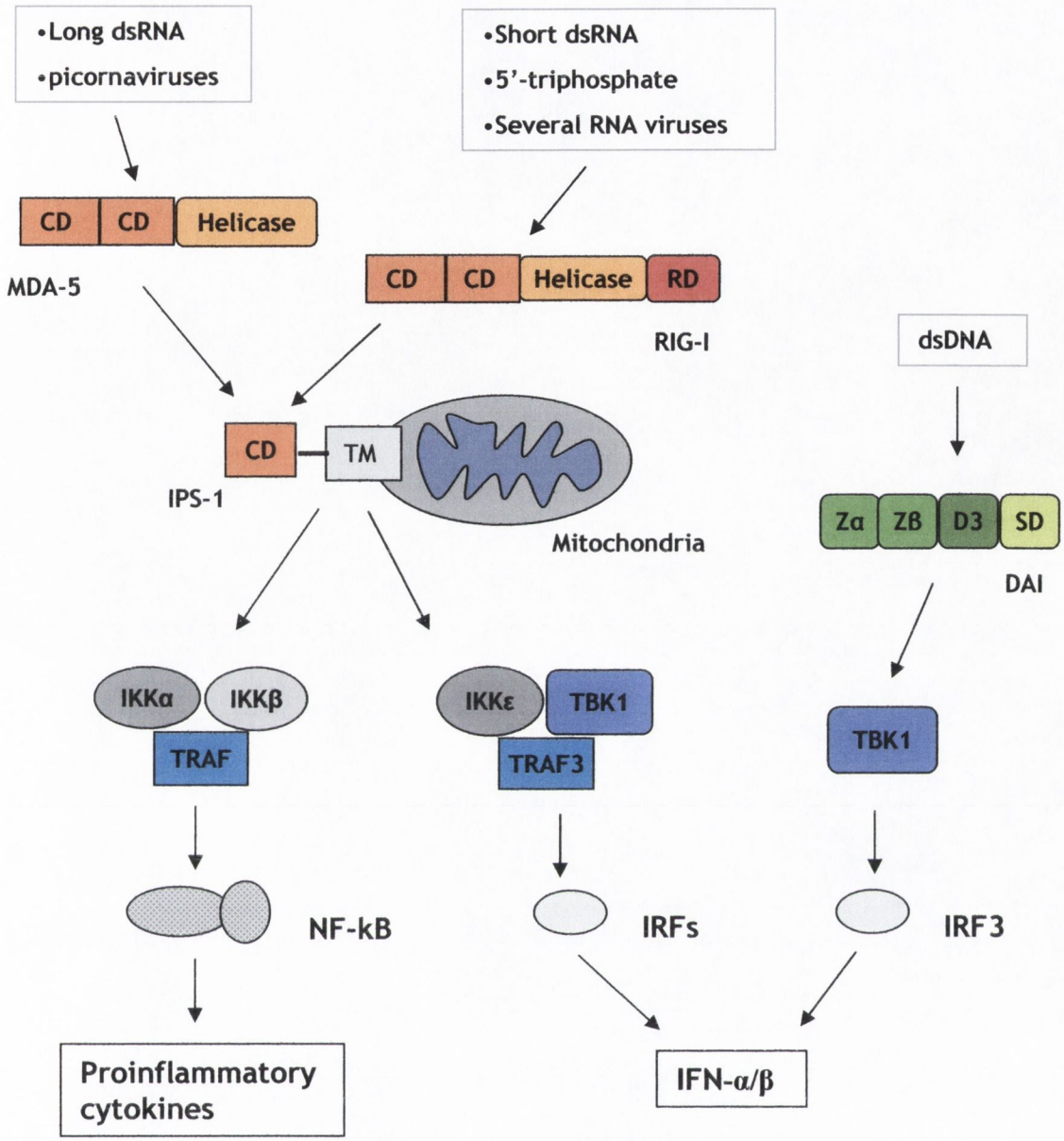

Figure 1.1 The cytosolic PRRs

RIG-I and MDA5 detect 5'-triphosphate single-stranded RNA or double-stranded RNA (dsRNA), respectively. They mediate antiviral signalling via CARD-CARD interactions with the adaptor IPS-1. The transmembrane domain of IPS-1 is anchored in the mitochondrial outer membrane and this localisation is required for it to transduce the signal to proinflammatory cytokine production and IFNα/β induction. Double-stranded DNA (dsDNA) in the cytoplasm is detected by DAI, leading to IFNα/β production. CD, card domain; TM, transmembrane domain; RD, repressor domain; Zα/β, Z-DNA binding domains; D3, DNA binding domain; SD, signalling domain.

1.2.2 IPS-1

The adaptor protein used by both RIG-I and MDA5 was identified simultaneously by four groups as IFN-β promoter stimulator (IPS)-1 (Kawai *et al.*, 2005), mitochondrial antiviral signalling (MAVS) (Chen *et al.*, 2005), CARD adaptor inducing IFNβ (Cardif) (Meylan *et al.*, 2005) and virus-induced signalling adaptor (VISA) (Xu *et al.*, 2005). The name IPS-1 will be used hereafter for clarity. IPS-1 contains an N-terminal CARD domain and this is required for interaction with the CARD domains of RIG-I and MDA5 (Hiscott *et al.*, 2006). The C-terminus of IPS-1 has a membrane-spanning domain that anchors the adaptor in the mitochondrial outer membrane, a localisation that is required for IPS-1 function (Hiscott *et al.*, 2006). In addition to synthetic RLR ligands, IPS-1 is required for type I IFN activation by both RIG-I and MDA-5 following RNA virus infection (Kumar *et al.*, 2006).

As indicated by the name, the main function of IPS-1 is to mediate IFNβ production (Figure 1.1). Following RLR stimulation, IPS-1 recruits numerous adaptor molecules and effector enzymes. In order to activate IFN regulatory factor 3 (IRF3), the non-canonical IκBα kinases, IKKε and TANK-binding kinase 1 (TBK1) are required (Johnson and Gale, 2006). Recently, the TNFR-associated death domain (TRADD) protein was found to bind to IPS-1 and to be required for RLR signalling (Michallet *et al.*, 2008). TRADD then recruits tumour necrosis factor receptor associated factor 3 (TRAF3) and TRAF-family member associated NF-κB activator (TANK) to form a complex at the mitochondria in association with IPS-1 (Michallet *et al.*, 2008). Subsequently, TANK recruits FAS-associated death-domain protein (FADD) and receptor-interacting protein (RIP-1) to the complex, likely mediated by interactions between the death domains of TANK, FADD and RIP-1 (Michallet *et al.*, 2008). This multi-protein complex subsequently recruits NF-κB essential modulator (NEMO), which then activates TBK1 and IKKε, leading to IRF3 phosphorylation (Michallet *et al.*, 2008). In addition, NEMO recruitment results in the

phosphorylation of IKKα and IKKß and consequently in the activation of NF-κB (Michallet *et al.*, 2008).

1.2.3 Cytosolic DNA Receptors

Long, double-stranded DNA (dsDNA) is able to activate TLR-independent innate immune pathways, leading to IRF3 and IFNß promoter activation (Figure 1.1; Ishii *et al.*, 2006). A cytosolic DNA receptor, DNA-dependent activator of IFN-regulatory factors or DAI (also called DLM-1 and ZBP1), has recently been found to induce type I IFN genes in response to dsDNA from many sources (Takaoka *et al.*, 2007). In a positive feedback mechanism, DAI expression is also upregulated in response to type I IFNs (Takaoka *et al.*, 2007). DAI interacts with TBK1 and this interaction is required for activation of IRF3 (Takaoka *et al.*, 2007). In addition, DAI interacts with IRF3 itself (Takaoka *et al.*, 2007). Since DAI-knockout mice were shown to be able to mount an immune response to dsDNA, it is likely that DAI is not the only cytosolic DNA sensor (Ishii and Akira, 2008). This is supported by the fact that knockdown of DAI with siRNA inhibited but did not completely block IFNß production in response to infection with a DNA virus, HSV-1 (Takaoka *et al.*, 2007). Furthermore, suppression of DAI expression inhibited dsDNA-induced IFNß induction in L929 cells but not in murine embryonic fibroblasts (MEFs) (Wang *et al.*, 2008).

1.2.4 Viral immune evasion of the cytosolic PRRs

Recognition of viral nucleic acids triggers the cytosolic PRRs to activate antiviral signalling pathways, many of which lead to type I IFN expression. Viruses have strategies to counteract the antiviral response, either by preventing detection by the PRRs or blocking the expression of IFN. In order to prevent detection by RIG-I, RNA viruses have devised ways to mask the 5'-triphosphate on their mRNA molecules, either by converting it to a 5'-monophosphate (Habjan *et al.*, 2008) or by stealing the 5' cap

from host cell mRNAs (Jin and Elliott, 1993). The pathogenic hantavirus NY-1 encodes a protein (G1) that inhibits RIG-I- and TBK1-directed type I IFN induction (Alff *et al.*, 2006). In addition, at least one virus, hepatitis C virus (HCV), targets IPS-1 as part of its immune evasion strategy (Hiscott *et al.*, 2006). The HCV NS3/4A protease cleaves IPS-1 at its C-terminus, disrupting its mitochondrial localisation and preventing NF-κB and IRF3 activation (Hiscott *et al.*, 2006).

1.3 TLRs

The link between TLRs and innate immunity was discovered in *Drosophila*, where the Toll receptor is crucial to the antifungal response (Kawai and Akira, 2006b). A human homologue of *Drosophila* Toll was discovered which induced NF-κB activation, the expression of pro-inflammatory cytokines and of co-stimulatory molecules (Medzhitov et al., 1997). A role for mammalian TLR4 in immunity was described following the discovery of a mutation (P712H) that rendered mice resistant to LPS (Poltorak *et al.*, 1998). It was thus hypothesised that TLR4 was required to detect LPS and transduce a signal within the cell (Poltorak *et al.*, 1998). Eleven TLRs have since been described in humans, while thirteen TLRs have been found in mice (Kawai and Akira, 2007).

1.3.1 TLRs and their ligands

TLRs are type I transmembrane proteins with a highly variable extracellular domain comprising leucine-rich repeats (LRRs), which are involved in ligand binding (Miggin and O'Neill, 2006). The cytoplasmic portions of the TLRs contain a conserved domain, the Toll-IL-1R (TIR) domain, which is also found in the IL-1 receptor superfamily (Figure 1.2; Kawai and Akira, 2007). The TIR domain is essential for signalling from the TLRs (O'Neill *et al.*, 2003). There are three conserved regions, denoted Box 1, Box 2 and Box 3, with Box 1 being the hallmark sequence of the TIR domain (O'Neill *et al.*, 2003). Both Box 2 and Box 3 contain sequences that are important for signalling. Residues

from Box 2 form the BB loop that may allow interaction with other TIR-domain containing signalling molecules or may mediate dimer formation between TLRs (reviewed in Jin and Lee, 2008). The structure of the TIR domains of TLR1 and TLR2 (Xu *et al.*, 2000), TLR10 (Nyman *et al.*, 2008) and a member of the IL-1 family, IL-1 receptor protein-like (IL-1RAPL) (Khan et al., 2004) have been solved and have a three-layered α-β-α sandwich secondary structure. The extracellular or lumenal region of the TLRs is very different from that of IL-1R: while TLRs possess the LRRs mentioned above, the IL-1R has three immunoglobulin-like domains (Uematsu and Akira, 2006). It is the extracellular or lumenal region of TLRs and IL-1R that interact with the ligands.

One or more ligands have been identified for most TLRs (Table 1.1). Although a ligand has not yet been identified for human TLR10, a constitutively-active CD4-TLR10 construct was able to bind to the TIR adaptor myeloid differentiation factor 88 (MyD88; see below) and to activate NF-κB (Hasan *et al.*, 2005). Thus, human TLR10 might have a physiological role in MyDD8-dependent innate immune signalling. TLRs can be classified based on the type of molecule that serves as the ligand for receptor activation (O'Neill, 2006). The TLRs and their ligands are described below.

1.3.1.1 Lipid-based ligands

a) TLR4

Following ligand stimulation, TLR4 forms a homodimer (O'Neill, 2006). The first ligand of TLR4 to be identified was lipopolysaccharide (LPS), which is found in the cell wall of Gram-negative bacteria (Kawai and Akira, 2006b). The lipid portion of LPS, known as lipid A, induces the majority of the pathogenic effects associated with Gram-negative bacterial infection (Akira *et al.*, 2006). LPS associates with LPS-binding protein (LBP) in the serum (Akira *et al.*, 2006). The LPS-LBP complex binds to CD14, a GPI-linked cell-surface protein of phagocytes (Akira *et al.*, 2006). The LPS is then transferred to MD-2

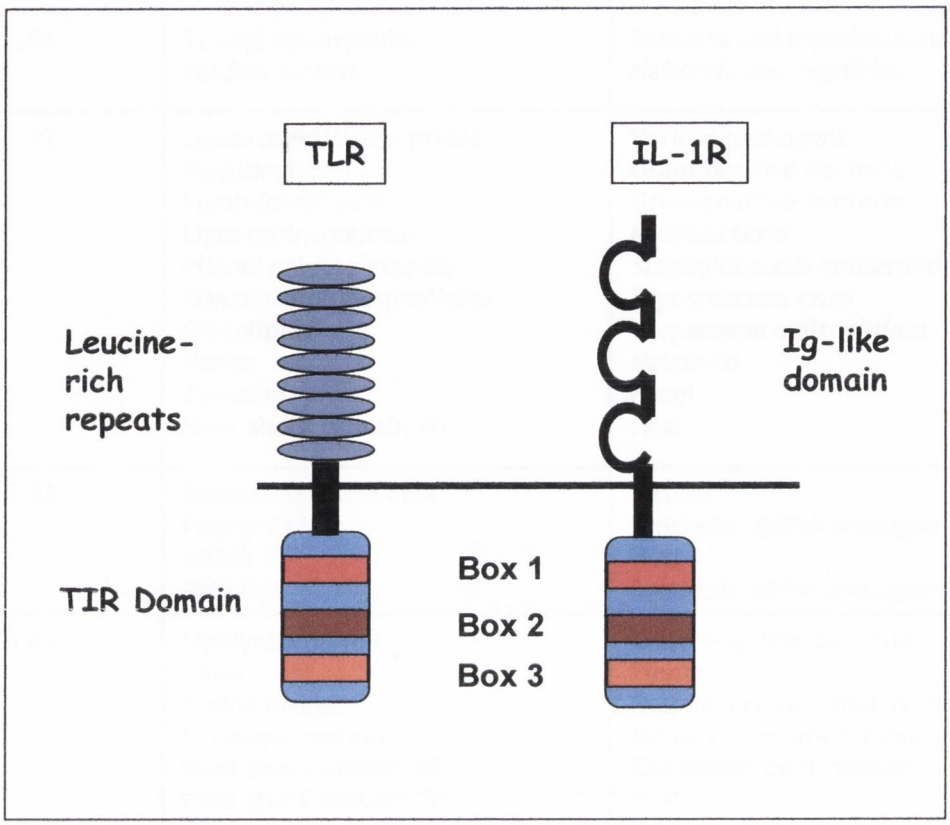

Figure 1.2 The TIR domain of IL-1R/TLRs

The intracellular TIR domain is a common feature of the TLRs and of members of the IL-1R superfamily. The TIR domain contains three recognised conserved regions, termed Box 1, Box 2 and Box 3. The extracellular domain in TLRs contains leucine rich repeats which may mediate ligand binding. In IL-1R family members, the extracellular domain consists of Ig-like domains. Figure adapted from Akira and Takeda, 2004.

Receptor	Ligand	Origin of Ligand
TLR1	Triacyl lipopeptides Soluble factors	Bacteria and mycobacteria *Neisseria meningitides*
TLR2	Lipoprotein/lipopeptides Peptidoglycan Lipoteichoic acid Lipoarabinomannan Phenol-soluble modulin Glycoinisitolphospholipids Glycolipids Porins Zymosan Heat-shock protein 70	Various pathogens Gram-positive bacteria Gram-positive bacteria Mycobacteria *Staphylococcus epidermidis* *Trypanosoma cruzi* *Treponema maltophilum* *Neisseria* Fungi Host
TLR3	Double-stranded RNA Poly (I:C) mRNA Poly (I)	Viruses Synthetic dsRNA analogue Host Synthetic ssRNA analogue
TLR4	Lipolysaccharide Taxol Fusion protein Envelope protein Heat-shock protein 60 Heat-shock protein 70 Fibrinogen Mannan Glucuronoxylomannan	Gram-negative bacteria Plants Respiratory syncytial virus Mouse mammary-tumour virus *Chlamydia pneumoniae* Host Host *Candida albicans* *Cryptococcus neoformans*
TLR5	Flagellin	Bacteria
TLR6	Diacyl lipopeptides Lipoteichoic acid Zymosan	*Mycoplasma* Gram-positive bacteria Fungi
TLR7	Imidazoquinoline Loxoribine Bropirimine Single-stranded RNA	Synthetic compounds Synthetic compounds Synthetic compounds Viruses
TLR8	Imidazoquinoline Single-stranded RNA	Synthetic compounds Viruses
TLR9	CpG-containing DNA Hemozoin	Bacteria and viruses *P. falciparum*
TLR10	N.D.	N.D.
TLR11	Profilin-like molecule	Toxoplasma gondii

Table 1.1 Ligands of Toll-like receptors.

The ligands and their origins of each Toll-like receptor (TLR) are listed. N.D., not determined. Adapted from Akira and Takeda, 2004 and Ishii *et al.* 2005.

which, in turn, associates with TLR4 and induces TLR4 dimerisation (Akira *et al.*, 2006). The crystal structure of the TLR4-MD-2 complex shows that TLR4 and MD2 interact via ionic and hydrogen bonds in two patches bearing opposite electrostatic charges (Kim *et al.*, 2007). The bound MD-2 molecule has an open ß cup fold that has hydrophobic residues in the internal pocket and a lining of positive charges around the opening, thereby permitting interaction with the amphipathic LPS molecule (Kim *et al.*, 2007). The binding of LPS to MD-2 induces the formation of an m-shaped heterotetramer, comprising two MD-2-bound TLR4 molecules (Kim *et al.*, 2007).

In addition, TLR4 responds to viral envelope glycoproteins, including the fusion (F) protein of respiratory syncytial virus (RSV) and the envelope (env) glycoprotein of mouse mammary tumour virus (MMTV) (Boehme and Compton, 2004). TLR4 also recognises fungal PAMPs, including mannan (*Candida albicans*) and glucuronoxylomannan (*Cryptococcus neoformans*) (Akira *et al.*, 2006). Another ligand of TLR4 is Taxol, an anti-tumour agent derived from the bark of the Western yew (*Taxus brevifolia*) (Kawasaki *et al.*, 2001). Despite being structurally unrelated to LPS, Taxol mimics the actions of LPS on murine (but not human) macrophages due to the differential use of cysteine residues in MD-2 (Kawasaki *et al.*, 2003). In addition, TLR4 has been shown to respond to several endogenous ligands, including heat shock proteins (e.g. HSP70) and fibronectin (Tsan and Gao, 2004). However, high concentrations of these ligands is required to activate TLR4 and it has been suggested that LPS contamination of these samples may be responsible for stimulating TLR4 (Tsan and Gao, 2004).

b) TLRs 1, 2 and 6

TLR2 forms heterodimers with either TLR1 or TLR6 (O'Neill, 2006). The ligands identified are all bacterial components, including peptidoglycan, lipopeptide and lipoprotein of Gram-positive bacteria (Kawai and Akira, 2006b). The TLR1 and TLR2 heterodimer responds to triacyl lipopeptide, while the TLR2 and TLR6 heterodimer responds to diacyl lipopeptide (Kawai and Akira, 2006b). Recently, the structures of the TLR1/2 and TLR2/6 heterodimers have been solved. Binding of the triacylated lipopeptide ligand induced TLR1/2 heterodimerisation, forming an m-shaped ectodomain with a lipid-binding channel at the interface of the two TLRs (Jin *et al.*, 2007). The dimerisation of the TLR1/2 ectodomains may promote dimerisation of the intracellular TIR domains, thereby initiating signalling (Jin *et al.*, 2007).

While TLR2 heterodimerisation is required for binding the triacyl and diacyl lipopeptides, it has been found that TLR2 can bind to certain lipids in the absence of TLR1 and TLR6 possibly by TLR2 homodimerisation (Buwitt-Beckmann *et al.*, 2006). Furthermore, TLR2 has been implicated in peptidoglycan (PG) recognition, though this is disputed (Akira *et al.*, 2006). Like TLR4, TLR2 is implicated in the response to fungal PAMPs, including zymosan (with TLR6), phospholipomannan, and glucuronoxylomannan, which is also a ligand for TLR4 (Akira *et al.*, 2006). Also like TLR4, TLR2 has been found to interact with the envelope glycoproteins of herpesviruses, including human cytomegalovirus (hCMV) and HSV-1 (Boehme and Compton, 2004).

1.3.1.2 Nucleic acid ligands

Nucleic acids from microbes or released from dying cells are important immunogens detected by both cytosolic PRRs and TLRs (Ishii and Akira, 2008). The TLRs that respond to microbial nucleic acids are localized to endosomes and are not expressed at the cell surface (Kawai and Akira, 2006b). TLR7, TLR8 and TLR9 have been found to have

specific localisation sequences in their transmembrane domain that direct them to the endosome, while TLR3 has a distinct localisation sequence between its transmembrane and TIR domains (Kajita *et al.*, 2006). These TLRs are only able to recognise nucleic acids that are released into the endosome following lysis of bacteria or disruption of viral capsids (Kawai and Akira, 2006b). Endosomal acidification has been found to be required for recognition of viral ssRNA by TLR7 (Lund *et al.*, 2004), of the synthetic dsRNA analogue poly (I:C) by TLR3 (de Bouteiller *et al.*, 2005) and of synthetic CpG oligodeoxynucleotides (ODN) by TLR9 (Zou *et al.*, 2003). Inhibition of endosomal acidification with agents such as chloroquine prevented TLR signalling following ligand stimulation (de Bouteiller *et al.*, 2005; Lund *et al.*, 2004; Zou *et al.*, 2003).

Since endosomes are used by viruses for entry, the TLRs localised to the endosome would be poised to engage with viral PAMPs at an early time following infection (Thompson and Iwasaki, 2008). The endosomal localisation is also important for sequestering viral nucleic acids and preventing access of the TLRs to host nucleic acids (Thompson and Iwasaki, 2008). However, the endosomal localisation poses a problem for the detection of viruses that do not enter endosomes as part of their lifecycle. One solution to this problem is the process of autophagy, which involves sampling the contents of the cytoplasm and digesting old proteins and organelles by fusion of the autophagosome with the endosome (Thompson and Iwasaki, 2008). The subsequent fusion of the endosome with the lysosome would permit degradation of viral nucleic acid-protein complexes and facilitate detection of otherwise masked viral PAMPs (Thompson and Iwasaki, 2008). In support of a role for autophagy in antiviral immunity, detection of vesicular stomatitis virus (VSV) was impaired in cells deficient in a protein (atg-5) involved in autophagy (Thompson and Iwasaki, 2008). Detection of viral nucleic acids in the cytosol would also be mediated by the other PRRs, RIG-I, MDA5 and DAI (see

above), which may be the more important PRRs for immediate detection of viral infection in the cytosol.

a) TLR3

TLR3 responds to poly (I:C) to activate NF-κB and induce type I IFNs (Alexopoulou *et al.*, 2001). $TLR3^{-/-}$ mice showed impaired responsiveness to poly (I:C) and to viral genomic RNA (Alexopoulou *et al.*, 2001). Stimulation with poly (I:C) or dsRNA upregulates expression of TLR3 and induces type I IFN production (Akira *et al.*, 2006). In addition, mRNA was found to be an endogenous ligand for TLR3, likely serving as a danger signal following injury or infection by obviating the need for detection of microbial PAMPs (Karikó *et al.*, 2004). Recently, TLR3 has also been found to respond to ssRNA in macrophages, dendritic cells and B cells (Marshall-Clarke *et al.*, 2007). Following stimulation, TLR3 is phosphorylated on cytoplasmic tyrosine residues and this modification is important for TLR3 signalling (Sarkar *et al.*, 2003; Vercammen *et al.*, 2008). The crystal structure of the TLR3 ectodomain has been solved (Choe *et al.*, 2005) and the dsRNA binding site identified in a glycan-free area near LRR20 (Bell *et al.*, 2006)

Viruses produce dsRNA during replication and TLR3 is thought to be a key antiviral PRR. However, TLR3 does not appear to be required for the first-line of defence against viruses (Akira *et al.*, 2006). $TLR3^{-/-}$ mice did not show increased susceptibility to infection with several viruses, including reovirus, which has a dsRNA genome (Akira *et al.*, 2006). In addition, $TLR3^{-/-}$ mice were more resistant to infection by West Nile virus (WNV) than wild-type mice (Wang *et al.*, 2004). In wild-type mice, WNV infection triggers a TLR3-dependent inflammatory response in the central nervous system (CNS) and an increase in inflammatory cytokines (IL-6 and TNF-α) in the circulation (Wang *et al.*, 2004). The TLR3-dependent inflammatory response causes the blood brain barrier

to break down, leading to leakiness that allows viral entry into the CNS and enhances WNV replication (Wang *et al.*, 2004). In $TLR3^{-/-}$ mice, there was a reduction in inflammatory cytokine production and in the viral load in the brain, making $TLR3^{-/-}$ mice less susceptible to WNV infection of the CNS and encephalitis (Wang *et al.*, 2004).

In addition to its role in the innate immune response, TLR3 has been found to play a role in cross-priming DCs (Schulz *et al.*, 2005). TLR3 is expressed in conventional DCs (cDCs), which phagocytose dying cells (Akira *et al.*, 2006). Phagocytosis of cells infected with viruses that do not normally infect DCs activates TLR3 signalling following fusion of the phagosome with the endosome (Schulz *et al.*, 2005). The detection of dsRNA from the phagocytosed cells by TLR3 in the endosomes of DCs augments the activation of cytotoxic T lymphocytes (CTLs) by the DCs (Schulz *et al.*, 2005).

b) TLRs 7 and 8

TLR7 and TLR8 are homologous proteins and recognise the same type of ligands, namely viral ssRNA and synthetic imidazoquinoline (Kawai and Akira, 2006b). In addition, TLR7 recognises loxoribine, a guanosine nucleoside analogue (Takeda and Akira, 2005). TLR7 recognises ssRNA from human immunodeficiency virus type I (HIV-1), vesicular stomatitis virus (VSV) and influenza virus (Kawai and Akira, 2006b). Murine TLR8 is non-functional but human TLR8 responds to viral ssRNA, including from Coxsackie B virus and Parechovirus I, as well as imidazoquinoline (Ishii et al, 2005). In particular, TLR7 and TLR8 recognise guanosine- or uridine-rich ssRNA (Takeda and Akira, 2005). The localisation of TLR7 and TLR8 to the endosome could be important for its recognition of viral and not host RNA, since host ssRNA should not normally be localised to the endosome (Takeda and Akira, 2005).

c) TLR 9

TLR9 recognises unmethylated CpG motifs from both viruses and bacteria (Kawai and Akira, 2006b). Single-stranded DNA with unmethylated CpG motifs common in bacteria and viruses and thus can act as PAMPs (Gilliet *et al.*, 2008). In addition to bacteria, DNA viruses have genomes that are rich in CpG motifs (Akira *et al.*, 2006). DNA from HSV-1, HSV-2 and murine cytomegalovirus has been shown to activate TLR9 (Akira *et al.*, 2006). A missense mutation in the *Tlr9* gene ($Tlr9^{CpG1}$) has been shown to render homozygous mice unresponsive to CpG-ODN and highly susceptible to infection by murine cytomegalovirus (Tabeta *et al.*, 2004).

The response to bacterial CpG requires endosomal acidification, reinforcing the importance of the endosomal localization of TLR9 (Zou *et al.*, 2003). CpG can also stimulate cells of the acquired immune system (B cells, macrophages and DCs) to produce cytokines, express co-stimulatory molecules and increase antigen presentation (Akira *et al.*, 2001). Stimulation with CpG activates a DNA-dependent protein kinase (DNA-PK), leading to NF-κB activation, though the mechanism is not fully determined (Akira *et al.*, 2001). Recently, it has been found that TLR9 recognises the sugar backbone of DNA in synthetic ODN (Haas *et al.*, 2008). While optimal TLR9 activation required a certain number of nitrogenous bases as well, the fact that TLR9 can recognise the deoxyribose might explain the weak induction of TLR9 in response to non-CpG DNA molecules (Ishii and Akira, 2008). The real ligand for TLR9 is still unclear.

1.3.1.3 Protein ligands

a) TLR5

The ligand for TLR5 is flagellin, the protein monomer from the flagella of bacteria (Kawai and Akira, 2007). Flagellin is also a proinflammatory factor, leading to NF-κB activation and nitric oxide synthetase expression (Kawai and Akira, 2007).

b) TLR11

Murine TLR11 recognises unknown components of uropathogenic bacteria and a profilin-like molecule of protozoa (Kawai and Akira, 2007). Human TLR11 is non-functional because of a premature stop codon in the gene (Akira *et al.*, 2006).

1.3.2 Downstream signalling pathways

Ligand-binding to TLRs stimulates a number of intracellular signalling pathways to the activation of transcription factors and mitogen-activated protein kinases (MAPK), leading to the regulation of gene expression and cytokine production. A core shared signalling pathway from TLRs leads to activation of NF-κB, AP-1 and of the regulatory MAP3K (Figure 1.3; O'Neill, 2006), via the TIR domain-containing adaptor molecule MyD88. Following ligand stimulation, MyD88 is presumed to interact with dimerised TLRs via TIR-TIR interactions. MyD88 then recruits members of the IRAK family, including IRAK1, IRAK4 and IRAK2. Subsequently, TRAF6 forms a complex with ubiquitin-conjugating enzymes and ubiquitin-binding proteins in order to recruit and activate TAK1. Activated TAK1 is able to phosphorylate the IKK complex and the MAP2K in order to activate NF-κB and MAPK-dependent transcription factors, respectively. While it is possible to generalize about TLR signalling, as in Figure 1.3, the situation is more complex and involves numerous other signalling molecules. There are a total of five TIR adaptor molecules, including MyD88, which will be described below. In addition, the recruitment of IRAK family members, TRAFs and other signalling adaptors and enzymes can vary between signalling pathways. The roles of these signalling molecules will be introduced, along with a brief discussion of the activation of MAPK and NF-κB.

1.3.2.1 Adaptor molecules

Adaptors mediate signal transduction from stimulated TLRs to downstream pathways. Following ligand stimulation, TLRs are thought to dimerise in order to initiate signal transduction and dimerisation has recently been demonstrated for TLR1/2 (Jin *et al.*, 2007), TLR3 (Bell *et al.*, 2006) and TLR4 (Kim *et al.*, 2007). The receptor TIR domains are thought to alter their conformation once dimerised so that they can interact with adaptor proteins containing TIR domains (O'Neill *et al.*, 2003). Five TIR domain-containing adaptors have been described and selectivity in adaptor usage by different TLRs accounts for at least some of the distinct signalling pathways from the receptors (O'Neill and Bowie, 2007). The current understanding of adaptor usage is shown schematically in Figure 1.4.

a) MyD88

The first TIR domain-containing adaptor protein identified was MyD88. MyD88 was found to have a role in IL-1 signalling (Muzio *et al.*, 1997) and subsequently in TLR signalling (Muzio *et al.*, 1998). Interaction between MyD88 and the TLRs is dependent upon the C-terminal TIR domain (Nishiya *et al.*, 2007). In addition to the TIR domain, MyD88 has a short N-terminal region, a death domain (DD) and an intermediate region between the DD and the TIR domains (Nishiya *et al.*, 2007). The non-TIR region of MyD88 is crucial for its subcellular localisation to an as yet unknown organelle and for its role in cell signalling (Nishiya *et al.*, 2007). The DD of MyD88 is required for its interaction with the DD of IRAK4 (O'Neill, 2006). MyD88 is crucial in mediating signal transduction from all TLRs, except TLR3, as well as from the Type I IL-1 receptor (O'Neill *et al.*, 2003).

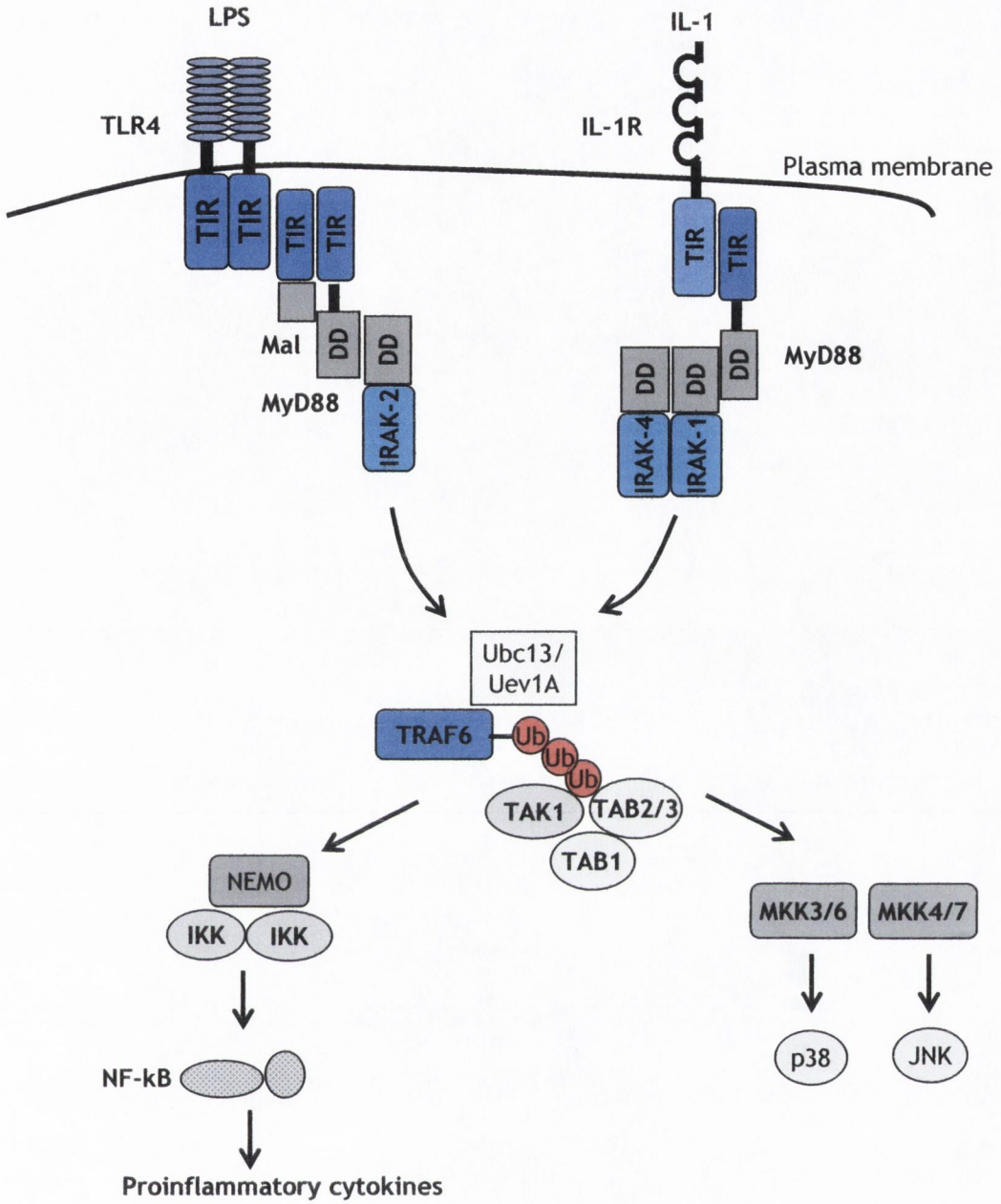

Figure 1.3 The core IL-1R/TLR signalling pathway using MyD88.

IL-1R and most TLRs signal via interaction with the adaptor MyD88, leading to the formation of a complex with the IRAKs and TRAF6. IRAK1 and IRAK4 have been found to have a role in IL-1R/TLR signal transduction from MyD88, with IRAK4 likely being the one that interacts with MyD88 itself (O'Neill and Bowie, 2007). IRAK2 has recently been found to have a role in TLR-induced NF-κB and MAPK activation (Keating *et al.*, 2007). Previous work established that IRAK2 interacted with Mal and MyD88 (see text). Activation of TRAF6 results in its polyubiquitination (K63-linked) and this is thought to recruit TAB2/3 and TAK1. Activated TAK1 then phosphorylates NEMO and the MAP3K to activate NF-kB and of MAPK, respectively.

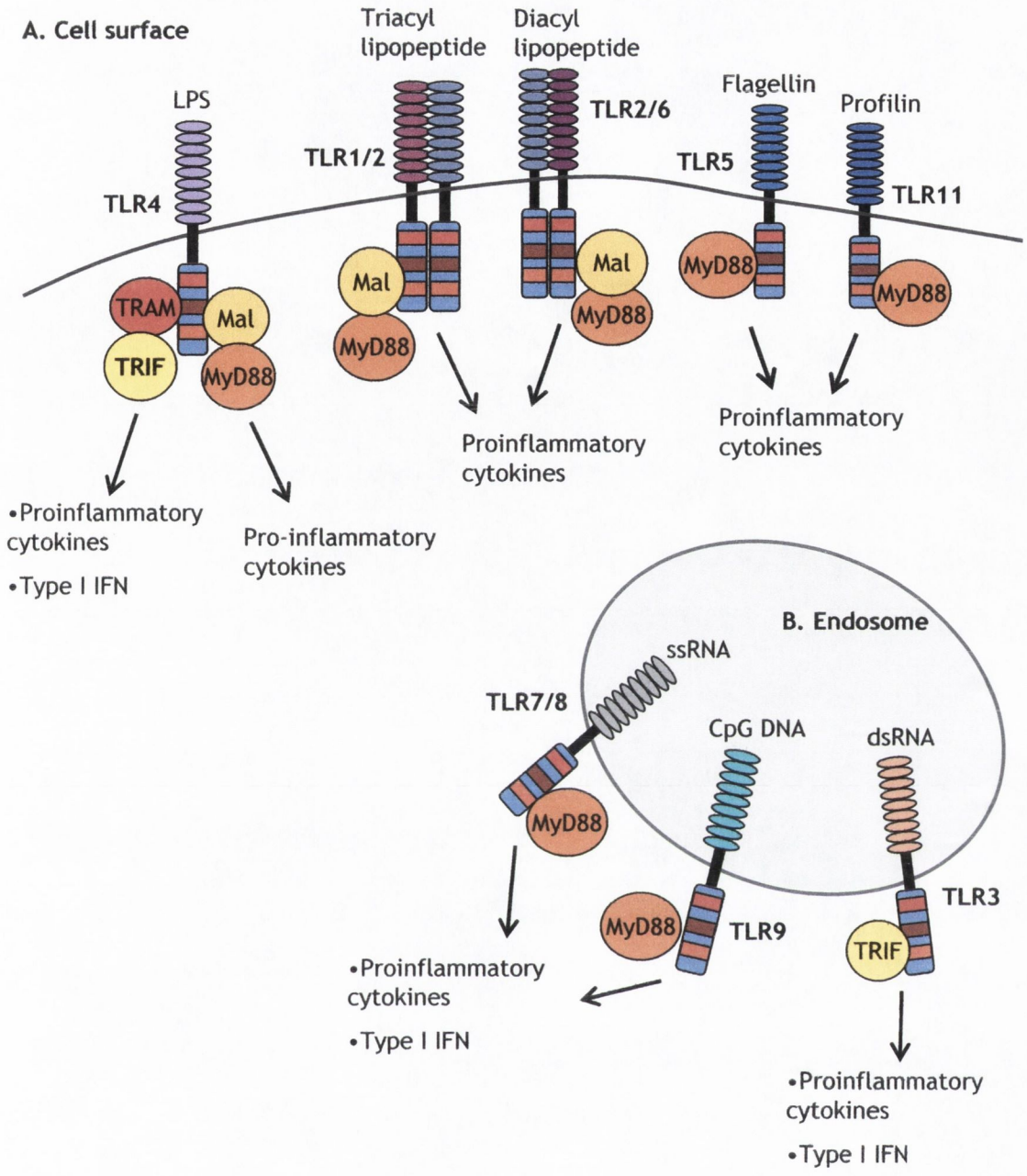

Figure 1.4 Toll-like receptors (TLRs) response to their respective ligands is mediated by intracellular TIR adaptor proteins.

TLRs that are localised to the cell surface and respond to lipid or protein ligands (A). Other TLRs are localised to the endosome and respond to nucleic acids (B). Ligand-binding induces receptor dimerization and the recruitment of intracellular adaptors (MyD88, Mal, TRIF and TRAM). Activation of the signalling pathways leads to production of inflammatory cytokines and type I IFN. Aside from TLR1/2 and TLR2/6 heterodimers, other receptor dimers are not shown for simplicity. Adapted from Kawai and Akira, 2006b.

b) Mal / TIRAP

The existence of a second adaptor protein was hypothesised based on the observation that LPS-induced signalling to NF-κB and JNK activation proceeded in MyD88-deficient cells, although with delayed kinetics (O'Neill *et al.*, 2003). The second TIR-containing adaptor protein was described simultaneously as MyD88-adapter-like (Mal; Fitzgerald *et al.*, 2001) and TIR domain-containing adaptor protein (TIRAP; Horng, *et al.*, 2001). The TIR domain in Mal/TIRAP has conserved residues in both box 1 and box 2 but does not have box 3 (Fitzgerald *et al.*, 2001). Mal/TIRAP has the BB loop described in the TIR domain of TLR2 and found to be essential for signalling (Fitzgerald *et al.*, 2001). In contrast to MyD88, Mal/TIRAP has a shorter N-terminus (75 amino acids) and lacks a death domain (Fitzgerald *et al.*, 2001). It was subsequently found that Mal/TIRAP was not specific to TLR4 signalling and did not participate in the LPS-induced MyD88-independent signalling pathway to IRF3 activation (Yamamoto *et al.*, 2002). Instead, it was found that Mal/TIRAP functioned similarly to MyD88 but that its role was restricted to signalling from TLR2 and TLR4 (Yamamoto *et al.*, 2002).

Mal/TIRAP can interact directly with TLR2 and TLR4 while MyD88 cannot, likely due to electrostatic repulsion of the TLR and MyD88 TIR domains (O'Neill and Bowie, 2007). Mal/TIRAP bridges the interaction between the TLR2 or TLR4 and MyD88 (O'Neill and Bowie, 2007). Mal is localised to the plasma membrane via a phosphatidylinositol 4,5-bisphosphate (PIP_2) binding domain which binds to the phospholipid (PIP_2) that is enriched in the membrane (Kagan and Medzhitov, 2006). Both the PIP_2-binding and TIR domains of Mal are needed for it to recruit MyD88 to the plasma membrane (Kagan and Medzhitov, 2006). Mal is thus hypothesised to be a sorting adaptor, required for the assembly of TLR signalling complexes (Kagan and Medzhitov, 2006).

In order to function in signalling, Mal has to be post-translationally modified. A 4kDa peptide at the C-terminus of Mal is cleaved by caspase-1 (Miggin *et al.*, 2007). In addition, phosphorylation of tyrosine residues in Mal (86, 106 and 159) is essential for activation (Piao *et al.*, 2008; Gray *et al.*, 2006).

c) TRIF

The third adaptor protein described was TIR domain-containing adaptor inducing IFNβ (TRIF; Yamamoto *et al.*, 2002). TRIF is an adaptor specific for TLR3 signalling to IRF3 and NF-κB activation (O'Neill *et al.*, 2003). In $TRIF^{-/-}$ mice, TLR3 and TLR4 signalling was found to be impaired (Yamamoto *et al.*, 2003). The TLR3 ligand, poly (I:C) failed to elicit any responses in $TRIF^{-/-}$ mice (Yamamoto *et al.*, 2003). While LPS-induced signalling via IRAK-1, NF-κB and MAP kinase were all normal in $TRIF^{-/-}$ mice, inflammatory cytokine production was impaired (Yamamoto *et al.*, 2003). It was thus proposed that TRIF is involved in signalling from TLR4 in a MyD88-independent pathway (Yamamoto *et al.*, 2003). TLR3 and TLR4 signal via TRIF to activate the IKK family kinase TBK-1, which phosphorylates IRF3 and thereby activates IFN-β (O'Neill, 2006). Mal has a TRAF6 binding motif (see below) which is required for signalling to NF-κB and MAP kinase activation (Mansell *et al.*, 2004). Recently, TRADD was found to be recruited to TRIF-dependent signalling complexes downstream of TLR3 and TLR4 (Ermolaeva *et al.*, 2008). TRADD is normally associated with TNF-induced signalling and it is required for TNF-induced apoptosis (Ermolaeva *et al.*, 2008). In TRIF-mediated signalling, TRADD has a role in recruitment of the signalling molecules, including RIP1, required to induce proinflammatory cytokine expression (Ermolaeva *et al.*, 2008).

d) TRAM

The TRIF-related adapter molecule (TRAM) is similar to TRIF and, like TRIF, induces NF-κB and IRF-3 activation (Fitzgerald *et al.*, 2003). TRAM-deficient mice showed impaired IRF3 activation and subsequent expression of IFN-inducible genes (Akira and Takeda,

2004). However, the response to TLR3 was normal in TRAM-deficient mice, suggesting that TLR3 recruitment of TRIF does not require TRAM (Akira and Takeda, 2004). Thus, TRAM is only involved in TLR4 signalling via a MyD88-independent and TRIF-dependent pathway (Akira and Takeda, 2004), where it interacts with TRIF. TRAM is localised to the plasma membrane via N-terminal myristoylation (Rowe *et al.*, 2006). Mutation of the predicted myristoylation site (TRAM-G2A) resulted in both a loss of plasma membrane localisation and an inability to function in TLR4 signalling (Rowe *et al.*, 2006). In addition, TRAM is phosphorylated at serine 16 by protein kinase Cε and this modification is also required for signalling (McGettrick *et al.*, 2006).

e) SARM

A fifth TIR adapter protein was described and termed SARM (for SAM and ARM protein) (O'Neill *et al.*, 2003). SARM contains a number of domains that are found in signalling proteins: two sterile α motif (SAM) domains and an Armadillo repeat motif (ARM) give the protein its name (O'Neill *et al.*, 2003). Human SARM has been found to have a role in negatively regulating TRIF-dependent signalling (Carty *et al.*, 2006). Suppression of SARM expression resulted in enhanced induction of TRIF-dependent genes (Carty *et al.*, 2006). Further, SARM co-immunoprecipitated with endogenous TRIF and the co-immunoprecipitation was enhanced by LPS stimulation (Carty *et al.*, 2006). The TIR and SAM domains of SARM are critical for its inhibitory function (Carty *et al.*, 2006).

1.3.2.2 IL-1 receptor-associated kinases (IRAKs)

Four members of the IRAK family have been described to date: IRAK1, IRAK2, IRAK4 and IRAK-M. The IRAKs are serine-threonine kinases and all have a kinase-like domain, with IRAK1 and IRAK4 having been found to have kinase activity (Gottipatti *et al.*, 2008). Recently, IRAK2 was also found to have kinase activity (Kawagoe *et al.*, 2008). In

addition, the IRAKs have an N-terminal death domain which is important for interaction with MyD88 (Suzuki *et al.*, 2002).

IRAK4 is essential in IL-1R/TLR signalling since the inability of a truncated form of MyD88 to recruit IRAK4 abolished NF-κB activation (Burns *et al.*, 2003). IRAK4 deficient ($IRAK4^{-/-}$) mice were completely resistant to lethal doses of LPS and had increased susceptibility to bacterial and viral infections (Suzuki *et al.*, 2002). IRAK4 was also required to mount a response to IL-1, CpG or poly (I:C) (Suzuki *et al.*, 2002). Furthermore, downstream signalling from IL-1R/TLR to NF-κB and MAP kinase activation was impaired in $IRAK4^{-/-}$ cells (Suzuki *et al.*, 2002). IRAK4 is likely recruited to the adaptors MyD88 and Mal, while TRAF6 acts downstream of IRAK4 (Suzuki *et al.*, 2002). IRAK1 is also involved in IL-1R/TLR signalling since macrophages lacking IRAK1 ($IRAK1^{-/-}$) showed impaired TLR2 and TLR4 signalling (Gottipatti *et al.*, 2008). $IRAK1^{-/-}$ mice were defective in response to IL-1, LPS and bacterial infection but the impairment was not as severe as that observed with $IRAK4^{-/-}$ mice (Suzuki *et al.*, 2002; Gottipatti *et al.*, 2008). Both IRAK1 and IRAK4 are needed for optimal signal transduction (Suzuki *et al.*, 2002), and are recruited to MyD88 via their death domains, which brings the two kinases into close proximity to allow IRAK4 to phosphorylate IRAK1 (Janssens and Beyaert, 2003).

IRAK2 has also been found to have a role in TLR signalling pathways. In TLR4 signalling, IRAK2 is recruited to the receptor via interaction with Mal and MyD88 (Fitzgerald *et al.*, 2001; Muzio *et al.*, 1997). In contrast, IRAK2 interacts directly with TLR3 (Keating *et al.*, 2007). Following ligand-induced TLR activation, IRAK2 is able to interact with and induce TRAF6 autoubiquitination (Keating *et al.*, 2007). Ubiquitinated TRAF6 recruits the TAB1/2 and TAK1 complex to activate MAP kinases and NF-κB (Keating *et al.*, 2007).

Recently, a study suggested that there was a temporal difference in IRAK 1 and IRAK2 usage in TLR signalling (Kawagoe *et al.*, 2008). While both IRAK1 and IRAK2 are needed in the early stages following TLR stimulation, IRAK2 is needed for sustained induction of proinflammatory cytokines (Kawagoe *et al.*, 2008). However IRAK2, and not IRAK1, induced TRAF6 polyubiquitination and this was found to be critical for IL-1R/TLR-induced NF-κB activation (Keating *et al.*, 2007). IRAK2 is thus critical in TLR-induced NF-κB activation, whereas IRAK1 may have a distinct role in selective activation of IRFs (Keating *et al.*, 2007).

In Drosophila, signalling from Toll is transmitted by the serine-threonine kinase Pelle and the Pelle-interacting protein, Pellino (Jiang *et al.*, 2003b). The mammalian counterpart, Pellino 1, is required in signalling from the IL-1R leading to NF-κB activation and interacts with IRAK1, IRAK4 and TRAF6 (Jiang *et al.*, 2003b). In addition to Pellino 1, there are also Pellino 2 and Pellino 3, all of which contain a RING (Really Interesting New Gene) domain and function as an E3 ubiquitin ligase (see section 1.3.2.3c below; Butler *et al.*, 2007). The Pellinos, IRAK1 and IRAK4 have a reciprocal relationship, with the Pellinos catalysing the ubiquitination of IRAK1 and IRAK4 (Butler *et al.*, 2007). Once active, IRAK 1 and IRAK4 phosphorylate Pellino proteins, thereby promoting their polyubiquitination and degradation (Butler *et al.*, 2007). In contrast, IRAK2 does not regulate the degradation of Pellinos (Butler *et al.*, 2007).

IRAK-M expression is induced by TLR stimulation in monocytes or macrophages (Kobayashi *et al.*, 2002). Following activation, IRAK-M prevents IRAK1/IRAK4 from dissociating from the TLR/MyD88 complex and inhibits the interaction of IRAK1 with TRAF6 (Kobayashi *et al.*, 2002). Thus, IRAK-M negatively regulates TLR signalling in order to prevent excessive cytokine secretion and endotoxic shock (Kobayashi *et al.*, 2002).

1.3.2.3 TRAFs

The TRAFs were initially described by Rothe and colleagues (1994) as cytoplasmic proteins that bound to the TNFRII (Arch *et al.*, 1998). It has since been found that the TRAFs serve as adaptor proteins to a variety of receptors, including other members of the TNFR superfamily, such as CD40, and IL-1R (Arch *et al.*, 1998). The TRAFs bind to the cytoplasmic region of the receptors and also interact with downstream effectors, including kinases and ubiquitin ligases, thereby providing the link between receptor activation and signal transduction (Zapata *et al.*, 2001). To date, seven human TRAFs have been identified and found to have distinct functions in signalling pathways and development (Zapata *et al.*, 2007b).

a) TRAF structure

The TRAF proteins have several domains in common (Figure 1.5). The characteristic domain of the family is the TRAF domain in the C-terminal region of the protein (Arch *et al.*, 1998). The TRAF domain is further subdivided into the TRAF-N and TRAF-C regions (Arch *et al.*, 1998). The TRAF-C domain is a region of high homology between the TRAFs and it mediates binding of the TRAFs to their respective receptors (Wajant *et al.*, 2001). The TRAF-N region is predicted to form a coiled-coil structure (Arch *et al.*, 1998) and to be required for signalling (Wajant *et al.*, 2001). Furthermore, it has been shown that receptor activation can induce some of the TRAFs to form homo- or heterotrimers (Wajant *et al.*, 2001) and this may be mediated by the TRAF-N domain (Wu and Arron, 2003). However, it is not clear if all the TRAFs form oligomers and, if they trimerise, whether they do so only following recruitment to the activated receptor. Moreover, the role of the TRAF domain in oligomerisation is uncertain since at least one member of the TRAF family, TRAF7, lacks the TRAF domain (Zapata *et al.*, 2007b).

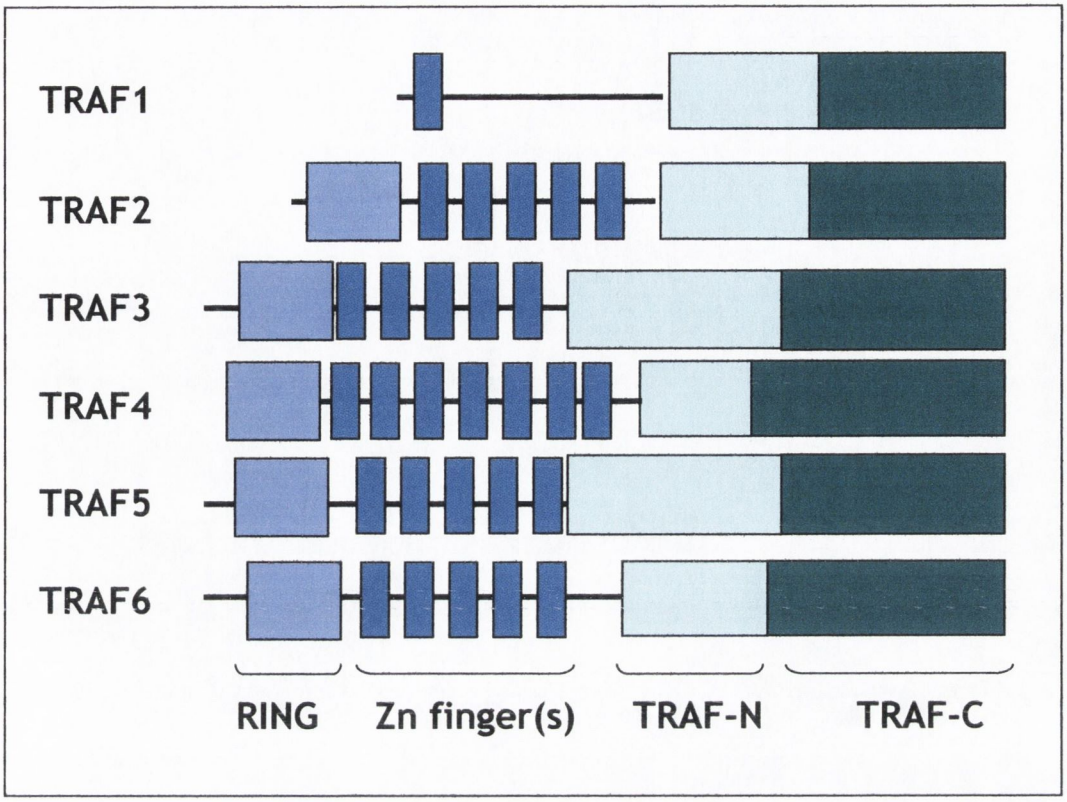

Figure 1.5 Tumour necrosis receptor factors (TRAFs) are multidomain proteins.

The TRAFS have a characteristic TRAF domain, consisting of the distinct subdomains TRAF-N and TRAF-C. In addition, there is a RING domain near the N-terminus in TRAF2, TRAF3, TRAF4, TRAF5 and TRAF6. Each TRAF has at least one zinc finger between the RING and TRAF domains. The higher molecular structure, the *C*-rich domain *a*ssociated with *R*ING and *T*RAF domains CART domain, would comprise the zinc fingers in each TRAF2 through TRAF6 . Figure adapted from Kobayashi *et al.*, 2004.

In addition to the TRAF domain, all of the TRAFs except TRAF1 have a RING (for really interesting new gene) domain near the N-terminus (Arch *et al.*, 1998). RING domains are characterised by a consensus sequence of cysteine and histidine residues (Borden, 2000). The TRAF RING domain is characteristic of the RING-HC (or C_3HC_4) subfamily, with the consensus sequence: $CX_2CX_{11,12}CX_1HX_2CX_2CX_{9,11}CX_2C$ (Wajant *et al.*, 2001). The cysteine and histidine residues bind to two zinc atoms in a cross-brace arrangement that allows the creation of two sites that can interact with different binding partners (Borden, 2000). An important function of RING domains is in the formation of macromolecular scaffolds (Borden, 2000), a role that is likely due to the ability of RINGs to bind to proteins at two sites (i.e. the two sites created by zinc binding). In particular, it has been found that RING domains are important in forming the macromolecular complexes that comprise E3 ubiquitin ligases, described below (Borden, 2000).

In TRAFs 2 through 6, several predicted zinc fingers lie between the RING and TRAF-N domain (Arch *et al.*, 1998). Interestingly, the zinc fingers are arranged in a regular pattern, with six amino acids between each finger (Wajant *et al.*, 2001). This arrangement of zinc fingers has been described as a higher order structure, the *C*-rich domain *a*ssociated with *R*ING and *T*RAF domains (CART), and has been described in TRAF2 (Régnier *et al.*, 1995). There is one predicted zinc finger in TRAF1 near the N-terminus (Wajant *et al.*, 2001). The function of these fingers in the TRAFs is not clear though they are generally known to mediate protein-protein interactions as well as to bind DNA (Arch *et al.*, 1998).

Based on their multidomain structure, the TRAFs are thought to function as protein adaptors, mediating signal transduction via receptor binding and the recruitment of other proteins to form signalling complexes (Arch *et al.*, 1998). In order to determine

how TRAFs interact with receptors, the receptors have been studied for specific TRAF binding sites. A common motif, (P/S/T/A)-X-(Q/E)-E, where X is any amino acid is recognised by TRAF2, TRAF3 and TRAF5 (Chung *et al.*, 2002), which accounts for their ability to bind several of the same receptors (Arch *et al.*, 1998). The TRAFs have diverse roles in signalling, mainly from TNFR family members. However, at least one TRAF, TRAF6, has a role in IL-1R/TLR signalling. TRAF6 was originally identified as a component of IL-1R signalling (Cao *et al.*, 1996) and has since been found to have a role in the activation of NF-κB and MAPK downstream of TLRs as well.

b) TRAF6

The domain organization of TRAF6 is similar to that of the other TRAFs described above (Figure 1.5). TRAF6 has an N-terminal RING domain, followed by five zinc fingers (Chung *et al.*, 2007a). The C-terminal TRAF domain consists of a TRAF-N and a TRAF-C domain (Chung *et al.*, 2007a). The TRAF domain of TRAF6 is the most divergent from other TRAFs in terms of structure, since the α-helices that link the two sheets of the β-sandwich have distinct orientations (Chung *et al.*, 2007a). As for the other TRAFs, the TRAF-C domain of TRAF6 is the site of interaction with other proteins, such as receptors or kinases. Proteins that interact with TRAF6 typically have a TRAF6 binding motif, which was defined by X-ray crystallography studies using peptides from known TRAF6 interaction partners (Ye *et al.*, 2002). The consensus motif was defined as P-X-E-X-X-Acidic (Ac)/Aromatic (Ar) residue (Ye *et al.*, 2002), where P, E and the Ac/Ar residues were found to be critical for the peptide-TRAF-C interaction (Ye *et al.*, 2002). This motif is slightly different from that used by the other TRAFs (see above).

Since its discovery, TRAF6 has been found to have a critical role in several signalling pathways. In particular, TRAF6 is an adaptor molecule in numerous pathways to NF-κB activation, including from CD-40, receptor activator of NF-κB (RANK) (Darnay *et al.*,

1999), IL-1R/TLR (Cao *et al.*, 1996), the T-cell receptor (Sun *et al.*, 2004), nerve growth factor (Wooten *et al.*, 2005) and LPS-stimulated caspase 4 (Lakshmanan and Porter, 2007). In addition, TRAF6 is required for MAPK activation in MyD88-dependent pathways since stimulation of $TRAF6^{-/-}$ MEFs with several different TLR ligands did not induce phosphorylation of the MAPK ERK, JNK and p38 (Godha *et al.*, 2004). TRAF6 has also been implicated in a number of signalling pathways induced by cytokines, including interleukin-17 (IL-17) signal transduction (Schwandner et al, 2000).

c) TRAF6 ubiquitination

Ubiquitin is a 76 amino acid protein monomer that can be linked to proteins via its lysine residues, either singly or in polyubiquitin chains (Schnell and Hicke, 2003). The attachment of ubiquitin involves a cascade of three enzymes: the E1 ubiquitin-activating enzyme, the E2 ubiquitin-conjugating enzyme and the E3 ubiquitin ligase (Figure 1.6; Schnell and Hicke, 2003). The E1 enzyme forms a thiol-ester bond between a cysteine in its active site and glycine 76 (G76) of ubiquitin (Fang and Weissman, 2004). Next, the activated ubiquitin moiety is transferred to an active site cysteine of the E2 enzyme by transesterification (Fang and Weissman, 2004). The E3 enzyme binds the ubiquitin-conjugated E2, as well as to the substrate protein, providing substrate specificity (Fang and Weissman, 2004). The E3 catalyses the formation of the isopeptide linkage between the G76 of ubiquitin and the ε-amino group of a lysine residue within the substrate protein (Fang and Weissman, 2004). There are several classes of E3 enzymes, including the HECT (Homologous to the E6-AP Carboxyl Terminus) and RING E3 ligases, so named for the presence of an eponymous domain (Di Fiore *et al.*, 2003). As mentioned above, the TRAFs, except for TRAF1, have a RING domain and TRAF2 and TRAF6 have been found to have E3 ubiquitin ligase activity.

The original role described for ubiquitination in the cell was in targeting proteins for degradation via the proteasome (Schnell and Hicke, 2003). Recent work has expanded this definition of ubiquitination to include numerous other functions. The number of ubiquitin moieties added and the particular lysine residue of ubiquitin used as a link residue determine the function of ubiquitination. Polyubiquitination with K48-linked chains is a well-known signal for protein degradation at the proteasome (Schnell and Hicke, 2003). K48-linked ubiquitination is important for turnover of cellular proteins but also has a role in the regulation of cell signalling pathways, since activation of NF-κB involves the phosphorylation and subsequent K48-linked ubiquitination of the inhibitory protein, IκBα (Roff *et al.*, 1996). In addition, TLR4 and TLR9 are targeted for degradation by Triad3A-mediated K48-linked ubiquitination in order to suppress TLR signalling (Chuang and Ulevitch, 2004).

In contrast, proteins that are either mono-ubiquitinated or K63-linked ubiquitinated are not degraded at the proteasome. Mono-ubiquitination has a role in receptor tyrosine kinase signalling, endosomal sorting and regulation of transcription factors (Di Fiore *et al.*, 2003). K63-linked polyubiquitination is important in IL-1R/TLR signal transduction, as described below for TRAF6 (Keating and Bowie, 2008). The K48- and K63-linked polyubiquitin chains are structurally distinct, with the K63-linked chains adopting a more elongated conformation compared to the K48-linked chains (Tenno *et al.*, 2004). The distinct conformations permit recognition of the linkages by different ubiquitin binding proteins (Tenno *et al.*, 2004). However, there is no reason that ubiquitin chains cannot contain mixed linkages though this has not been demonstrated *in vivo* (Pickart and Fushman, 2004). It is also possible for one E3 enzyme to conjugate both K48- and K63-linked ubiquitin chains, depending upon the E2 enzyme that interacts with the E3 (Windheim *et al.*, 2008b). Furthermore, polyubiquitin linkages through a few of the

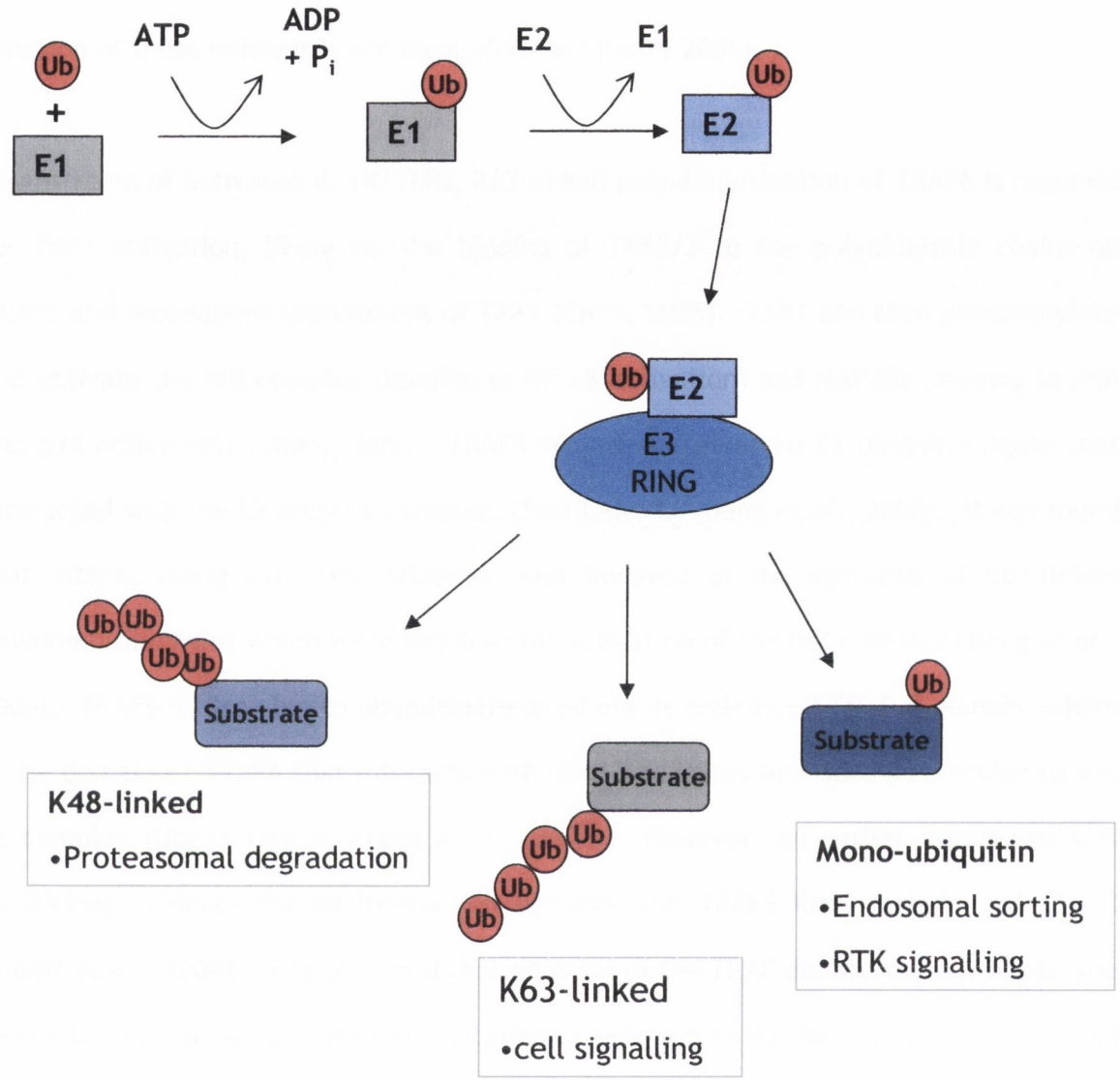

Figure 1.6 The ubiquitin pathway

The conjugation of ubiquitin to the E1 activating enzyme requires ATP. Once activated, the ubiquitin is transferred to the E2 conjugating enzyme. The E2 can then transfer the ubiquitin to the E3 ligase for conjugation to the substrate. Alternatively, the E2 with bound ubiquitin can bind to the E3 but then transfer the ubiquitin directly to the substrate. Ubiquitin can be added as a monomer or as a polyubiquitin chain, linked through any of the seven lysine residues (only K48 and K63 shown for simplicity). Ub, ubiquitin; ATP, adenosine triphosphate; RING, really interesting new gene; RTK, receptor tyrosine kinase.

other lysine residues (K6, K11 and K29) of ubiquitin have been described though the function of these linkages is not clear (Gao and Karin, 2005).

Downstream of activated IL-1R/TLRs, K63-linked polyubiquitination of TRAF6 is required for TAK1 activation, likely via the binding of TAB2/3 to the polyubiquitin chains on TRAF6 and subsequent recruitment of TAK1 (Chen, 2005). TAK1 can then phosphorylate and activate the IKK complex (leading to NF-κB activation) and MAP3Ks (leading to JNK and p38 activation) (Chen, 2005). TRAF6 was identified as an E3 ubiquitin ligase that interacted with the E2 enzyme complex, Ubc13/Uev1A (Deng *et al.*, 2000). It was found that TRAF6, along with Ubc13/Uev1A, was involved in the synthesis of K63-linked polyubiquitin chains which were required for activation of the IKK complex (Deng *et al.*, 2000). TRAF6 is also able to ubiquitinate itself via its coiled-coil TRAF-N domain, which is the domain of TRAF6 that interacts with Ubc13 and thus functions as a bridge to the E2 complex (Ubc13/Uev1A) (Yang *et al.*, 2004). However, an earlier report provides conflicting evidence for an interaction between the TRAF6 RING domain and Ubc13 (Wooff *et al.*, 2004). They observed that deletion of the TRAF domain did not impair the TRAF6-Ubc13 interaction, whereas mutation or deletion of the RING and zinc fingers did (Wooff *et al.*, 2004). Interestingly, ß-arrestin negatively regulates TRAF6 function by binding to the TRAF-N domain (Wang *et al.*, 2006), possibly by preventing access of the E2 complex. The binding of ß-arrestin to the TRAF-N domain prevents TRAF6 auto-ubiquitination and oligomerisation, thereby inhibiting NF-κB and AP-1 activation (Wang *et al.*, 2006).

Finally, it is possible that a scaffolding protein, such as the p62 or sequestosome 1 (SQSTM1), is required to regulate TRAF6 ubiquitination. The need for p62 in TRAF6 oligomerisation and ubiquitination has been demonstrated in nerve growth factor-induced NF-κB activation (Wooten *et al.*, 2005). While a role for p62 in IL-1-induced

NF-κB activation has been postulated (Wooten *et al.*, 2005), the need for TRAF6-p62 interaction in IL-1R/TLR signalling has not been characterised. It is possible that another scaffolding protein interacts with TRAF6 to regulate its ubiquitination IL-1R/TLR signalling.

1.3.2.4 Activation of NF-κB

NF-κB is a dimeric transcription factor belonging to the Rel-homology domain containing protein family (Kawai and Akira, 2006b). This family comprises p65/RelA, p50/NF-κB1, p52/NF-κB2, RelB and c-Rel (Kawai and Akira, 2006b). Generally, NF-κB is a heterodimer of p65 and p50 (Kawai and Akira, 2006b). NF-κB is kept in the cytoplasm in an inactive state by its interaction with inhibitor of NF-κB (IκB) proteins (Kawai and Akira, 2006b). Following TLR stimulation, the IKK complex phosphorylates IκB proteins, targeting them for K48-linked ubiquitination and subsequent degradation via the proteasome (Akira *et al.*, 2006). The free NF-κB is then able to translocate to the nucleus and to bind to κB elements (Kawai and Akira, 2006b).

1.3.2.5 Activation of MAPK and AP-1 transcription factor

TLR signalling also leads to the activation of the regulatory proteins of the mitogen-activated protein (MAP) kinases. The MAP kinase cascade consists of a series of protein kinases: a serine-threonine kinase MAPKKK (MAP3K) activates a dual specificity kinase (MAP2K), which then activates the MAP kinase (Figure 1.7; Symons *et al.*, 2006). The three classes of kinases activated are extracellular signal-regulated protein kinases (ERK 1 and 2), c-Jun amino-terminal kinases (JNK 1, 2 and 3) and the p38 MAP kinases (α, β, γ and δ) (Symons *et al.*, 2006). Twenty-one MAP3K have been identified and they activate the MAP2K by phosphorylation (Symons *et al.*, 2006). While it is thought that there is cell-type and receptor specificity in the use of the MAP3K, the specific MAP3K involved in TLR signalling are still being elucidated (Symons *et al.*, 2006). For example,

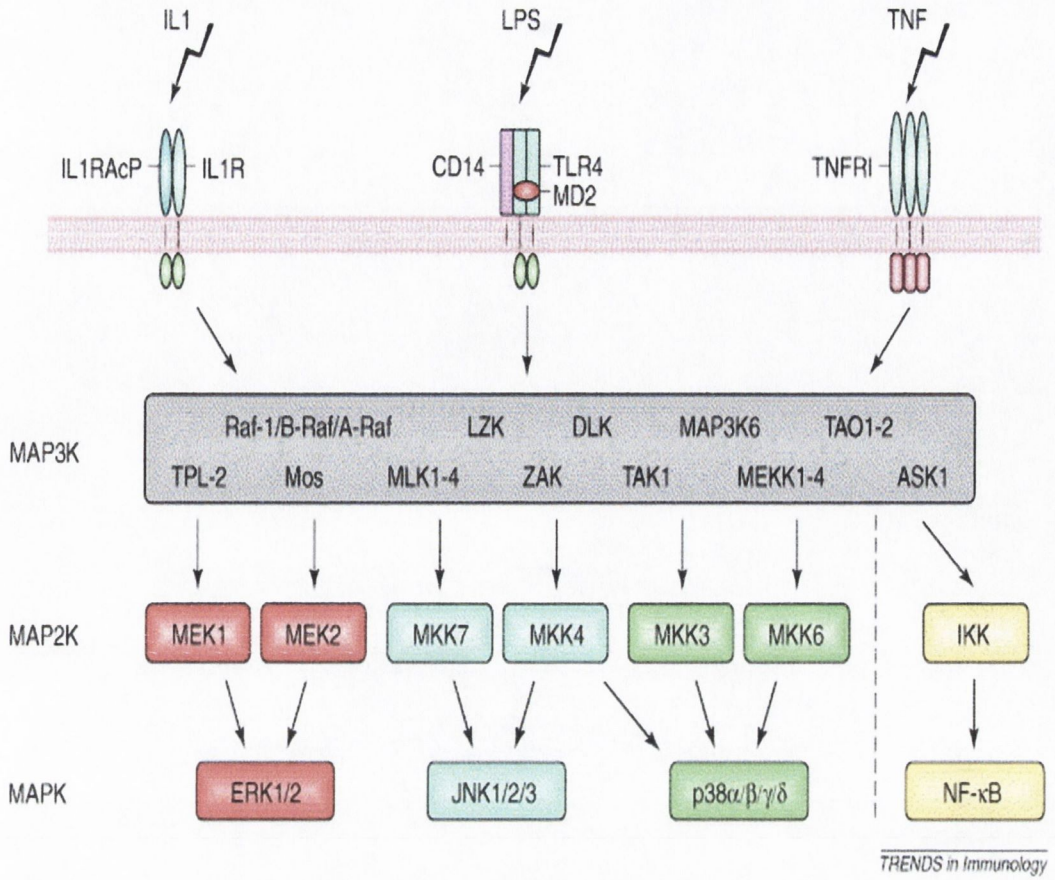

Figure 1.7 MAP kinase activation by TLRs, IL-1R and TNFR.

In response to stimulation by IL-1, TLR ligands or TNF, the respective receptors are activated and trigger intracellular MAP kinase cascades. The MAP3K activate the MAP2K which, in turn, activate the MAPK. The MAP2K and the MAPK they activate have been determined but the specific MAP3K involved in each pathway are still being determined. The MAP3K are: ASK1, apoptosis signal-regulating kinase 1; DLK, dual leucine zipper kinase; LZK, leucine zipper bearing kinase; MAP3K6; MEKK1-4, MAPK/ERK kinase (MEK) kinases 1-4; MLK1-4, mixed-lineage kinases 1-4; Mos, Moloney murine sarcoma viral oncogene v-mos homologue; TAK1, transforming growth factor β (TGFβ)-activated kinase 1; TAO1-2, thousand and one amino acid kinase 1-2; TPL-2, tumour progression locus 2; ZAK, leucine-zipper (LZ) and sterile-α motif (SAM) kinase. The MAP2K are: MEK 1-2, ; MAPK kinases (MKK) 3, 4, 6 and 7. The MAPK are: ERK1/2, extracellular-signal-regulated kinases 1/2; JNK1/2/3, Jun N-terminal kinases 1/2/3; and p38 isoforms α/β/γ/δ. Taken from Symons et al., 2006.

TLR stimulation induced the phosphorylation of the MAP3K, MEKK2/3, but the precise role for MKK2/3 in JNK and p38 activation is unclear and might be cell-type specific (Zhang *et al.*, 2006). One MAP3K, TAK1, is activated by recruitment to the TRAF6/TAB1/TAB2 complex downstream of activated TLRs (Wang *et al.*, 2001). TAK1 activates the MAP2K, MKK4/7 and MKK3/6, which subsequently activate JNK and p38, respectively (Katsoulidis *et al.*, 2005). TLR stimulation induced the phosphorylation of the MAP3K, MEKK2/3, on specific serine residues (Zhang *et al.*, 2006). Both MEKK2 and MEKK3 have been implicated in signalling to p38 and JNK activation, although their roles might be cell-type specific (Zhang *et al.*, 2006).

Once active, the MAPK phosphorylate and thereby activate transcription factors. For example, active p38 phosphorylates numerous transcription factors including CHOP, p53 and activating transcription factors (ATF1, ATF2 and ATF6) (Katsoulidis *et al.*, 2001). In addition, activating protein-1 (AP-1) is activated by the MAPK, including JNK, p38 and ERK, following TLR stimulation (Kawai and Akira, 2006b). AP-1 is a dimeric basic region leucine zipper (bZIP) protein (Kawai and Akira, 2006b). The subunits are members of the Jun, Fos, ATF and Maf subfamily which bind TPA- or cAMP-response elements (Kawai and Akira, 2006b).

1.3.2.6 IRFs and induction of IFN

Activation of IRFs occurs downstream of several PRRs, including the TLRs and RLRs discussed above. IRFs regulate type I IFN production as well as the expression of several other genes (O'Neill, 2006). In particular, IRF3 and IRF7 were found to be crucial for the induction of type I IFNs following viral infection (Takaoka and Yanai, 2006). TLR3 and TLR4 activate a TRIF-dependent pathway leading to the induction of type I IFN, especially IFNß (Kawai and Akira, 2006b). In addition, TRAM associates with TRIF to mediate signalling from TLR4 to type I IFN induction (Akira *et al.*, 2006). Following TLR

activation, IRFs are activated by the noncanonical IKKs, TRAF TBK1 and IKKε (Fitzgerald *et al.*, 2003; Hemmi *et al.*, 2004).

a) IRF3

As mentioned above, both TLR3 and TLR4 signal through TRIF to activate IRF3 (Doyle *et al.*, 2002). While TLR3 interacts directly with TRIF, TLR4 must first bind to TRAM, which then recruits TRIF to the cytoplasmic domain of IRF3 (Fitzgerald *et al.*, 2003). In addition, TLR4 but not TLR3 requires the p65 subunit of NF-κB for activation of IRF3 and the subsequent IRF3-dependent IFN-sensitive response element (ISRE) (Wietek *et al.*, 2003). Following stimulation of TLR3 and TLR4, IRF3 is phosphorylated, leading to its dimerisation and interaction with the histone acetyltransferase nuclear proteins CBP and p300 (Servant *et al.*, 2002). The IRF3-CBP-p300 complex then translocates to the nucleus, where it regulates expression of IFNß (Jefferies and Fitzgerald, 2005). IRF3 is phosphorylated by either IKKε or TBK-1 (Jefferies and Fitzgerald, 2005). TBK-1-deficient embryonic fibroblasts were impaired in their ability to activate IRF3 or to induce IRF3-dependent genes (Jefferies and Fitzgerald, 2005). The ability of TBK1-deficient fibroblasts to phosphorylate IRF3 was restored by the exogenous addition of IKKε, suggesting that TBK-1 and IRF3 are functionally redundant when expressed in the same cell (Jefferies and Fitzgerald, 2005). TBK-1 has been found to be expressed in most cell types, while IKKε is limited to lymphoid cells (Jefferies and Fitzgerald, 2005). Recently, a role for the DEAD box helicase, DDX3, in the activation of IRF3 and IRF7 (below) was described (Schröder *et al.*, 2008).

b) IRF5

Activation of IRF5 occurs in response to a select group of viruses and is not induced by dsRNA or poly (I:C) stimulation (Jefferies and Fitzgerald, 2005). IRF5 is activated by several TLRs and is downstream of MyD88 (O'Neill, 2006). In contrast to the induction

of IRF3 and IRF7 (see below), the activation of IRF5 uses the MyD88-IRAK1-TRAF6 pathway (Takaoka *et al.*, 2005). Stimulation of $IRF5^{-/-}$ pDCs and macrophages with the TLR9 ligand CpG impaired expression of the proinflammatory cytokines IL-6, IL-12 and TNF-α (Takaoka *et al.*, 2005). In addition, the production of IL-6, IL-12 and TNF-α in response to other TLR ligands, including LPS, poly(I:C) and flagellin, was impaired in cells from *Irf5*$^{-/-}$ mice (Takaoka *et al.*, 2005). Thus IRF5 may have a broad role in TLR-induced proinflammatory cytokine expression.

c) IRF7

As with IRF3, IRF7 activation leads to induction of type I IFNs (O'Neill, 2006). However, IRF7 induction leads to a systemic antiviral type I IFN response and increased serum levels of IFNα and IFNß (Jefferies and Fitzgerald, 2005). IRF3 and IRF7 likely form a heterodimer to bind to and activate the IFNß enhanceosome (Jefferies and Fitzgerald, 2005). By a positive feedback mechanism, the production of type I IFNs leads to an increase in the expression of IRF7 and a consequent amplification of the type I IFN produced (Takaoka and Yanai, 2006). It has been shown that IRF7 is an important regulator of IFN-α induction following stimulation of TLR7, TLR8 and TLR9 (Kawai *et al.*, 2004). IRF7 interacts with IRAK-1 and IRAK-4 (O'Neill, 2006). IFN-α production in response to TLR7 and TLR9 is completely impaired in IRAK-1-deficient mice (Gottipati *et al.*, 2008). In addition, the activation of IRF7 in response to TLR7 stimulation depends upon the NF-κB-inducing kinase (NIK) catalysed phosphorylation of IKKα (Wang *et al.*, 2008). Like IRF5, IRF7 interacts with MyD88 and TRAF6 (Kawai *et al.*, 2004; Honda *et al.*, 2004). In addition, TRAF6-dependent ubiquitination is required for IRF7 activation (Kawai *et al.*, 2004).

d) IFN and IFN-stimulated genes (ISGs)

The IRFs bind to the promoter elements of type I IFN genes and thereby induce IFN expression. The IFNs are secreted by the infected cell and act in both an autocrine and a paracrine manner to induce an antiviral state (Randall and Goodbourn, 2008). In addition, there is a constitutive level of type I IFN that primes cells for an antiviral response (Takaoka and Yanai, 2006). All type I IFNs signal by binding to the IFN receptor (IFNAR), which is composed of two parts (IFNAR1 and IFNAR2) (Takaoka and Yanai, 2006). There are also two other classes of IFNs that are involved in other processes than antiviral innate immunity. IFN stimulation upregulates two enzymes for dealing with dsRNA: 2'-5'-oligoadenylate synthetase (OAS) and protein kinase R (PKR) (Langland and Jacobs, 2002). The upregulation of OAS leads to the activation of RNaseL, which cleaves cytosolic mRNA and rRNA (Langland and Jacobs, 2002). Activated PKR phosphorylates and inactivates eukaryotic initiation factor 2α (eIF2α), thereby inhibiting translation (Mogensen and Paludan, 2005). The result of both of these pathways is the inhibition of protein synthesis, a strategy that prevents the cellular translation machinery from being hijacked by viruses. In addition, PKR can activate innate immune signalling pathways, leading to the induction of cytokine expression (Mogensen and Paludan, 2005). PKR interacts with TRAF6 and MKK6 (a MAP kinase kinase) to activate NF-κB and p38 MAP kinase, respectively (Mogensen and Paludan, 2005). Intriguingly, PKR is activated downstream of some TLRs and associates with Mal (Jiang *et al.*, 2003a; Horng *et al.*, 2001). Thus, there may be cross-talk between the TLRs and the IFN-induced effector enzymes.

1.3.3 TLRs and viral immune evasion

Similar to the RLRs, viruses have strategies to evade detection by TLRs and to inhibit TLR-induced signalling pathways. The study of signalling pathways downstream of IL-1R/TLRs has been advanced by the use of knockout mice lacking various components of

the pathways. While informative, these studies may not reflect IL-1R/TLR usage in human biology. The relevance of TLRs in viral infection and, in particular, in the context of human immune system function will be discussed herein.

It is now widely accepted that TLRs have a role in antiviral innate immunity. The evidence that this was the case was three-fold: (1) TLRs recognise viral PAMPs, (2) TLR signalling leads to the induction of the IFN response and thus the production of an antiviral state, and (3) there are viral strategies for evading or subverting TLRs (Bowie and Haga, 2005). There are several viral products that have been shown to serve as ligands for TLRs (Table 1.1). As for bacteria, the viral motifs that interact with TLRs are essential for the viability of the virus and thus are not subject to mutation (Rassa and Ross, 2003). While sequences of viral nucleic acids can mutate, the non-sequence-dependent chemical features of the nucleic acids are unchangeable and thus can serve as PAMPs (Thompson and Iwasaki, 2008). This hypothesis is supported by the recent discovery that the phosphodiester 2' deoxyribose of DNA can trigger TLR9 independently of the nitrogenous base sequence (Haas *et al.*, 2008). This implies that the viral motifs recognised by TLRs are conserved because they are immutable chemical features rather than specific nucleotide or amino acid sequences.

The response of TLRs to viral infections is expected to protect the host against viral infection. As discussed above, the sensing of viral PAMPs by TLRs triggers antiviral signalling pathways. For example, loss-of-function mutations in TLR3 result in severe viral infections with influenza and HSV-1 (Thompson and Iwasaki, 2008). Naturally-occurring polymorphisms in TLR2 affect the severity of HSV-2 infections (Thompson and Iwasaki, 2008). However, TLR-induced proinflammatory cytokines can lead to problems by exacerbating or prolonging inflammation. In bacterial infections, septic shock can result from excessive LPS-induced TLR4 stimulation without the normal feedback

mechanism to produce endotoxin tolerance via recruitment of IRAK-M (Kobayashi *et al.*, 2002). A similar situation of prolonged TLR activation and production of proinflammatory cytokines is possible following viral infection, resulting in inflammation that is deleterious to the host but advantageous to the virus (Thompson and Iwasaki, 2008), such as in the case of HIV-1 infection (see below).

The prolonged activation of TLRs has been found to benefit HIV-1 replication. The progression from HIV-1 infection to the development of AIDS is, in part, characterised by the occurrence of opportunistic infections with other pathogens (Equils *et al.*, 2003). The innate immune response to the other infections can create a milieu that favours HIV-1 replication. For example, the activation of NF-κB can trigger HIV-1 replication since the binding of NF-κB and the HIV *trans*-activator (Tat) to the viral long-terminal repeats (LTRs) activates transcription of viral genes (Equils *et al.*, 2003). LPS-induced activation of TLR4-induced NF-κB activation resulted in activation of the HIV-LTRs (Equils *et al.*, 2001). Opportunistic infections in HIV-positive patients resulted in activation of TLR2 and TLR9, which then enhanced HIV-1 replication (Equils *et al.*, 2003). Furthermore, co-stimulation with a combination of TLR4 and either TLR2 or TLR9 ligands resulted in an additive increase in HIV-1 replication, possibly mimicking the effect of numerous opportunistic infections *in vivo* (Equils *et al.*, 2003). However, it has been reported that some opportunistic infections could repress HIV-1 replication, likely due to the production of type I IFNs (Simard *et al.*, 2008).

TLR adaptors and effector enzymes in human disease

The importance of the TIR adaptor protein MyD88 in the response to infections has recently been analysed in children with naturally-occurring mutations in MyD88 that abrogated expression of the adaptor (von Bernuth *et al.*, 2008). The affected children showed increased susceptibility to pyogenic bacterial infections early in life (von

Bernuth *et al.*, 2008). Otherwise, the children showed normal immune responses to other pathogens, including viruses (von Bernuth *et al.*, 2008). Thus the role of MyD88 may be less important later in life, potentially due to compensation by the adaptive immune system (von Bernuth *et al.*, 2008).

Mutations that disrupt TIR adaptor binding to TLRs can reduce susceptibility to infection. In another TIR adaptor, Mal/TIRAP, a single nucleotide polymorphism (S180L) renders heterozygotes resistant to bacterial infections (tuberculosis and pneumococcal pneumonia) and malaria (Khor *et al.*, 2007). The binding of S180L Mal/TIRAP to TLR2 is impaired, thereby dampening the inflammatory response to the aforementioned pathogens (Khor *et al.*, 2007).

In contrast to the above, mutations in IRAK4 such as Q293X resulted in increased susceptibility to bacterial infections (Medvedev *et al.*, 2005; Davidson *et al.*, 2006). Interestingly, the Q293X mutation in IRAK4 abrogates MAP kinase signalling but only partially inactivates NF-κB signalling (Davidson *et al.*, 2006). Another patient suffering from recurrent bacterial infections was found to have mutations in the IRAK4 gene that resulted in protein with a truncated kinase domain (Medvedev *et al.*, 2005). IL-1R signalling was defective in these patients, since IRAK4 recruitment to the IL-1R was reduced (Medvedev *et al.*, 2005). In addition, truncated IRAK4 interacted with MyD88 constitutively rather than in an IL-1-inducible manner (Medvedev *et al.*, 2005).

Given the crucial role of TRAFs in signalling pathways, it is not surprising to discover that they are targeted by viral immune evasion or subversion strategies. The best characterised example of viral targeting of TRAFs is the Epstein-Barr virus (EBV) latent membrane protein 1 (LMP1). LMP1 has a role in suppressing viral replication by negatively regulating the activity of the viral DNA replication origin, *oriP*, in order to

maintain latent EBV infection (Shirakata *et al.*, 2001). It was found that the TRAF binding site of LMP1 was essential for its role in suppressing *oriP* (Shirakata *et al.*, 2001). This site binds to TRAF1 and TRAF3 with high affinity and to TRAF2 and TRAF5 with lower affinity (Luftig *et al.*, 2003). LMP1 induces activation of NF-κB, as well as MAP kinases (p38, JKN and ERK) and Janus kinase 3 (Shirakata *et al.*, 2001). Activation of NF-κB by LMP1 is crucial for the survival of B lymphocytes infected with EBV (Luftig *et al.*, 2003). TRAF6 was also found to be needed for LMP1-induced NF-κB activation but interacted with LMP1 at a distinct site to the other TRAFs (Luftig *et al.*, 2001). Moreover, TRAF6 recruitment to LMP1 is a TRAF2- and TRADD-dependent (Schultheiss *et al.*, 2001) and is mediated by another adaptor protein, BS69 (Wan *et al.*, 2006). The interaction between the TRAFs and LMP1 is required to suppress viral replication and to prolong the survival of virally-infected B cells.

Moreover, different viruses have been found to activate NF-κB via targeting TRAF6, including HSV (Liu *et al.*, 2008), human cytomegalovirus (Poole *et al.*, 2006), *herpesvirus ateles* (Heinemann *et al.*, 2006) and *herpesvirus saimiri* (Garcia *et al.*, 2007; Jeong *et al.*, 2007). Several of the herpes viruses activate NF-κB via TRAF6 in order to promote transformation and oncogenesis (Garcia *et al.*, 2007; Jeong *et al.*, 2007; Heinemann *et al.*, 2006), suggesting that TRAF6-mediated induction of NF-κB might be an anti-apoptotic pathway.

There are several poxviral proteins that target NF-κB, either preventing its activation by IL-1R/TLR signalling or by inhibiting the activation of NF-κB-dependent genes (Johnston and McFadden, 2005). For example, VACV protein K1 inhibits NF-κB activation likely by preventing the degradation of IκBα (Shisler and Jin, 2004). In addition, M2 inhibits NF-κB activation by preventing phosphorylation of ERK2 and blocks nuclear translocation of NF-κB (Gedey *et al.*, 2006).

The VACV protein A46 was identified as having a putative TIR domain and A52 was found by a BLAST search with the A46 sequence (Bowie *et al.*, 2000). A52 and A46 were initially described as potential antagonists of IL-1R/TLR signalling (Bowie *et al.*, 2000). A46 inhibited IL-1-stimulated NF-κB activation (Bowie *et al.*, 2000). It also inhibited multiple TLRs by sequestering the adaptor molecules (Stack *et al.*, 2005). A52 was initially found to inhibit IL-1, TLR4 and IL-18 signalling (Bowie *et al.*, 2000). It was a more potent inhibitor of NF-κB activated by IL-1R/TLRs than A46 (Stack *et al.*, 2005). Both A46 and A52 failed to inhibit TNF-induced NF-κB activation, indicating that their effects are specific for TIR-dependent signalling (Bowie *et al.*, 2000).

1.4 Poxviruses

The family *Poxviridae* is composed of enveloped DNA viruses that replicate within the cytoplasm of infected cells (Moss, 2006). Poxviruses are widely-known due to the once prevalent and lethal disease, smallpox. Smallpox is caused by infection with variola major virus (the more virulent form) or variola minor virus (see Figure 1.8A; Smith and McFadden, 2002). Mature variola virus has a distinctive brick-shape (Figure 1.8B) and replicating virus can be observed within the cytoplasm of infected cells (Figure 1.8C). Smallpox originally emerged in Asia and was brought to Europe by returning Crusaders (Smith and McFadden, 2002). From that time until the late twentieth century, smallpox was a widespread disease with a high mortality rate among infected individuals (Smith and McFadden, 2002). Smallpox was officially eradicated from the world in 1977 in the WHO Global Smallpox Eradication Program. Declared stocks of Variola virus are held in two laboratories, Centres for Disease Control, Atlanta, U.S.A. and Novosibirsk, Russia (Smith and McFadden, 2002). The variola stocks were to be destroyed following eradication but this did not occur and there has been debate over whether they should be destroyed or not, particularly in light of the risk of variola major virus being used as a bioterrorism agent (Mahy, 2003; Mayr, 2003). In addition, there are concerns that

there may be undeclared stocks of the variola virus and that these could be used to develop biological weapons against which the global population now has little or no protection (Smith and McFadden, 2002; Mahy, 2003). In the absence of global vaccination of the population, there is a risk that variola infection would not be detected until after smallpox develops and there are no effective antivirals to treat the illness at this stage (Mahy, 2003). In addition, variola major could be engineered to make it a more potent bioterrorism agent (Mayr, 2003). For example, it has been found that recombinant poxviruses expressing cytokines, such as IL-4, are more potent pathogens based on their inhibition of host immune responses and thus could be effective bioterrorism agents (Kerr *et al.*, 2004; Jackson *et al.*, 2001). Since the respiratory tract is a key route of entry for poxviruses, it is not surprising to find that alveolar macrophages can limit poxviral replication (Rivera *et al.*, 2007). Understanding the local immune responses of respiratory epithelial cells and macrophages could help to develop effective anti-poxviral treatments (Rivera *et al.*, 2007). The mechanisms by which poxviruses counteract the innate immune response are diverse and understanding them might provide useful targets for treatment in the case of infection.

The virus used in the vaccination campaign against smallpox was Vaccinia virus (VACV), an orthopoxvirus closely related to variola (Smith and McFadden, 2002). VACV is the prototype poxvirus and it has been studied extensively. In the following discussion of poxviruses, the genes described are from VACV strain Western Reserve (WR) unless otherwise stated.

1.4.1 Poxviral structure

Poxviruses are large, DNA-containing viruses with a complex particle structure. Recently, a study using deep-etch electron microscopy clarified the structure of the viral particle of VACV (Heuser, 2005). The mature virion (MV) of VACV consists of a

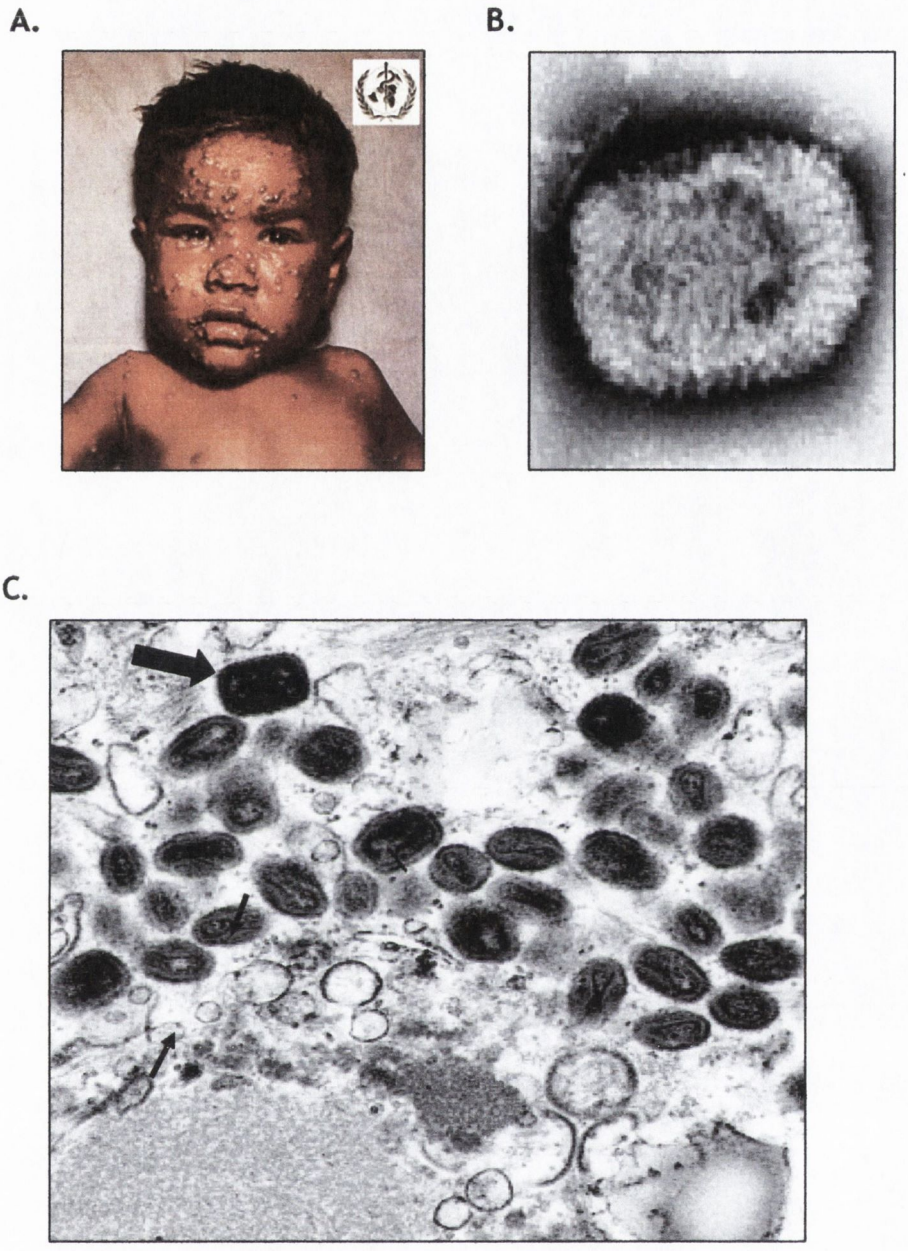

Figure 1.8 Variola virus is the causative agent of smallpox.

A. Smallpox lesions on the face of a child due to infection with Variola virus (World Health Organisation, www.WHO.int). B. Electron micrograph of an isolated Variola virus virion detected by negative stain electron microscopy. It is from a skin lesion taken during the WHO Global Smallpox Eradication Program (www.phene.cpmc.columbia.edu/Images/Murphy/smallpoxns.htm).

C. Electron micrograph of Variola virus replicating within chick embryo cells. There are brick-shaped mature virions (block arrow) as well as immature forms (line arrows) (www.phene.cpmc.columbia.edu /Images/Murphy/smallpox.htm).

DNA-containing core particle surrounded by a single membrane (Heuser, 2005). Surrounding the core is a palisade layer and there are two lateral bodies between the palisade layer and the viral membrane (Heuser, 2005).

Within the core particle is the linear double-stranded DNA genome. The termini of the DNA form covalently-closed hairpin loops (Johnston and McFadden, 2005). The genome of poxviruses ranges in size from 130kbp to 300kbp and encodes up to 260 open reading frames (Johnston and McFadden, 2005; Broyles, 2003). At the termini are flanking terminal inverted repeat regions (Johnston and McFadden, 2005). Genes that are centrally located within the genome are conserved and are essential for replication and virion assembly (Johnston and McFadden, 2005).

1.4.2 Summary of the poxvirus life cycle

The VACV infection and replication cycle has been well-characterised. Both the MV and the extracellular enveloped virus (EEV) are infectious (McFadden, 2005). Following fusion of the MV or EEV to the cell, the core particle is released into the cytoplasm and early gene transcription and protein synthesis can proceed (Schramm and Krijnse Locker, 2005). The core structure is then dissolved by an unknown mechanism, releasing the DNA genome into the cytoplasm (McFadden, 2005). Following core uncoating, the DNA genome is replicated and intermediate and late genes are transcribed (Schramm and Krijnse Locker, 2005). Virion assembly occurs, beginning with the formation of crescent-shaped membranes that form immature virions (IVs) in the perinuclear region where viral DNA has accumulated (Schramm and Krijnse Locker, 2005). The DNA is then packaged into the IVs, leading to the production of the brick-shaped MVs (Schramm and Krijnse Locker, 2005). The MV is wrapped by membranes derived from the *trans*-Golgi network (TGN), referred to as intracellular enveloped virion or the wrapped virion (WV; Moss, 2006). The WV is transported to the plasma

membrane by the polymerisation of actin on one side of the virion (Smith and Law, 2004). The WV fuses with the plasma membrane and is released in the form of the MV (Moss, 2006). If the wrapped MV (WV) is released from the cell by lysis, the WV is then known as the EEV (Moss, 2006). This brief outline of VACV replication belies the complexity of the system; a few of the steps in the cycle are described in more detail below.

1.4.3 Poxvirus virion and viral entry into host cells

Poxvirus entry into host cells has been studied for many years but the viral fusion proteins have only recently been described (reviewed in Moss, 2006). The host cell surface receptor used by the virus is still unknown (Moss, 2006). As described above, there are two infectious forms of VACV, the MV and the EEV, both of which have the same DNA-protein core but EEV has an additional membrane compared to MV (Schramm and Krijnse Locker, 2005). In order for virus-cell fusion to proceed, the wrapping membrane of the EEV must be disrupted in order to expose the MV membrane containing the fusion protein(s) (Moss, 2006). Lipid rafts might be required for entry of MVs since this was blocked by depletion of cholesterol from the plasma membrane (Moss, 2006). Attachment of the MV, but not the EEV, particles induces cell signalling events (Moss, 2006).

The mechanism of entry of the MV particle has been studied extensively. The MV membrane contains numerous non-glycosylated proteins that form an entry/fusion complex (EFC) (Moss, 2006). It has been shown that the MV enters the cell by fusion of its single lipid membrane with the plasma membrane and release of the core into the cytoplasm (Carter *et al.*, 2005). Recently, another MV membrane protein, L1, was found to associate with the EFC and to be required for fusion of the MV to the plasma membrane (Bisht *et al.*, 2008). Fusion of MV to the cell membrane can occur at neutral

pH but is enhanced by low pH and thus likely occurs in the endosome following acidification (Townsley *et al.*, 2006).

1.4.4 Transcription and replication

Following virus-cell fusion, the viral core particle is delivered intact into the cytoplasm (Broyles, 2003). The interior of the viral core remains a mystery, though it is known to contain all of the components required for early gene transcription (Broyles, 2003). Replication occurs in viral factories that are enclosed by ER membranes (Schramm and Krijnse Locker, 2005). VACV replication requires phosphorylation of the cellular MAP kinase, extracellular signal-regulated kinase 1/2 (ERK1/2), and replication of VACV can be blocked by the treatment of cells with an agent (aurintricarboxylic acid) that specifically inhibits ERK phosphorylation (Myskiw *et al.*, 2007).

Genome replication and virion assembly are regulated temporally and at the level of transcription initiation, with a cascade of genes being transcribed at early, intermediate or late stages (Broyles, 2003). For example, proteins required for intermediate gene transcription are translated during the early stage (Broyles, 2003). Early gene transcription occurs within the core particle, which remains intact throughout the early phase of transcription (Broyles, 2003). The core contains all of the enzymes and other proteins required to synthesise mature mRNA (Broyles, 2003). In fact, it has been hypothesized that the early transcription machinery assembles onto early promoters during morphogenesis and virion assembly (Broyles, 2003).

The transition from early to intermediate transcription requires uncoating of the viral core, followed by release of the genomic DNA (Schramm and Krijnse Locker, 2005). If DNA replication is blocked, the virus does not progress from early to intermediate transcription (Broyles, 2003). The proteins required for intermediate gene transcription

are mostly virus-encoded and are translated during the early phase (Broyles, 2003). The replication of VACV DNA, as well as intermediate and late transcription, occurs in viral factories (Schramm and Krijnse Locker, 2005). Late genes encode proteins required for virion assembly (Schramm and Krijnse Locker, 2005). Virion assembly occurs when the nascent DNA is taken up by the immature virions (Schramm and Krijnse Locker, 2005). The immature virions gain infectivity following condensation of the core and proteolytic cleavage of several capsids proteins (Smith and Law, 2004). The resulting mature virions consist of the viral core surrounded by the palisade layer and a single membrane, as described above (Heuser, 2005).

1.4.5 Poxviral exit and cell-to-cell spread

The WV, but not the MV, are transported to the cell surface on microtubules in a process requiring a kinesin-associated motor (Smith and Law, 2004). Once the WV reaches the plasma membrane, it fuses with the membrane to produce a cell-associated enveloped virus (CEV) on the cell surface by exocytosis (Smith and Law, 2004). The CEV can either be released as MV or remain attached to the cell (Smith and Law, 2004). If the CEV remains attached to the cell, it is pushed towards neighbouring cells by polymerisation of an actin tail within the plasma membrane beneath the CEV (Smith and Law, 2004). The actin tail enables efficient cell-to-cell spread of the virus and thus CEV remains associated with the cell in order to promote polymerisation of the actin tail (Smith and Law, 2004).

In addition to cell-to-cell spread by the MV or the CEV, there are two other ways that VACV can spread to neighbouring cells. Lysis of the cell releases the WV, which can then infect adjacent cells (Smith and Law, 2004). Cell-to-cell fusion and even syncytium formation has been observed with mutant poxviruses (Smith and Law, 2004). Syncytium formation occurs late in infection and depends on extracellular CEV particles

that express all of the viral entry and fusion proteins (Bisht *et al.*, 2008). Syncytium formation is not considered to be a common mechanism of poxvirus transmission (Smith and Law, 2004).

1.4.6 Poxvirus detection by PRRs

Infection with poxviruses is now known to activate different TLRs. A protective role for TLR4 in innate immunity to respiratory VACV infection has recently been demonstrated (Hutchens *et al.*, 2008). Interestingly, the production of the antimicrobial peptide, LL-37, in cultured keratinocytes is induced through activation of TLR3 in response to VACV infection of keratinocytes (Howell *et al.*, 2006). TLR3-deficient mice produce significantly less of the murine LL-37 homologue than wild-type mice, as do patients who develop atopic dermatitis following vaccination with VACV (Howell *et al.*, 2006). Another study found that the response to VACV depended upon TLR2 (Zhu *et al.*, 2007). In mice, infection with ectromelia virus was lethal in the absence of TLR9 (Samuelsson *et al.*, 2008). In addition, innate immunity to VACV has also been found to require TLR-independent induction of type I IFN (Zhu *et al.*, 2007). A TLR-independent pathway to IFN induction involves the RLRs, which signal via IPS-1. Recently, infection with VACE lacking the E3 protein (see below) was found to activation an IPS-1-dependent innate immune response (Deng *et al.*, 2008). Thus, it is evident that poxviruses have a need for tactics to evade detection by PRRs since the processed of infection and replication elicit an innate immune response.

1.4.7 Poxviral innate immune evasion strategy

In order to replicate efficiently within cells, poxviruses need to suppress or evade the host cell immune response. Poxviral genomes encode numerous immunomodulatory proteins that are directed at a broad range of host cell proteins (Johnston and McFadden, 2005). A number of these proteins are homologues of mammalian proteins

that are involved in the immune response, such as IFN-γ, complement regulators and cytokine receptors (Jackson *et al.*, 2005). There are three main strategies employed by viruses to evade the immune system: virostealth proteins, virotransducers and viromimetics (Johnston and McFadden, 2005). While the adaptive immune response is also inhibited by VACV, only innate immune evasion will be discussed here.

1.4.7.1 Virostealth

This method of immune evasion consists in masking the hallmarks of infection from immune surveillance (Johnston and McFadden, 2005). One important antiviral strategy in mammals is the complement-mediated lysis of infected cells. VACV encodes a complement control protein (VCP) that is secreted from and binds to the surfaces of infected cells (Girgis *et al.*, 2008). The expression of another VACV protein (A56) is required for VCP to bind to the cell surface since A56 is a transmembrane protein localised to the plasma membrane (Girgis *et al.*, 2008). VCP bound to A56 on the extracellular surface of infected cells protects the cells from complement-mediated lysis (Girgis *et al.*, 2008). Thus the VCP-A56 complex masks the fact that the cell is infected from immune surveillance.

1.4.7.2 Virotransduction

In virotransduction, the virus interrupts the transmission of signals that indicate that the cell is infected. There are a number of strategies employed, including inhibition of apoptosis, modulation of caspase activity and modulation of the IFN response (Johnston and McFadden, 2005). VACV infection can trigger apoptosis following viral entry and it is thus not surprising that VACV expresses numerous proteins to counteract apoptosis induction by distinct pathways (Taylor and Barry, 2006). For example, the VACV F1 protein localises to the mitochondria and inhibits the pro-apoptotic protein, Bak (Taylor and Barry, 2006). In addition, a new human anti-apoptotic protein, Golgi anti-apoptotic

protein or h-GAAP, was discovered and found to have a homologue in the VACV v-GAAP protein (Gubser *et al.*, 2007). The v-GAAP rescued cells from apoptosis following depletion of h-GAAP, suggesting that the two proteins have the same function (Gubser *et al.*, 2007). The expression of v-GAAP by VACV likely blocks apoptosis induced by viral infection and thus contributes to virulence (Gubser *et al.*, 2007). Finally, structural studies of the VACV protein N1 revealed a Bcl-2-like fold and a surface groove similar to that of the anti-apoptotic Bcl-2 family member, Bcl-x_L (Cooray *et al.*, 2007). N1 interacted with the pro-apoptotic proteins Bid, Bad and Bax via the surface groove and thereby inhibited staurosporine-induced apoptosis (Cooray *et al.*, 2007). Thus, N1 may function as an anti-apoptotic survival factor, allowing infected cells to survive and viral progeny to be produced.

In addition to inhibition of apoptosis, VACV expresses proteins to inhibit other antiviral signalling pathways. The VACV *E3L* gene encodes two gene products (p20 and p25), both of which have a dsRNA-binding motif (Langland and Jacobs, 2002; Garcia *et al.*, 2002). By sequestering dsRNA, E3 prevents activation of either PKR or OAS (Langland and Jacobs, 2002). In addition to sequestering dsRNA, E3 can also bind PKR directly and inhibit its activity (Johnston and McFadden, 2005). In addition, the binding of dsRNA by E3 is postulated to downregulate host gene expression, thereby preventing expression of cellular antiviral genes (Langland *et al.*, 2006). Intriguingly, E3 also inhibits dsRNA-induced apoptosis (Taylor and Barry, 2006) but this might permit cellular transformation and thus E3 might be oncogenic (Garcia *et al.*, 2002).

1.4.7.3 Viromimetics: virokines and viroceptors

Poxviruses are known to encode a number of mimics of host cytokines and cytokine receptors. Viroceptors are viral proteins that are related to cellular receptors (Johnston and McFadden, 2005). They function by competitively inhibiting ligand

binding to the cell receptors, thereby preventing the antiviral or inflammatory signalling pathways (Johnston and McFadden, 2005). For example, TNF-induced apoptosis following poxviral infection is inhibited by the secretion of soluble TNF receptor homologues that inhibit TNF binding to cell surface receptors (Taylor and Barry, 2006). Virokines are secreted and mimic host molecules, including cytokines, complement regulators and their inhibitors (Johnston and McFadden, 2005).

IFN is a crucial cytokine that induces antiviral signalling pathways (Seet *et al.*, 2003). The species barrier of at least one poxvirus (myxoma virus) is due to the induction of ERK-dependent type I IFN production in non-permissive cells types, showing that IFNs can specifically block poxvirus infection (Wang *et al.*, 2004). IFNγ limits poxviral infection and IFNγ$^{-/-}$ mice are more susceptible to VACV infection (reviewed in Seet *et al.*, 2003). It is not surprising then to find that all poxviruses encode a viral homologue of the IFNγ-receptor (IFNγ-R) to competitively antagonise IFNγ-induced signalling (Seet *et al.*, 2003). The *B8R* gene of VACV encodes a soluble IFNγ-R homologue that sequesters IFNγ of several species and thereby prevents it from binding to the cellular receptor (Symons *et al.*, 2002).

One of the cytokines mimicked by viruses is Il-10. This cytokine has both immunosuppressive and immunostimulatory roles in many cell types (Seet *et al.*, 2003). Viral IL-10 homologues are encoded by several poxviruses, with the ORFV-IL10 protein from Orf virus being the best characterized (Seet *et al.*, 2003). ORFV-IL-10 was found to suppress macrophage activation and IFNγ expression, thereby mimicking the immunosuppressive effects of Il-10 (Johnston and McFadden, 2005). Another poxvirus gene, *Y134R*, has been found to encode a protein with similarities to members of the IL-10-related cytokine family, namely IL-19, IL-20 and IL-24 (Bartlett *et al.*, 2004). Secreted Y134 bound to class II cytokine receptors and activated STAT1 and STAT3

(Bartlett *et al.*, 2004). Interestingly, a recombinant Vaccinia virus with the *Y134R* gene was tested in an intranasal mouse model and found to attenuate VACV infection (Bartlett *et al.*, 2004). It was hypothesised that Y134 has immunostimulatory activity and thus induces a potent antiviral response (Bartlett *et al.*, 2004).

1.4.7.4 Ubiquitin ligases

Several viruses have been described that encode E3 ubiquitin ligases in order to evade the host immune system, likely by inducing degradation or downregulation of crucial immune system proteins (Liu, 2004). Several poxviruses (excluding VACV strains Copenhagen and WR) encode a RING protein, p28, which is an E3 ubiquitin ligase (Nerenberg *et al.*, 2005). In the presence of p28, viral factories were enriched for ubiquitin, likely due to both the auto-ubiquitination of p28 and the ligation of ubiquitin to as yet unknown substrates (Nerenberg *et al.*, 2005). The function of p28 is not entirely clear, though it has been linked to inhibition of apoptosis and to virulence (Taylor and Barry, 2006). In addition, myxoma virus encodes another ubiquitin ligase, M153, which targets immune receptors for degradation (Nerenberg *et al.*, 2005). Thus, modulation of the ubiquitination system by poxviruses could be a general mechanism used to enhance virulence, evade the immune response and inhibit apoptosis (Nerenberg *et al.*, 2005).

1.4.8 A52

A52 was initially identified as an antagonist of IL-1R/TLR signalling since it inhibited IL1, TLR4 and IL-18 signalling (Bowie *et al.*, 2000). A52 was subsequently found to inhibit NF-κB activation by multiple TLRs (Harte *et al.*, 2003). It was found to interact with IRAK2 and TRAF6, downstream effectors in TLR signalling, and not with TIR domain-containing adaptor proteins Mal and MyD88 (Harte *et al.*, 2003). A52 interacted

specifically with the TRAF domain of TRAF6 (Harte *et al.*, 2003). In addition, A52 disrupted IRAK2/Mal interactions and IRAK2-mediated signalling (Harte *et al.*, 2003).

While it inhibits NF-κB activation, A52 potentiates IL-1-induced p38 MAP kinase activation (Maloney *et al.*, 2005). Furthermore, it is able to drive p38 MAP kinase and JNK activation in unstimulated cells (Maloney *et al.*, 2005). The ability to drive p38 and JNK was found to be TRAF6-dependent (Maloney *et al.*, 2005). As discussed above, A52 interacts with the TRAF domain of TRAF6 (Harte *et al.*. 2003). A C-terminal deletion of A52 (ΔA52) interacts with IRAK2 but no longer binds to TRAF6 yet still inhibits NF-κB (Maloney *et al.*, 2005). The ΔA52 construct could no longer drive p38 or JNK activation, implicating the A52-TRAF6 interaction in the ability of full-length A52 to drive MAP kinases (Maloney *et al.*, 2005).

A52 also enhanced the TLR-induced, p38-dependent gene IL-10 in a TRAF6-dependent manner (Maloney *et al.*, 2005). It had been found that LPS-induced IL-10 production was p38-dependent (Ma *et al.*, 2001). Since A52 was found to activate p38, it was possible that it would also affect induction of the p38-dependent gene IL-10 (Maloney *et al.*, 2005). A52 was able to induce the IL-10 promoter in a dose-dependent manner in normal cells but not in $TRAF6^{-/-}$ MEFs (Maloney *et al.*, 2005). This suggested that A52 induction of the IL-10 promoter was TRAF6-dependent and, moreover, that the A52-TRAF6 interaction was crucial for A52-enhanced LPS-induced IL-10 expression (Maloney *et al.*, 2005).

1.5 Aims

In this study, the interaction between TRAF6 and the VACV protein A52 will be investigated. Previous work showed that A52 interacted with over-expressed TRAF6. The potential interaction between A52 and the other TRAFs will be tested. It has been

found that the C-terminal region of A52 is required for interaction with TRAF6. In order to further map the interaction, potential sites within A52 which may interact with TRAF6 will be tested by mutagenesis. The mechanism by which A52 activates p38 will be examined. Since the activation of p38 by A52 is TRAF6-dependent, elucidating the mechanism of activation will involve a further study of the effects of A52 on TRAF6 functions. In particular, the effect, if any, of A52 on TRAF6 ubiquitination or the role of TRAF6 as an E3 ubiquitin ligase will be investigated. The TRAF6-mediated activation of MAPK involves recruitment to the TAB1/TAB2/TAK1 complex and the effect, if any, of A52 on this signalling complex will be examined.

Chapter Two: Materials and Methods

2.1 Materials

2.1.1 Reagents and Molecular Biology Kits

General laboratory chemicals were purchased from Sigma-Aldrich (Poole, U.K.). Protease inhibitor cocktail set III, containing 4-(2-Aminoethyl) benzenesulphonyl fluoride hydrochloride (AEBSF), aprotinin, bestatin, E64 protease inhibitor, leupeptin, and pepstatin, was obtained from Calbiochem (Novagen/Merck). Iodoacetamide, sodium orthovanadate, aprotinin solution, and phenylmethylsulphonyl fluoride (PMSF) were from Sigma-Aldrich. Agar, yeast extract and tryptone were purchased from Unitech Limited (Dublin, Ireland). LB broth and LB-agar mixes were obtained from Chromatrin (Dublin, Ireland). Isopropyl ß-D-1-thiogalactopyranoside (IPTG) and reduced glutathione were from Sigma-Aldrich. Glutathione sepharose 4B beads and thrombin protease were purchased from GE Healthcare (Amersham, U.K.). Protogel (30% (w/v) acrylamide and 0.8% (w/v) bis-acrylamide) from National Diagnostics was obtained from Biosciences (Dun Laoghaire, Ireland). Millipore Immobilon™-P polyvinylidene fluoride (PVDF) transfer membrane was purchased from Sigma-Aldrich. Enhanced chemiluminescence (ECL) Western blotting detection reagent was obtained from GE Healthcare (Amersham, U.K.). SuperSignal® West Pico chemiluminescent substrate was purchased from Pierce (Medical Supply Co., Dublin, Ireland). Homemade enhanced chemiluminescence (ECL) Western blotting detection reagent solution A was made from 250mM luminol and 90mM p-Coumaric acid, both dissolved in DMSO, diluted in 100mM Tris buffer pH8.5 (all chemicals from Sigma-Aldrich). Solution A was mixed with an equal volume of solution B, comprising 0.6mM H_2O_2 in a final concentration of 100mM Tris buffer pH8.5, immediately before use. Reblot western blot stripping reagent was purchased from Chemicon International (Hampshire, U.K.). All ELISA kits were purchased from R&D Systems.

Cell culture reagents, including Minimum Essential Medium (MEM), Dulbecco's MEM (DMEM), gentamicin, trypsin-EDTA and L-glutamine were obtained from Sigma-Aldrich. DMEM with added pyruvate and nonessential amino acids was obtained from Gibco (Biosciences). DMEM containing Glutamax was obtained from Gibco (Biosciences). Low-endotoxin foetal calf serum (FCS) was purchased from BioWest (Ringmer, East Sussex, U.K.). Cell culture plasticware was purchased from Corning (Schipol-Rijk, The Netherlands) or Greiner Bio-one (Cruinn Diagnostics Limited, Dublin, Ireland). GeneJuice™ transfection reagent was from Novagen (Merck Biosciences, Nottingham, United Kingdom). Passive lysis buffer was from Promega (Medical Supply Co.).

Lipofectamine 2000 transfection reagent was purchased from Invitrogen (Biosciences). Ultrapure lipopolysaccharide (LPS) was purchased from Alexis Biochemicals (Lausanne, Switzerland). Human rIL-1α and rIL-1β were obtained from the National Cancer Institute (Frederick, Washington, U.S.A.). The synthetic dsRNA analogue, polyinosinic:polycytidylic acid (poly (I:C)), was purchased from GE Healthcare.

The UltraMobius™ 1000 plasmid purification kit and the competent Escherichia coli strain NovaBlue™ Singles were obtained from Novagen (Merck Biosciences). BL21 and Rosetta-Gami2 competent cells for protein expression were also obtained from Novagen. The FastPlasmid miniprep kit was purchased from Eppendorf (Unitech Limited). The Quicklyse plasmid miniprep and PCR cleanup kits were purchased from Qiagen. The gel extraction kit was obtained from Eppendorf (Unitech Limited).

The ExSite™ PCR-based and Quikchange® Site-directed Mutagenesis kits were purchased from Stratagene (Technopath, Limerick, Ireland). *PfuTurbo*® DNA polymerase was also from Stratagene (Technopath). Restriction enzymes, 2-log DNA ladder (0.1-10.0kb), deoxynucleotide solution set and broad range pre-stained protein markers (6-175kDa)

were from New England Biolabs (ISIS, Wicklow, Ireland). KOD DNA polymerase was from Toyobo (Merck Biosciences). Clonables Ligation/Transformation kit was obtained from Novagen (Merck Biosciences). Quick DNA ligase and calf intestinal alkaline phosphatise were both from New England Biolabs (ISIS).

2.1.2 Antibodies

Polyclonal anti-A52 was raised to a GST-A52 fusion protein (described in Harte *et al.*, 2003). Anti-FLAG M2 antibody, anti-FLAG M2 conjugated agarose, monoclonal anti-ß-actin (clone AC-74) and anti-myc monoclonal antibody (clone 9E10) were all from Sigma-Aldrich. Polyclonal antibodies to the C-terminus of human TRAF2 (C-20; rabbit), the N-terminus of murine TRAF3 (M-20; rabbit), the N-terminal 274 residues of human TRAF6 (H-274; rabbit), full-length murine TAK1 (M-579; rabbit), a C-terminal peptide of human TAB2 (K-20; goat), and human ubiquitin (FL-76; rabbit) were obtained from Santa Cruz Biotechnology (California, U.S.A.). A mouse monoclonal antibody to full-length GFP (clone B-2) was obtained from Santa Cruz Biotechnology. A mouse monoclonal antibody to polyubiquitinated proteins (clone FK1) was purchased from Biomol® International (Exeter, U.K.). Antibody to phosphorylated IκBα (Ser32) was from Cell Signaling Technology (ISIS). A monoclonal antibody to IκBα was provided by R. Hay (University of Dundee, Scotland). Phospho-p38 MAP kinase (Thr^{180}/Tyr^{182}), total p38 MAP kinase, and total JNK polyclonal antibodies were purchased from Cell Signalling Technology (ISIS). A rabbit polyclonal antibody to phospho-JNK1 and 2 ($pTpY^{183/185}$) was from Biosource (Biosciences). A mouse monoclonal antibody to the HA peptide CYPYDVPDYASL (clone 16B12) was purchased from Covance (Cambridge Biosciences, U.K.). A rabbit polyclonal antibody to an IRAK2 peptide was made by Inbiolabs (Tallinn, Estonia). All HRP-conjugated secondary antibodies were purchased from Sigma-Aldrich.

2.1.3 Cells

The human embryonic kidney cell line 293 (HEK 293) and HEK293 cells stably transfected with the IL-1R1 (R1s) were provided by Tularik Inc (San Francisco, California, U.S.A.). HEK 293 cells with a mutation in IRAK1 (I1A) were obtained from Katherine Fitzgerald (University of Massachusetts Medical School, Worcester, Massachusetts, U.S.A). In addition, HEK 293 cells stably transfected with the large T antigen (HEK 293Ts) were obtained from European Collection of Animal Cell Cultures (ECACC; Salisbury, U.K.). The human hepatocarcinoma cell line HepG2 was obtained from the ECACC (Salisbury, U.K.). Wild-type and TRAF6$^{-/-}$ MEFs were a gift from Z.J. Chen (University of Texas Southwestern Medical Centre, Dallas, Texas, U.S.A.). Wild-type and IRAK2$^{-/-}$ MEFs were a gift from S. Akira (Osaka University, Japan). Monkey BS-C-1 and human TK^{-}143B osteosarcoma cells were from G.L. Smith (Imperial College London, London, U.K.)

2.1.4 DNA expression vectors

The FLAG-TRAF1-6 constructs in pRK5 expression vector were provided by Tularik, Inc. (San Francisco, California, U.S.A.). In each case, a FLAG epitope was fused to the full-length TRAF. The FLAG-TRAF was then cloned into the multiple cloning site of pRK5 using different combinations of restriction enzymes. The A52R construct was made by amplifying the VV open reading frame (ORF) of the Western Reserve strain by PCR amplification using primers that incorporated an *EcoR*I site upstream and a *Hind*III site downstream of the ORF (described in Bowie *et al.*, 2000). The *A52R* ORF, flanked by *EcoR*I and *Hind*III sites, was then ligated into the pRK5 expression vector. The myc-tagged and HA-tagged ubiquitin constructs were provided by A. Mansell (Monash University, Melbourne, Australia). Both myc-ubiquitin and HA-ubiquitin are under the control of the CMV immediate early promoter in the pMT123 vector (Treier *et al.*, 1994). CD4-TLR4 was provided by R. Medzhitov (Yale University, New Haven,

Connecticut, U.S.A.). TLR3 was obtained from D. Golenbock (University of Massachusetts Medical School, Worcester, Massachusetts, U.S.A). Full-length MyD88 with an N-terminal AU1 tag was cloned into pcDNA3 and was provided by M. Muzio (Muzio *et al.*, 1997). FLAG-TAK1 was from H. Sakurai (Tanabe Seiyaku Co., Osaka, Japan). The TAK1 (K63W) dominant negative construct was made by insertion in an expression vector under the control of the CMV promoter (Ninomiya-Tsuji *et al.*, 1999).

2.1.5 Reporter plasmids

The NF-κB-luciferase reporter plasmid was provided by R. Hofmeister (University of Regensburg, Germany). It consists of five κB elements and is inserted in the pGL3Basic vector (Promega). The phRL-TK vector has the herpes simplex virus thymidine kinase (HSV-TK) promoter upstream of the synthetic Renilla luciferase gene (hRluc; Promega). For the MAP kinase reporter assays, the transcription activators (c-Jun, CHOP, and Elk) were fused to the DNA-binding domain of Gal4, which was then inserted into the pFA-CMV plasmid. The trans-activator-Gal4 fusion plasmids (c-Jun-Gal4, CHOP-Gal4, and Elk-Gal4) were obtained from Stratagene (Technopath, Limerick, Ireland). The pFR-luciferase reporter plasmid has a synthetic promoter with five tandem repeats of the yeast Gal4 binding sites which control the expression of the *Photinus pyralis* (American firefly) luciferase gene (Stratagene). The human IL-10 promoter reporter plasmid was from L. Zeigler-Heitbrock (GSF-National Research Centre, Gauting, Germany).

2.2 Methods

2.2.1 Cell Culture

The HEK 293, HEK 293T, R1s, I1A, and BS-C-1 cell lines were maintained in DMEM supplemented with 10% (v/v) FCS, 100μg/mL gentamicin and either 2mM L-glutamine and or Glutamax (Gibco). The TK$^-$143B osteosarcoma cells were maintained in MEM and supplemented with 10% FCS, 100 μg/mL gentamicin and 2mM L-glutamine. The HepG2

cell line was cultured in DMEM with Glutamax containing pyruvate, glucose and nonessential amino acids, as well as being supplemented with 10% (v/v) FCS and 100µg/mL gentamycin. MEFs were maintained in DMEM pluss Glutamax, which was supplemented with 10% (v/v) FCS, 100µg/mL and 1X non-essenttial amino acids (NEAA). All cell lines were maintained at 37°C in a humidified atmosphiere containing 5% (v/v) CO_2.

All HEK 293 cell lines were sub-cultured every two to three days. The old medium was removed and the cells were washed with 10mL sterile 1X phosphate-buffered saline (PBS). Next, 5mL of Trypsin-EDTA (0.05mg/mL) was added to the cells and they were returned to the incubator (37°C, 5% CO_2) for three to five minutes. Following the incubation, 10mL of complete medium was added to the trypsinized cells and the cells were resuspended by pipetting. The cell suspension was then centrifuged at 1000xg for five minutes. The supernatant was discarded and the cell pellet was resuspended in 1mL of complete medium. The density was determined by counting the cells in a 10µL sample of the cell suspension with a haemocytometer and a light microscope. Flasks were seeded at 1.5 x 10^5 cells/mL in a volume of either 15mL (T75 flask) or 30mL (T175 flask) of complete medium. For immunoprecipitation experiments, 100mm dishes were seeded at a density of 1.5 x 10^5 cells/mL in 10mL of complete medium. For NF-κB and MAPK activation assays, cells were seeded at 1.5 x 10^5 cells/mL in a volume of 200µL per well of a 96-well plate. For expression studies, cells were seeded at 1.5 x 10^5 cells/mL in 2mL of complete medium per well of a 6-well plate.

MEFs were sub-cultured approximately every two to three days. The old medium was removed and the cells were washed with 10mL sterile 1X PBS. Next, 5mL of Trypsin-EDTA (0.05mg/mL) was added to the cells and they were returned to the incubator (37°C, 5% CO_2) for three to five minutes. Following the incubation, 10mL of complete

medium was added to the trypsinised cells and the cells were resuspended by pipetting. The cells were seeded in a final volume of 20mL (T75 flask) or 10mL (100mm dishes) at a ratio that gave a 75% confluent monolayer 24- to 36-hours later. For wild-type MEFs, the ratio was approximately 1:10. TRAF6$^{-/-}$ and IRAK2$^{-/-}$ null MEFs were typically seeded at a ratio of 1:4.

The BS-C-1 and TK^{-}143B cells were cultured in T175 flasks and allowed to grow until the monolayer was fully confluent. Both cell lines were sub-cultured as described above for the HEK 293 cell lines but the cell density was not determined. Instead, a volume of the cell suspension was used to seed flasks and the flasks were used once the monolayer was confluent. In the case of BS-C-1 cells, the cell suspension was also used to seed 6-well plates for plaque assays (see below).

For cryopreservation, 9mL of FCS was mixed with 1mL of tissue culture-grade dimethyl sulphoxide (DMSO). Next, the cells were harvested by trypsinisation, as described above. The density of the 1mL cell suspension was determined using a haemocytometer as described. The volume of the cell suspension to obtain 1 x 10^6 cells/mL in a final volume of 10mL was calculated. The requisite volume of the cell suspension was combined with sufficient FCS-DMSO to obtain a final volume of 10mL. The cell suspension in FCS-DMSO was then divided into 1mL aliquots in cryovials. The aliquots were placed in a cryo-freezing container (Nalgene) containing isopropanol and placed at -80°C over night. The following day, the aliquots were transferred to liquid nitrogen.

Cryopreserved cells were resuscitated by bringing to room temperature immediately upon removal from liquid nitrogen. The vial was placed in a 37°C water bath to quickly thaw the cells. The whole aliquot was transferred to a T75 flask containing 15mL of pre-warmed complete medium. The flask was incubated overnight under normal

maintenance conditions (37°C, 5% CO_2). The following day, the old medium (containing DMSO from the cryopreservation process) was replaced with fresh complete medium. The cells were then maintained under the normal conditions as described above.

2.2.2 Site-directed Mutagenesis

Single amino acid changes and a deletion construct of A52 were made with the Quikchange® Mutagenesis Kit from Stratagene. For the point mutations, primers were designed that bound to a region of approximately 20 nucleotides of the wild-type *A52R* sequence. The mutated nucleotides were at or near the centre of the primers and were flanked on either side by ten or more bases of wild type sequence. The primers for the deletion construct were made with approximately 20 nucleotides complementary to wild-type sequence on either side of the 18 nucleotides that were deleted. The *PfuTurbo* DNA polymerase extends the primers, incorporating the mutation or deletion into nicked daughter strands. For the point mutations, the polymerase chain reaction (PCR) was cycled 12 times. The deletion construct was made by increasing the number of cycles from 12 to 18. Following the mutagenesis reaction, the PCR products were treated with the DpnI restriction enzyme at 37°C for one hour. Subsequently, the DpnI-treated PCR product was transformed into competent cells for miniprep (see below). The sequences of the primers are listed in Table 2.1, with the mutated bases underlined.

Primer Name	Primer Sequence (5' to 3')
R149A positive	GGT AGA TGT TTG GGC AAA TGA GAA ACT G
R149A negative	CAG TTT CTC ATT TGC CCA AAC ATC TAC C
E151A positive	GAT GTT TGG AGA AAT GCG AAA CTG TTT TCT AG
E151A negative	CTA GAA AAC AGT TTC GCA TTT CTC CAA ACA TC
K152A positive	GAT GTT TGG AGA AAT GAG GCA CTG TTT TCT AGA TGG
K152A negative	CCA TCT AGA AAA CAG TGC CTC ATT TCT CCA AAC ATC
F154A positive	GGA GAA ATG AGA AAC TGG CTT CTA GAT GG
F154A negative	CCA TCT AGA AGC CAG TTT CTC ATT TCT CC
ΔT6BM positive	CAT GCG TGG TAG ATG TTT GGTC TAG ATG GAA ATA TTG TTT AC
ΔT6BM negative	GTA AAC AAT ATT TCC ATC TAG ACC AAA CAT CTA CCA CGC ATG

Table 2.1 Primers used in Quik-change® site-directed mutagenesis.

2.2.3 Cloning

Primers were designed to the coding sequence of each of the TRAFs 1-5 which also had engineered *EcoRI* and *XhoI* restriction sites. The primer sequences are shown in Table 2.2, with the restriction sites underlined.

PRIMER NAME	SEQUENCE
TRAF1 positive	GCG CGA ATT CGG ATG GCC TCC AGC TCA GGC
TRAF1 negative	GCG TGG AGC TCT TTA GAG CCC TGT CAG GTC
TRAF2 positive	GCG CGA ATT CGGATG GCT GCA GCT AGC GTG
TRAF2 negative	GCG TGG AGC TCT TTA GAG CCC TGT CAG GTC
TRAF3 positive	GCG CGA ATT CGG ATG GAG TCG AGT AAA AAG
TRAF3 negative	GCG TGG AGC TCT TTA TCA GGG ATC GGG CAG
TRAF4 positive	GCG CGA ATT CGG ATG CCT GGC TTC GAC TAG
TRAF4 negative	GCG TGG AGC TCT TCA GCT GAG GAT CTT CCG
TRAF5 positive	GCG CGA ATT CGG ATG GCT TAT TCA GAA GAG
TRAF5 negative	GCG TGG AGC TCT CTA GAG ATC CTC CAG GTC

Table 2.2 Primers used in HA-TRAFs cloning.

The primers were used to amplify the TRAFs from the FLAG-tagged construct by PCR and the PCR products were analysed on an agarose gel. TRAF2 PCR conditions required further optimisation before observing a product. Following PCR, the products were purified with the Qiagen PCR purification kit. The PCR products were then cut with the EcoRI/ XhoI restriction enzymes for at least three hours. The digested products were electrophoresed run on a 1% (w/v) agarose gel and then gel-purified. The pCMV-HA vector was digested overnight with the EcoRI/ XhoI enzymes. The digested vector was

purified with the Qiagen PCR purification kit. The concentration of the DNA was assessed with a UV spectrophotometer at 260 nm.

Subsequently, the TRAFs were ligated to the pCMV-HA vector using the T4 DNA ligase of the Quick Ligation kit (New England Biosciences). The reaction components were set up on ice according to the manufacturer's directions. Fifty nanograms of vector were combined with a ten-fold molar excess of insert (calculated using the Promega BioCalculator at www.promega.com). The volume was made up to 10μL with distilled water and then 10μL of 2X Quick Ligation Buffer was added. Finally, 1μL of Quick Ligase was added. Then the reaction was mixed with the pipette tip, centrifuged briefly and incubated at room temperature for five minutes. The ligation reaction was chilled on ice briefly. The ligation reaction (1.5μL) was subsequently transformed into 10μL of NovaBlue Singles competent cells.

Following ligation and transformation, individual colonies were selected, cultured and screened for successful insertion of the TRAFs by digestion with EcoRI/XhoI restriction enzymes. The minipreps that appeared to contain the insertions were maxiprepped, then sequenced and tested for expression in R1 cells.

2.2.4 Plasmid transformation

In order to prepare plasmid DNA, 1μL of the plasmid of interest was transformed into 25μL of competent E. coli cells and incubated on ice for five minutes. The cells were then heat shocked by being placed in a 42°C water bath for 30 seconds. Next, the cells were placed on ice for 2 minutes. Following the incubation on ice, 250μL of room temperature super optimal broth with catabolite repression (SOC) medium was added and 100μL of the cell suspension was plated on Luria-Bertani (LB)-agar plates containing the appropriate antibiotic. The plates were incubated overnight at 37°C. Individual

colonies were selected for plasmid purification. For standard plasmid preparation, NovaBlue singles (Novagen) were used routinely. Following mutagenesis reactions, the XL-1 blue cells (Stratagene) provided with the mutagenesis kits were transformed according to the method described above.

2.2.5 Plasmid DNA Preparation

Following transformation of the plasmids, as described above, a number of individual colonies were selected and used to inoculate 5mL of LB containing the appropriate antibiotic (usually ampicillin). The culture was incubated for eight hours at 37°C with shaking (approximately 150rpm).

For miniprep purification, 1mL of the 5mL culture was harvested by centrifugation at 16100xg for 10 minutes in a benchtop centrifuge (Eppendorf 5415D). The supernatant was discarded and the cell pellet resuspended in resuspension buffer. The cells were lysed and the DNA was collected on a filter. Following washing of the bound DNA with ethanol, the DNA was eluted into nuclease-free water. The purification steps were performed with reagents from either the Wizard SV (Promega) or the Fast plasmid mini (Eppendorf) kits.

For maxipreps, the 8mL culture was used as a starter culture. This culture was used to inoculate a 100mL-overnight culture which was also incubated at 37°C with shaking (approximately 200 rpm). The 100mL culture was harvested by centrifugation at 5000xg for 10 minutes at 4°C. The supernatant was discarded and the cell pellet was resuspended in 8mL of chilled resuspension buffer. The cells were lysed for five minutes at room temperature with 8mL lysis buffer. The lysis reaction was stopped by the addition of 8mL of neutralisation buffer and incubation on ice for five minutes. The lysates were then centrifuged at 10 000xg for two minutes at 4°C. The supernatant was

added to the filter columns (provided with the kit) and centrifuged for three minutes at 2000xg. The filter was discarded and 2.4mL Detox agent was added to the cleared lysate. The lysate was incubated on ice for 15 minutes. During this time, the DNA-binding column was equilibrated with 10mL equilibration buffer. The lysate was added to the column. The plasmid DNA in the lysate bound to the column and the rest of the cell debris flowed through the column and was discarded. The column was washed twice with 10mL wash buffer. The plasmid DNA was then eluted using 5mL elution buffer. The DNA was precipitated by the addition of 3.5mL of molecular biology-grade isopropanol. The precipitate was divided into approximately 1mL aliquots and centrifuged at 16100xg in a benchtop centrifuge for 20 minutes. The DNA pellet was washed twice with 70% (v/v) ethanol and then the pellet was allowed to air-dry. The pellet in each tube was resuspended in 100µL nuclease and endotoxin-free water. The total plasmid DNA was pooled and analysed by Spectrophotometry and agarose gel electrophoresis. The Ultramobius 1000 kit (Novagen) was used exclusively for maxiprep DNA purification.

2.2.6 Spectrophotometry

DNA preparations were quantified with a UV spectrophotometer (Eppendorf Biophotometer) by measuring the absorbance at 260nm. The purity of the preparations was indicated by an A260/A280 ratio of 1.75 to 1.95. The DNA preparations were also analysed by agarose gel electrophoresis to confirm the spectrophotometer reading.

2.2.7 Transfection

Cells were seeded in 96 well plates, 6 well plates or 100mm dishes as described above (section 2.2.1). Plasmid DNA was transfected into cells using GeneJuice™ according to the manufacturer's directions. The volume of DNA required was aliquoted and the total quantity of DNA was kept constant by the addition of empty vector (pRK5 or

pcDNA3.1) where necessary. The requisite quantities of GeneJuice™ and serum-free DMEM were mixed and allowed to stand at room temperature for five minutes. The GeneJuice and DMEM mixture was then mixed with the previously-aliquoted DNA and allowed to stand at room temperature for 15 minutes before being added to the cells. The quantities of DNA, serum-free DMEM and GeneJuice™ are indicated in Table 2.3. For 96-well plates, the quantities of DNA, GeneJuice™ and serum-free DMEM were scaled up (multiplied by a factor of 3.5) in order to perform the experiment in triplicate. The mixture of DNA, GeneJuice™ and serum-free DMEM was then divided between three wells (10µL per well). The cells were incubated overnight at 37°C. The following day, the cells were stimulated with IL-1 or a TLR agonist, if required, and then harvested.

	DNA	Serum-free DMEM	GeneJuice™
96-well plate	2.3ng	9.2µL	0.8µL
6-well plate	2.3µg	92µL	8µL
100mm dishes	8µg	235µL	15µL

Table 2.3 GeneJuice™ transfection

2.2.8 Immunoprecipitation

R1s were seeded at a density of 1 x 10^5 cells/mL in 100mm dishes containing 10mL DMEM supplemented as described above (section 2.2.1). The cells were incubated at 37°C for 24 hours prior to transfection. The cells were then transfected with a total of 8µg of DNA using GeneJuice™ according to the manufacturer's protocol. The cells were then returned to the incubator and left for 24 to 48 hours. They were harvested on ice by scraping into ice-cold PBS and centrifuged at 1500xg in a benchtop centrifuge at 4°C. The supernatant was removed and the cells were washed with a further 1mL of ice-cold PBS. They were then centrifuged again at 1500xg for three minutes at 4°C. The

supernatant was discarded and the cell pellet was resuspended in lysis buffer (50mM HEPES, pH 7.5, 1mM EDTA, 100mM NaCl, 0.5% (v/v) NP40, 10% (v/v) glycerol) containing protease inhibitors (Aprotinin, 1mM PMSF, and 1mM sodium orthovanadate) and then lysed on ice for 20 minutes. Of the cell lysate, 50µL was reserved and the remaining 800µL was divided into two samples and used in immunoprecipitation. The 50µL lysate was boiled in SDS-containing sample buffer and set aside for analysis by SDS-PAGE.

Lysates were immunoprecipitated with antibody which was pre-coupled to protein A-or protein G-sepharose beads or with anti-FLAG conjugated agarose (Sigma-Aldrich). The protein A or protein G sepharose was washed twice with lysis buffer and then the desired amount of antibody (1-4µL per reaction) was added. The antibody was allowed to couple to the protein A- or protein G-sepharose with continuous rolling at 4°C for two hours to overnight. The pre-coupled antibody was washed twice with lysis buffer and then resuspended in the requisite volume. To each sample, 30µL of the pre-coupled antibody or the commercial FLAG beads were added and the immunoprecipitation was incubated with continuous rolling at 4°C for two hours to overnight. The samples were harvested by centrifugation, washed twice in lysis buffer and boiled with SDS-sample buffer.

2.2.9 Western blotting

The lysates and immunoprecipitates were analysed by sodium dodecyl sulphate-polyacrylamide (SDS-PAGE) electrophoresis. Depending on the size of the proteins of interest, a 10-12% SDS-PAGE was used to resolve the samples. The gels were run at 85V through the stacking gel and then at 100V through the resolving gel. Following electrophoresis, the gels were transferred to Imobilon-P PVDF (Millipore) using a wet-transfer system. The transfer was performed at 100V for 45 to 75 minutes, depending upon the size of the protein and the thickness of the gel (0.75mm or 1.5mm).

Alternatively, a semi-dry transfer method was employed. In this method, the protein in the gels was transferred to PVDF at a current of 75-90mA per gel. If four gels were transferred at the same time, the current used was 300mA. The transfer was performed for 55 minutes.

Following transfer, the blots were allowed to dry in order to fix the proteins into the membrane. The blots were then reactivated in methanol, rinsed in water and washed once in PBS-Tween (0.1% (v/v)). A blocking solution of 5% (w/v) dry milk in PBS-Tween was used to block the blots, either at room temperature for one hour or overnight at 4°C with continuous rolling. The blots were washed three times in PBS-Tween and then incubated with the primary antibody solution, diluted in either 3% (w/v) BSA (in TBS-Tween) or in the blocking solution. The blots were subsequently washed three times in PBS-Tween prior to incubation with the secondary antibody for one hour at room temperature (or overnight at 4°C). Next, the blots were washed twice in PBS-Tween and then once in PBS alone. Finally, a substrate solution was added to the blots and left on them for two minutes. The blots were then exposed to film (Kodak X-Omat LS or Fujifilm Super RX) and the film developed.

2.2.10 Assay of IκB phosphorylation and degradation

R1 cells were seeded in 6-well plates at a density of 1.5×10^5 cells/mL in a total volume of 2mL/well. The next day, the cells were transfected with the DNA of interest according to the method above (section 2.2.6). The cells were stimulated with IL-1α 24 hours post-transfection. Following stimulation, the medium was removed and 100μL of 1x SDS-containing sample buffer was added to each well. The cells were scraped into the sample buffer and removed to microcentrifuge tubes. In order to lyse the cells, the samples were sonicated for ten pulses and then boiled for five minutes. The lysates were then analysed by SDS-PAGE and western blotting, as described above. The blots

were probed with antibodies to phospho-IκB (phospho-IκB assay) or for IκB (degradation assay). The blots were stripped using 1x Reblot and reprobed for A52 and ß-actin.

2.2.11 Phosphorylated p38 assay

The cells were seeded, transfected and harvested as described above for the phosphorylated IκB and IκB degradation assays (2.2.9). The samples were analysed by SDS-PAGE and western blotting. The blots were stripped with Reblot and then reprobed with antibodies to phospho-p38, total p38 and A52.

2.2.12 Ubiquitination assays

2.2.12.1 Ubiquitination of endogenous TRAF6 in R1s and HepG2s

R1 or HepG2 cells were seeded at a density of 1.5 x 10^5 cells/mL in 10mL of DMEM in 100mm dishes. The following day, the cells were stimulated with IL-1 for either 7 minutes or a time course of 3, 7, 15 and 30 minutes. The cells were harvested by scraping into ice-cold 1xPBS. The cells were subsequently lysed in 850µL lysis buffer (50mM HEPES, pH 7.5, 1mM EDTA, 100mM NaCl, 0.5% (v/v) NP40, 10% (v/v) glycerol) and then TRAF6 was immunoprecipitated as described above. The immunoprecipitation samples were analysed by SDS-PAGE and western blotting. The blots were probed with antibodies to ubiquitin, polyubiquitin and TRAF6.

2.2.12.2 Ubiquitination of over-expressed TRAF6

R1 cells were seeded at a density of 1.5 x 10^5 cells/mL in 10mL of DMEM in 100mm dishes. The cells were transfected with pcDNA3.1 (8µg) or FLAG-TRAF6 (8µg). The cells were stimulated with 20ng/mL of IL-1α for several times points. The cells were harvested by scraping them into 1X PBS, followed by centrifugation at 16100xg for five minutes. The cells were lysed in 850µL lysis buffer (50mM HEPES, pH 7.5, 1mM EDTA, 100mM NaCl, 0.5% (v/v) NP40, 10% (v/v) glycerol) for 20 minutes. The lysates were

immunoprecipitated for FLAG as described above. The blots were probed with antibodies against ubiquitin, polyubiquitin or FLAG.

2.2.12.3 Ubiquitination of endogenous TRAF6 in the presence of A52

HepG2 cells were seeded in 100mm dishes at a density of 1 x 10^5 cells/mL in 15 mL DMEM. The next day, the cells were transfected with either pRK5 or A52R according to the transfection method described above. Twenty-four hours post-transfection, the cells were stimulated with IL-1α for 7 minutes and then harvested by scraping into ice-cold 1X PBS, followed by centrifugation at 16100xg for five minutes. The cells were lysed 850µL lysis buffer (50mM HEPES, pH 7.5, 1mM EDTA, 100mM NaCl, 0.5% (v/v) NP40, 10% (v/v) glycerol) for 20 minutes. The lysates were divided into two 400µL samples and immunoprecipitated for either TRAF6 or A52. The immunoprecipitated samples were analysed by SDS-PAGE and western blotting. The blots were probed with antibodies against polyubiquitin, TRAF6 or A52.

2.2.12.4 Overexpressed myc-ubiquitin in R1s

R1s were seeded at 1.5 x 10^5 cells/mL in 100mm dishes in 10mL of complete medium. The cells were transfected the following day with pcDNA3.1 (8µg) or myc-ubiquitin expression vector (8µg) using GeneJuice. The cells were stimulated with 20ng/mL IL-1ß for 5, 10 or 15 minutes and then harvested in 1X PBS. The cells were centrifuged at 16100xg for five minutes. The cells were lysed in 850µL lysis buffer (50mM HEPES, pH 7.5, 1mM EDTA, 100mM NaCl, 0.5% (v/v) NP40, 10% (v/v) glycerol) for 20 minutes and the lysates immunoprecipitated for TRAF6. The lysates and immunoprecipitates were resolved by SDS-PAGE and western blotting. The blots were probed for myc (to detect myc-ubiquitin) or TRAF6.

2.2.12.5 Overexpression of HA-ubiquitin in R1s

R1 cells were seeded at 1.0 x 10^5 cells/mL and transfected 36h later with HA-ubiquitin expression vector (4μg) or A52 (4μg) using GeneJuice™. The cells were stimulated with IL-1α (20ng/mL) for 5 or 10 minutes. The cells were harvested by scraping into ice-cold 1X PBS, followed by centrifugation at 16100xg for five minutes. The cells were lysed for one hour on ice in 850μL lysis buffer (50mM HEPES, pH 7.5, 1mM EDTA, 100mM NaCl, 0.5% (v/v) NP40, 10% (v/v) glycerol) supplemented with protease inhibitors including iodoacetamide and protease inhibitor cocktail (Calbiochem). During the lysis, the cells were resuspended by vortexing approximately every 15 minutes. The lysates were immunoprecipitated for TRAF6. The lysates and immunoprecipitates were resolved on a 10% SDS-polyacrylamide gel and transferred to Immobilon PVDF using a wet transfer system. The blots were probed with antibodies to either HA, TRAF6 or A52.

2.2.13 Native PAGE

Six-well plates were seeded with R1 cells at 1x10^5 cells/mL in 2mL DMEM per well. Twenty-four hours later, the cells were transfected with FLAG-TRAF6 or A52 expression vector, if required. The next day, the cells were stimulated with IL-1α (20ng/mL) for different time periods. The cells were harvested by scraping into ice-cold PBS and centrifuged at 16100xg for 5 minutes to pellet the cells. The supernatant was removed and the cells were lysed in 60μL NP-40 lysis buffer (50mM HEPES, pH 7.5, 1mM EDTA, 100mM NaCl, 0.5% (v/v) NP40, 10% (v/v) glycerol) for one hour on ice with vortexing every fifteen minutes. The lysates were then centrifuged at 16100xg for 10 minutes. The total cell extract was divided into two, with one half mixed with non-denaturing sample buffer and the other half mixed with denaturing sample buffer. The sample mixed with denaturing sample buffer was boiled for five minutes, then immediately chilled on ice. The denatured samples were analysed by SDS-PAGE, followed by transfer using a semi-dry transfer system.

The sample treated with non-denaturing buffer was analysed by native PAGE. The running buffer was Tris-glycine, supplemented with 1% (w/v) sodium deoxycholate in the upper buffer chamber. The 7% native gels were pre-run for 30 minutes at 40mA. The samples were then loaded on to the gels. The gels were run for one hour at either 25mA (one gel) or 35mA (two gels). Following the run, the gels were transferred to PVDF by a semi-dry transfer system.

2.2.14 A52 and GFP-A52 oligomerisation assay

R1 cells were seeded at 1x 10^5cells/ml in 10mL DMEM in 100mm dishes. The cells were transfected 36 hours later with pRK5 (8μg), GFP-A52 (4μg), wild-type A52 (4μg), F154A (4μg), or ΔT6BM (4μg) expression vectors using GeneJuice™ according to the manufacturer's directions. The cells were harvested 24 hours post-transfection by scraping into ice-cold 1X PBS and centrifuging at 16100xg for five minutes. The cell pellets were lysed for one hour on ice in 850μL lysis buffer supplemented with protease inhibitors. The lysates (800μL) were immunoprecipitated with 1μL anti-GFP pre-coupled to protein A. The immunoprecipitation was allowed to incubate overnight at 4°C. The lysates and immunoprecipitations were analysed by SDS-PAGE (12%) and the gels were transferred to PVDF by a semi-dry system. The blots were incubated with antibodies to GFP or A52.

2.2.15 Luciferase reporter gene assays

These assays take advantage of the different enzyme structures and substrates of firefly and Renilla luciferases. The firefly luciferase oxidises the beetle luciferin in the presence of ATP, Mg^{2+} and O_2, generating a flash of light. The signal is stabilised by the presence of coenzyme A (CoA) in the luciferase assay mix. The Renilla luciferase uses coelenterate-luciferin (coelentrazine) and O_2 to produce coelenteramide, CO_2 and a luminescent signal.

2.2.15.1 NF-κB Reporter Gene Assay

The effect of A52, E151A and F154A on the activity of the NF-κB-luciferase reporter plasmid was assayed by transient co-transfection with NF-κB-luciferase and Renilla luciferase (phRL-TK). A 96-well plate was seeded with R1 cells at 1.5 x 10^5 cells/mL in a total volume of 200μL 24 hours prior to transfection. The cells were then transfected with a total of 230ng of DNA per well using GeneJuice™, as described above. The reporter plasmids NF-κB-luciferase (60ng) and phRL-TK (20ng) were co-transfected with up to 150ng of the expression plasmids of interest. The total amount of DNA was kept constant with empty vector.

The following day, the cells were stimulated with either IL-1α or TNFα at a final concentration of 50ng/mL. The cells were harvested six hours after stimulation and were lysed in passive lysis buffer for 15 to 20 minutes with vigorous shaking. The lysates were then analysed for firefly luciferase and renilla luciferase activity by taking 20μL of each well into two separate assay plates. To one plate, 40μL of luciferase assay mix (20mM tricine, 1.07mM $(MgCO_3)_4Mg(OH)_2 \cdot 5H_2O$, 2.67mM $MgSO_4$, 0.1M EDTA, 33.3mM DTT, 270mM coenzyme A, 470mM luciferin and 530mM ATP) was added. To the other plate, 40μL of the renilla substrate coelentrazine (2μg/mL in 1x PBS) was added. The samples were analysed using a luminometer.

2.2.15.2 MAP kinase activation

To test the effect of A52 on MAP kinase activation, the Stratagene Path Detect® system was used. The system uses a trans-activator plasmid, consisting of the activation domain of a transcription activator fused with the DNA-binding domain of the yeast Gal4 (residues 1-147). In the MAP kinases assays described herein, the activation domain of either the c-Jun, Elk1 or CHOP transcription activator was fused to Gal4. The transcription activators c-Jun, Elk1 and CHOP are phosphorylated and activated by c-

Jun N-terminal kinase (JNK), extracellular signal-regulated protein kinases (ERK) and p38, respectively. In this system, the ability of JNK, ERK and p38 MAP kinase to phosphorylate and activate their respective transcription factors (i.e. c-Jun, Elk1 and CHOP) is assayed. There are five tandem repeats of the gal4 binding site at the promoter of the pFR-luciferase reporter gene construct. When activated by phosphorylation, the gal4-transcription activator fusion protein can bind to the pFR-luciferase construct and induce transcription of the luciferase.

A 96-well plate was seeded with R1s at 1.5 x 10^5 cells/mL in a volume of 200µL/well 24 hours before transfection. The cells were then transfected with a total of 230ng of DNA, including 60ng of pFR-Luciferase and 20ng of pHRL-TK (Tk-Renilla) and up to 150ng of the DNA of interest. For the CHOP assay, 0.25ng of the CHOP-Gal4 trans-activator plasmid was transfected into the cells. The total amount of DNA was kept constant with empty vector. The DNA was transfected with GeneJuice transfection reagent as described above. The cells were stimulated the following day and harvested 6 hours post-stimulation. The cells were lysed using passive lysis buffer and the lysates were analysed as described above for the NF-κB activation assay.

For the analysis of JNK activation, the above protocol was followed with the substitution of 0.25ng of the c-Jun trans-activator plasmid for the CHOP-Gal4 plasmid. To examine ERK activation, the CHOP-Gal4 plasmid was substituted with 2ng of the Elk-1 *trans*-activator plasmid.

2.2.16 GST-A52 Expression

GST-A52 had previously been cloned into the pGEX-4T2 bacterial expression vector (Harte *et al.*, 2003). GST-A52 (2µL) was added to BL-21 cells (50µL), gently mixed with the pipette tip and then incubated on ice for 30 minutes. Following the incubation, the

cells were heat-shocked at 42°C for one minute. The cells were returned to ice for a further two minutes, followed by the addition of 1mL of LB medium containing no antibiotic. The cells were then grown at 37°C for one hour with shaking at approximately 150rpm. The culture was centrifuged for five minutes at 2300xg. Most of the supernatant was removed but approximately 50µL was left to cover the cell pellet. The cells were resuspended in the LB and the suspension was spread on an LB-agar plate containing ampicillin. The plate was incubated overnight at 37°C.

The next day, the plate was removed from the incubator and placed at 4°C. At the end of the day, one colony was selected and grown in 10mL LB broth containing ampicillin overnight at 37°C and with shaking at 150rpm. The next morning, the overnight culture was added to 1L LB broth containing ampicillin. The culture was incubated at 37°C with shaking at 150rpm until an optical density (O.D.) at 600nm of 0.6 was attained. At this point, a pre-induction sample (50µL) was removed, mixed with sample buffer and stored at -20°C for gel analysis. In addition, a pre-induction sample (600µL) was mixed with 400µL 50% glycerol and stored at -80°C. The culture was then induced with 500µL 1M IPTG and incubated at 25°C for four more hours. At this point, post-induction samples (50µL each) were taken and mixed with either denaturing or non-denaturing sample buffer. The cultures were centrifuged at 2600xg for 20 minutes and the supernatant was discarded. The pellets were either lysed immediately or stored at -80°C for later processing.

In order to purify the GST-A52 protein, the cell pellet was resuspended in 20mL extraction buffer (300mM NaCl in 1X PBS with 1% Triton X-100) supplemented with protease inhibitors. The suspension was sonicated four times for two minutes each time (with the probe sonicator set at 25% duty cycle, 0.25 power). The suspension was kept on ice throughout the sonication steps. Between the sonication steps, the suspension

was mixed by inversion and incubated on ice for five minutes. The lysates was then transferred to centrifuge tubes and centrifuged at 17211xg for 30 minutes. The supernatant was recovered and a 50 µL sample was taken for gel analysis. A small sample of the pellet (or insoluble fraction) was also taken and mixed with sample buffer for gel analysis. The glutathione sepharose beads (2mL/litre of culture) were loaded onto a purification column and allowed to settle. The beads were washed twice with extraction buffer and the flow-through discarded. The supernatant from the bacterial cell lysates was then loaded onto the column and the column was kept at 4ºC for the incubation period (five hours total). The lysate was allowed to flow-through the column and the beads were washed three times with extraction buffer (with protease inhibitors added) to remove any unbound protein. In order to elute untagged A52, 0.5mL elution buffer (10mM reduced glutathione in 50mM Tris, pH8) containing thrombin (10µL) was added to the column and allowed to incubate overnight at 4ºC. The next morning, the fractions containing eluted protein were collected and the samples analysed by SDS-PAGE.

Since protein expression levels seemed low in the BL-21 competent cells, another cell type was used to improve expression. Rosetta-Gami 2 cells (Novagen) have the pRARE2 plasmid (chloramphenicol-resistant, *Cam*^{r}) which supplies seven tRNA codons that are rare in *E. coli*. They also have mutations in the thioredoxin reductase (*trxB*) and glutathione reductase (*gor*) genes and are kanamycin-sensitive. The combination of the pRARE2 plasmids and the mutant enzymes improves expression of heterologous proteins and enhances disulphide bond formation in the cytoplasm. The Rosetta-Gami2 cells were transformed and cultivated as described above for the BL-21 cells. The LB-agar plates used initially had chloramphenicol and tetracycline, as well as ampicillin, but only ampicillin was added to the liquid broth. The omission of chloramphenicol and tetracycline probably reduced the overall yield of protein and should be included in

both agar plates and broth. The presence of the extra plasmids in Rosetta-Gami cells increases the amount of time taken for the culture to reach the log growth phase. It can take several hours (five or more) to reach an O.D. of 0.6, compared to the two-three hours for the BL-21 cells.

The protein purification method described above was similar to that used for the Rosetta-Gami2 cells. At the end, the protein was eluted off the column with either 1% (w/v) SDS or a modified elution buffer (20mM reduced glutathione in 50mM Tris, pH8.0, with 1% Triton X-100). Following elution, the eluate was dialysed overnight in 1X PBS at 4°C to remove the glutathione and the Triton X-100. The purified protein was analysed by SDS-PAGE and then sent to Inbiolabs for antibody production.

2.2.17 VACV infection

2.2.17.1 Growth and purification of VACV working stocks

In order to be used in further experiments, wild-type Western Reserve strain (WR) and the deletion virus lacking A52 (ΔA52) had to be cultivated and purified of contaminating cell debris. Five large (T175) flasks of TK cells were grown until they were fully confluent. The medium was removed and replaced with inoculum containing 15μL virus from master stocks diluted in 25mL DMEM supplemented with 10% FCS, gentamicin and either L-glutamine or Glutamax. The inoculum was left on the cells for one hour with gentle rocking. The inoculum was then removed and replaced with 20mL DMEM supplemented as above. The cells were returned to the incubator and left for three days. The infection was monitored by the development of cytopathic effect (c.p.e.), with the infected cells appearing more rounded compared to uninfected cells.

The cells were harvested by scraping into the culture medium. The cell suspensions from each flask were pooled to give approximately 100mL cell suspension total divided

between two 50mL tubes. The cells were centrifuged at 5000xg for five minutes at 4°C. The supernatant was discarded and the cell pellets were re-suspended in 5mL hypotonic buffer (10mM Tris, pH9). The cell suspensions in hypotonic buffer were then pooled to give 10mL total. The suspension was incubated on ice for 20 minutes. Following the incubation, the suspension was transferred to a Dounce homogeniser and the cells were lysed by 25 to 30 strokes with the homogeniser. The homogenate was transferred to a 50mL tube and centrifuged at 5000xg for five minutes at 4°C. The supernatant was reserved and the pellet discarded. To the supernatant, hypotonic buffer was added to bring the volume up to approximately 16mL total. The diluted supernatant was transferred to a centrifuge tube for use in the ultracentrifuge. To the supernatant, 16mL of sucrose solution (36% sucrose in hypotonic buffer) was added gently to avoid mixing with the supernatant. The swinging bucket rotor (Beckman L8-M ultracentrifuge, rotor SW 41) was taken from the fridge and the centrifuge tubes added to the buckets. The buckets were balanced and then replaced on the rotor. The samples were centrifuged for 80 minutes at 4°C at 32 000xg. Following centrifugation, the pellet was observed at the bottom of the tube. The sucrose was aspirated and the pellet was resuspended in 1mL 1X PBS. The purified virus was then stored at -80°C until titrated by the plaque assay.

2.2.17.2 Plaque assay

BS-C-1 cells were seeded into 6-well plates and were allowed to incubate until they were fully confluent. The virus to be titrated was subject to three freeze-thaw cycles, then sonicated for five minutes in the water bath sonicator (100% amplitude). The serial dilutions were then set up in 15mL tubes with DMEM (any concentration of FCS is acceptable). For the first two dilutions (10^{-2} and 10^{-4}), 5mL media was added to each of the tubes. For the other dilutions (10^{-5}, 10^{-6}, 10^{-7} and 10^{-8}), 4.5mL media was added to each of the tubes. The stock virus (50µL) was added to the first tube (10^{-2}). The tube

was vortexed and then 50µL of the dilution was added to the second tube (10^{-4}). This tube was then vortexed and 500µL was taken into the next tube (10^{-5}). For the next three dilutions (10^{-6}, 10^{-7} and 10^{-8}), 500µL of the previous dilution was added and then the tube was vortexed. Once the dilutions were set up, the media was aspirated from the 6-well plates. To each well, 500µL of the appropriate dilution was added. Each dilution was done in duplicate. The plates were returned to the incubator for 90 minutes, with gentle rocking every 15 minutes. Meanwhile, the overlay (50:50 carboxymethylcellulose (CMC) and DMEM with 5% FCS) was prepared. The inoculum was removed and 2mL of the overlay solution was added to each well. The plates were returned to the incubator and left for 48 hours.

Two days later, the inoculum was removed and 2mL of crystal violet was added to each well. The plates were rocked gently and then the crystal violet was left on the cells for one hour. Following the incubation, the crystal violet was removed and the plates were washed gently with water in order to remove the excess stain but without damaging the monolayer. The plates were then inverted and allowed to dry. Once dry, the plaques in each well were counted and the average for the two wells for each dilution (10^{-6}, 10^{-7} and 10^{-8}) determined. Since 500µL of each dilution was added to each well, the number of plaques counted was multiplied by two in order to get a value for particle-forming units (pfu)/mL. All counts were then converted to values raised to the power of 10^{8} and the average was taken to give the titre used in further experiments.

2.2.17.3 HA-Ubiquitination of TRAF6 and VACV A52 in VACV-infected R1s or MEFs

The cells were seeded into 100mm dishes twenty-four hours prior to transfection (see above). The next day, the cells were transfected with 8µg of HA-ubiquitin. The following morning, the dishes were either mock-infected or infected with VACV. First, the medium was removed from all the dishes and replaced with 5mL DMEM

supplemented with 2.5% FCS, gentamicin and L-glutamine or Glutamax. The virus had been thawed, sonicated and vortexed. The virus used for the infections had been titrated and the approximate cell density for a confluent dish of the cells had been determined. A multiplicity of infection (MOI) of five was used based on previous studies in the lab. The volume of virus stock required for each dish was determined by the following formula:

$$\text{Volume of virus stock (mL)} = \frac{\text{MOI x density (cells/mL) x volume of medium (mL)}}{\text{Virus titre}}$$

The previously-determined volume of virus was added to the dishes and the dishes were returned to the incubator for one hour. The mock infected dishes did not have any virus added but were otherwise treated the same. The dishes were rocked gently every fifteen minutes. After the hour incubation, the inoculum was removed and replaced with fresh DMEM containing 10% FCS, as well as gentamicin and L-glutamine or Glutamax. The cells were harvested either eight or 24 hours later by scraping into ice-cold PBS. The cells were centrifuged at 16100xg (Eppendorf 5415D centrifuge), the supernatant removed and the cell pellets either lysed for immunoprecipitation or stored at -20°C for later processing.

2.2.18 Bioinformatics

The *A52R* nucleotide sequence and A52 amino acid sequence were analysed *in silico* using programs available on the Internet at www.expasy.ch (Expasy; Gasteiger *et al.*, 2003), www.justbio.com, and www.ch.embnet.org (Swiss EMBnet). The *A52R* nucleotide sequence was translated and the nucleotide/amino acid alignment performed with the Translator tool (www.justbio.com). Comparisons of the *A52R* nucleotide or amino acid sequences with those of other proteins were made using several different alignment programs, including DIALIGN (Morgenstern, 2004; http://bibiserv.techfak.uni-

bielefeld.de/dialign/) and ClustalW (Thompson *et al.*, 1994; http://www.ch.embnet.org/software/ClustalW.html).

To determine protein topology, the hydrophobicity of the amino acid residues was measured using the method of Kyte and Doolittle (1982). The location of a transmembrane domain was predicted with several programs, including TMPred (Hofmann and Stoffel, 1993), HMMTOP (Tusnády and Simon, 2001) and TopPred (von Heinje, 1992; Claros and von Heinje, 1994). The secondary structure of A52 was analysed using PSIPRED (McGuffin *et al.*, 2000). To determine if there were significant motifs in the protein, a comparison was made to a database of existing motifs using Prosite (Falquet *et al.*, 2002) and ELM (Puntervoll *et al.*, 2003; www.eu.elm.org). The presence of sumoylation sites was analysed using SUMOplot™ (Abgent; http://www.abgent.com/doc/sumoplot).

The TRAF6 binding motif is not searchable using a computer algorithm yet. The motif was obtained from the literature (e.g. Ye *et al.* 2002) and the sequence of A52 was studied to determine if it contained this sequence.

Chapter Three: Results I

The interaction between A52 and the TRAFs

3.1 Introduction

A52R is an immediate-early gene of the VACV western reserve strain (WR) and is thus among the first genes expressed upon infection (Assarsson *et al.*, 2008). This class of genes are expressed to very high levels, with the transcript levels peaking two hours post-infection (Assarsson *et al.*, 2008). The proteins expressed from immediate-early transcripts are involved in immune evasion and virulence, as well as DNA replication and transcription (Assarsson *et al.*, 2008). Consistent with this function of the immediate-early gene products, the A52 protein has a role in immune evasion, blocking IL-1R and TLR signalling to NF-κB activation (Bowie *et al.*, 2000, Harte *et al.*, 2003).

A52 was previously found to interact with the signalling molecules IRAK2 and TRAF6 (Harte *et al.*, 2003), both of which are required for signal transduction from activated TLRs and IL-1R (Keating *et al.*, 2007). A52 was not found to interact with another TRAF family member, over-expressed TRAF2, nor with IRAK1 (Harte *et al.*, 2003). Recently, IRAK2 was found to be required for all TLR-mediated pathways leading to NF-κB activation (Keating *et al.*, 2007). Moreover, the interaction between A52 and IRAK2, in the absence of any A52-TRAF6 interaction, was sufficient for A52 to inhibit NF-κB activation by multiple TLRs (Keating *et al.*, 2007).

In contrast to its role as an inhibitor of NF-κB, A52 is also able to activate p38 and JNK MAPK (Maloney *et al.*, 2005). This is intriguing since the activation of NF-κB and MAPK utilise common signalling pathways. While the inhibition of NF-κB by A52 depends upon its interaction with IRAK2 and not with TRAF6, p38 MAP kinase activation by A52 requires TRAF6 and does not occur in $TRAF6^{-/-}$ MEFs (Maloney *et al.*, 2005). Further, A52 interacts specifically with the TRAF domain of TRAF6 (Maloney *et al.*, 2005). Co-expression of the TRAF domain of TRAF6 and A52 resulted in inhibition of A52-induced p38 MAPK activation, consistent with the TRAF domain acting as a dominant negative

(Maloney *et al.*, 2005). Moreover, the co-expression of the TRAF domain of TRAF6 and A52 inhibited the interaction between A52 and endogenous TRAF6 (Maloney *et al.*, 2005). Thus, the interaction between A52 and TRAF6 is required for p38 MAPK activation by A52 (Maloney *et al.*, 2005).

There are seven TNF-receptors associated factors (TRAFs) found in humans (Zapata *et al.*, 2007b). The TRAFs are considered to be adaptor molecules in signalling pathways based on their multidomain structure (Arch *et al.*, 1998). The TRAFs belong to the MATH (meprin and TRAF-C homology domain) superfamily because they have the typical MATH domain - a fold of seven or eight anti-parallel ß-sheets - in their TRAF-C domain (Zapata *et al.*, 2007b, Wajant *et al.*, 2001). All the TRAFs, except TRAF7, are related by the presence of the C-terminal TRAF domain, which is subdivided into a TRAF-N and TRAF-C (or MATH) domain (Figure 1.6). The TRAF-C domain has been crystallised and found to be the site of a cleft where TRAF6 interaction partners bind (Ye *et al.*, 2002). At least some of the TRAFs have been found to associate in trimers, linked by interactions between the coiled coils of the TRAF-N domains of each monomer (Zapata *et al.*, 2007b). In addition, all of the TRAFs have a RING domain near the N-terminus (except TRAF1) and one or more zinc fingers, typically between the RING and TRAF domains (Zapata *et al.*, 2007b).

Several TRAFs, including TRAFs 1,2 3 and 5, have previously been shown to interact with members of the TNFR superfamily and to mediate downstream signalling (Zapata *et al.*, 2007b). There are two pathways of NF-κB activation by CD40, leading to the nuclear translocation of either the canonical p50/RelA dimer or of the noncanonical p52/RelB dimer (Hauer *et al.*, 2005). CD40 signalling via TRAF6 induced activation and nuclear translocation of the p50/RelA dimer (Hauer *et al.*, 2005). Interestingly, CD40 signalling via TRAF2/5 resulted in nuclear translocation of either the p50/RelA or the p52/RelB

dimer (Hauer *et al.*, 2005). However, there is also evidence of cooperation between TRAF2 and TRAF6 in mediation of CD-40-induced NF-κB and JNK activation (Davies *et al.*, 2005; Wu and Arron, 2003). Another TRAF family member, TRAF3, inhibited TRAF2/5-mediated CD40 signalling to NF-κB activation and thereby indirectly enhanced TRAF6-mediated NF-κB activation (Hauer *et al.*, 2005).

In addition to mediating signalling from TNFR family members, some TRAFs have since been found to have a role in IL-1R/TLR signal transduction. TLR signalling via MyD88 and TRIF is differentially regulated by recruitment of either TRAF3 or TRAF6. Following TLR4 or TLR9 stimulation, both TRAF3 and TRAF6 were recruited to the receptor and interacted with MyD88 (Häcker *et al.*, 2005). TLR-induced MyD88 dimerisation leads to recruitment of both TRAF3 and TRAF6 in equal quantities (Häcker *et al.*, 2005). TRAF3 is recruited to TIR signalling complexes via interactions with the adaptor proteins MyD88 and TRIF (Häcker *et al.*, 2005). TRAF6 is required for signalling via MyD88-dependent but not TRIF-dependent pathways (Häcker *et al.*, 2005). Signalling via TRAF6 results in activation of MAPK, as well as AP-1 and NF-κB and results in the induction of pro-inflammatory cytokines (Häcker *et al.*, 2005). In contrast, TRAF3 is not required for MAPK activation or the production of proinflammatory cytokines. Instead, TRAF3 promotes the production of type I interferon and the anti-inflammatory cytokine IL-10 (Häcker *et al.*, 2005). Further, TLR4-induced, TRIF-dependent activation of type I IFN and IL-10 expression utilised TRAF3 and not TRAF6 (Häcker *et al.*, 2005; Oganesyan *et al.*, 2005). Another TRAF family member, TRAF7, has been found to function in conjunction with TRAF6 to mediate signalling from TLR2 (Yoshida *et al.*, 2005). In addition, TRAF4 has been identified as a potential inhibitor of TLR signalling, negatively regulating TRIF and TRAF6 function (Takeshita *et al.*, 2005).

As mentioned above, TRAF6 is required for TLR-induced MAPK activation. Some of the

other TRAFs also have a role in assembling the components of the MAP kinase pathways (Bradley and Pober, 2001). For example, TNF or IL-1 stimulation induces the interaction of MEKK1 with TRAF2 or TRAF6, respectively, leading to JNK activation (Wajant *et al.*, 2001). The importance of the TRAFs in MAPK activation is evident from studies with $TRAF2^{-/-}$ mice, in which TNF-induced JNK activation was impaired, whereas NF-κB activation was unaffected (Bradley and Pober, 2001). TRAF proteins have also been shown to interact with germinal centre kinase (GCK) family members (Inoue *et al.*, 2000). The GCK are constitutively active kinases that can activate the MAP3Ks, TAK1 and MEKK1, and JNK (Wajant *et al.*, 2001; Zhong and Kyriakis, 2004). TLR/IL-1R-induced GCK stabilisation is mediated by TRAF6, which binds to GCK to prevent its degradation and thus to promote JNK activation (Zhong and Kyriakis, 2004). Finally, TRAF7 has been found to interact with directly with MEKK3 and to potentiate MEKK3-induced activation of the transcription factors, AP-1 and CHOP (Xu *et al.*, 2004).

In addition to TNFR and IL-1R/TLR signalling, a role for the TRAFs in RLR signalling has been identified. TRAF3 interacts with the adaptor, IPS-1, to mediate type I IFN production (Saha *et al.*, 2006). IPS-1 has a TRAF3-specific TRAF-interaction motif, mutation of which abrogates TRAF3-dependent IFN production (Saha *et al.*, 2006). In parallel with the distinct roles for TRAF3 and TRAF6 in TLR signalling, TRAF3 is required for IPS-1-induced type I IFN expression but not for NF-κB activation (Saha *et al.*, 2006), whereas TRAF6 is required for the latter (Lad *et al.*, 2008).

The purpose of this chapter was to investigate the potential interactions between A52 and the TRAFs. Although A52 was shown to interact with TRAF6 and not TRAF2, it was hypothesised that it might interact with one or more other TRAFs. There is a high level of homology among the TRAFs, particularly in the TRAF domain. Previous studies used over-expressed FLAG-tagged TRAFs to investigate A52-TRAF2 and A52-TRAF6

interactions (Harte *et al.*, 2003). The other FLAG-TRAFs were acquired and tested for an interaction with A52. In addition, while the A52-TRAF6 interaction was necessary for p38 MAP kinase activation by A52, the role of other binding partners could not be ruled out. In particular, it was possible that the A52-TRAF6 interaction was indirect, occurring via the recruitment of TRAF6 to IRAK2. The ability of A52 to bind to TRAF6 in the absence of IRAK2 was examined to test this hypothesis.

The A52 antibody used in previous studies had been raised to GST-A52 (Harte *et al.*, 2003). That antibody immunoprecipitates A52 and detects A52 on western blots. However, it also detects non-specific proteins on western blots and may not exclusively immunoprecipitate A52. Thus, in order to make a more specific antibody, GST-A52 was produced with the intention of cleaving the GST-tag and thereby producing recombinant A52. In addition, antibodies were also raised to an immunogenic peptide of A52 in order to create an antibody directed at a specific epitope of A52. Improving the antibody to A52 was undertaken in order to create an effective tool for looking at interactions between A52 and cell signalling proteins. The GST-A52 produced could also be used for pulldowns to detect and interaction between the recombinant protein and the TRAFs in eukaryotic cell lysates.

3.2 Results

3.2.1 GST-A52 can be expressed in *E.coli* and purified

Full-length A52 was previously cloned into the pGEX-4T2 bacterial expression vector downstream of GST (Harte *et al.*, 2003). The resulting fusion protein is predicted to be 46kDa, since A52 is 22kDa and GST is 24kDa. Initially, a 46kDa protein that is likely GST-A52 was expressed in the BL-21(DE3) strain of *E. coli* following induction with IPTG (Figure 3.1, lanes 3 and 4). Although expression of the fusion protein was detectable,

only a small amount of the soluble protein was produced (Figure 3.1, lane 3). There appeared to be protein of the same molecular mass in the insoluble pellet (Figure 3.1, lane 5). Furthermore, digestion of the fusion protein with the protease thrombin did not produce detectable untagged A52 (Figure 3.1, lanes 7-10). No protein of approximately 22kDa was observed on the gel following thrombin cleavage (Figure 3.1, lanes 7-10).

In order to improve expression of GST-A52, a different strain of E. coli was used. The Rosetta-Gami2™ (Novagen/Merck) strain has an extra plasmid encoding tRNAs that are rare in *E.coli* and this improves expression of eukaryotic proteins. In addition, they have the Origami2 mutations that favour disulphide bond formation, thereby enhancing protein folding. GST-A52 was expressed in Rosetta-Gami2 cells following induction with IPTG (Figure 3.2, lanes 2 and 3). The thrombin cleavage was once again unsuccessful at cleaving free A52 from the GST-A52 on the beads (Figure 3.2, lanes 6-9).

Since thrombin cleavage was not successful, GST-A52 was instead purified to be used for pull-downs and antibody production. Although GST-A52 was expressed (Figure 3.3, lanes 3 and 4) and bound to glutathione sepharose beads (lanes 6, 7 and 8), it could not be eluted with 10mM glutathione (lane 9). It was possible to elute the GST-A52 from the glutathione sepharose beads with 1% SDS (Figure 3.4, lane 10). However, the presence of 1% SDS in the protein sample meant that it could not be used to inoculate rabbits for antibody protein. The fusion protein was produced again and bound to glutathione sepharose beads (Figure 3.5, lanes 3 and 4). The GST-A52 was eluted using buffer containing 20mM reduced glutathione and 1% Triton-X-100. The eluate was dialysed against phosphate buffered saline overnight in order to remove the glutathione and Triton-X-100 (Figure 3.5, lane 5). The resulting eluate containing purified GST-A52 was used to inoculate rabbits for antibody production.

3.2.2 The antibodies produced in response to GST-A52 do not detect over-expressed A52

The antibodies were made by immunising rabbits (L114 and L116) with GST-A52. The resulting serum was used to detect over-expressed A52 in cell lysates by western blotting (figure 3.6). The antibody produced in rabbit L114 detected a band below the 25kDa marker only in the lane with over-expressed A52 and not the lane with empty vector (Figure 3.6A). Unfortunately, the same protein was not found with the serum from rabbit L116 (Figure 3.6B). The result was not reproducible since subsequent western blots probed with L114 and L116 did not detect A52 (Figure 3.7, both panels). The antisera detect only non-specific bands in the lysates. The antisera was only weakly immunogenic in ELISAs performed by the company (Appendix 2), which could explain the difficulty in detecting A52 by western blotting with the L114 and L116 antisera. The recombinant protein was not examined by western blotting to determine if the antisera could detect GST-A52 while not being able to detect the untagged A52.

3.2.3 Antibodies raised against a peptide of A52 detect a protein in VACV-infected cells that is not A52

Since the antibodies produced in response to GST-A52 were not very specific, antibodies were produced by immunising two rabbits with a peptide from A52. The A52 peptide, KYGRLFNEI (residues 75-83), had been shown to be immunogenic (Tscharke *et al.*, 2006). This peptide was synthesised and conjugated to BSA, then used to inoculate the rabbits. Serum from rabbit SG-4608 detected fewer non-specific bands than serum from rabbit SG-4607 and thus further antibody testing was done with SG-4608 only (SG-4607 data not shown). Serum from both rabbits detected a VACV protein in VACV-infected cells at about 25kDa on a western blot, as shown for serum from rabbit SG-4608 (Figure 3.8, panel A). However, the 25kDa protein detected by SG-4608 was found in cells infected with VACV that lacks A52 (Figure 3.8, panel A, lane 3). Furthermore, SG-4608

did not detect over-expressed A52 in cell lysates (Figure 3.8, panel A, lane 5). In comparison, the A52 antibody previously generated as described in Harte *et al.* (2003) detected a protein in both WR-infected and A52 over-expressed cell lysates (Figure 3.8, panel B, lanes 7 and 10). The protein detected was below the 25kDa marker and is not found in the DD-infected cells (Figure 3.8, panel B, lanes 7 and 8). In addition, when SG-4608 was used in an immunoprecipitation of WR- or ΔA52-infected cells and subsequently in the western blot, it detected a protein of 25kDa that was in both WR and ΔA52 (data not shown). In contrast, the A52 antibody immunoprecipitated and detected the 22kDa A52 in WR-infected cells only (data not shown). Thus, the protein detected by SG-4608 is unlikely to be A52 but may be another VACV protein. Interestingly, a search of a database of VACV proteins with the peptide sequence KYGRLFNEI only matched with A52. Furthermore, the titre from an ELISA performed by Sigma suggested that the antisera were only weakly immunogenic and this could account for the difficulty in detecting A52 by western blotting with these antisera (Appendix 2). Thus, the original A52 antibody made against GST-A52 (as described in Harte *et al.*, 2003) was used in future experiments.

3.2.4 The FLAG-TRAFs are expressed in R1s

In order to determine whether the interaction of A52 with TRAF6 was specific, the potential interactions between A52 and TRAFs1-6 were examined. It was previously reported that A52 interacts with TRAF6 and not with TRAF2 (Harte *et al.*, 2003). In order to confirm this observation and to examine other potential interactions of A52 with members of the TRAF family, expression plasmids encoding FLAG-tagged TRAF1-TRAF6 were employed. First, the expression of the FLAG-tagged human TRAF constructs was confirmed. The FLAG-TRAF constructs were expressed in R1s and then the total cell lysates were analysed for TRAF expression by western blotting. The blots were probed with anti-FLAG antibody and developed with enhanced chemiluminescence

(ECL). As shown in Figure 3.9, all of the FLAG-TRAFs are detected by the anti-FLAG antibody. The predicted sizes of the FLAG-TRAFs mostly correspond to the observed molecular masses for the human TRAFs. FLAG-TRAF1 is predicted to be 46kDa, running just below the 47.5kDa standard (Lane 2), while FLAG-TRAF2 is predicted to be 55kDa and runs just above the 47.5 kDa standard (Lane 3). FLAG-TRAF3 is predicted to be 64.5kDa and runs at or slightly above the level of the 62kDa standard (Lane 4). In lane 5, FLAG-TRAF4 (53.5kDa) migrated at approximately the same level as FLAG-TRAF2 (55.9kDa). FLAG-TRAF5 (64.4kDa) is predicted to be larger than FLAG-TRAF6 (59.6kDa), but they both migrated just below the 62kDa standard and appeared to have roughly the same molecular mass (Compare lanes 6 and 7).

Numerous other higher and lower molecular weight species were detected in the FLAG-TRAF3 sample. It is unclear why these bands are present. It is possible that they are modified forms of TRAF3, such as ubiquitinated forms due to auto-activation when the FLAG-TRAF3 is over-expressed. In addition, the bands could be due to degradation or to impurity of the sample. A fresh DNA preparation was made and expressed but the bands were still present when FLAG-TRAF3 was used in FLAG-TRAF and A52 co-immunoprecipitation experiments (see below). The FLAG-TRAFs were also transfected into R1s for immunoprecipitation. Both the lysates (not shown) and the FLAG immunoprecipitates (Figure 3.10) were probed for FLAG and the same molecular mass of each of the FLAG-TRAFs in the blot in Figure 3.9 was observed.

3.2.5 The FLAG antibody detects A52

Co-immunoprecipitation experiments were performed with all of the FLAG-TRAFs. Initial experiments showed non-specific interactions between the FLAG antibody and A52 (data not shown). The cell lysis and immunoprecipitation conditions were made more stringent in order to try to eliminate the non-specific interactions. The stringency

was increased by using a greater concentration of NaCl (from 100mM to 250mM) and a higher percentage of NP-40 (from 0.5% to 1%) in the lysis buffer. Also, the cell lysates were incubated for shorter periods of time with the antibodies during the immunoprecipitations. Finally, the antibody concentrations for the western blot were decreased. Figure 3.10 shows the blots obtained from the experiments performed with greater stringency.

In lane 1, A52R was transfected into the cells without any of the FLAG-TRAFs. Here, A52 is clearly detected in FLAG immunoprecipitates, despite there being no FLAG-tagged proteins in the sample (Figure 3.10, top panel, lane 1). The FLAG antibody was still pulling down A52 and thus it is impossible to conclude whether or not A52 interacts with any other FLAG-TRAFs. In each of lanes 2 through 7, there is a band (top panel) which would indicate that A52 and each of the FLAG-TRAFs interact. However, this is obviously not the case due to the non-specific pull-down of A52 by the FLAG antibody (Figure 3.10, top panel). Immunoprecipitation of A52 followed by immunoblotting for FLAG was also attempted but the results of these experiments were inconclusive (data not shown).

An alternative to the above experiment was devised whereby the FLAG-TRAFs were co-transfected with GFP-A52. The lysates were immunoprecipitated with FLAG or with GFP antibodies and the potential interactions examined by western blotting (data not shown). In both experiments attempted, the results were non-specific. For example, the GFP antibody precipitated FLAG-TRAF3 and FLAG-TRAF6 in samples that lacked GFP-A52, suggesting that the GFP antibody could detect the FLAG-tagged proteins (data not shown). Thus, a different strategy was required to compare the ability of A52 to interact with different TRAFs.

3.2.6 Cloning of the TRAFs into the pCMV-HA vector was unsuccessful

The ability of the FLAG antibody to detect A52 made it difficult to determine if there was a specific interaction between the FLAG-TRAFs and A52. In order to circumvent this problem, the TRAFs were subcloned into the pCMV-HA vector. The resulting HA-tagged TRAFs would then be used to test for an interaction with A52, either by co-immunoprecipitation or by using the GST-A52 in pull-downs. TRAF6 had already been subcloned into the pCMV-myc vector using the EcoRI/ XhoI restriction sites. The TRAF6 insert was successfully cleaved from the myc vector and ligated into the pCMV-HA vector. The HA-TRAF6 construct was sequenced and found to be correct.

The coding sequences for the human TRAFs 1-5 were obtained from the NCBI database and then primers were designed that hybridised to the coding sequence of each TRAF. The primers were designed with *EcoRI* (forward) and *XhoI* (reverse) restriction sites. The TRAFs were then amplified by PCR with the KOD high-fidelity polymerase after first optimising the PCR conditions for each TRAF (Figure 3.11, panel A). The number of bases of each TRAF insert corresponded approximately to the length of each PCR product based on a comparison with the reference bands of the 2-log DNA ladder (Figure 3.11, panel A).

The PCR products were digested with EcoRI and XhoI, followed by gel cleanup and then ligation into pCMV-HA that had also been cut with EcoRI/ XhoI and purified. Following ligation and transformation, the colonies were selected and cultured for mini-preparation of plasmid DNA. This was attempted numerous times without success, possibly due to vectors ligating to other vectors rather than the insert (data not shown). To prevent the vectors from ligating to each other, the EcoRI/ XhoI-cut vector was treated with calf intestinal alkaline phosphatase and the ligation was re-done but without success (data not shown). Many parameters were altered to improve the

ligation efficiency, such as altering the insert-vector ratio and using a different ligase (data not shown). The use of the Quick Ligase enzyme and a 10:1 ratio insert to vector ratio seemed to have produced successful constructs (see below).

The DNA was then subjected to digestion with EcoRI/ XhoI enzymes in order to test for insertion of the TRAF DNA into the vector (Figure 3.11, panel B). The agarose gel shows that only TRAF5 and TRAF6 had been inserted (Figure 3.11, panel B, last two lanes). TRAF1 was previously found to be inserted by the same method on another agarose gel (not shown). In addition, the plasmid preparations had also been digested with EcoRI alone as it was hypothesised that a step-wise digest with each EcoRI/ XhoI on their own might be more effective (not shown). Following the EcoRI digest, the samples were analysed by gel electrophoresis and the TRAFs 2-5 showed a size shift relative to the empty vector alone consistent with insertion of the respective TRAF PCR products (not shown).

Given the evidence that the TRAF DNA had potentially been inserted into the vector, all the plasmids were sequenced. TRAFs 2 and 5 came back with the correct sequence, while the plasmids for TRAFs 1, 3 and 4 failed to sequence correctly. The reason for the failed sequencing reactions is unknown and attempts to re-do the reactions proved unsuccessful (data not shown).

While waiting for the sequencing data, the HA-TRAF constructs were tested for expression by transfection into R1s with either GeneJuice or calcium phosphate. The cells were harvested, lysed and analysed by SDS-PAGE and western blotting. Incubation with the HA antibody failed to detect any HA-tagged TRAF proteins (not shown). When the sequencing results suggested only TRAFs 2 and 5 were correctly inserted into the vector, the expression study was performed again, along with the HA-TRAF6 construct

that had also had the correct sequence. A HA-tagged protein known to express well, HA-p65, was used as a positive control. Only HA-p65 is expressed as a HA-tagged protein (Figure 3.12, lane 8).TRAF2 (lanes 2 and 3), TRAF5 (lanes 4 and 5) and TRAF6 (lanes 6 and 7) are either not HA-tagged or do not express following transfection (Figure 3.12). It was suggested that the problem could be due to a mix up in the pCMV-HA and pCMV-myc vectors. Both vectors have the same multiple cloning site sequences. Furthermore, the original cloning of TRAF6 into the pCMV-myc vector had used the *EcoRI/XhoI* restriction sites. To test this hypothesis, the same samples used to test for expression of the HA-tagged constructs were loaded onto a gel, transferred to PVDF and the blot incubated with myc antibody (Figure 3.13). The TRAF6 construct that was thought to be HA-tagged appeared to be myc-tagged (Figure 3.13, lane 8). There was likely too much protein loaded on the gel, which could account for the smear instead of a distinct band for myc-TRAF6. Close examination of the blots revealed a band at the correct size for TRAF6 but this is difficult to distinguish from the smear of bands on the blot. Curiously, neither TRAF2 (lanes 2 and 3) nor TRAF5 (lanes 4 and 5) are expressed as myc-tagged proteins (Figure 3.13), despite the fact that sequencing showed that the TRAFs were correctly inserted into the vector. A previous set of constructs had been made and had not expressed as determined at the time by probing the blot with the HA antibody (not shown). In order to test whether these constructs were actually myc-tagged, the old blots were stripped and reprobed for myc but only TRAF6 was myc-tagged (data not shown). While it is possible that the pCMV-myc and pCMV-HA vectors were mixed up, this does not rule out other problems with the vector or with the cloning that could prevent expression of the tagged protein.

3.2.7 A52 immunoprecipitates with endogenous TRAFs 2, 3 and 6

Given the antibody cross-reactivity observed with A52 and the FLAG-TRAFs (section 3.5) and the problems with cloning and expression of the HA-TRAFs (section 3.6), the next

strategy was to immunoprecipitate the endogenous TRAFs. To do so, antibodies to TRAF2, TRAF3 and TRAF6 were acquired and coupled to protein A sepharose beads. Whole cell extracts from R1s transfected with 8μg of either pRK5 or A52 were incubated with the antibody-protein A beads. The immunoprecipitation was allowed to incubate overnight. The following day, the beads were collected by centrifugation and washed three times in lysis buffer. The initial result obtained indicated that A52 was present with TRAF2, TRAF3 and TRAF6 in immunoprecipitates (data not shown).

Since previous work with over-expressed FLAG-TRAF2 had found that A52 did not co-immunoprecipitate with TRAF2 (Harte *et al.*, 2003), it was conceivable that the endogenous immunoprecipitation results were non-specific. In order to address this possibility, the lysis and immunoprecipitation conditions were made more stringent. The endogenous TRAF immunoprecipitation was incubated for only two hours and the beads were washed three times in a high salt lysis buffer (250mM NaCl). The same result was obtained, suggesting that A52 might interact with each TRAF2, TRAF3 and TRAF6 (data not shown). In order to further increase the stringency of the co-immunoprecipitation experiments and given that the A52 construct expresses very well following transfection, the amount of A52 transfected was reduced from 8μg to 1μg for the third experiment. The immunoprecipitation was once again allowed to proceed for two hours and the beads were washed with the high salt buffer. Once again, A52 appeared to co-immunoprecipitate with endogenous TRAF2, TRAF3 and TRAF6 (Figure 3.14, top panel). The amount of A52 expressed is still abundant and could probably be reduced further (Figure 3.14, bottom panel). It was surprising to find that both TRAF2 and TRAF3 could co-immunoprecipitate with A52. Further work is needed to determine if these interactions are specific. For the remainder of the thesis, the nature and function of the A52-TRAF6 interaction was studied.

3.2.8 A52 interacts with TRAF6 in the absence of IRAK1 and IRAK2

A52 has been found to interact with both TRAF6 and IRAK2. Since IRAK2 and TRAF6 are known to interact themselves, an immunoprecipitation experiment for TRAF6 was done in IRAK2$^{-/-}$ MEFs to determine if the A52-TRAF6 interaction was independent of IRAK2 (Figure 3.15). This experiment was possible due to the recent generation of IRAK2$^{-/-}$ mice (described in Kawagoe *et al.*, 2008). The wild-type and IRAK2$^{-/-}$ MEFs were provided by S. Akira (see Chapter 2). Immunoprecipitation of TRAF6 followed by blotting for A52 detected an interaction band in IRAK2$^{-/-}$ MEFs (Figure 3.15, top panel, lane 4), suggesting that A52 could interact with TRAF6 in the absence of IRAK2. Unfortunately, the interaction band was not detected in the IRAK2 wild-type MEFs (Figure 3.15, top panel, lane 2). This might suggest that A52 and TRAF6 interact better in the absence of IRAK2, which would be consistent with previous work showing that A52-IRAK2 (Keating *et al.*, 2007) and A52-TRAF6 (Maloney *et al.*, 2005) interactions are independent. For example, the absence of one or the other binding partner might make the site of interaction with the other partner more accessible to A52. A52 had previously been found not to interact with IRAK1 (Harte *et al.*, 2003) and thus it was likely that A52 would still interact with TRAF6 in the absence of IRAK1. To confirm this, the ability of A52 to co-immunoprecipitate with TRAF6 in the absence of IRAK1 was tested using IRAK1-deficient cells (I1A). In the I1A cells, there was a clear interaction band, indicating that A52 binds to TRAF6 in the absence of IRAK1 (Figure 3.15, top panel, lane 6). TRAF6 immunoprecipitates itself equally in the different cell types, resting just above the heavy chain (Figure 3.15, middle panel). Unfortunately, while A52 is expressed in the three cell types, the blot is very dark and it is difficult to discern the bands (Figure 3.15, bottom panel). The level of expression was lower in the MEFs than in the I1A cells (Figure 3.15, bottom panel, compare lanes 2 and 4 to lane 6). This experiment could not be attempted again in the MEFs due to difficulty with culturing the cells for more than one ore two passages and the lack of sufficient cell numbers to

set down the 100mm dishes required. While preliminary, this experiment provides initial evidence that A52 interacts with TRAF6 independently of IRAK1 or IRAK2.

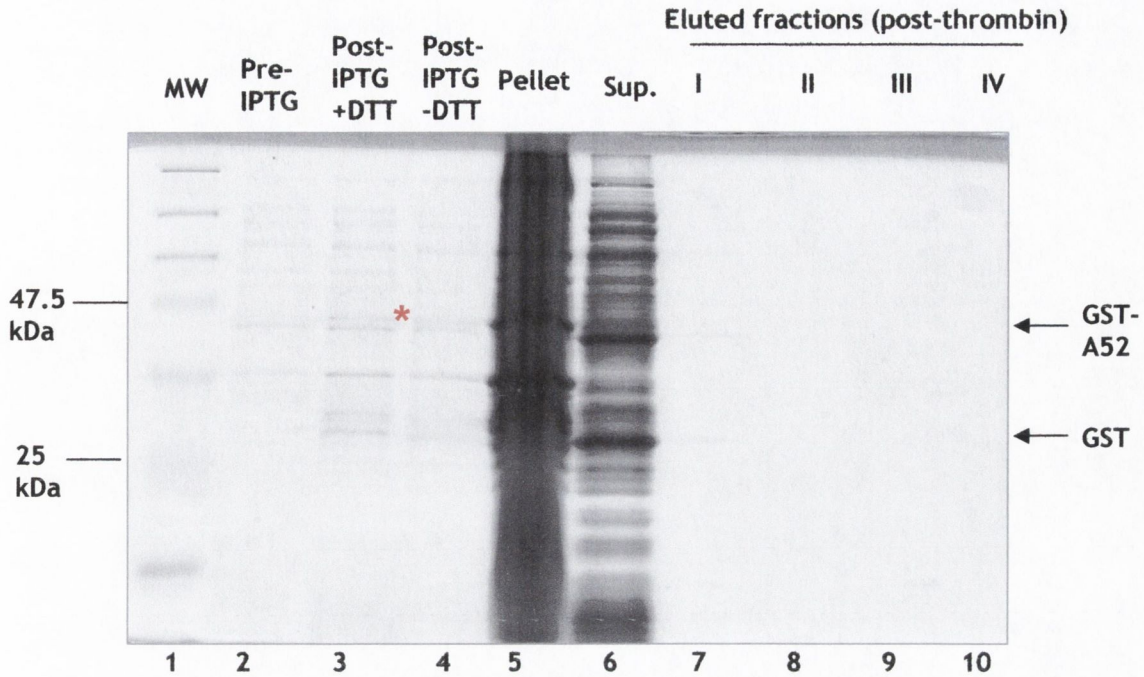

Figure 3.1 GST-A52 is weakly expressed in BL21(DE3) *E. coli* cells.

A single colony of BL21(DE3) cells transformed with pGEX-4T2 encoding GST-A52 was selected and cultured in LB broth until an OD of 0.6 was reached (lane 2). Protein expression was induced by addition of IPTG. The bacterial culture was harvested four hours post-induction and samples were taken (lane 3 and 4). The bacterial cells were pelleted by centrifugation, the cells were lysed in extraction buffer (300mM NaCl in PBS and 1% Triton-X-100) with sonication and then the lysate was centrifuged again. Samples of the pellet (lane 5) and the supernatant (lane 6) were reserved for gel analysis. The supernatant was incubated with glutathione sepharose beads for two hours and then the beads were washed several times in the extraction buffer. The GST-A52-bound beads were incubated with thrombin to cleave the A52 from the GST tag and fractions were collected that should have contained free A52 (lanes 7-10).

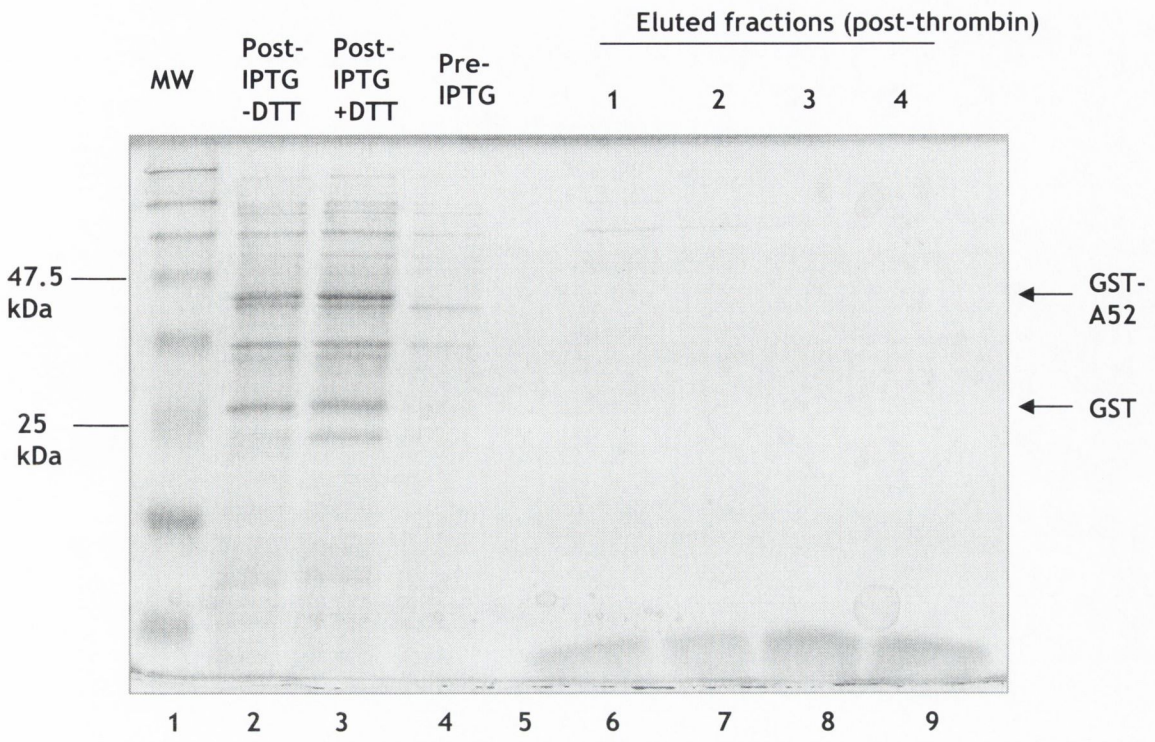

Figure 3.2 GST-A52 is expressed more strongly in Rosetta-Gami 2 cells.

GST-A52 was transformed into the E. coli cell line Rosetta-Gami 2 and a single colony was used to inoculate 10mL of LB media, which was incubated overnight at 37°C. The overnight culture was used to inoculate 1L of LB broth and the culture was incubated at 37°C for approximately four hours until an OD of 0.6 was attained. An aliquot of the pre-induction culture was harvested at this point (lane 4). Protein expression was then induced by the addition of 500µL 1M IPTG. The culture was incubated for a further six hours at 25°C. Two samples of the culture were taken, one mixed with denaturing sample buffer (lane 3) and the other mixed with nondenaturing sample buffer (lane 2). The cells were then pelleted by centrifugation and the protein was subsequently extracted with sonication in a low salt buffer (300mM NaCl in PBS and 1% Triton-X-100) containing protease inhibitors. The supernatant containing the soluble fraction of the GST-A52 protein was incubated with glutathione sepharose beads. The beads were washed several times, incubated with thrombin and the fractions collected (lanes 6-9). The samples were analysed by SDS-PAGE followed by staining with Coomassie blue.

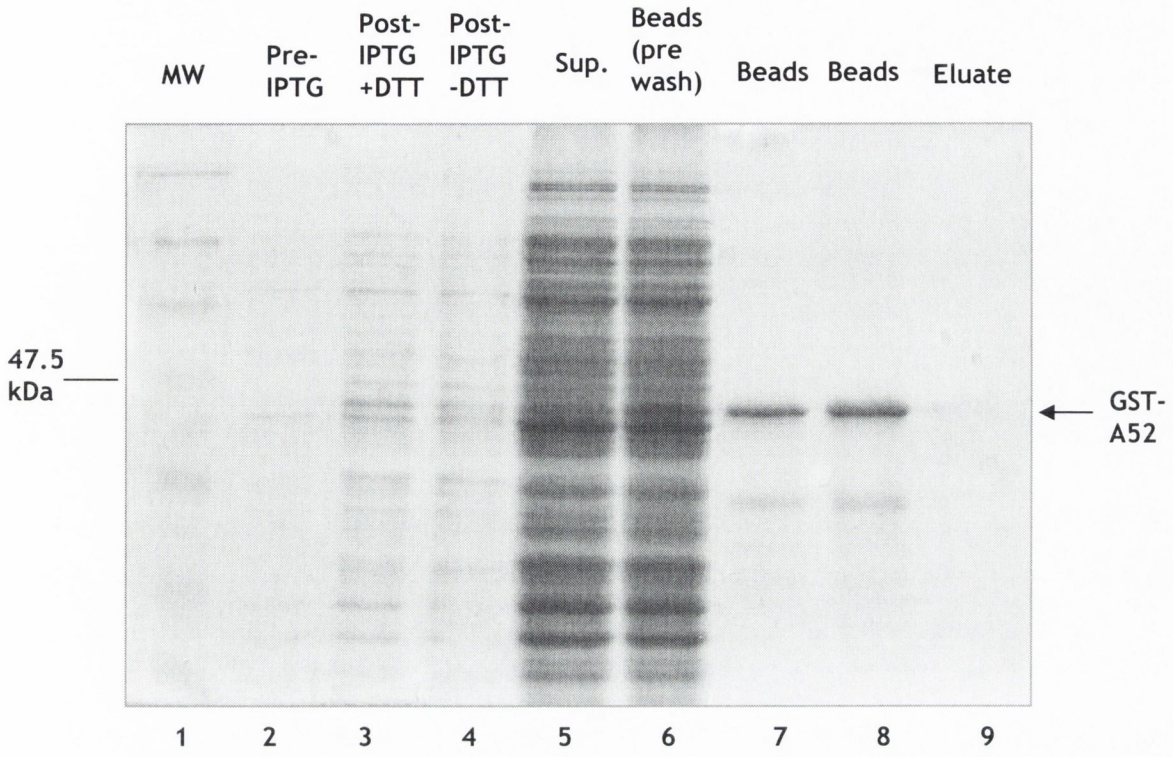

Figure 3.3 GST-A52 does not elute from glutathione beads with 10mM reduced glutathione.

GST-A52 is expressed in Rosetta-Gami 2 cells following induction with IPTG (lanes 3 and 4). The cells were lysed by sonication in extraction buffer (PBS with 300mM NaCl and 1% Triton-X-100) supplemented with protease inhibitors. The supernatant from the lysed bacterial cells (lane 5) was incubated with glutathione sepharose beads (lane 6). The beads were washed four times with extraction buffer (lane 7). The beads were washed twice more with high salt (600mM NaCl) extraction buffer (lane 8). The beads were then incubated with elution buffer (50mM Tris pH 8.0, 10mM reduced glutathione) for 90min at 4°C and the eluate was collected (lane 9).

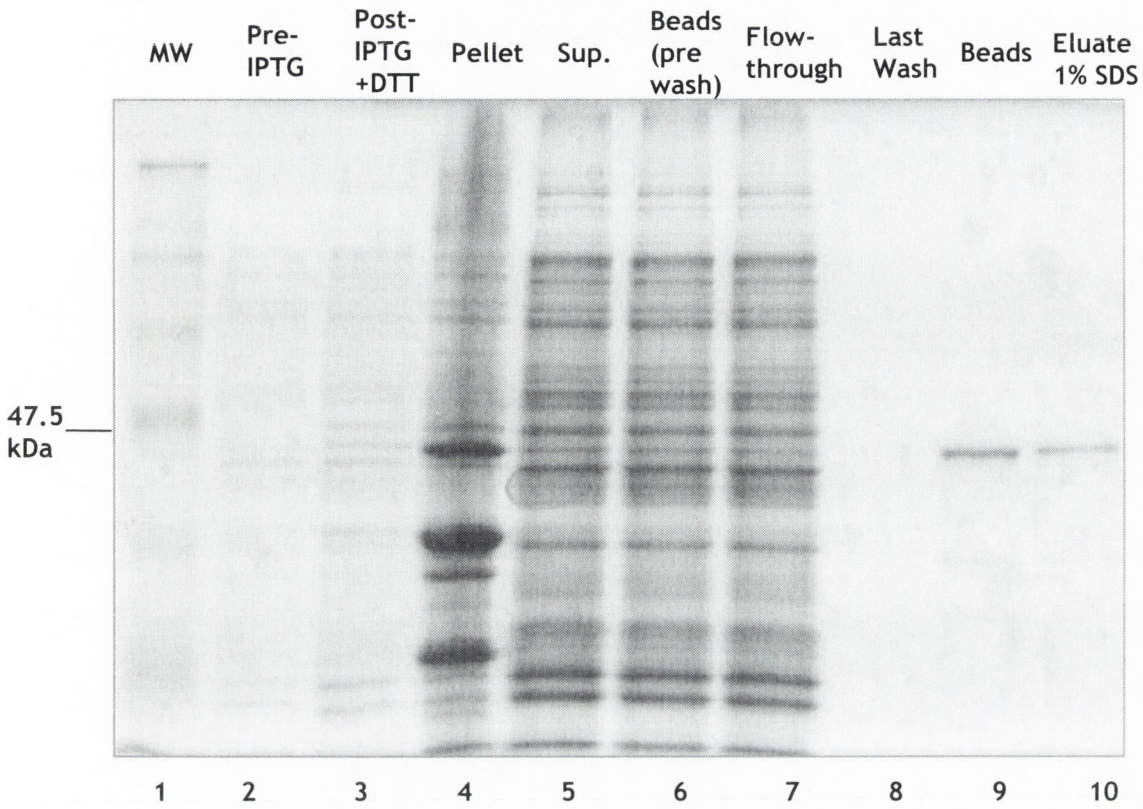

Figure 3.4 GST-A52 is eluted from glutathione sepharose beads with 1% SDS.

GST-A52 was transformed into the Rosetta-Gami2 competent cells and a single colony was cultured in LB broth until an OD of 0.6 was reached (lane 2). The culture was induced with 1M IPTG and incubated for a further four hours at 25°C (lane 3). The cells were lysed by sonication in extraction buffer (PBS with 300mM NaCl and 1% Triton-X-100) supplemented with protease inhibitors. The lysate was centrifuged, a sample of the insoluble pellet was taken (lane 4) and the supernatant (lane 5) was incubated with glutathione sepharose beads (lane 6). The beads were loaded into a column and allowed to settle. A sample of the flow-through was taken (lane 7). The beads were washed four times with high salt (600mM NaCl) extraction buffer and samples of the last wash flow-through (lane 8) and the washed beads (lane 9) were taken for gel analysis. The beads were then incubated with elution buffer (50mM Tris pH 8.0, 10mM reduced glutathione, 1% SDS) for 10min at 4°C and the eluate was collected (lane 10).

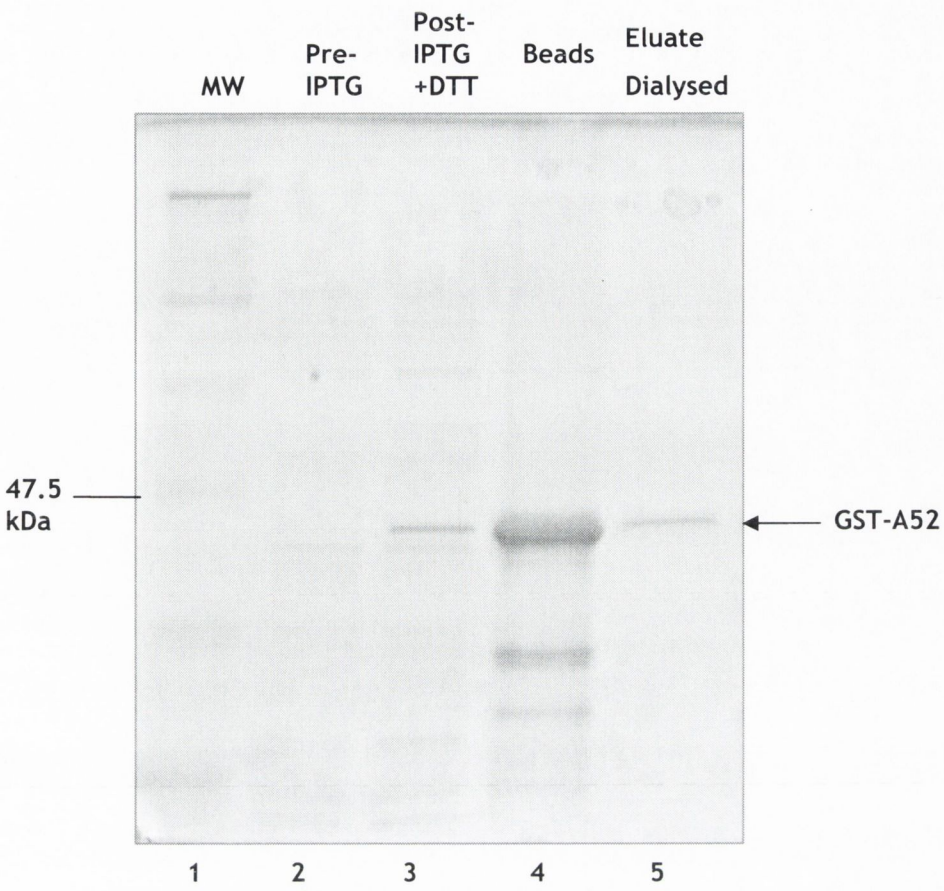

Figure 3.5 GST-A52 eluted with 20mM reduced glutathione is used for antibody production.

GST-A52 was transformed into the Rosetta-Gami2 competent cells and a single colony was cultured in LB broth until an OD of 0.6 was reached (lane 2). The culture was induced with 1M IPTG and incubated for a further four hours at 25°C (lane 3). The cells were lysed by sonication in extraction buffer (PBS with 300mM NaCl and 1% Triton-X-100) supplemented with protease inhibitors. The lysate was centrifuged and the supernatant was incubated with glutathione sepharose beads. The beads were loaded into a column and allowed to settle. The beads were washed four times with high salt (600mM NaCl) extraction buffer and a sample of the washed beads (lane 4) was reserved for gel analysis. The beads were then incubated with elution buffer (50mM Tris pH 8.0, 20mM reduced glutathione, 1% Triton-X-100) for 10min at 4°C and the eluate was collected. The eluate was dialysed against PBS overnight to remove the glutathione and Triton-X-100 (lane 5). The resulting purified GST-A52 fusion protein was used for antibody production.

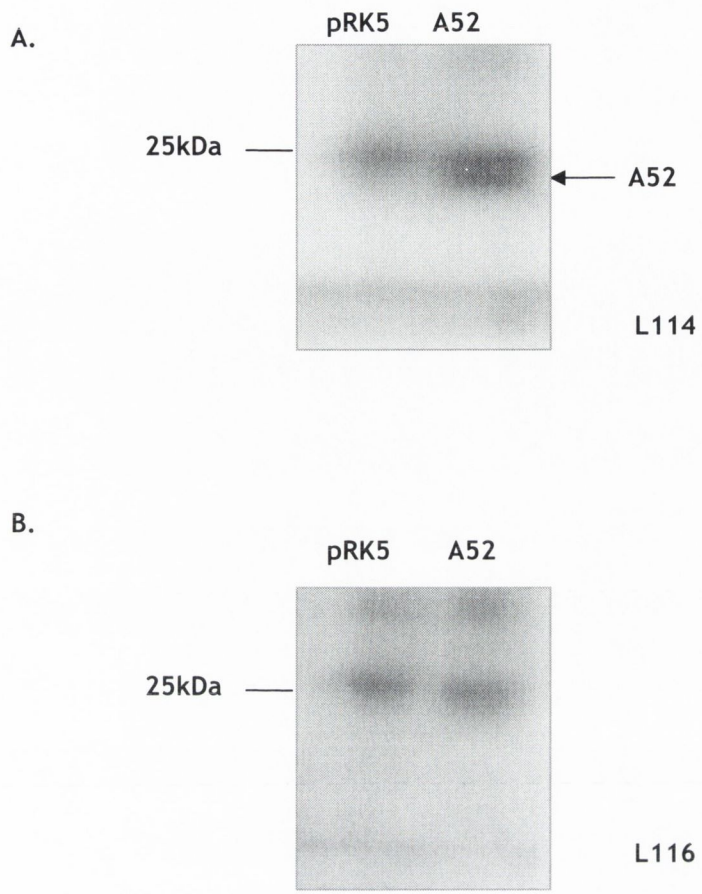

Figure 3.6 Antibodies raised to GST-A52 in rabbit L114 may detect A52 over-expressed in R1s.

R1s were seeded at 1 x 10^5 cells/mL in 6-well plates and then were transfected 36 hours later with 2.3 µg of either empty vector (pRK5) or A52. The cells were harvested 24 hours later by scraping into sample buffer. Following sonication and boiling to disrupt the cell membranes, the samples were resolved by SDS-PAGE and transferred to PVDF. The resulting blots were incubated with serum from either rabbit L114 (panel A) or rabbit L116 (panel B). A band corresponding to A52 was detected on the blot incubated with serum L114 (arrow, panel A) but not with serum L116 (panel B).

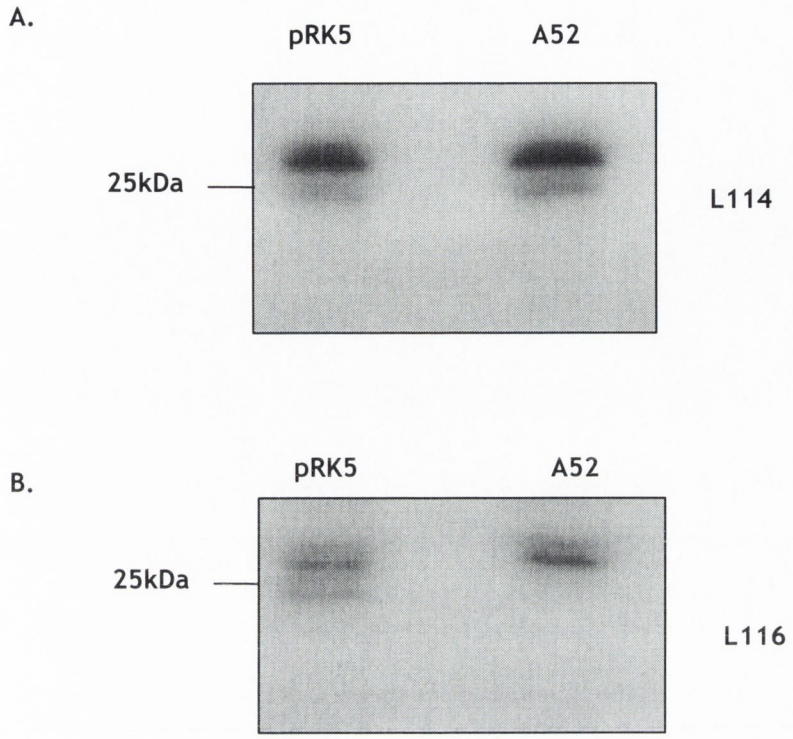

Figure 3.7 Antibodies to GST-A52 do not detect A52 over-expressed in R1s.

R1s were seeded at 1 x 10^5 cells/mL in 6-well plates and then were transfected 24 hours later with pRK5 (2.3 μg) or A52 (1μg). The cells were harvested 24 hours later by scraping into sample buffer. Following sonication and boiling to disrupt the cell membranes, the samples were resolved by SDS-PAGE and transferred to PVDF. The resulting blots were incubated with serum from either rabbit L114 (panel A) or rabbit L116 (panel B). A52 was not detected on either blot.

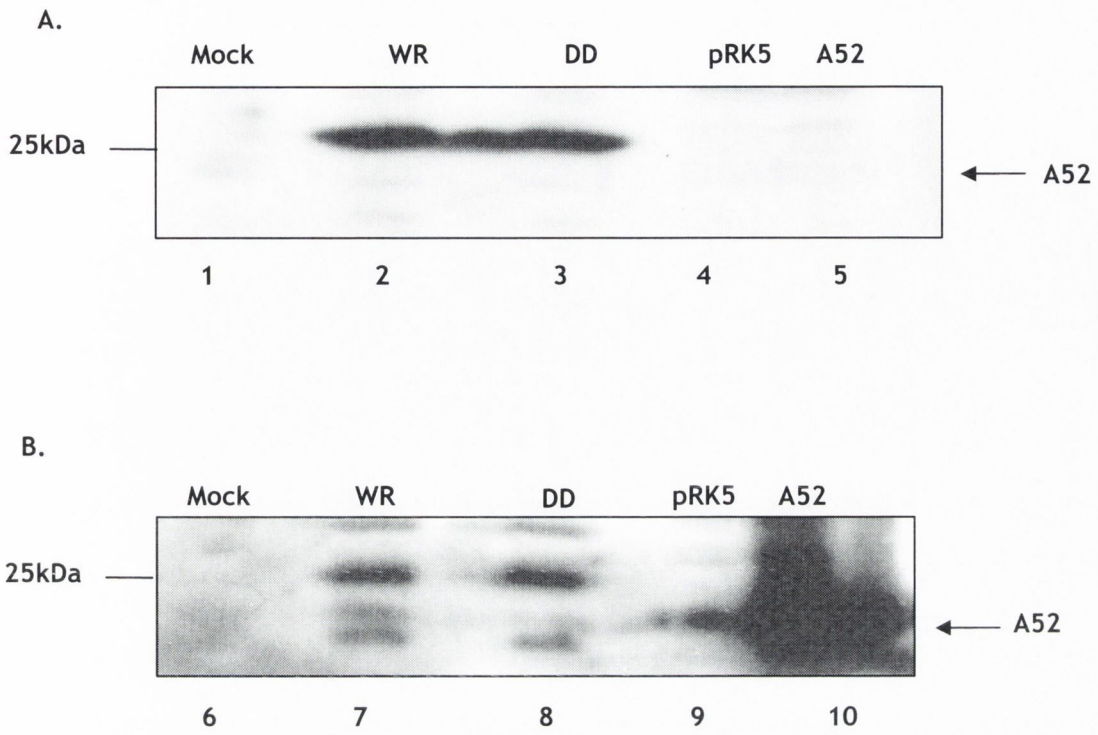

Figure 3.8 Antibodies raised against a peptide of A52 do not detect the over-expressed A52.

R1s were seeded at 1 x 10^5 cells/mL in 100mm dishes 24 hours prior to transfection. The following day, the cells were transfected with 8μg of pRK5 (lanes 1-4) or A52 (lane 5). The next day, the cells were infected with VACV by removing the media (10% FCS) and replacing it with minimal media (2.5% FCS) containing the required volume of either WR or DD, a VACV lacking both A46R and A52R ORFs (lanes 2 and 3). The infection was allowed to proceed for one hour with gentle rocking of the dishes. The inoculum was replaced with fresh media (10% FCS) and the cells were harvested 8 hours later. The mock infection (lane 1) was treated as the VACV-infected cells but with no virus in the inoculum. The infected (lanes 1-3) and transfected cells (lanes 4 and 5) were harvested at the same time by scraping into sample buffer followed by sonication and boiling. The samples were then resolved by SDS-PAGE and transferred to PVDF using a semi-dry transfer system. The blot was incubated with serum from rabbit SG-4608 which had been immunised with the A52 peptide (panel A). The blot in panel A was stripped and reprobed with the antibody to A52 made as described in Harte *et al.*, 2003(panel B).

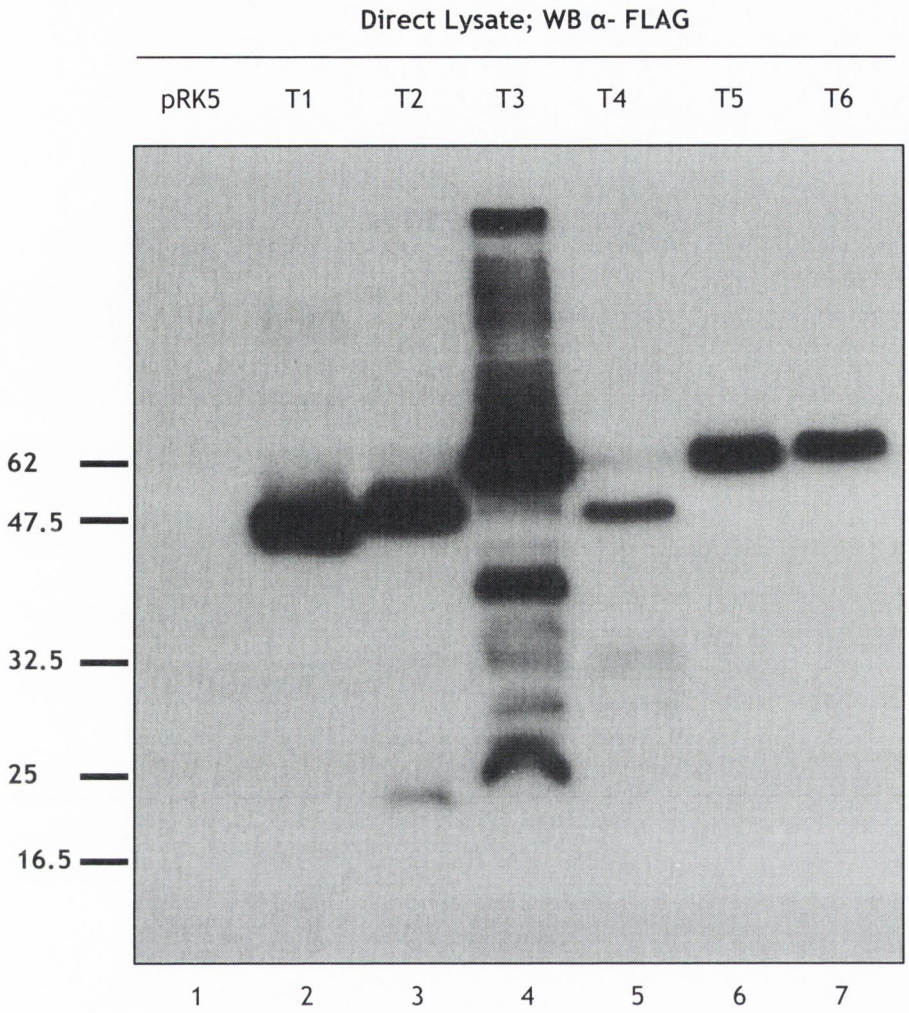

Figure 3.9 The FLAG-TRAFs are expressed and are detected with the FLAG antibody

HEK-293 R1 cells were seeded at 1.5 x 10^5 cells/mL in 100mm dishes 24 hours prior to transfection. Cells were transfected with 8μg of empty vector (pRK5) or of expression vectors encoding FLAG-TRAFs 1-6 (T1-T6) using GeneJuice™ according to the manufacturer's directions. The cells were harvested 24 hours post-transfection and were lysed in SDS-containing sample buffer. The lysates were resolved by SDS-PAGE. The proteins were transferred to Immobilon PVDF membrane by a wet transfer system. The blot was probed with antibody specific to FLAG. Representative of one experiment by the direct lysis method described above.

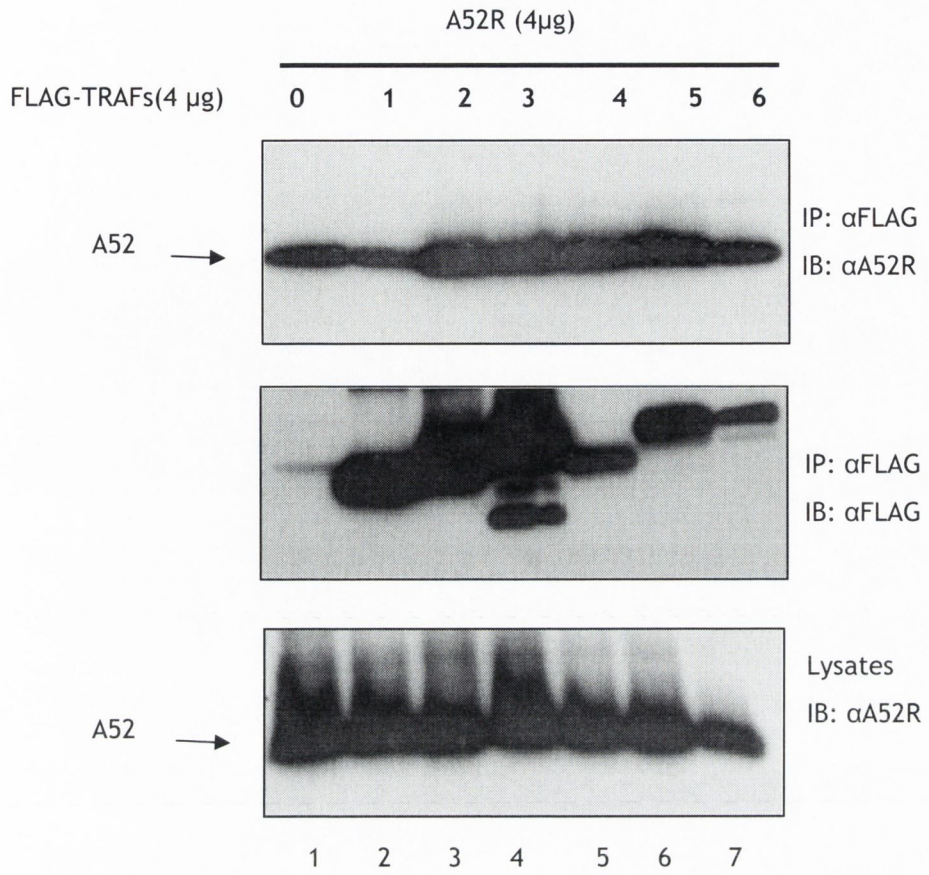

Figure 3.10 The FLAG antibody cross-reacts with A52R.

HEK-293 R1 cells were seeded at 1x 10^5 cells/mL in 100mm dishes 24 hours prior to transfection. Cells were co-transfected with A52R (4μg) and each of the FLAG-TRAFs 1-6 (4μg) using GeneJuice™ according to the manufacturer's directions. The cells were harvested 24 hours post-transfection and were lysed using NP40- and glycerol-containing lysis buffer. The lysates were immunoprecipitated for either A52R or FLAG and then resolved by SDS-PAGE. The proteins were transferred to Immobilon using a wet transfer system. The blot was probed with anti-A52 or anti-FLAG antibodies. Representative of four experiments.

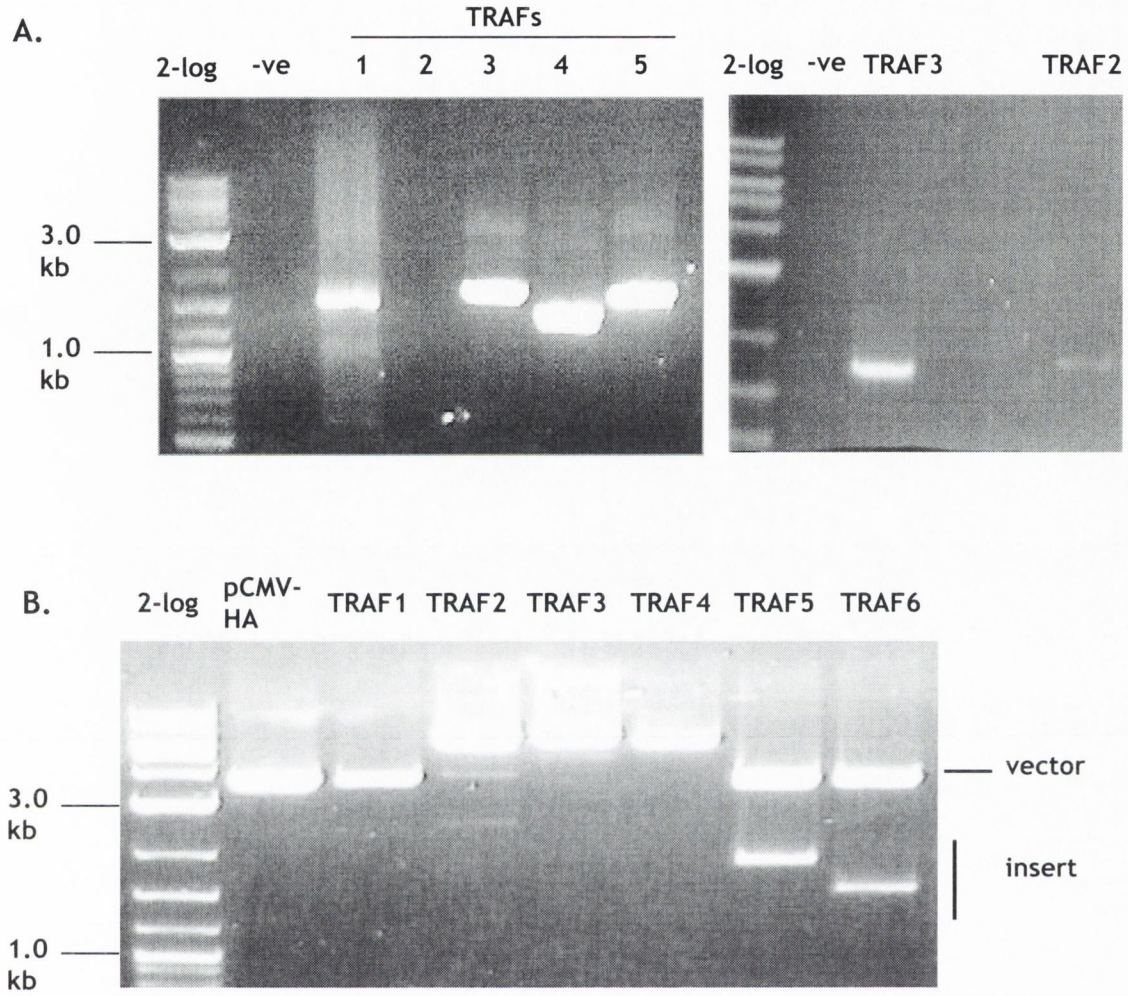

Figure 3.11 Sub-cloning of the TRAFs into the pCMV-HA vector.

Primers were designed to the coding sequence of each of the TRAFs 1-5 which also had engineered EcoRI and XhoI restriction sites. The primers were used to amplify the TRAFs from the FLAG-tagged construct by PCR and the PCR products were analysed on an agarose gel (Panel A, left-hand gel). TRAF2 PCR conditions required further optimisation before observing a product (Panel A, right-hand gel). Following ligation and transformation (see Methods, Chapter 2), individual colonies were selected, cultured and screened for successful insertion of the TRAFs by digestion with EcoRI/XhoI (panel B). 2log refers to the DNA marker. The negative (-ve) control in the PCR reactions was a reaction done without primers.

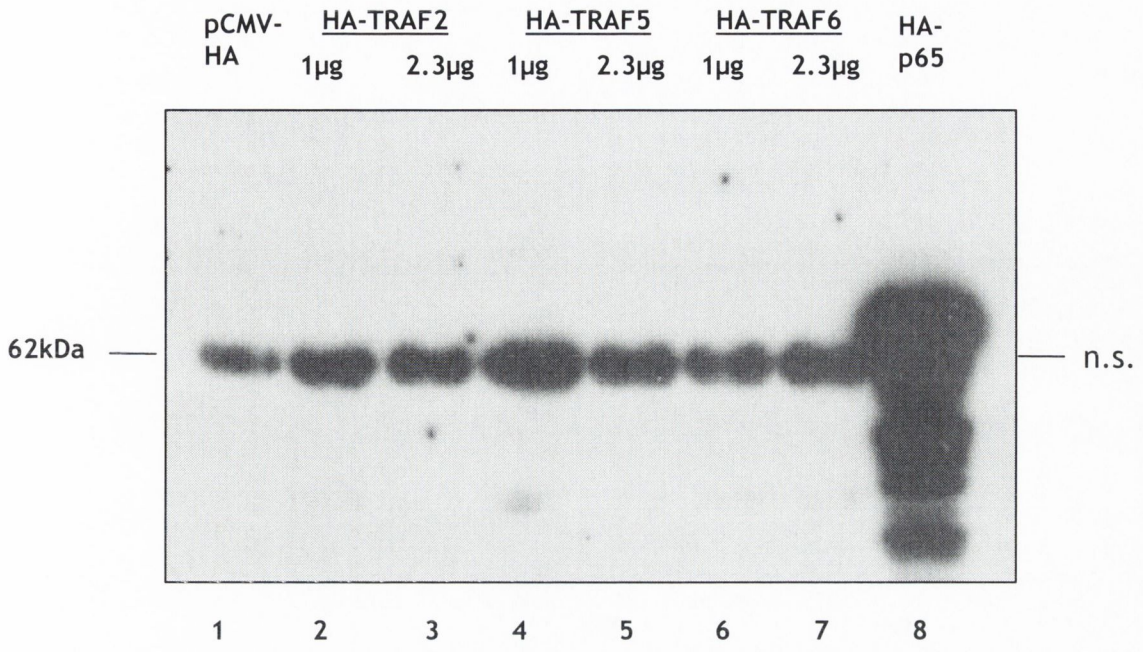

Figure 3.12 The HA-TRAFs are not expressed.

HEK-293 R1 cells were seeded at 1x 10^5 cells/mL in 6-well plates 24 hours prior to transfection. Cells were transfected with each of the HA-TRAF2, HA-TRAF5 or HA-TRAF6 (1 or 2.3µg) using GeneJuice™ according to the manufacturer's directions. The cells were harvested 24 hours post-transfection by scraping into sample buffer. The samples were sonicated, boiled and then resolved by SDS-PAGE. The proteins were transferred to PVDF and the resulting blot was incubated with HA antibody. n.s., non-specific band detected in all lanes

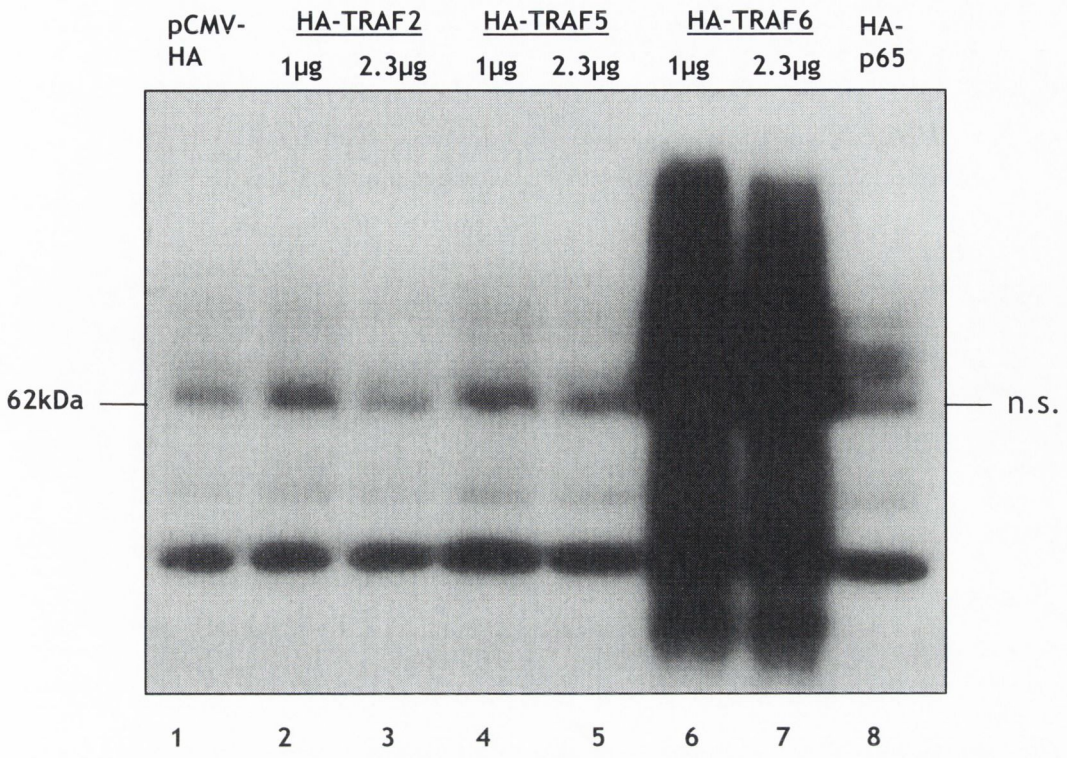

Figure 3.13 HA-TRAF6 is myc-tagged and the other TRAFs are not expressed.

HEK-293 R1 cells were seeded at 1x 10^5 cells/mL in 6-well plates 24 hours prior to transfection. Cells were transfected with each of the HA-TRAFs 2,5 or 6 (1 or 2.3μg) using GeneJuice™ according to the manufacturer's directions. The cells were harvested 24 hours post-transfection by scraping into sample buffer. The samples were sonicated, boiled and then resolved by SDS-PAGE. The proteins were transferred to PVDF and the resulting blot was incubated with myc antibody. n.s., non-specific band detected in all lanes

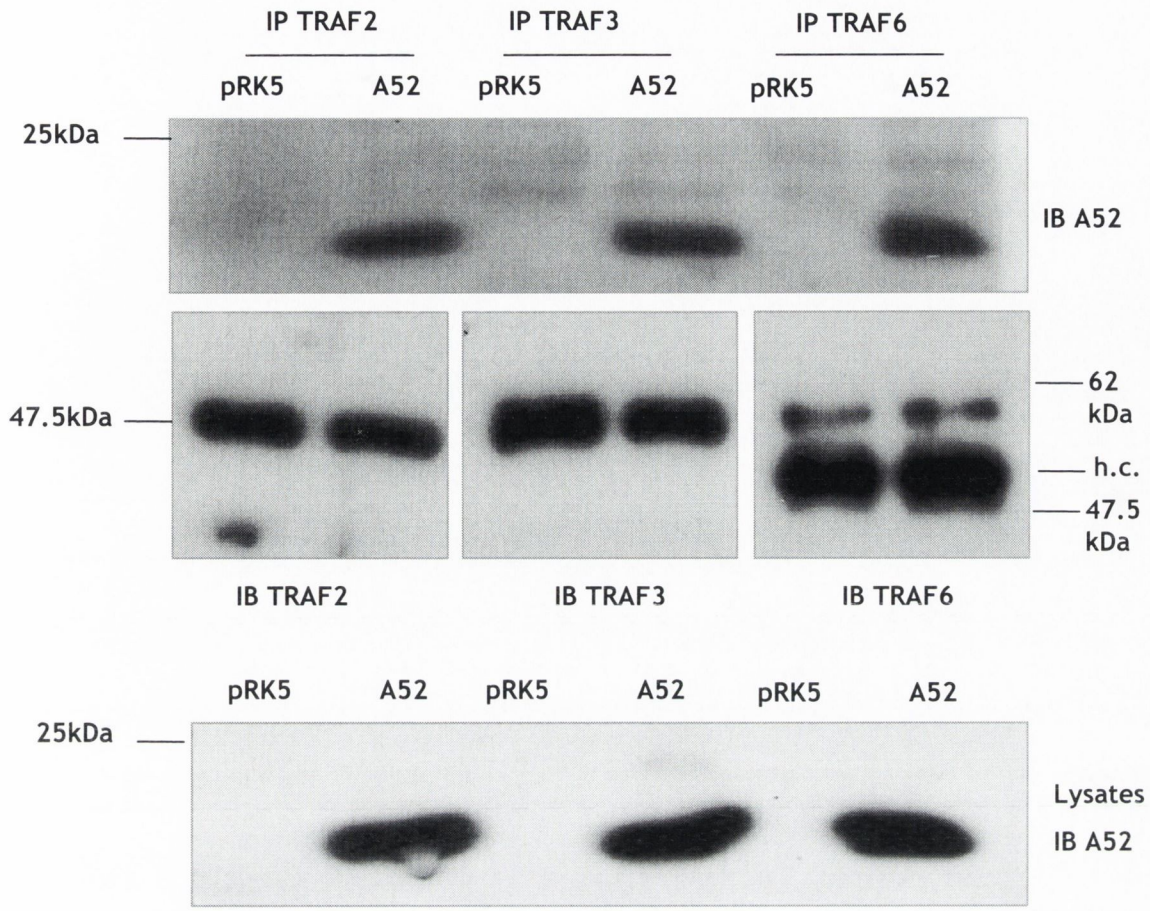

Figure 3.14 A52 interacts with endogenous TRAF2, TRAF3 and TRAF6.

R1 cells were seeded at 1x 10^5 cells/mL in 100mm-dishes 24 hours prior to transfection. Cells were transfected with either pRK5 (8μg) or A52 (1μg) using GeneJuice™ according to the manufacturer's directions. The cells were harvested 24 hours post-transfection. The cells were lysed in lysis buffer (50mM HEPES, 100mM NaCl, 1mM EDTA, 10% glycerol, 0.5% NP-40) supplemented with protease inhibitors. The cell extract was incubated with either TRAF2, TRAF3 or TRAF6 antibodies coupled to protein A sepharose beads for two hours. Subsequently, the beads were collected washed in a high salt stringent buffer (50mM HEPES, 250mM NaCl, 1mM EDTA, 10% glycerol, 1% NP-40). The final wash buffer did not have glycerol or NP-40. All the buffers used were supplemented with protease inhibitors. The samples were mixed with sample buffer, boiled and resolved by SDS-PAGE. The proteins were transferred to PVDF and the resulting blots were probed with antibodies to A52 or to either TRAFs 2, 3 or 6, as indicated. No heavy chain was detected in IP/IB TRAF2 and TRAF3 blots but it was observed in the IP/IB TRAF6 blot. TRAF2 and TRAF3 migrated to above the 47.5kDa marker, while TRAF6 migrated to just below the 62kDa marker. h.c., antibody heavy chain

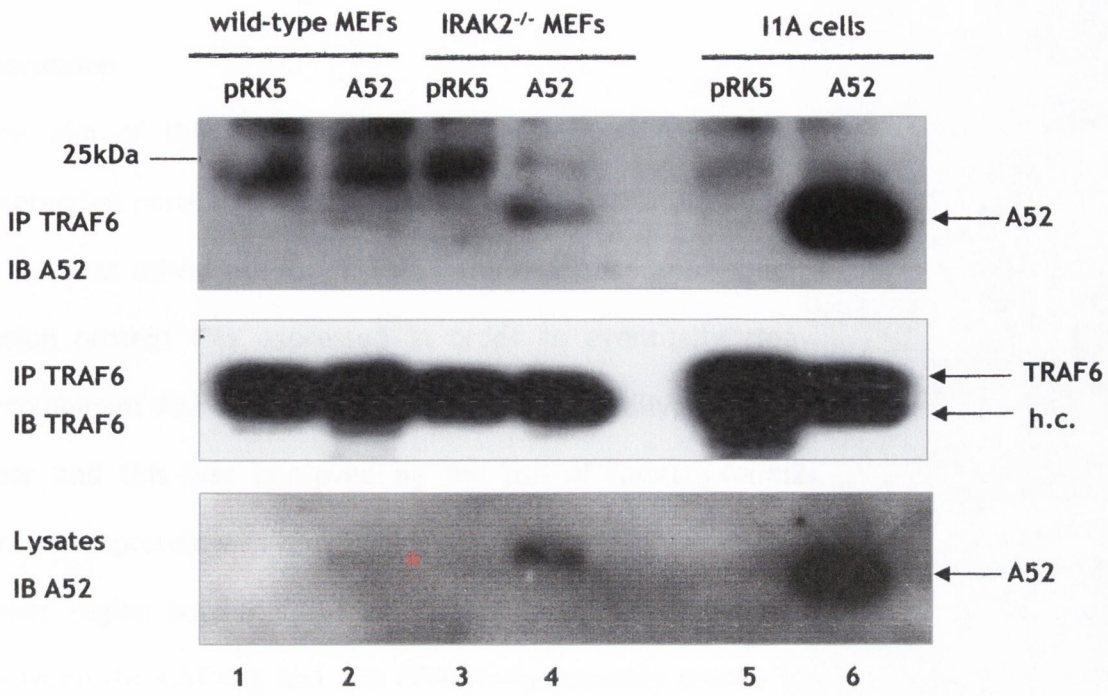

Figure 3.15 A52 interacts with endogenous TRAF6 in IRAK2 knock out MEFs and IRAK1-deficient 293 HEKs.

IRAK2 wild-type or knockout MEFs were seeded into 100mm dishes 24 hours prior to transfection. HEK-293 IRAK1-deficient cells were seeded at 1x 10^5 cells/mL in 100mm-dishes 24 hours prior to transfection. Cells were transfected with either pRK5 or A52 (8μg) using GeneJuice™ according to the manufacturer's directions. The cells were harvested 24 hours post-transfection, lysed in lysis buffer (50mM HEPES, 100mM NaCl, 1mM EDTA, 10% glycerol, 0.5% NP-40) supplemented with protease inhibitors, and the resulting cell extract incubated with protein A sepharose beads coupled to TRAF6 antibody. The beads were collected by centrifugation and washed three times is the lysis buffer containing protease inhibitors. The final wash step used buffer lacking NP-40 and glycerol. Sample buffer was added to the beads, which were then boiled and analysed by SDS-PAGE. The proteins were transferred from the polyacrylamide gel to PVDF and the blot was then probed with either the A52 or TRAF6 antibodies, as indicated. * The expression of A52 in the IRAK2 wild-type MEFs.

Discussion

One aim of this project was to improve the tools required to search for novel interaction partners of A52. In particular, a better antibody was required since the one in use was raised against GST-A52 and recognised non-specific proteins. The GST-A52 fusion protein was expressed in order to eventually cleave the GST, leaving free recombinant A52 for antibody production. Initially, expression of GST-tagged A52 was poor and this was improved by the use of Rosetta-Gami2 competent cells. Once sufficient protein was obtained, all that remained was to cleave the fusion protein at a linker region between GST and A52. However, thrombin did not cleave the linker between the GST-tag and A52 effectively, possibly due to low activity of the enzyme. Folding of the fusion protein may have excluded the enzyme from its cleavage site, thereby making it impossible for the GST to be removed. There are more effective proteases, such as the Prescission Protease from GE Healthcare, which could be used to cleave the GST-tag in order to generate free recombinant A52 protein.

In order to proceed with antibody production, GST-A52 was used to immunise rabbits in the hope that the antiserum would be able to detect A52. This strategy had been employed previously (Harte *et al.*, 2003), producing an antibody that was able to detect A52, whilst also detecting non-specific proteins. In the present study, the antiserum from rabbit 114 did detect A52 the first time it was tested by western blotting. Although this was not observed when the experiment was repeated, it is possible that purification of the antiserum would improve the detection of A52. Antiserum from rabbit L116 did not detect over-expressed A52 at all. The antisera from both L114 and L116 were not specific, binding to other proteins than A52 in the lysates. The antiserum raised to the GST-A52 in the present study could be purified in order to make it more specific, possibly by incubating it with GST to remove any GST-specific antibodies. It is also possible to affinity purify the antibody but this would require more recombinant

A52, preferably not fused to GST. Since it did not work in the past, it may be difficult or impossible to cleave the fusion protein to produce untagged A52. Alternatively, A52 was successfully cloned into the pHis-parallel 1 vector (data not shown), though the expression of this construct was not tested. If His-A52 expresses well, it could be easier to cleave the His-tag and thus to obtain untagged A52 for antibody production or affinity purification.

The antibodies raised against the peptide from A52 detected a VACV protein that is not A52. This was a curious observation given the immunogenicity of this epitope from A52 (Tscharke *et al.*, 2006). Furthermore, when the peptide was submitted in a search of a poxvirus protein database, the only hits were VACV A52 from numerous strains including WR or the related protein from variola. Thus, if another protein than A52 is detected by the SG-4608 antibody, it must be due to cross-reactivity of the antibody and not because the same epitope is found in another protein. The attempts to produce better A52 antibodies failed. Though it may be possible to improve them by purification, the remainder of the project used the older antibody generated to GST-A52.

The goal of the chapter was to compare the ability of A52 to interact with the TRAFs. Due to the cross-reactivity of the FLAG antibody for A52 and the FLAG-TRAFs, it has been difficult to show which TRAFs interact with A52. This technical difficulty could be overcome by subcloning the TRAFs into vectors with another epitope tag, such as HA. However, as discussed above, the subcloning of the TRAFs into the pCMV-HA vector was problematic and ultimately a failure. Other groups have constructed HA-TRAFs (e.g. Oganesyan *et al.*, 2006) and these could likely be obtained. One strategy that was explored was the use of GST-A52 to pulldown the FLAG-TRAFs. Unfortunately, these experiments are impossible to control since the antibody to A52 also detects GST (data not shown). Ideally, the pulldowns could be repeated once an antibody to A52 and not

GST-A52 is made. The problems with antibody cross-reactivity made it difficult to compare the TRAFs directly so another method had to be used.

In order to investigate A52-TRAF interactions, antibodies to the endogenous TRAFs were to be used. However, the isolation of endogenous TRAFs first required optimisation. Initially, endogenous TRAF6 was immunoprecipitated from whole cell extracts following a twenty-minute lysis period but very little TRAF6 was detected by western blotting following this method. TRAFs are usually found dispersed in the cytoplasm or in punctuate intracellular structures prior to stimulation (Chung *et al.*, 2002). Following stimulation, they have been found to migrate to cytoplasmic membranes or to plasma membrane patches (Ardila-Osorio *et al.*, 2005; Chung *et al.*, 2002; Arch *et al.*, 2000). In the latter case, the TRAFs could be recruited to lipid rafts along with activated receptors, such as CD40 (Chung *et al.*, 2002). The raft localisation is of functional significance since the TRAFs that activate JNK MAPK are found in rafts (Dadgostar and Cheng, 2000). Further, the forced localisation of TRAF3 is sufficient to activate JNK even though TRAF3 normally does not activate MAPK (Dadgostar and Cheng, 2000). Thus, it may be that stimulation of IL-1R/TLR signalling results in the re-localisation of the TRAFs to subcellular membrane systems (mitochondria, endosomes) such that it is relatively insoluble (Li *et al.*, 2006). The subcellular localisation of the TRAFs, particularly if they are localised to insoluble membrane fractions even in the absence of stimulation, can hinder isolation of the TRAFs by usual lysis methods. Thus lysis period was extended to one hour, with frequent vortexing to help solubilise the TRAFs by disrupting the subcellular membranes. The lysis buffer already contained NP40, a non-ionic detergent that can disrupt lipid-lipid and lipid-protein interactions, and thus should have enabled isolation of membrane-associated proteins such as the TRAFs. Endogenous TRAF6 was subsequently isolated by this method and found to interact with over-expressed A52. When lysing the cells for immunoprecipitation of the other

endogenous TRAFs, the same lysis conditions were used. Isolation of the TRAFs by this method worked well for TRAF2 and TRAF6 but did not extract much endogenous TRAF3. TRAF3 is more soluble than TRAF2 (Dadgostar and Cheng, 2000) so there could be other reasons for the difficulty with detection of immunoprecipitated TRAF3 by western blotting. The antibody used for TRAF3 had been used by other researchers (Häcker *et al.*, 2005), so it should be able to detect TRAF3. It could also be that R1s do not express much TRAF3 though other studies using the related cell line HEK 293Ts detected ample TRAF3 (Dadgostar and Cheng, 2000).

Although not able to directly compare all of the TRAFs by using an antibody to A52, it was more expedient to assay the A52-TRAF interactions by immunoprecipitating the endogenous TRAFs and then western blotting for A52. Since TRAF3 has been shown to have a role in TLR signalling (Häcker *et al.*, 2005), it was selected to see if it interacted with A52. As discussed in section 3.7, each TRAF2, TRAF3 and TRAF6 appeared to interact with A52 by this method as A52 was found to be present in immunoprecipitates of endogenous TRAF2, TRAF3 and TRAF6. However, based on previous studies, it was thought that A52 interacts with over-expressed TRAF6 and does not interact with over-expressed TRAF2 (Harte *et al.*, 2003). This finding is consistent with the inhibitory role of A52 in signalling via IL-1R/TLRs but not via TNFR (Harte *et al.*, 2003). As anticipated from other experiments, A52 interacted with endogenous TRAF6. While this was predicted based on the observation that A52 interacts with over-expressed TRAF6 (Harte *et al.*, 2003), the endogenous interaction was not observed in the initial experiments.

In light of the aforementioned role of TRAF3 in both TNFR and IL-1/TLR signalling pathways, it was exciting to observe that TRAF3 could interact with A52. This could be part of the overall strategy of A52 to inhibit NF-κB, since TRAF3 has been proposed to have a regulatory or inhibitory role and acts to suppress the antiviral immune response

(Zapata *et al.*, 2007b). TRAF3 is considered to be an important regulator of TLR-dependent signalling; by directly associating with MyD88 and TRIF, TRAF3 induces the formation of a complex with IRAK1, TBK-I and IKKε, ultimately leading to the activation of IRF3 and IRF7, as well as the induction of type I interferons (Häcker et al, 2005; Oganesyan *et al.*, 2005). Furthermore, TRAF3 regulates LPS-induced type I IFN and IL-10 production by a TRIF-dependent pathway (Häcker et al, 2005). A52 has also been shown to modulate IL-10 production following LPS stimulation (Maloney *et al.*, 2005). If A52 is also able to interact with TRAF3, it may be another mechanism by which A52 can regulate IL-10 production. However, TRAF3 is not known to have a role in MAPK activation so it is unlikely that A52 would target TRAF3 as part of its mechanism of activation of p38 MAPK.

Overall, TRAF3 is considered to be an important regulator of the interferon-dependent response to viral infection (Zapata *et al.*, 2007a,b). In addition to the TLR signalling pathways, TRAF3 is also important in TLR-independent antiviral signalling (Oganesyan *et al.*, 2005). A role for TRAF3 in TLR-independent interferon induction was described prior to the discovery of the RIG-I pathway (Oganesyan *et al.*, 2005). TRAF3 is required for the RIG-I-dependent induction of interferons (Saha *et al.*, 2006). The TRAF domain of TRAF3 interacts with a TRAF-interaction motif in Cardif, the adaptor protein in the RIG-I signalling (Saha *et al.*, 2006). Thus, an interaction between TRAF3 and A52 would suggest that A52 might also affect non-TLR-dependent antiviral signalling. However, since A52 has no effect on IRF activation (Keating *et al.*, 2007, Stack *et al.*, 2005), it may not affect the non-TLR-dependent pathway to IRF activation mediated by TRAF3.

However, this finding is tempered by the fact that A52 also co-immunoprecipitated with endogenous TRAF2. The interaction between endogenous TRAF2 and A52 could be another non-specific interaction due to cross-reactivity of the TRAF2 antibody with the

A52 protein. In this chapter, attempts were made to increase the stringency of the lysis and immunoprecipitation conditions in order to reduce the likelihood of observing a non-specific interaction. Nonetheless, A52 still appeared in TRAF2 immunoprecipitates. It is possible that the TRAF antibodies are all non-specifically immunoprecipitating However, given the evolutionary divergence of these proteins, it is likely that they present distinct epitopes and thus that the antibodies against each TRAF would be distinct. In conjunction with the aforementioned stringent conditions, it is possible that the co-immunoprecipitation of A52 and each of the TRAFs tested is specific. The use of the matched pre-immune serum for the TRAF antibodies or else pre-clearing the lysate with the protein A/G beads could help to validate the results. Alternatively, other methods to assess the interaction of A52 and the TRAFs could be explored, including pull-downs with His-tagged A52.

In conclusion, A52 appeared to co-immunoprecipitate with TRAF3 and this potential new interaction partner should be investigated further. As expected, A52 was able to co-immunoprecipitate with endogenous TRAF6. Previously, A52 was found to interact with over-expressed TRAF6 and A52-induced p38 activation was found to require TRAF6 (Maloney *et al.*, 2005). Moreover, preliminary evidence presented herein suggests that the A52-TRAF6 interaction is independent of the A52-IRAK2 interaction and, further, does not need IRAK1. Thus, A52 might to target TRAF6 directly and independently of other signalling molecules in order to activate MAPK. The interaction between A52 and TRAF6 was explored further in subsequent chapters in order to elucidate the mechanism by which A52 activates MAPK.

Chapter Four: Results II

Identification and characterisation of a non-canonical TRAF6 binding motif in A52

4.1 Introduction

In the previous chapter, A52 was observed to co-immunoprecipitate with endogenous TRAF2, TRAF3 and TRAF6 (Chapter 3). This result is surprising since previous work had found that A52 interacted with over-expressed FLAG-TRAF6 but not FLAG-TRAF2 (Harte *et al.*, 2003). In this chapter, the interaction between A52 and TRAF6 was explored in more detail.

Although the TRAFs are related by their characteristic TRAF domain, they also possess specialised functions that parallel the divergent evolution of this family. The TRAF domain emerged early in eukaryotic evolution and has become associated with other domains (RING, zinc finger) thereby generating the functional diversity of the TRAFs (Zapata *et al.*, 2007b). The ancestral TRAFs, TRAF6 and TRAF4, diverged from a common ancestor in metazoan evolution and have distinct functions in cell signalling and development, respectively (Zapata *et al.*, 2007b). TRAF3 diverged from TRAF4 and TRAF3 subsequently gave rise to TRAFs 1, 2 and 5 (Zapata *et al.*, 2007b). While pair-wise comparisons of the TRAF domains from all the TRAFs show an overall identity of between 31% and 69%, there is a clear distinction between TRAF6 and the other TRAFs, consistent with the divergent evolution outlined above (Zapata *et al.*, 2001). The TRAF domain of TRAF6 is 30-35% identical to that of the other TRAFs, whereas the TRAF domains of TRAFs 1, 2,3 and 5 are between 55 and 69% identical to each other (Zapata *et al.*, 2001). Thus, TRAF6 shares the least identity in its TRAF domain to any other TRAF.

Distinct functions and protein-protein interaction motifs were first described for the TRAFs interacting with TNFR family members, CD40 and RANK. TRAF6 was originally identified as a novel member of the TRAF family that bound to the cytoplasmic tail of CD40 in an N-terminal region that was distinct from the site with which the other TRAFs

interacted with CD40 (Ishida *et al.*, 1996). Furthermore, the TRAF domain of TRAF6, and not of TRAF2, acted as a dominant negative to inhibit CD40L-induced NF-κB activation from the deletion construct of CD40 (Ishida *et al.*, 1996). This suggested that TRAF6 bound CD40 independently of the other TRAFs in order to activate NF-κB by a distinct mechanism (Ishida *et al.*, 1996). TRAF6 was subsequently found to interact with RANK, another TNFR family member, via a distinct interaction motif from that which bound to TRAF2 (Darnay *et al.*, 1999). Numerous other TNFR family members that associate with TRAFs 1, 2, 3 and 5 do not interact with TRAF6 (Ishida *et al.*, 1996).

The initial evidence that TRAF6 had a role in IL-1R signalling was that overexpression of the TRAF domain of TRAF6 had a dominant negative effect on IL-1-induced NF-κB activation (Cao *et al.*, 1996). In contrast, over-expression of N-terminally truncated TRAF2 or TRAF5 inhibited TNF- but not IL-1-induced NF-κB activation (Cao *et al.*, 1996). TRAF6 thus has a role in IL-1-induced NF-κB activation, whereas TRAF2 and TRAF5 are needed for TNF-induced NF-κB activation (Cao *et al.*, 1996). Subsequently, TRAF6 was also found to be required in TLR4 signalling following LPS stimulation (Lomaga *et al.*, 1999). Originally, it was the only TRAF required for IL-1R/TLR signalling but TRAF3 has recently been found to be recruited to activated TLR4 along with TRAF6 (Chapter 3; Häcker *et al.*, 2005). The downstream pathways from TRAF3 and TRAF6 are still distinct, with TRAF3 being more important in TRIF-mediated signalling to induce type I IFN and IL-10 production (Häcker *et al.*, 2005). Thus TRAF6 has unique roles in several signalling pathways and is functionally distinct from other TRAFs.

A feasible explanation for the distinct functions of TRAFs has to do with the aforementioned divergence in the TRAFs, in particular in the TRAF domain. As discussed above, the TRAF domain of TRAF6 is the least like that of any other TRAF. The fact that TRAF6 and TRAF2 bind to CD40 at different locations via their TRAF

domains is consistent with the differences that exist in these domains. The C-terminal portion of the TRAF domain, the TRAF-C domain, mediates interactions with cell surface receptors, other TRAFs and adaptor proteins (Arch *et al.*, 1998). The crystal structures of the TRAF-C domain of TRAF6 and TRAF2 were solved both on their own and in complex with peptides derived from CD40 and RANK (Ye *et al.*, 2002). The TRAF-C domain has surface pockets which are the sites of interaction between the TRAF and the binding peptides (Ye *et al.*, 2002). Characteristic differences between TRAF2 and TRAF6 were observed in the surface clefts, the sequences of the bound peptides and the types of intermolecular bonds between the peptides and the TRAFs.

From the crystallography studies of the TRAFC domain, a consensus motif was identified in peptides that interacted with TRAF6: P-X-E-X-X-Ac/Ar, where Ac is an acidic residue and Ar is an aromatic residue (Ye *et al.*, 2002). Based upon the binding of peptides from TRAF6-interacting proteins, it was found that the consensus motif bound to a cleft in the TRAF-C domain (Ye *et al.*, 2002). The strength of the interaction between the peptide and the cleft on the TRAFC domain was measured by the surface area of the peptide residues buried in the pocket of the TRAFC (Ye *et al.*, 2002). From these studies, three residues of the peptide, denoted P_{-2}, P_0 and P_3, were found to be crucial for the peptide-TRAF-C interaction (Ye *et al.*, 2002). The glutamate residue is the central or P_0 residue of the motif and it was shown to be the critical residue for binding to the TRAF-C domain (Ye *et al.*, 2002). The carboxylate of glutamate forms hydrogen bonds to the amide nitrogen atoms of Leu457 and Ala458 (Ye *et al.*, 2002). In addition, the aliphatic side chain of glutamate binds tightly to the TRAF6 surface (Ye *et al.*, 2002). The proline residue (P_{-2}) also fits into a pocket formed by the Phe 471 and Tyr 473 residues of TRAF6 (Ye *et al.*, 2002). The third key residue is the acidic or aromatic residue at position P_3, which binds to aromatic and basic residues of TRAF6 (Ye *et al.*, 2002).

Given that the glutamate was found to be the critical residue for the interaction with TRAF6, numerous studies of TRAF6 interacting proteins have focussed on this residue and have examined its importance by site-directed mutagenesis. However, mutation of the glutamate of TRAF6 binding motif within a protein is not always sufficient to abolish interaction (Ye *et al.*, 2002; Sato *et al.*, 2003). Where more than one TRAF6 binding motif is present in the protein, mutation of the glutamate residue in all the motifs did result in both a loss of interaction and of function (Ye *et al.*, 2002; Sato *et al.*, 2003; Keating *et al.*, 2007). Thus, there are likely other residues in the protein outside the TRAF6 binding motif that contribute to or stabilise the interaction with TRAF6 (Zapata *et al.*, 2006).

In comparison to the TRAF6 binding motif, proteins that interact with the other TRAFs have the consensus sequence (P/S/T/A)-X-(Q/E)-E, where X is any amino acid (Chung *et al.*, 2002). The structure of the TRAF domain of TRAF2 is distinct from that of TRAF6. There is a 40-degree difference in the chain direction of peptides bound to TRAF2 versus those bound to TRAF6 (Ye *et al.*, 2002). The surface clefts in the TRAF domains of TRAF6 and TRAF2 are completely different (Ye *et al.*, 2002). The peptides that bind to TRAF6 have a ß-conformation, whereas those that bind to TRAF2 have a poly-proline II helix (Ye *et al.*, 2002). The P_0 residue of the TRAF2 binding peptide is either glutamic acid or glutamine and it interacts with the hydroxyl groups of three serine residues (453-455) in TRAF2 (Ye *et al.*, 2002). Not only do TRAF2 and TRAF6 differ in the sequence of amino acids recognised but the orientation of binding of the peptide and the bonds formed between the TRAF domain and the peptide are distinct for the two TRAFs. Thus it seems likely that the two TRAFs would interact either with different protein partners or that interaction with the same protein would necessitate the use of different binding sites, as observed for CD40.

Since A52 has been found to interact with TRAF6, it is feasible that A52 has a TRAF6 binding motif. Further, it is likely that the ability of A52 to bind to TRAF6 is required for A52 function. Previous work showed that A52 could inhibit NF-κB activation from numerous TLRs and from the IL-1R (Harte *et. al.*, 2003; Maloney *et al.*, 2005). A deletion construct of A52 lacking the C-terminal 46 amino acids (ΔA52) was able to bind to IRAK2 but not to TRAF6 (Maloney *et al.*, 2005). Further, ΔA52 was still able to inhibit IL-1-induced NF-κB activation, suggesting that interaction with IRAK2 and not TRAF6 was required for A52 to inhibit NF-κB activation (Keating *et al.*, 2007). In addition to its inhibitory function, A52 was found to enhance IL-1R/TLR-induced p38 MAP kinase activation (Maloney *et al.*, 2005). A52 was also able to activate p38 and JNK MAP kinases in the absence of any ligand and in a TRAF6-dependent manner (Maloney *et al.*, 2005). Thus, the A52-TRAF6 interaction is more important for MAPK activation by A52, whereas the interaction between A52 and IRAK2 is necessary for the inhibition of IL-1R/TLR signalling by A52.

The interaction between A52 and TRAF6 was examined further by identification and mutation of a putative TRAF6 binding motif. The ability of wild-type and mutant A52 to interact with TRAF6 was tested by co-immunoprecipitation and western blotting. The mutants were compared to wild-type A52 for their ability to inhibit ligand-induced NF-κB activation and to activate p38 in the absence of stimulation.

4.2 Results

4.2.1 TRAF6 is needed for A52 to activate p38 and JNK MAP kinases

The importance of TRAF6 in p38 and JNK MAPK activation was investigated in wild-type and $TRAF6^{-/-}$ MEFs. The CHOP assay had been used to study MAPK activation by A52 and

the mutants in R1s (see below). However, numerous attempts at using this assay in the MEFs proved inconclusive (data not shown). Thus, another method had to be used to study MAPK activation in the MEFs.

The phosphorylation of the MAPKs JNK and p38, as well as the p38-dependent transcription factor ATF-2, were assayed by western blotting. The phosphorylation of ATF-2 would indicate that p38 was not only phosphorylated but also able to phosphorylate one of its substrates. Initial experiments showed that the amount of protein obtained from 6-well plates was insufficient (data not shown). The experiment was scaled up to 100mm-dishes in order to overcome this limitation. In addition, the cells were difficult to count accurately using the haemocytometer due to aggregation. In order to obtain approximately equivalent cell densities, the cell suspension obtained from a fully confluent flask of each cell type was divided equally between 100mm dishes and the dishes were then transfected when the monolayer was 75% confluent. In wild-type MEFs, stimulation with IL-1 or A52 overexpression caused phosphorylation of p38 and JNK, as well as of ATF-2 (Figure 4.1, left-hand panels). The phosphorylation of p38 induced by A52 was not as intense as that induced by IL-1 stimulation. The phosphorylation of p38, JNK and ATF-2 was not observed in the $TRAF6^{-/-}$ MEFs in response to IL-1 (Figure 4.1, right-hand panels). While A52 did not induce phosphorylation of ATF-2 in the $TRAF6^{-/-}$ MEFs, there appeared to be a slight induction of phosphorylation of both p38 and JNK in response to A52 over-expression (Figure 4.1, right-hand panels). The level of protein loading was tested by immunoblotting for ß-actin and found to be equal (Figure 4.1, bottom panels). A52 was expressed in both wild-type and $TRAF6^{-/-}$ MEFs (Figure 4.1). Since IL-1-induced phosphorylation of MAPKs was only observed in the wild-type MEFs, the activation of JNK and p38 by IL-1 requires TRAF6. Although p38 and JNK phosphorylation appeared to be slightly induced in $TRAF6^{-/-}$ MEFs, p38-dependent phosphorylation of ATF-2 was not observed in these cells.

Thus, the A52-dependent phosphorylation of p38 alone might not be sufficient to induce function of p38 in the absence of TRAF6.

4.2.2 A52 has a non-canonical TRAF6 bind motif

The TRAFs are known to interact with different proteins via distinct motifs. Since A52 was found to co-precipitate with TRAFs 2 and 3 as well as TRAF6, it was hypothesised that there would be at least two discrete motifs in A52 that would mediate these interactions. The TRAFs other than TRAF6 recognise a consensus sequence of [PSAT]-X-[QE]-E (Chung *et al.*, 2002). Using the algorithm ELM (Puntervoll *et al.*, 2003; www.eu.elm.org), a putative TRAF binding motif TIEE (residues 96-99) was identified in the A52 primary sequence (Figure 4.2A).

As mentioned above, A52 has been shown to interact directly with the TRAF domain of TRAF6 (Harte *et al.*, 2003). The C-terminal 46 amino acids of A52 were required to mediate the interaction with TRAF6 (Maloney *et al.*, 2005). Proteins that interact with the TRAF domain of TRAF6 have been shown to possess a TRAF6 binding motif (P-X-E-X-X-Ac/Ar) which interacts with a cleft in the TRAF-C domain (Ye *et al.*, 2002). Since A52 was shown to interact with the TRAF domain of TRAF6 (Harte *et al.*, 2003), it was hypothesised that there could be a TRAF6 binding motif in A52 that allows it to interact with TRAF6. The C-terminal region of A52 was scanned and a putative TRAF6 interaction motif was identified at amino acids 149-154: RNEKLF (Figure 4.2A). The major difference between the potential TRAF6 interaction motif in A52 and the canonical sequence is the presence of an arginine (residue 149) instead of a proline (Figure 4.2A). Since proline is structurally unique, with a cyclic structure and a secondary amine group, the existence of an arginine in place of a proline would be anticipated to give quite a different structure.

To determine if this short sequence of amino acids was indeed a TRAF6 binding motif, four point mutations of A52 were generated by site-directed mutagenesis: R149A, E151A, K152A and F154A (Figure 4.2B). In addition, a deletion construct lacking the entire TRAF6 binding motif of A52 (ΔT6BM) was made by a modified mutagenesis protocol (Figure 4.2B). The point mutants and ΔT6BM were sequenced and found to contain the desired mutations. The integrity of the wild-type and mutant A52 plasmids was checked by cleavage with EcoRI followed by agarose gel analysis (data not shown). Different quantities of the point mutants were transfected into HEK 293 cells (Figure 4.3). When the total cell lysates were analysed by western blotting, it was found that the point mutants were detected with the antibody raised against A52 (Harte *et al.*, 2003) and expressed at comparable levels (Figure 4.3). Point mutants E151A (Figure 4.3A, middle panel) and K152A (Figure 4.3C) express as well as wild-type A52. The F154A (Figure 4.3A, bottom panel) and R149A (Figure 4.3B) point mutants express slightly less than wild-type A52. The initial ΔT6BM construct used did not express very well and was barely detectable by western blotting (data not shown). Further clones that had been sequenced and found to contain the deletion were prepared and tested for expression (Figure 4.4). The three preparations of the ΔT6BM construct tested expressed equally well to each other (Figure 4.4, lanes 3-5). However, none of the preparations expressed as well as either wild-type A52 or the F154A mutant (Figure 4.4, compare lanes 3-5 with lanes 2 and 6).

4.2.3 Deletion of the TRAF6 binding motif of A52 abrogates the A52-TRAF6 interaction

The FLAG antibody non-specifically precipitates A52, making it impossible to use in co-precipitations with the FLAG-TRAFs (Chapter 3). Therefore, to determine if the mutant proteins could interact with TRAF6, the mutants and wild-type A52 were transfected into R1s and tested for their ability to interact with endogenous TRAF6. The total cell

extracts were immunoprecipitated with antibodies to either A52 or TRAF6. The immunoprecipitates were resolved by SDS-PAGE and Western blotting. The blots were probed with antibodies to A52 and TRAF6. Initial results failed to detect endogenous TRAF6 in the immunoprecipitates (data not shown). As previously discussed (Chapter 3), the TRAFs, including TRAF6, are known to be localised to insoluble subcellular fractions (Arch *et al.*, 2000). In order to extract TRAF6 into the soluble fraction, buffer including the non-ionic detergent NP-40 was used. In addition, the lysis period was extended from twenty minutes to one hour and the cells were vortexed three times during the lysis (Chapter 3). Similar levels of endogenous TRAF6 were detected in TRAF6 immunoprecipitates in all samples as a band above the heavy chain following this longer lysis period (Figure 4.5, middle panel). When TRAF6 immunoprecipitates from lysates containing A52, E151A or F154A were immunoblotted for A52, a band was detected indicating that endogenous TRAF6 co-precipitates with A52 and the two mutants (Figure 4.5, top panel). This co-immunoprecipitation between the mutants and TRAF6 was observed despite the fact that the mutants did not express as well as wild-type A52 in this experiment (bottom panel).

Since point mutations in the TRAF6 binding motif did not impair the co-precipitation of A52 with TRAF6, it was hypothesised that deletion of the entire motif would be required to abrogate the A52-TRAF6 interaction. Consistent with this, the ΔT6BM construct failed to co-precipitate with endogenous TRAF6 (Figure 4.6, top panel). The immunoprecipitation of TRAF6 was equal in all samples (Figure 4.6, middle panel). Neither F154A nor ΔT6BM expressed as well as wild-type A52 (Figure 4.6, bottom panel). However, both F154A and ΔT6BM have been shown to be expressed and at more comparable levels to wild-type A52 in other experiments (Figs 4.3 and 4.4). Despite the relatively low level of expression, F154A clearly co-precipitated with TRAF6 (Figure 4.6, top panel). It could be that ΔT6BM does interact weakly with TRAF6 and that it is just

not detectable due to the compounding low expression levels, but this is unlikely since low expression of F154A did not impede its detection in complex with TRAF6.

Since ΔT6BM did not co-precipitate with TRAF6, the ability of ΔT6BM to interact with IRAK2 was examined. Wild-type A52 co-precipitated with endogenous IRAK2 whereas the ΔT6BM construct did not (Figure 4.7, top panel). Endogenous IRAK2 was equally precipitated in each of the samples (Figure 4.7, middle panel). In this experiment, comparable quantities of wild-type A52 and ΔT6BM were detected in the lysates (Figure 4.7, bottom panel).

4.2.4 The TRAF6 binding motif mutants of A52 inhibit NF-κB activation

IL-1-induced NF-κB activation has previously been found to be inhibited by A52 (Maloney *et al.*, 2005). The TRAF6 binding motif mutants were tested in order to determine whether this inhibitory function was impaired. The NF-κB reporter plasmid, along with TK-Renilla and varying amounts of each wild-type and mutant A52 were co-transfected into R1s. Relative luciferase activity was measured following IL-1 stimulation. Wild-type A52 inhibited IL-1-induced NF-κB activation in R1s (Figure 4.8A). In the experiment shown, IL-1 induced NF-κB activity by approximately 10-fold and the addition of 150ng of wild-type A52 reduced this to 4-fold (Figure 4.8A). However, the inhibition of IL-1-induced NF-κB by wild-type A52 was not dose-dependent (Figure 4.8A). By comparison, the mutant F154A (150ng) inhibited IL-1-induced NF-κB activity to 4-fold, whereas addition of E151A (150ng) completely blocked IL-1-induced NF-κB activitation (Figure 4.8C and E, respectively). The other mutants (R149A, K152A and ΔT6BM) also inhibited IL-1-induced NF-κB activation to varying degrees (Figure 4.8 B, D and F). Thus, all of the TRAF6 binding motif mutants inhibited IL-1-induced NF-κB activation in R1s, typically to a comparable degree to inhibition by wild-type A52.

Since A52 wild-type and mutants were able to inhibit IL-1-induced NF-κB activation, inhibition of signals emanating from TLRs was next examined. A52 has previously been shown to inhibit NF-κB activation in HEK-293 cells transiently transfected with CD4-TLRs (Harte *et al.*, 2003). The chimeric CD4-TLRs are constitutively active and thus do not require ligand stimulation to activate the NF-κB reporter plasmid (Harte *et al.*, 2003). R1s were co-transfected with CD4-TLR4, reporter gene plasmids and varying amounts of A52, E151A and F154A. As expected, wild-type A52 inhibited CD4-TLR4-induced NF-κB activation (Figure 4.9A). Both mutants tested, F154A and E151A, inhibited CD4-TLR4-induced NF-κB activation (Figure 4.9B and C). K152A was tested and found to inhibit CD4-TLR4-induced NF-κB in one experiment (data not shown). The other mutants (R149A and ΔT6BM) were not tested in this assay.

Activation of NF-κB leads to the expression of genes for proinflammatory cytokines including IL-8. An ELISA was performed in order to determine if the TRAF6 binding motif mutants could inhibit IL-8 production. Consistent with published data (Maloney *et al.*, 2005), A52 was found to inhibit LPS-induced IL-8 production in TLR4 cells (Figure 4.10A). The A52 mutants E151A (Figure 4.10B) and F154A (Figure 4.10C) also inhibited LPS-induced IL-8 production. The inhibition of LPS-induced IL-8 production was observed three or more times but the inhibition was not always dose-dependent.

In addition to TLR4-induced NF-κB activation, wild-type A52 and the F154A mutant were found to inhibit p(I:C)/TLR3-induced NF-κB activation (data not shown). The other mutants (R149A, E151A, K152A, ΔT6BM) were not tested in this assay.

To further examine the effects of wild-type A52 and the A52 mutants on NF-κB activation, phosphorylation and degradation of the regulatory protein IκBα was examined. Degradation of IκBα is considered a marker of NF-κB activation. In order to

be degraded, IκBα must first be phosphorylated, which targets it for ubiquitination and degradation via the proteasome (Ravid and Hochstrasser, 2004). A52, F154A and ΔT6BM were each transfected into R1s. Twenty-four hours post-transfection, the indicated cells were stimulated with IL-1α and then harvested in SDS-containing sample buffer. The lysates were sonicated and then analysed by Western blotting.

IL-1 induced degradation of IκBα (Figure 4.11, top panel, lane 2). This degradation was inhibited by wild-type A52 and both ΔT6BM and F154A (Figure 4.11, top panel, compare lanes 6-8 to lane 2). The mutants were not expressed as well as A52 (Figure 4.11, second panel from bottom, lanes 4, 5, 7 and 8). Despite the lower expression, the mutants inhibit degradation of IκBα as well as wild-type A52. In order to be degraded, IκBα must first be phosphorylated and phosphorylation of IκBα is used as a marker for activation. Accordingly, IL-1 induced phosphorylation of IκBα (Figure 4.11, second panel from top, lane 2). Surprisingly, IL-1-induced phosphorylation of IκBα was enhanced by wild-type A52 (Figure 4.11, second panel from top, lane 6). The A52 mutants, ΔT6BM and F154A, did not significantly alter the level of IL-1-induced phosphorylation of IκBα (Figure 4.11, second panel from top, compare lanes 7 and 8 to lane 2). The absence of an effect on IL-1-induced phosphorylation of IκBα by F154A and ΔT6BM could be due to the lower level of expression of the mutants compared to wild-type A52. The ß-actin blot shows that the protein loading was equal (Figure 4.11, bottom panel). Inhibition of IL-1-induced IκBα degradation was observed four times for wild-type A52 and F154A and twice for ΔT6BM. The enhancement of IL-1-induced phosphorylation of IκBα by wild-type A52 was observed three times. The F154A mutant has either had no effect or inhibited IL-1-induced phosphorylation of IκBα in five separate experiments. The ΔT6BM construct was found to have no effect on the phosphorylation of IκBα in two experiments. Thus, IκBα phosphorylation was not inhibited by A52 and the mutants and it is possible that the inhibition of IκBα

degradation occurs by another mechanism, such as by the prevention of ubiquitination. This has not been tested for A52 or the mutants.

4.2.5 The F154A and ΔT6BM mutants of A52 do not drive p38 activation

It was reported previously that A52 can activate p38, leading to IL-10 production in a TRAF6-dependent manner (Maloney *et al.*, 2005). Therefore, the ability of wild-type A52 and the mutants to activate p38 was compared to determine whether mutating the putative TRAF6-binding site compromised the activation of TRAF6 signalling by A52. Activation of p38 was measured by the PathDetect® CHOP *trans*-Reporting system as discussed previously (Materials and Methods). Wild-type A52 activated p38 in a dose-dependent manner although the level of activation overall was low (Figure 4.12A). The E151A mutant was able to activate p38 to the same extent or more than the wild type A52 (Figure 4.12C). In addition, the point mutants R149A and K152A did not affect the ability of A52 to activate p38 (Figure 4.12B and D). In contrast, the F154A mutant was not able to drive p38 activation (Figure 4.12E). Thus, a single residue, F154, is critical to the ability of A52 to activate p38 via TRAF6. As was observed for F154A, the ΔT6BM construct was unable to activate p38 (Figure 4.12F).

The ability of A52, E151A (an active mutant in terms of being able to stimulate p38) and F154A (an inactive mutant) to activate other MAPKs was examined. In order to test for the activation of JNK, the activation of a Gal4-dependent reporter by c-Jun-Gal4 was tested in a trans-reporting system similar to the CHOP assay (see Materials and Methods). In accordance with the finding that F154A does not activate p38 activation in the CHOP assay, it was also observed that it does not drive JNK activation (Figure 4.13C). Both A52 and E151A stimulated JNK activation in a dose-dependent manner (Figure 4.13 A and B). Thus the F154A mutant failed to activate p38 and JNK MAPK, highlighting the importance of this residue in MAPK activation by A52.

Following the discovery of the crucial residue of A52 required for p38 and JNK activation, the ability of A52, F154A and ΔT6BM to induce p38 and JNK phosphorylation was examined. The assay, described previously (see Materials and Methods), involves the detection of phosphorylated p38 and JNK in cell lysates by immunoblotting with a phospho-p38 or phospho-JNK specific antibody. Given the above finding that F154A and ΔT6BM do not drive p38 or JNK activation in reporter gene assays, it was anticipated that there would be no phosphorylated p38 or JNK in samples containing F154A. In the IL-1 control, an intense band shows that there is strong phosphorylation of p38 (Figure 4.14, top blot, lane 2). Surprisingly, A52 wild-type did not appear to induce phosphorylation of p38 in this assay (Figure 4.14, top panel, lane 3). ΔT6BM and F154A did not induce phosphorylation of p38 on their own (Figure 4.14, top panel, lanes 4 and 5). Wild-type A52 and both ΔT6BM and F154A did not alter the level of IL-1-induced phosphorylation of p38 (Figure 4.14, top panel, lanes 6-8). Total p38 was difficult to detect on the blots but was equal in all lanes (Figure 4.14). As observed for phospho-p38, phosphorylation of JNK was not detected following transient transfection of wild-type A52, ΔT6BM or F154A (Figure 4.14). IL-1 induced phosphorylation of JNK (lane 2) and this appeared to be enhanced by wild-type and mutant A52 (lanes 6, 7 and 8). Once again, the total JNK was difficult to detect following stripping of the blots but it was found to be equal in the samples (Figure 4.14). The amount of ß-actin in each sample was measured to control for protein loading and found to be equal in all lanes (Figure 4.14). The difficulty in detection of phosphorylated MAPK by A52 could be cell type-dependent since wild-type A52 induced phosphorylation of JNK, p38 and ATF-2 in MEFs (Figure 4.1). While it was possible to detect IL-1-induced MAPK phosphorylation in HEK 293 cell lines, it might be that this assay is not sensitive enough to detect phosphorylation of MAPK in response to over-expression of proteins, possibly due to transfection efficiency.

IL-10 production has been found to be regulated by p38 MAPK. A52 has been found to activate the IL-10 promoter in HEK 293 cells (Maloney *et al.*, 2005). Since the A52 mutant, F154A, was unable to drive p38 MAPK, it was hypothesised that it would be unable to activate the IL-10 promoter. The IL-10 promoter luciferase construct was co-transfected into R1s with doses of either wild-type A52 or F154A. Wild-type A52 weakly activated the promoter approximately 1.5-fold at the middle and top doses (Figure 4.15). F154A activated the promoter approximately 1.2-fold at the top dose, which is the same amount of activation observed with the lowest dose of wild-type A52 (Figure 4.15). In the same experiment, the positive control IL-1 activated the IL-10 promoter 2.5-fold (Figure 4.15). This result has been observed twice, with the IL-10 promoter only being weakly activated in both cases. Thus, wild-type A52 weakly activates the IL-10 promoter in the absence of ligand stimulation but not to the same extent as observed following stimulation with IL-1. It could be that the activation of the IL-10 promoter is weaker due to the efficiency of the co-transfection of the plasmids when compared to exogenous addition of a ligand. Nonetheless, the F154A mutant was not able to activate the IL-10 promoter to the same extent as wild-type A52 and this is consistent with the inability of F154A to activate MAPK.

4.2.6 Secondary structure of A52

Initially, there was no model or predicted structure of A52 and thus it was unknown where the TRAF6 binding motif was with respect to any secondary structure in the A52 protein. In order to investigate the potential structural consequences of the TRAF6 binding motif and particularly the F154 residue, the secondary structure of A52 was examined using computer algorithms. The secondary structure of A52 was predicted using PSIPRED, which gives predictions based on a Blast search of structures (McGuffin *et al.*, 2000). It is estimated to give predictions with a 78% per residue accuracy (Bryson *et al.*, 2005). A52 is predicted to have a mainly beta-strand structure in the N-

terminal 19 amino acids (Figure 4.16). C-terminal to the beta-strands is an extended coiled region from residues 19 to 53 (Figure 4.16). The remaining 137 amino acids (residues 53 to 190) form alpha helices, interspersed with short coiled regions (Figure 4.16). The putative TRAF6 binding motif (residues 149-154) lies mainly in a coiled region between two helices, suggesting that it could be exposed on the surface of the protein. Only the phenylalanine residue (F154) is predicted to be at the beginning of an adjacent alpha helix.

4.2.7 Oligomerisation of A52 is not altered by the F154A mutation

It was hypothesised that A52 could form dimers or higher-order oligomers. In order to examine this, native PAGE was employed to examine the oligomerisation of A52 under non-denaturing conditions. Initially, wild-type A52 was tested on its own to determine if it dimerised and if this could be detected. R1s were transfected with empty vector (pcDNA3.1), A52 (2.3µg) or doses of A52 (0.5, 1 and 2.3 µg). The samples were harvested under non-denaturing conditions and analysed by native PAGE (Figure 4.17, top panel). In the lanes in which A52 is transfected, there is a fast migrating form of protein near the bottom of the blot which could represent monomeric A52 (Figure 4.17, top panel, lanes 5-10). It is not the front of protein migration through the gel since the molecular mass marker migrated below this point on the gel (data not shown). Above the fast migrating form of the protein, there is a distinct band that is only found in the lanes containing A52 and not in those with empty vector (Figure 4.17, top panel, compare lanes 5-10 to lanes 1-4). Moreover, with increasing doses of A52, the intensity of this band increases somewhat though the there is aberrant migration of the protein in the last lane that makes it difficult to interpret (Figure 4.17, top panel, lanes 9 and10). The band likely represents a slower migrating form of A52, which would be consistent with it being an oligomer, possibly a dimer.

It is difficult to assess the molecular masses of proteins under non-denaturing conditions. Molecular mass markers for use with non-denaturing PAGE were used. Since they were not pre-stained, the PVDF membrane was stained with Ponceau S solution after the transfer in order to detect the markers (data not shown). The most reliable marker was found to be a 14kDa monomeric protein, lactalbumin. In the lane in which lactalbumin was present, it migrated to a position lower than the bottom of the fast-migrating form of A52 (data not shown). The fast-migrating form of the protein is thus likely to be greater than 14kDa. Other molecular mass markers representing monomers and dimers of other known proteins were difficult to detect and thus it was not possible to gauge the size of the putative monomeric or dimeric A52 further. The two forms of A52 were detected three times in independent experiments. A52 was expressed well, as determined by denaturing PAGE of the same samples (Figure 4.17, bottom panel).

Since wild-type A52 appeared to oligomerise in native PAGE, this assay was also used to examine the mutants. If F154 was important for A52 dimerisation, then it was hypothesised that the F154A mutant would be unable to dimerise and that this might explain the inability of this mutant to activate MAPK. The deletion of the TRAF6 binding motif might also preclude oligomerisation, possibly due to altered folding or to the loss of the F154 residue. The native PAGE experiment was repeated twice with increasing doses of A52, F154A and ΔT6BM (data not shown). The faster migrating form of A52 was detected for wild-type, F154A and ΔT6BM, but the slower migrating form could not be seen observed in any of the samples (data not shown). Since the results obtained by native PAGE were inconclusive with the mutants, another assay was devised to examine A52 oligomerisation.

A52 oligomerisation was also assessed by using GFP-A52 and untagged A52 in co-immunoprecipitation experiments. GFP-A52 migrates slower in SDS-PAGE than

unlabelled A52 due to the presence of the tag: GFP is 27kDa and the GFP-A52 fusion protein is predicted to be 49kDa. If GFP-A52 and A52 co-immunoprecipitate, two bands would be observed on the western blot at the distinct molecular masses of A52 (22kDA) and GFP-A52 (49kDA). Thus, the presence of a band at 22kDa and a second band at 49kDa would indicate that untagged and GFP-tagged A52 co-precipitated. Untagged wild-type A52 and F154A were co-transfected with GFP-A52. Following immunoprecipitation with GFP antibody, the precipitates were analysed by western blotting for A52 (Figure 4.18). Wild-type A52 and F154A co-precipitated with GFP-A52 (Figure 4.18, top panel, lanes 4 and 5). ΔT6BM did not co-precipitate with GFP-A52 but the control immunoprecipitation of GFP was also unsuccessful (data not shown). It was thus not possible to conclude if ΔT6BM could dimerise in this assay. A faint band was observed in the lane containing A52 in the absence of GFP-A52 (Figure 4.18, top panel, lane 3). This band could be bleed-through from the adjacent lane containing wild-type A52. From this assay, the F154A mutation did not appear to significantly alter the dimerisation of A52. Thus, the inability of F154A to activate MAPK is unlikely to be due to impairment of A52 dimer formation. Rather, the mutation may directly inhibit the ability of A52 to activate TRAF6.

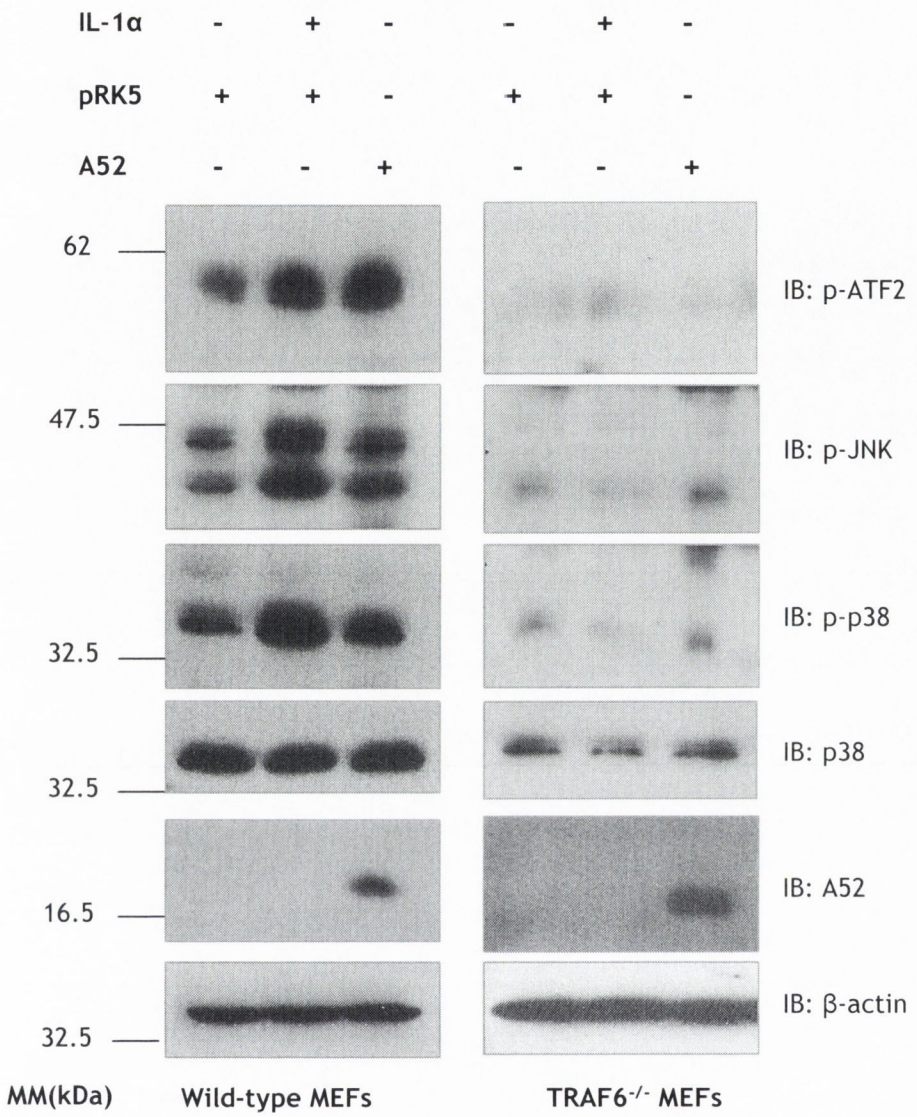

Figure 4.1 A52 can activate MAP kinases in wild-type but not in TRAF6-/- MEFs

MEFs were seeded in 100mm dishes twenty-four hours prior to transfection. The cells were transfected 24 hours later when the dishes were approximately 75% confluent with pRK5(8μg) or A52R (8μg) using GeneJuice™ according to the manufacturer's directions. The following day, the indicated cells were stimulated with IL-1α for 7 minutes. All cells were then harvested in sample buffer and lysed by sonication. The total cell lysates were analysed by SDS-PAGE and western blotting. The blots were incubated with the indicated antibodies overnight at 4°C. The phospho-specific antibodies were incubated in 3% BSA dissolved in TBS with 0.1% Tween 20. The molecular masses (MM) of relevant protein standards are indicated on the left in kildaltons (kDa).

A.

(NH_2)-^{1}MDIKIDISISGDKFTVTTRRENEERKKYLPLQKEKTT

DVIKPDYLEYDDLLDRDEMSTILEEYFMYRGLLGLRIKYG

RLFNEIKKFDNDAEEQFGTIEELKQKLRLNSEEGADNFID

YIKVQKQDIVKLTVYDCISMIGLCACVVDVWRNEKLFSR

WKYCLRAIKLFINDHMLDKIKSILQNRLVYVEMS^{190}-(COOH)

B.

Consensus motif		P X E X X Ac/Ar
A52 motif and mutations:		
1.	A52 w.t.	^{149}R N E K L F^{154}
2.	R149A	^{149}A N E K L F^{154}
3.	E151A	^{149}R N A K L F^{154}
4.	K152A	^{149}R N E A L F^{154}
5.	F154A	^{149}R N E K L A^{154}
6.	ΔT6BM	^{149} _ _ _ _ _ ^{154}

Figure 4.2 The C-terminus of A52 has a non-canonical TRAF6-binding motif

A. A potential TRAF6 binding motif was identified in A52 (a.a. 149-154), shown in blue. There is also a predicted TRAF2 binding site (a.a. 96-99), shown in red. **B.** The potential TRAF6 binding motif in A52 is similar to the consensus sequence of the binding motif but it lacks the initial proline residue. Four point mutations, R149A, E151A, K152A and F154A, and a deletion construct (ΔT6BM) lacking the entire motif were made in the *A52R* sequence using the Quikchange site-directed mutagenesis kit (Stratagene).

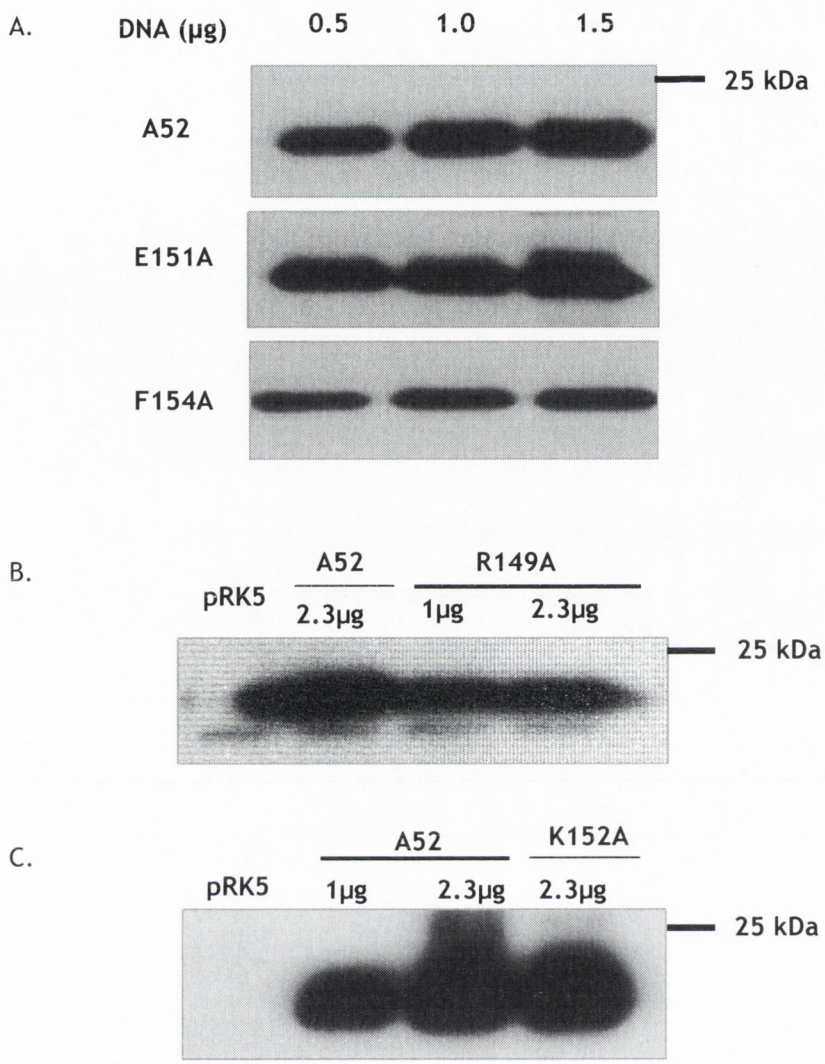

Figure 4.3 The TRAF6 binding motif mutants are expressed and are detected by the A52 antibody

Cells were seeded at 1x 10^5 cells/mL in 6-well plates 24 hours prior to transfection. A. HEK-293Ts were transfected with A52R, E151A or F154A (0.5, 1.0, 1.5 µg). B. R1s were transfected with pRK5 (2.3µg), A52 (2.3µg), or R149A (1 or 2.3µg). C. R1s were transfected with pRK5, A52 (1 or 2.3 µg) or K152A (2.3µg). All cells were transfected using GeneJuice™ according to the manufacturer's directions. The cells were harvested 24 hours post-transfection in sample buffer with DTT and then lysed by sonication. The lysates were resolved by SDS-PAGE and the proteins were transferred to Immobilon using a wet (A) or semi-dry (B and C) transfer system. The blots were probed with antibody specific for A52.

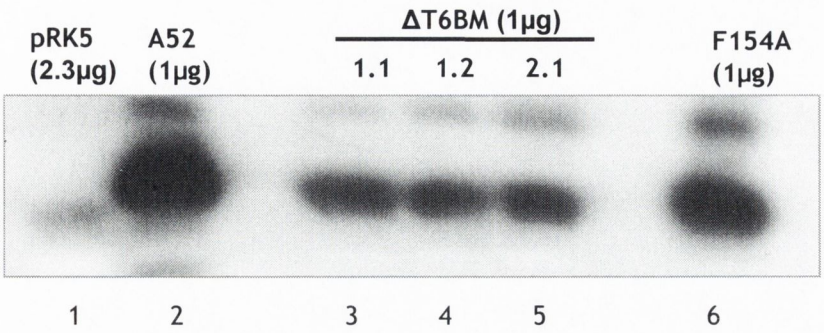

Figure 4.4 The TRAF6 binding motif deletion construct is expressed and detected by the A52 antibody

HEK-293R1s were seeded at 1x 10^5 cells/mL in 6-well plates 24 hours prior to transfection. The cells were transfected with pRK5, A52, ΔT6BM (1.1, 1.2, 2.1 are three different DNA preps) or F154A using GeneJuice™ according to the manufacturer's directions. The cells were harvested 24 hours post-transfection in 1x sample buffer with DTT and then sonicated. The lysates were resolved by SDS-PAGE and the proteins were transferred to Immobilon using a semi-dry transfer system. The blots were probed with antibody specific for A52.

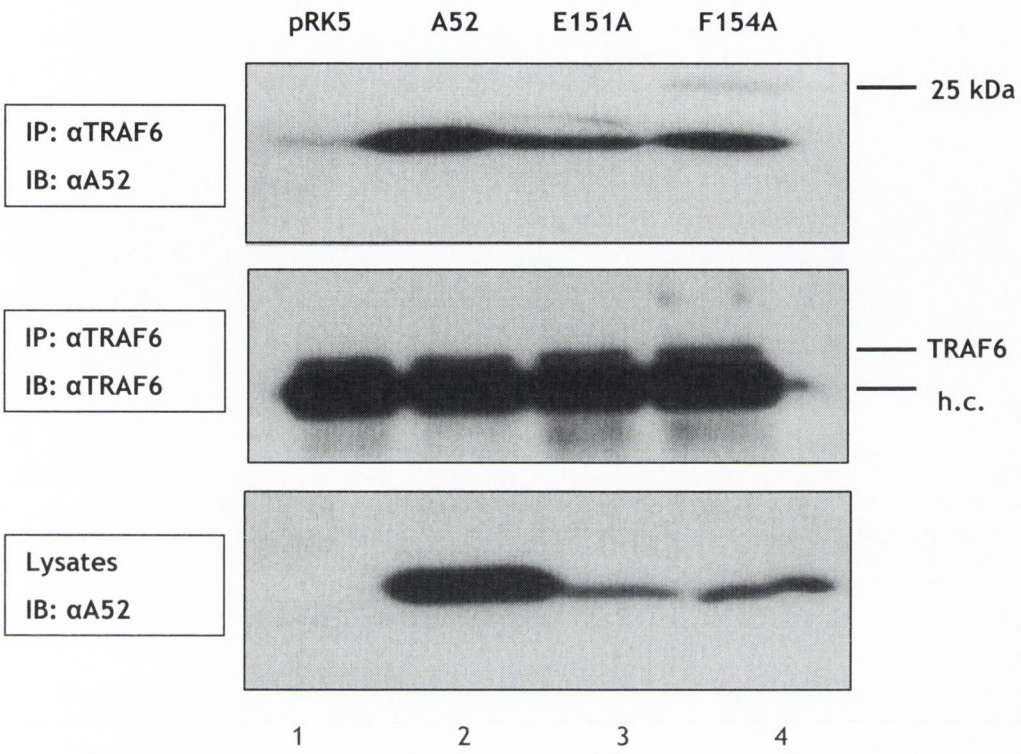

Figure 4.5 The TRAF6 binding motif mutants E151A and F154A bind to TRAF6

HEK-293T cells were seeded at 1x 10^5 cells/mL in 100mm dishes 24 hours prior to transfection. Cells were transfected with A52R, E151A or F154A (8μg) using GeneJuice™ according to the manufacturer's directions. The cells were harvested 24 hours post-transfection and lysed in NP-40 lysis buffer (50mM HEPES, 100mM NaCl, 1mM EDTA, 10% glycerol, 0.5% NP-40). Whole cell extracts were incubated with TRAF6 antibody coupled to protein A sepharose. The immunoprecipitates and lysates were resolved by SDS-PAGE and the proteins were transferred to Immobilon using a wet transfer system. The blots were probed with antibody specific for A52 or TRAF6, as indicated. Representative of two experiments. h.c., antibody heavy chain

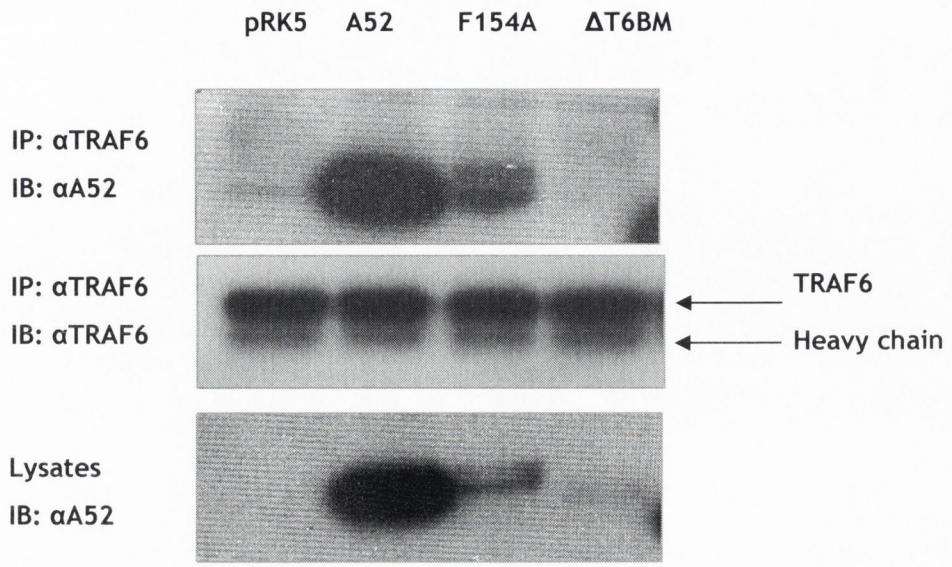

Figure 4.6 The TRAF6 binding motif deletion construct does not co-precipitate with TRAF6

R1s were seeded at 1x 10^5 cells/mL in 100mm dishes 36 hours prior to transfection. Cells were transfected with pRK5 (8μg), A52R (4μg), F154A (8μg) or ΔT6BM (8 μg) using GeneJuice™ according to the manufacturer's directions. The cells were harvested 24 hours post-transfection in PBS, followed by lysis in NP-40 lysis buffer (50mM HEPES, 100mM NaCl, 1mM EDTA, 10% glycerol, 0.5% NP-40). Whole cell extracts were incubated with TRAF6 antibody pre-coupled to protein A sepharose. The immunoprecipitates and lysates were resolved by SDS-PAGE and the proteins were transferred to Immobilon using a semi-dry transfer system. The blots were probed with antibody specific for A52 or TRAF6, as indicated. This is representative of two experiments.

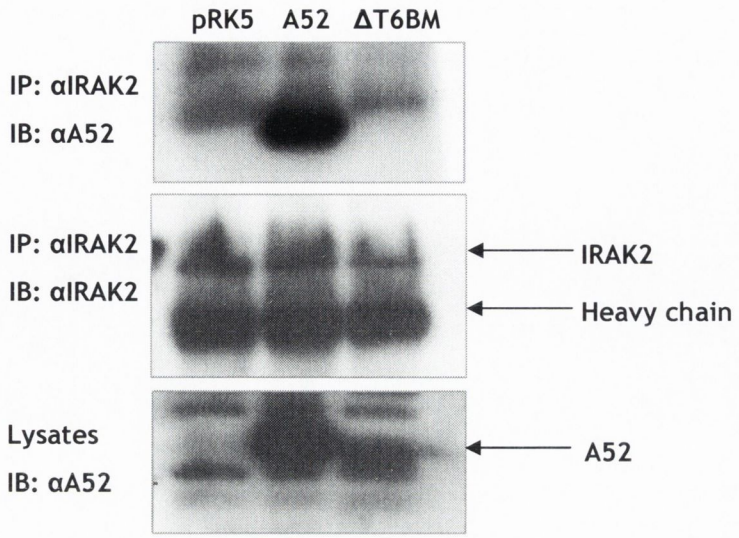

Figure 4.7 The TRAF6 binding motif deletion construct does not interact with endogenous IRAK2

R1s were seeded at 1x 10^5 cells/mL in 100mm dishes 36 hours prior to transfection. Cells were transfected with pRK5 (8μg), A52R (2μg) or ΔT6BM (8 μg) using GeneJuice™ according to the manufacturer's directions. The cells were harvested 24 hours post-transfection in PBS, followed by lysis in NP-40 lysis buffer (50mM HEPES, 100mM NaCl, 1mM EDTA, 10% glycerol, 0.5% NP-40). Whole cell extracts were incubated with IRAK2 antibody pre-coupled to protein A sepharose. The immunoprecipitates and lysates were resolved by SDS-PAGE and the proteins were transferred to Immobilon using a semi-dry transfer system. The blots were probed with antibody specific for A52 or IRAK2, as indicated. This represents one experiment.

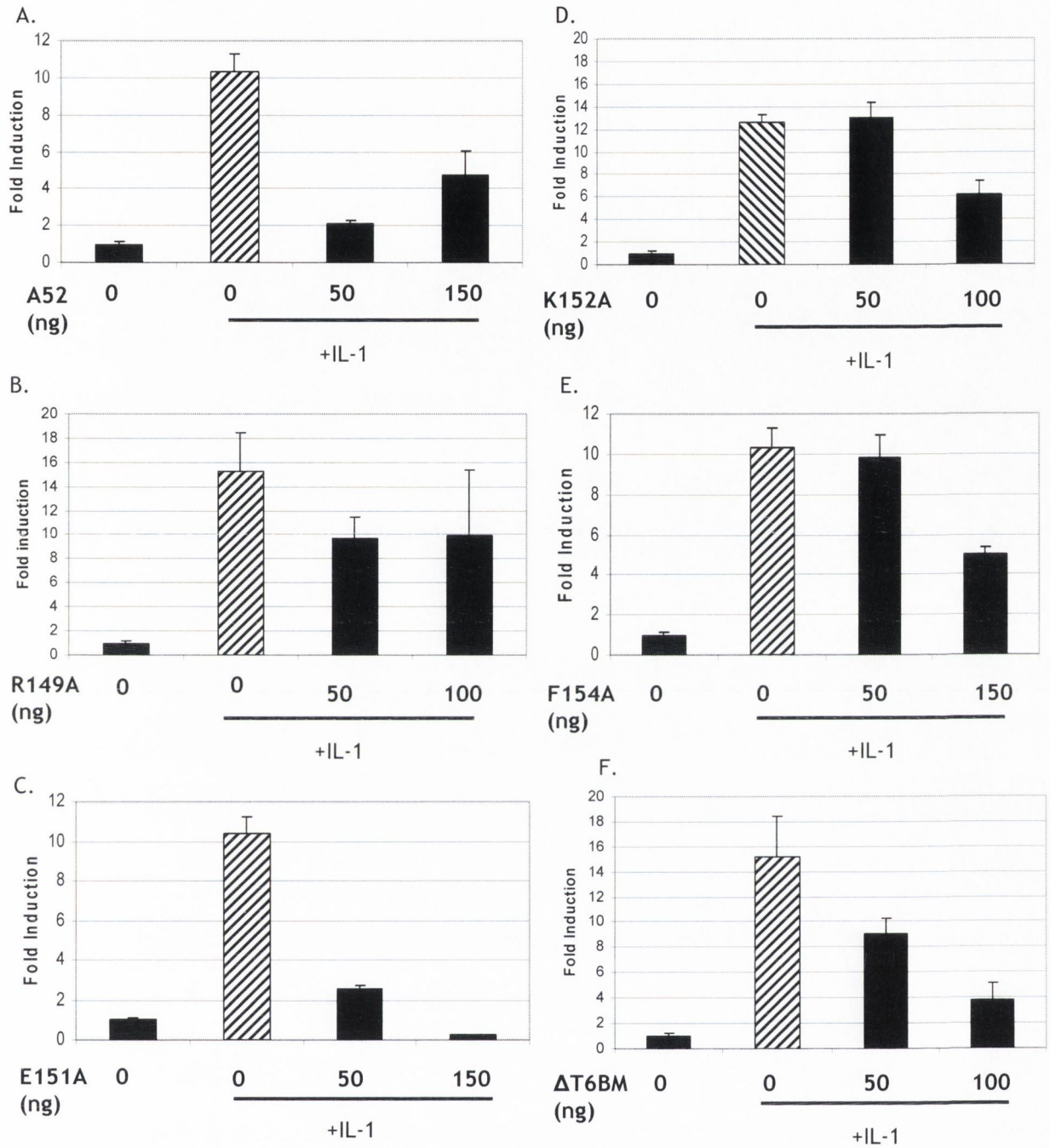

Figure 4.8 A52 mutants F154A and ΔT6BM still inhibit IL-1-induced NF-κB

R1 cells were seeded at 1.0 x 105 cells/mL 24 hours before transfection. The cells were co-transfected with κB-luciferase reporter plasmid (60ng), Tk-Renilla (20ng), and with A52R, R149A, E151A, K152A, F154A or ΔT6BM (50 and 100 or 150ng, as indicated) using GeneJuice™ transfection reagent (Novagen). The following day, the cells were stimulated with IL-1, harvested 6 hours later and the luciferase activity measured. Data are expressed as mean fold induction ± S.D. relative to control levels . Representative of more than three experiments, each performed in triplicate.

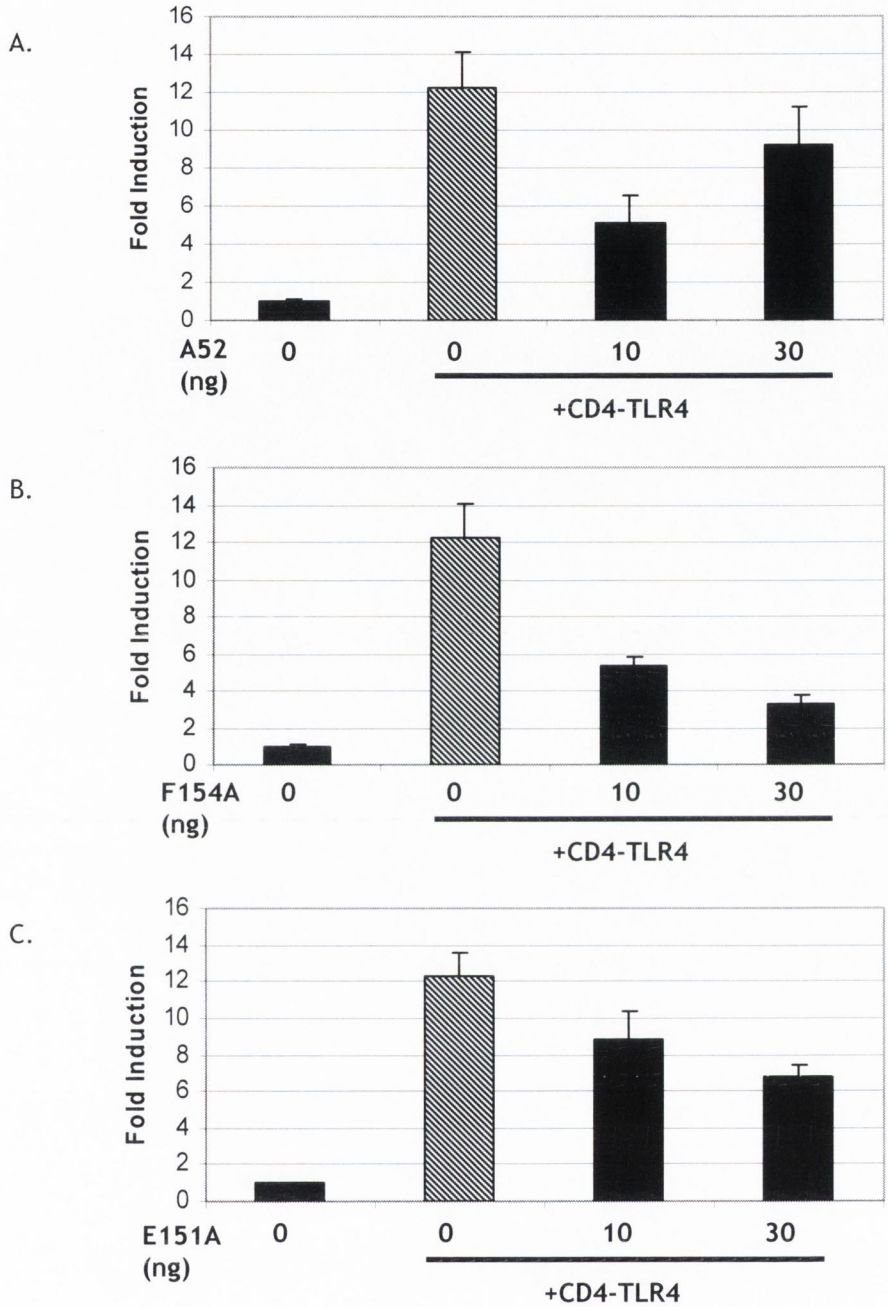

Figure 4.9 A52 mutant F154A inhibits CD4-TLR4-induced NF-κB

R1s were seeded at 1.0 x 10^5 cells/mL in 96-well plates and co-transfected with NF-κB luciferase reporter plasmid (60ng), Tk-Renilla (20ng), and CD4-TLR4 (100ng) using GeneJuice™ transfection reagent. The indicated wells were transfected with A52R, F154A or E151A (10, 30 or 50ng). Data are expressed as mean fold induction ± S.D. relative to control levels . Representative of three experiments, each performed in triplicate.

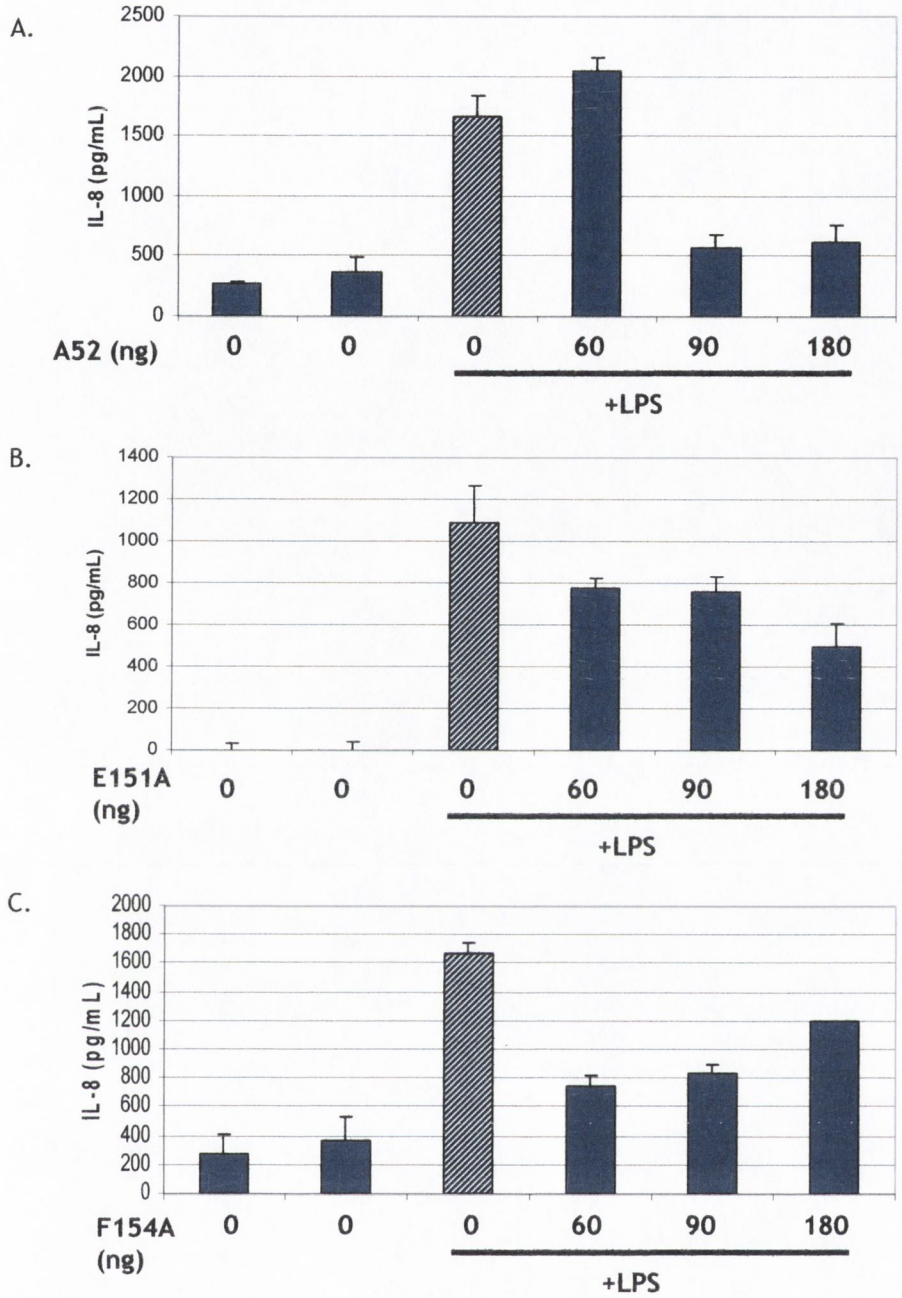

Figure 4.10 A52, F154A and ΔT6BM inhibit LPS-induced IL-8 production in TLR4 cells.

TLR4 cells were seeded at $1x10^5$ cells/mL in 96-well plates. Twenty-four hours later, cells were transfected with the pcDNA3.1 or with increasing doses of A52, E151A or F154A (60, 90 or 180ng) using GeneJuice™. The following day, the indicated wells were stimulated with LPS (50ng/mL final concentration). The cell supernatants were harvested twenty-four hours post-stimulation and assayed for IL-8 production using the human IL-8 ELISA kit from R&D systems according to the manufacturer's directions. Inhibition of LPS-induced IL-8 production was observed three times.

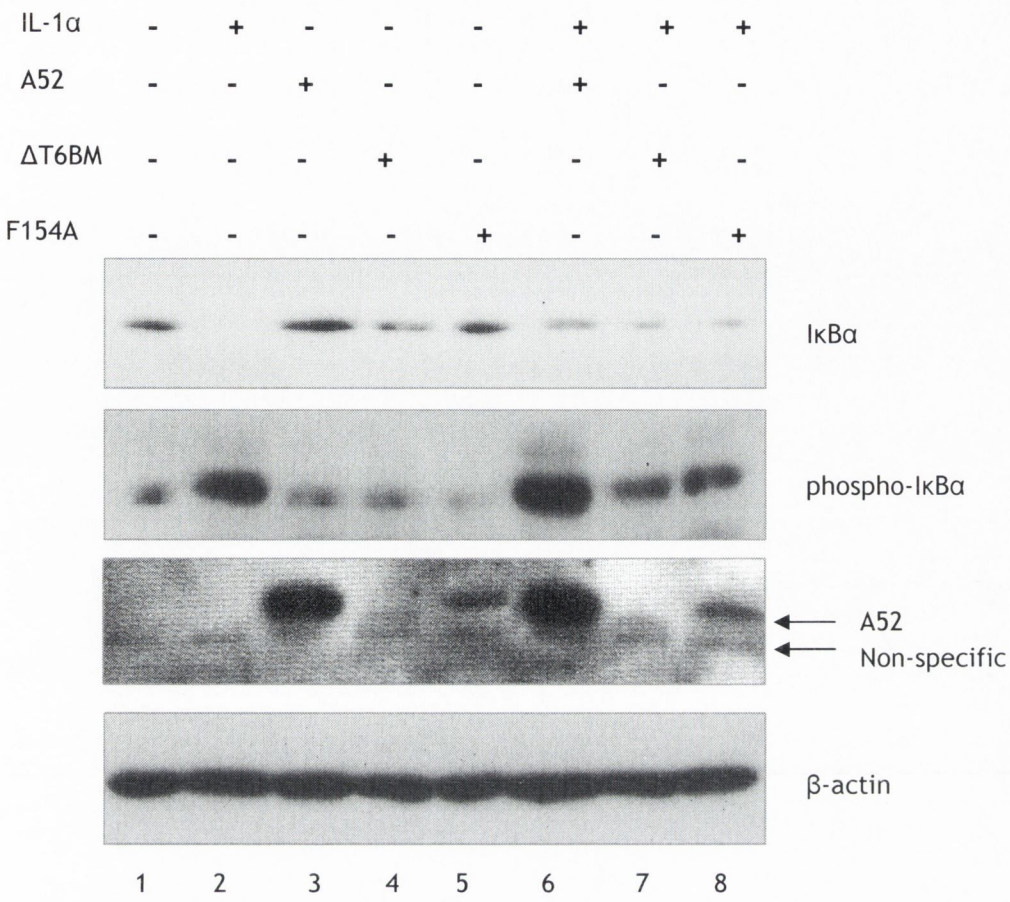

Figure 4.11 A52, F154A and ΔT6BM inhibit IL-1-induced IkB degradation.

R1s were seeded at $1x10^5$ cells/mL in six well plates. Twenty-four hours later, cells were transfected with the indicated plasmids using GeneJuice™. Prior to harvesting, the appropriate wells were stimulated with IL-1α (20ng/mL final concentration) for seven minutes. The cells were harvested in sample buffer and lysed by sonication. The total cell extracts were resolved by SDS-PAGE and the proteins were transferred to Immobilon PVDF membrane by a semi-dry transfer system. The blots were incubated with antibodies specific for IκBα, phospho- IκBα, A52 and β-actin, as indicated. This result has been observed four times for A52 and F154A and twice for ΔT6BM.

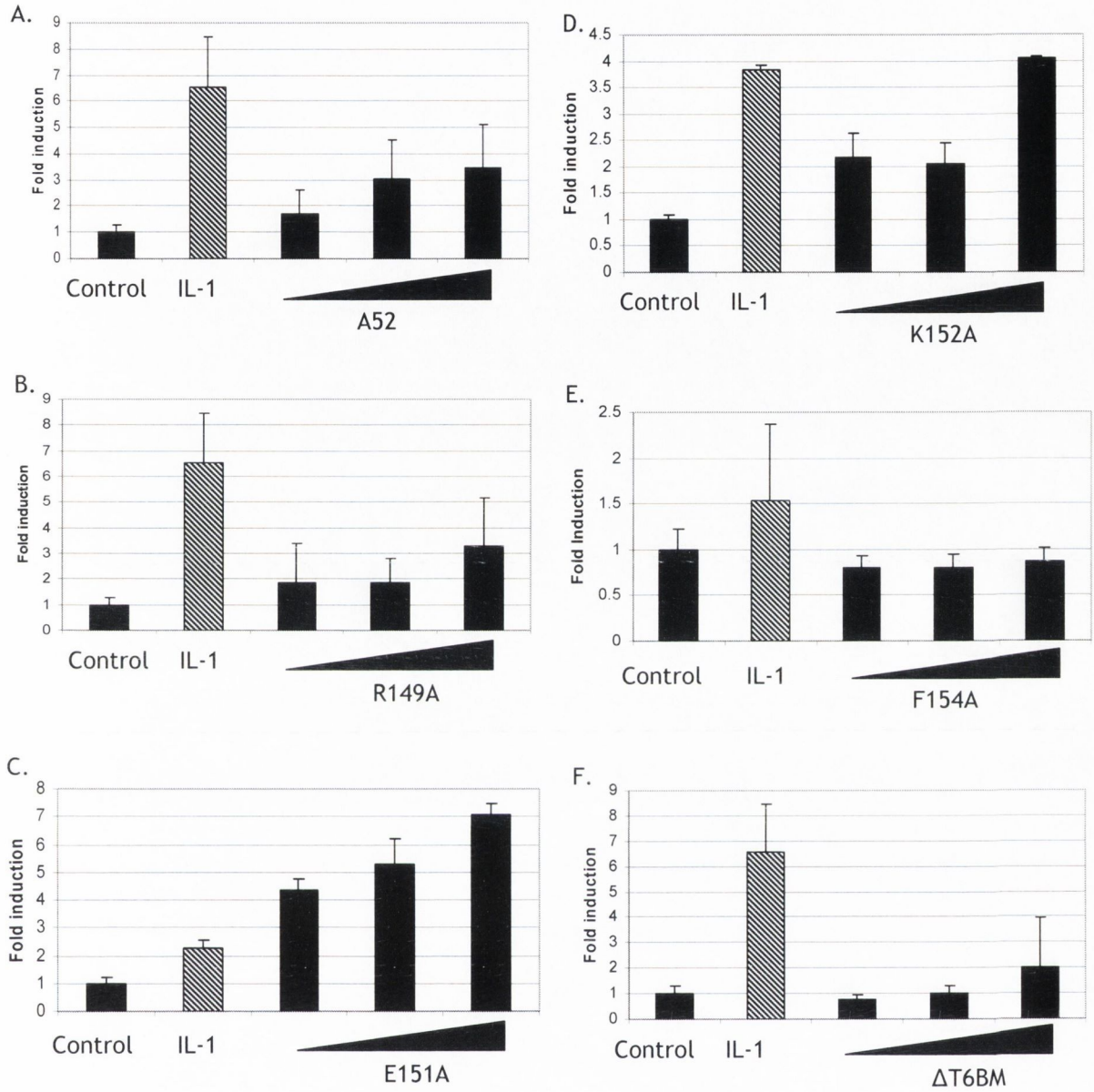

Figure 4.12 A52 mutants F154A and ΔT6BM do not drive p38 activation

R1s were seeded at 1.0 x 10^5 cells/mL 24 hours prior to transfection. The cells were co-transfected with pFR luciferase reporter plasmid (60ng), Tk-Renilla (20ng) and CHOP-Gal4 *trans*-activator plasmid (0.25ng) using GeneJuice™ transfection reagent. The indicated wells were transfected with increasing doses of A52R, R149A, E151A, K152A, F154A and ΔT6BM (10, 30 and 100ng). The following day, the indicated wells were stimulated with IL-1$^{\alpha}$ (20ng/mL final concentration). The cells were harvested 6 hours post-stimulation and the fluorescence was measured. Data are expressed as mean fold induction ± S.D. relative to control levels. Representative of more than three experiments, each performed in triplicate.

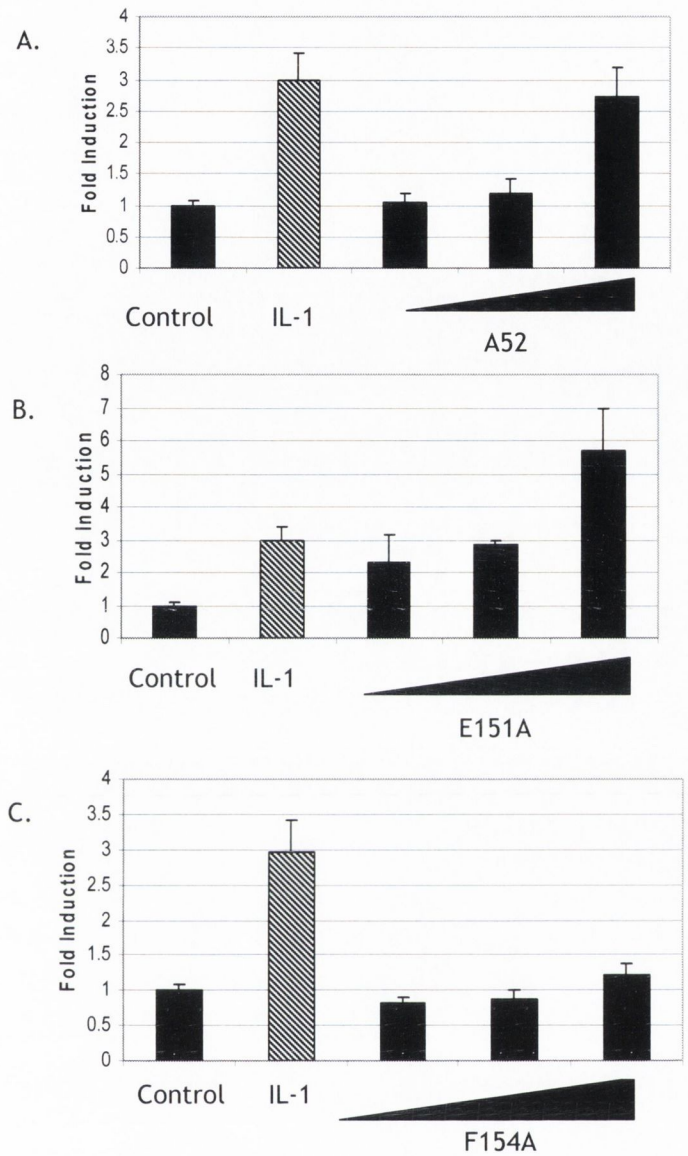

Figure 4.13 A52 mutant F154A does not drive JNK activation

R1s were seeded at 1.0 x 10^5 cells/mL 24 hours prior to transfection. The cells were co-transfected with pFR luciferase reporter plasmid (60ng), Tk-Renilla (20ng) and either the cJun-Gal4 (0.25ng) *trans*-activator plasmid using GeneJuice™ transfection reagent. The indicated wells were transfected with increasing doses of A52R, E151A and F154A (10, 30 and 100ng). The following day, the indicated wells were stimulated with IL-1α (20ng/mL) for 6 hours. Data are expressed as mean fold induction ± S.D. relative to control levels. Representative of three experiments performed in triplicate.

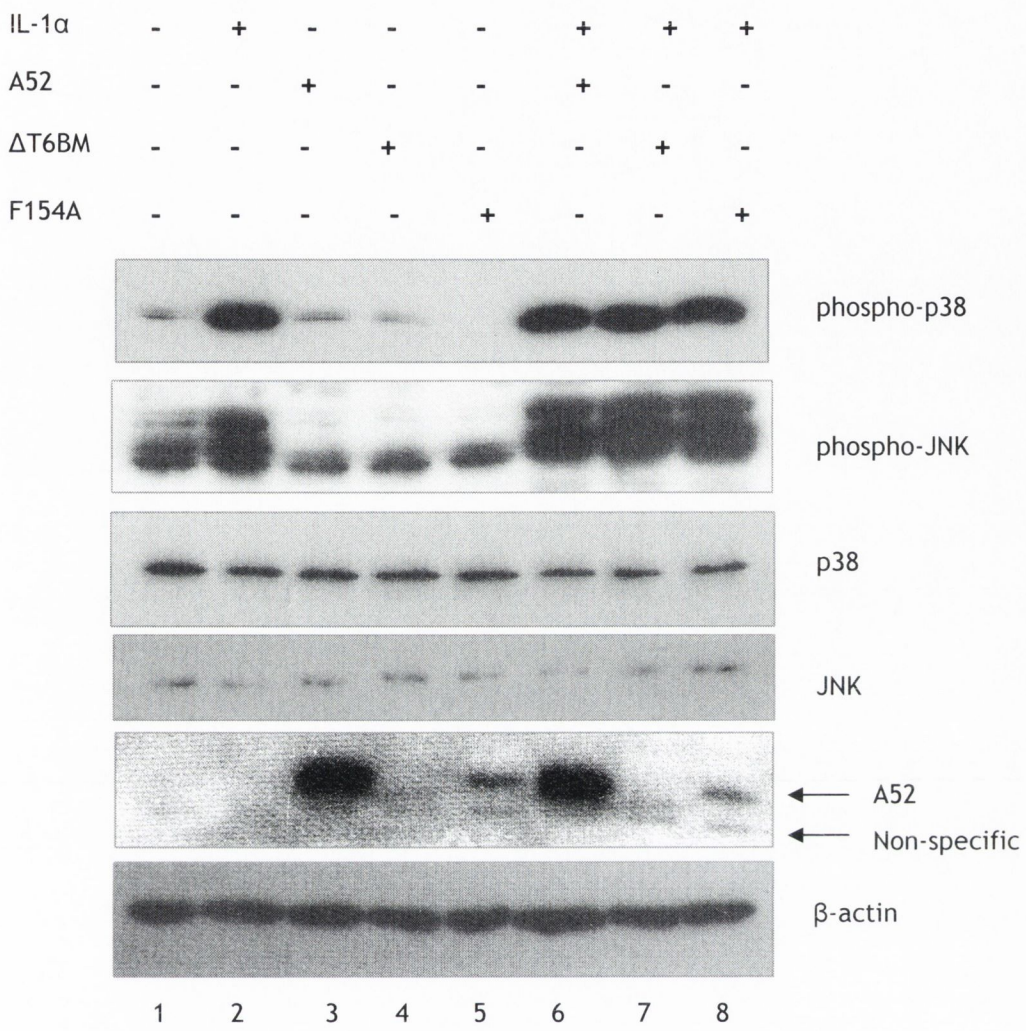

Figure 4.14 A52, F154A and ΔT6BM do not induce phosphorylation of p38 and JNK MAPK

R1s were transfected with 2.3μg of each A52, F154A or ΔT6BM using GeneJuice™ according to the manufacturer's directions. Prior to harvesting, the appropriate wells were stimulated with IL-1α (20ng/mL final concentration) for seven minutes. Cells were harvested in denaturing sample buffer and lysed by sonication. The total cell extracts were analysed by SDS-PAGE and immunoblotting. The blots were incubated with antibodies to phospho-p38, phospho-JNK, total JNK, total p38, A52 and β-actin, as indicated. This result has been observed twice for ΔT6BM and three times for wild-type A52 and F154A.

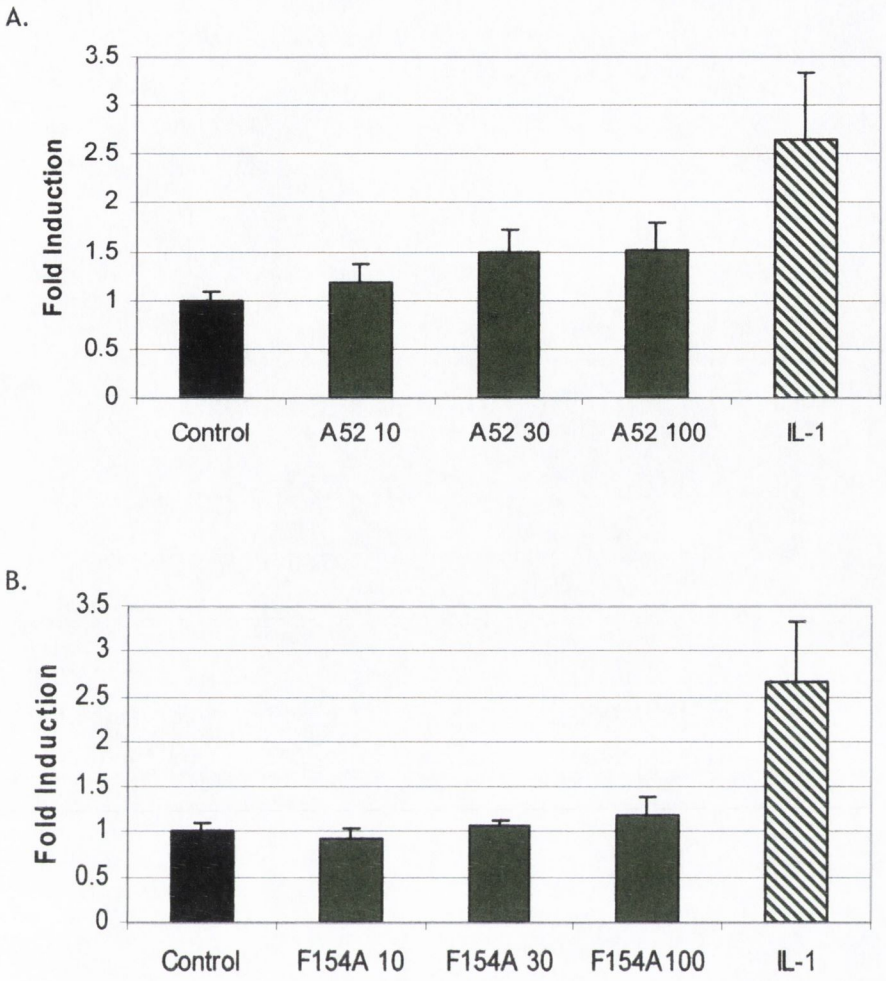

Figure 4.15 A52 activates the human IL-10 promoter weakly in R1s

R1s were seeded at 1.0 x 10^5 cells/mL 24 hours prior to transfection. The cells were co-transfected with human IL-10 promoter reporter plasmid (60ng), Tk-Renilla (20ng) either A52 or F154A (10, 30 and 100ng) using GeneJuice™ transfection reagent. The following day, the indicated wells were stimulated with IL-1α and then harvested 6 hours later. Data are expressed as mean fold induction ± S.D. relative to control levels Representative of three experiments performed in triplicate.

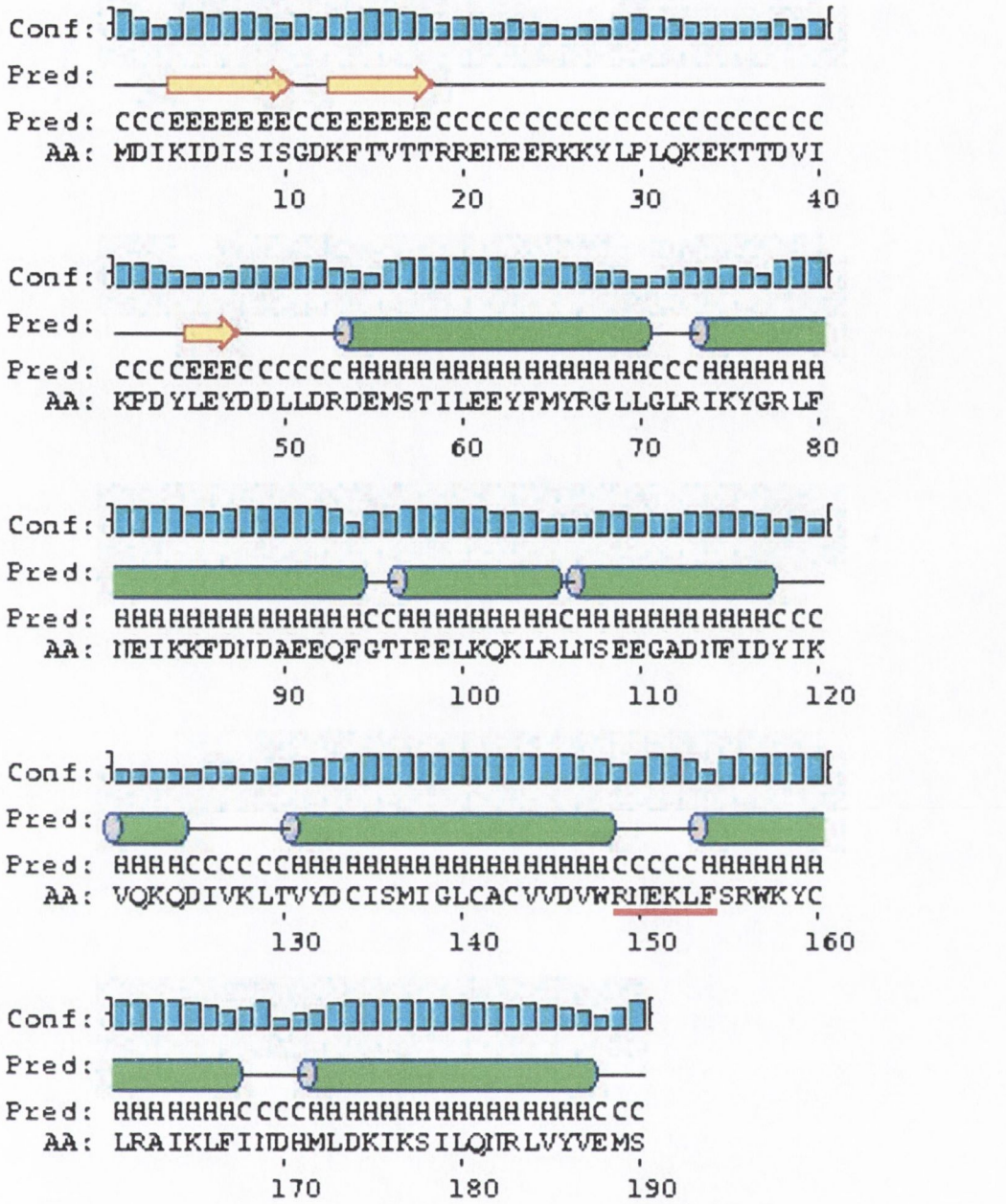

Figure 4.16 Predicted secondary structure of A52

The amino acid sequence of A52 was entered into the PSIPRED server in order to predict the secondary structure (McGuffin et al., 2000). The putative TRAF6 binding motif lies in a coiled region between two helices (underlined in red).

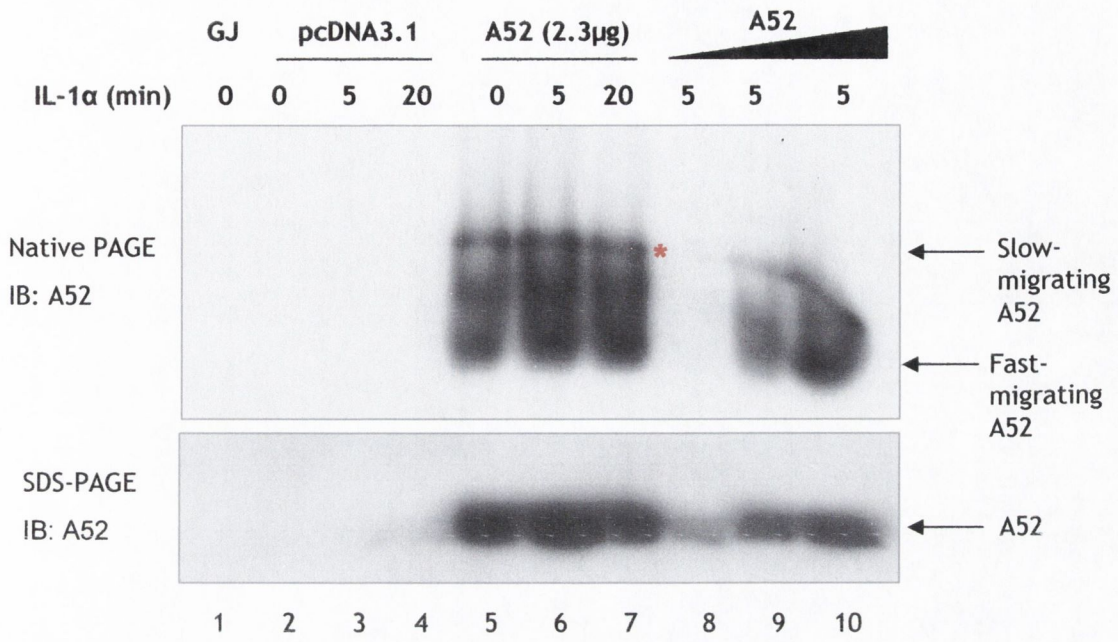

Figure 4.17 Wild-type A52 forms a homodimer under non-denaturing conditions

R1s were seeded at 1x105 cells/mL in 6-well plates 24 hours prior to transfection. The cells were transfected with GeneJuice™ alone (GJ) or with pcDNA3.1 (2.3µg), A52 (2.3µg) or with increasing doses of A52 (0.5, 1, 1.5µg). The indicated samples were stimulated with IL-1α (20ng/mL)for 5 or 20 minutes prior to harvesting the cells. Cells were harvested in phosphate-buffered saline and then lysed with NP-40 lysis buffer (50mM HEPES, 100mM NaCl, 1mM EDTA, 10% glycerol, 0.5% NP-40). Whole cell extracts were divided in half and treated with either non-denaturing (top panel) or denaturing (bottom panel) sample buffer. The samples treated with non-denaturing buffer were analysed by 7% native PAGE (top panel). The denatured samples were analysed for A52 protein expression by SDS-PAGE (bottom panel). The proteins were transferred to Immobilon PVDF by a sem-dry transfer system. The blots were incubated with A52 antibody. The fast migrating form of A52 is indicated with an arrow. The slow migrating form is indicated with an asterisk.

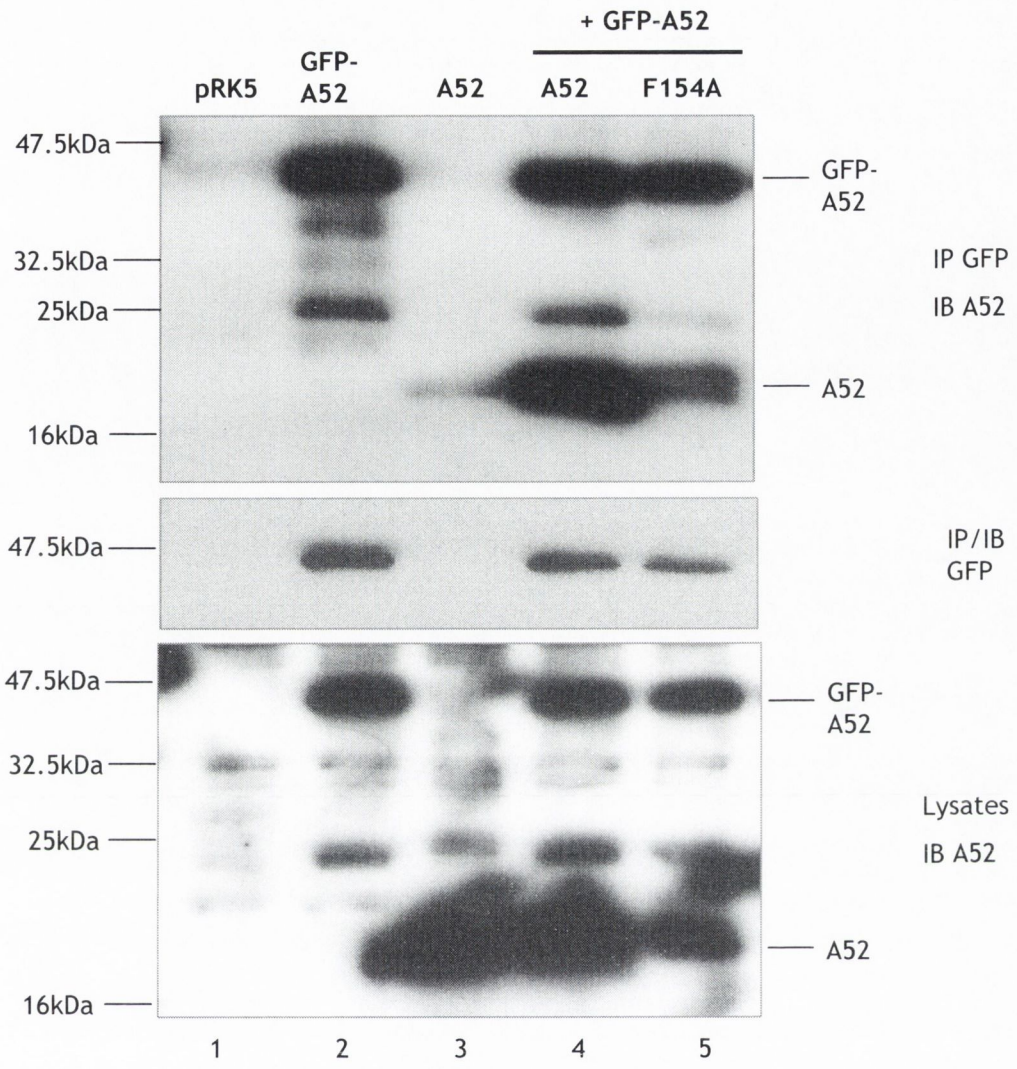

Figure 4.18 Wild-type A52 forms a dimer with GFP-A52

R1s were seeded at 1x105 cells/mL in 6-well plates 24 hours prior to transfection. The cells were transfected with pRK5 (8μg), GFP-A52 (4μg), untagged A52 (4μg) or F154A (4μg). Cells were harvested in phosphate-buffered saline and then lysed with NP-40 lysis buffer (50mM HEPES, 100mM NaCl, 1mM EDTA, 10% glycerol, 0.5% NP-40). The total cell extracts were immunoprecipitated with GFP antibody (1μL) pre-coupled to protein A sepharose. The immunoprecipitates and the lysates were analysed by SDS-PAGE followed by transfer to Immobilon PVDF by semi-dry transfer. The blots were incubated with antibodies to A52 or GFP, as indicated.

4.3 Discussion

In this chapter, a critical residue of A52 required for MAPK activation was identified. While point mutation of this residue did not impair co-precipitation of A52 with TRAF6, the ability of A52 to drive p38 and JNK MAPK activation was abrogated. The requirement of A52 for TRAF6 in order to activate p38 MAPK was previously described (Maloney *et al.*, 2005). MAPK activation in wild-type and TRAF6$^{-/-}$ MEFs further demonstrated a role for TRAF6 in both IL-1 and A52-induced MAPK activation. In wild-type MEFs, both IL-1 and A52 induced phosphorylation of JNK and p38 MAPKs, as well as the p38-dependent transcription factor, ATF-2 (Figure 4.1). Phosphorylation of JNK, p38 and ATF-2 was not observed in IL-1-stimulated TRAF6$^{-/-}$ MEFs, suggesting that TRAF6 is required for their activation in response to IL-1. In terms of IL-1-dependent signalling, this finding is consistent with a requirement for TRAF6 to activate the MAP3K, TAK1 (Chen, 2005). Interestingly, A52 induced phosphorylation of JNK and p38 weakly in TRAF6-/- MEFs but did not induce the phosphorylation of ATF2. This suggests that A52-induced phosphorylation of MAPK is TRAF6-independent but the full activation of the MAPK such that they can activate transcription factors requires TRAF6. It is unclear at this stage how A52 could induce the phosphorylation of the MAPK in the absence of TRAF6, although it is possible that another interaction partner is involved.

In the previous chapter, A52 was found to interact with endogenous TRAFs 2, 3 and 6. At first, this finding is incongruous with the divergent evolution of the TRAFs and the fact that they recognise distinct motifs in binding partners. There are precedents for proteins to interact with both TRAF6 and one or more of TRAFs 1, 2 3 or 5, such as CD-40. Typically, such proteins contain separate consensus binding motifs for TRAF6 and the other TRAFS. The *herpesvirus saimiri* oncoprotein STP-A has been found to interact with TRAF6 via an N-terminal TRAF6 binding motif and this interaction is critical for STP-A-induced NF-κB activation (Garcia *et al.*, 2007). Mutation of the central glutamate

in the TRAF6 binding motif of STP-A (E12A) results in a loss of interaction with TRAF6 and the concomitant loss of the ability to activate NF-κB (Garcia *et al.*, 2007; Jeong *et al.*, 2007). STP-A also has a centrally-located TRAF2 interaction motif that is independent of the TRAF6 binding motif (Garcia *et al.*, 2007). Furthermore, the two motifs were functionally distinct in that the STP-A-TRAF6 interaction is more important than the STP-A-TRAF2 interaction for NF-κB activation (Garcia *et al.*, 2007; Jeong *et al.*, 2007).

The role of the TRAF6 binding motif in the association of proteins with TRAF6 is controversial. Mutation of one or more TRAF6 binding motifs in a given protein does not typically result in a loss of interaction with TRAF6. In contrast, mutation of the TRAF6 binding motif is usually associated with a loss of function of the protein. The TIR adaptor molecule TRIF has three TRAF6 binding motifs in its N-terminal region (Sato *et al.*, 2003). Mutating one of the motifs (E88A) did not inhibit NF-κB activation or TRAF6 binding (Sato *et al.*, 2003). However, both a double (E88/252A) and a triple mutant (E88/252/3A) showed reduced NF-κB activation (Sato *et al.*, 2003). Only the triple mutant (E88/252/3A) was unable to bind TRAF6 (Sato *et al.*, 2003). Thus, mutation of one glutamate within the one TRAF6 binding motif is not sufficient to affect the physical association of TRAF6 and TRIF. Moreover, it is interesting that none of the three TRAF6 binding motifs was the preferred site of interaction with TRAF6.

Mal is another TIR domain-containing adaptor protein that mediates signalling from activated TLRs. Mal was found to contain a TRAF6 binding motif (Mansell *et al.*, 2004). Mutation of the TRAF6 binding motif (E190A) did not result in a loss of interaction with TRAF6 (Mansell *et al.*, 2004). However, the Mal E190A mutant could not activate NF-κB, JNK or p42/p44 MAP kinase (Mansell *et al.*, 2004). Thus, mutation of the TRAF6 binding motif in Mal results in a loss of function but does not affect the interaction with TRAF6.

TRAF6 was found to interact with IRAK after IL-1 stimulation (Cao *et al.*, 1996). Human IRAK has three TRAF6 binding motifs (Ye *et al.*, 2002). Mutation of the central glutamate residues (P_0 position) in all three motifs is required in order to reduce NF-κB activation (Ye *et al.*, 2002). The three motifs are likely to be functionally redundant (Ye *et al.*, 2002). Whether any or all of the mutations altered the ability of IRAK to interact with TRAF6 was not published (Ye *et al.*, 2002).

The IRAK family member IRAK2 contains two TRAF6 binding motifs (Ye *et al.*, 2002). Mutation of the central glutamate of each of these residues individually or together did not alter the ability of IRAK2 to interact with TRAF6 (Keating *et al.*, 2007). Mutation of the second TRAF6 binding motif (E528A) inhibited the ability of IRAK2 to activate NF-κB and p38 MAP kinase (Keating *et al.*, 2007). The loss of function observed with the E528A mutant correlated with the abrogation of IRAK2-induced TRAF6 polyubiquitination (Keating *et al.*, 2007). Thus, while the motif is crucial for function of IRAK2, it does not appear to be essential for the IRAK2-TRAF6 interaction.

Since A52 interacts with the endogenous TRAFs 2, 3 and 6, the amino acid sequence of A52 was examined for TRAF-interaction motifs. A TRAF interaction motif TIEE (residues 96-99) was identified by the program ELM. This motif could account for the ability of A52 to interact with TRAF2 and TRAF3, though the functionality of this motif was not tested. In addition, a putative TRAF6 binding motif was identified in A52 at residues 149-154 (Figure 4.2A). The putative TRAF6 binding motif in A52 (RNEKLF) does not match the consensus sequence (P-X-E-X-X-Ac/Ar) since it has an arginine in place of the proline in the consensus sequence. Despite this difference, the pattern and two of the other conserved residues were present. A52 has the central glutamate residue, which was found to be the most critical residue for mediating the interaction with TRAF6 (Ye

et al., 2002). In addition, the C-terminal residue is a phenylalanine in A52 and thus fits the consensus sequence since it is an aromatic amino acid. Moreover, the motif was located in a C-terminal region of A52 that had been found to be required for interaction with TRAF6 and activation of p38 (Maloney *et al.*, 2005). Thus, further studies were carried out to determine if the potential TRAF6 binding motif was functional.

Mutation of the putative TRAF6 binding motif at individual residues did not inhibit the co-precipitation of A52 with TRAF6 (Figure 4.5). While mutation of a single residue within the TRAF6 binding motif was sufficient to abrogate the TRAF6-caspase 4 interaction (Lakshmanan and Porter, 2007), disruption of the interaction with TRAF6 has not been observed following point mutation of the motif in most TRAF6-interacting proteins studied. Individual point mutations of the central glutamate of the TRAF6 binding motif in Mal did not prevent interaction with TRAF6 (Mansell *et al.*, 2004). Furthermore, mutation of the glutamate in both of the TRAF6 binding motifs in IRAK2 did not disrupt the interaction with TRAF6 (Keating *et al.*, 2007). In other proteins, such as caspase 8 and MALT1, mutation of the central glutamate residue in both motifs within each protein resulted in a loss of interaction with TRAF6 (Bidère *et al.*, 2006; Noels *et al.*, 2007). Thus, mutation of more than one residue within a motif or of multiple motifs, when present in the protein, may be necessary to abrogate the interaction with TRAF6. It has been suggested that the consensus motif provides the specificity for interaction with TRAF6 but that other neighbouring residues could contribute to the stability of the interaction (Zapata *et al.*, 2006). Whether or not a single mutation within the core motif is sufficient to abrogate the TRAF6 interaction likely depends upon the contribution of neighbouring residues in the protein to the overall interaction with the TRAF domain.

In this chapter, deletion of the entire motif appeared to have disrupted the A52-TRAF6 interaction (Figure 4.6). The ΔT6BM construct did not express as well as wild-type A52 or F154A and this low level of expression could make it more difficult to detect an interaction with TRAF6. However, though the level of expression was lower than for wild-type and the point mutants, ΔT6BM was expressed and was detectable with the A52 antibody (Figure 4.4). The ΔT6BM protein may not fold correctly due to the large deletion and thus structural features required for the interaction with TRAF6 could be disrupted. Altered folding could also mask an epitope that is detected by the A52 antibody, making it more difficult to detect ΔT6BM by immunoprecipitation.

Since wild-type A52 inhibits IL-1-induced NF-κB activation, the TRAF6 binding motif mutants of A52 were analysed to determine if they retained this function. Several lines of evidence suggest that A52 and all of the mutants can inhibit NF-κB activation. First of all, wild-type and mutant A52 can inhibit IL-1-induced NF-κB activation (Figure 4.8). Secondly, A52 and the point mutants tested (E151A and F154A) could inhibit CD4-TLR4- and poly (I:C)/TLR3-induced NF-κB inhibition. Thirdly, the LPS-induced production of IL-8 in TLR4 cells was inhibited by wild-type A52, E151A and F154A. IL-8 is a chemokine that is both induced by and can induce production of NF-κB (Manna and Ramesh, 2005). Inhibition of LPS-induced IL-8 production in TLR4 cells by wild-type A52 was described previously (Maloney *et al.*, 2005). Finally, the IL-1-induced degradation of IκBα was inhibited by A52, F154A, ΔT6BM (Figure 4.11) and E151A (data not shown). Mutation of the TRAF6 binding motif in A52 did not impair the ability of A52 to inhibit ligand-induced NF-κB activation. In fact, some mutations seemed to enhance the inhibitory effect of A52, with E151A and ΔT6BM always inhibiting NF-κB reporter gene activation better than the wild-type. The ability of A52 and the mutants to inhibit ligand-induced NF-κB activation and the expression of NF-κB-dependent genes suggests that the TRAF6 binding motif is not required for the mechanism of inhibition. This is consistent with

the hypothesis that it is the A52-IRAK2 interaction that is more important for the inhibition of NF-κB, while the A52-TRAF6 interaction is needed for MAPK activation by A52.

Interestingly, wild-type and mutant A52 were found to either enhance or not alter the level of phosphorylation of IκBα (Figure 4.11). In two experiments, F154A appeared to inhibit IL-1-induced phosphorylation of IκBα slightly but in several other experiments it had no effect on the level of phosphorylation. It was thus hypothesised that A52 did not inhibit phosphorylation of IκBα but prevented the phosphorylated IκBα from being degraded. In contrast to these findings, a peptide derived from the sequence of A52 (p13) was found to inhibit phosphorylation of IκBα (McCoy *et al.*, 2005). The peptide p13 inhibited LPS/TLR4-induced IκBα phosphorylation (McCoy *et al.*, 2005), while A52 enhances IL-1-induced IκBα phosphorylation (Figure 4.11). The western blots for IκBα phosphorylation are not shown (McCoy *et al.*, 2005) so it is impossible to compare them with the blots in this chapter. Moreover, the effects of a peptide could differ from those of a whole protein so it is difficult to compare the p13 results with those obtained from the study of over-expressed A52. The contradictory findings could also be due to differences in TLR4 and IL-1R signalling. Indeed, studies of p13 function were conducted following stimulation by TLR ligands, including LPS, CpG and poly(I:C) but did not look at IL-1-induced signalling pathways (McCoy *et al.*, 2005; Tsung *et al.*, 2007). Phosphorylation of IκBα following TLR stimulation and the effect of A52 thereon was not studied in this chapter.

A52 also has a stimulatory function in that it can activate p38 and JNK MAP kinases in the absence of ligand stimulation and in a TRAF6-dependent manner (Maloney *et al.*, 2005). The TRAF6 binding motif mutants of A52 were analysed to determine if they too could activate MAP kinases. All of the mutants except F154A and ΔT6BM were able to

activate p38 in the CHOP assay (Figure 4.12). F154A was also unable to activate JNK (Figure 4.13) and ERK (data not shown) MAP kinases in similar reporter gene assays. ΔT6BM was not tested in the JNK and ERK reporter gene assays. The phosphorylation of p38 and JNK was also analysed by western blotting. Since wild-type A52 was unable to induce phosphorylation of either p38 or JNK in R1s in the absence of ligand stimulation, it was impossible to discern any altered functionality in F154A or ΔT6BM (Figure 4.14).

Mutation of the TRAF6 binding motif may not always disrupt interaction with TRAF6, as discussed above, but it is frequently linked to a loss of function. It could be that the core motif, in addition to providing the specificity of binding, also contributes to activation of TRAF6 function. Peptides corresponding to the core TRAF motifs can activate TRAF-dependent signalling pathways in the absence of CD40 receptor stimulation (Zapata *et al.*, 2006). In addition, peptides derived from the RANK TRAF6 binding motif are able to block osteoclast differentiation (Ye *et al.*, 2002; Poblenz *et al.*, 2007). The role of the TRAF6 binding motif in function has been confirmed by numerous mutation studies on different TRAF6-interacting proteins. Mutation of the TRAF6 binding motif in Mal results in the loss of the ability of Mal to drive an NF-κB reporter gene and to induce p65 transactivation (Mansell *et al.*, 2004). In addition the mutant Mal is unable to activate JNK and p44/p42 MAP kinases (Mansell *et al.*, 2004). Likewise, mutation of one of the two TRAF6 binding motifs in IRAK2 (E528A) results in the loss of the ability of IRAK2 to activate an NF-κB reporter gene and to induce IL-8 production (Keating *et al.*, 2007). Interestingly, mutation of the other TRAF6 binding motif in IRAK2 does not alter the function of the protein, suggesting that the two motifs are not redundant (Keating *et al.*, 2007).

The p38 MAP kinase is important in antiviral immunity since it promotes type I interferon gene transcription (Katsoulidis *et al.*, 2005). At first glance therefore, the

ability of A52 to activate p38 seems counterintuitive; since p38 is critical to the antiviral response, it would seem more likely that a virus would endeavour to inhibit p38 activation. However, the induction of p38 MAP kinase by other viruses has been described for varicella-zoster virus (Rahaus *et al.*, 2004) and the SARS coronavirus (Kopecky-Bromberg *et al.*, 2006). In the case of varicella-zoster virus, the temporal regulation of p38 and JNK activation is required for viral replication since MAPK-induced cellular transcription factors transactivate varicella-zoster genes (Rahaus *et al.*, 2004). Thus, modulation of p38 MAPK activation could be an immune subversion mechanism, whereby a protective signalling pathway of the host is used to favour viral replication.

One downstream target gene of p38 is IL-10, a Th2 cytokine that suppresses both inflammation and cell-mediated immunity in order to maintain homeostasis (Ma *et al.*, 2001). Following LPS stimulation, p38 MAPK activates Sp1, a transcription factor which binds to the human IL-10 promoter and induces IL-10 expression (Ma *et al.*, 2001). One viral immune subversion strategy is to induce IL-10 production in order to dampen the immune response and a number of viruses, including hepatitis B virus, Epstein-Barr virus and HIV, encode proteins that up-regulate IL-10 production (Mogensen and Paludan, 2001). The HIV protein Tat induces IL-10 production by p38-dependent activation of the Sp1, CREB-1 and Ets-1 transcription factors (Gee *et al.*, 2007; Li and Lau, 2007). Thus, A52 could activate p38 in order to induce the production of IL-10 and to suppress the immune response (Maloney *et al.*, 2005).

A52 was previously found to activate the IL-10 promoter in the absence of ligand stimulation (Maloney *et al.*, 2005). In this chapter, wild-type A52 and F154A were analysed for their ability to drive the IL-10 promoter. While wild-type A52 was able to activate the promoter, it did so weakly in comparison to IL-1 (Figure 4.15). F154A did not activate the IL-10 promoter as much as wild-type (Figure 4.15). Although this result

was reproducible, the IL-10 promoter was never strongly activated by wild-type A52 and it is thus difficult to conclude that the F154A mutant cannot activate it. In addition, previous studies showed that A52 could enhance LPS-induced IL-10 production (Maloney *et al.*, 2005), a pathway that is p38-dependent (Ma *et al.*, 2001). The effect of the TRAF6 binding motif mutants on LPS-induced IL-10 was not determined due to difficulties with transfection of the RAW 264.7 murine macrophage cell line.

Recently, the crystal structure of an N-terminally truncated form of A52 has been solved and found to adopt a Bcl-2-like fold (Figure 4.19; Graham *et al.*, 2008). The Bcl-2-like fold in A52 is similar to that determined for the other VACV proteins N1 (Cooray *et al.*, 2007) and B14 (Graham *et al.*, 2008). The model of A52 predicted by bioinformatics (Figure 4.16) is very similar to the crystal structure, with the putative TRAF6 binding motif an exposed, coiled region between two alpha helices. As predicted, the F154 residue is the first residue of the second alpha helix.

The three-dimensional structure of another VACV protein, N1, is similar to that of Bcl-x_L, a Bcl-2 family member (Cooray *et al.*, 2007). The Bcl-x_L protein is anti-apoptotic and contains a surface groove that binds to BH3 motifs of pro-apoptotic proteins (Cooray *et al.*, 2007). Structural studies revealed a similar surface groove in N1 (Cooray *et al.*, 2007), which was confirmed by crystallography studies on N1 bound to BH3 peptides (Aoyagi *et al.*, 2007). In addition to having a similar three-dimensional structure to Bcl-x_L, N1 interacts with the pro-apoptotic proteins and inhibits staurosporine-induced apoptosis (Cooray *et al.*, 2007). Thus, N1 may function as an anti-apoptotic survival factor, allowing infected cells to survive and viral progeny to be produced. While A52 was found to adopt a Bcl-2-like fold, it did not have the BH3 peptide-binding groove (Graham *et al.*, 2008). Unlike N1, A52 was unable to inhibit staurosporine-induced apoptosis and thus retains the Bcl-2-like structure whilst not

having anti-apoptotic activity (Graham *et al.*, 2008). The conserved fold might serve other, as yet undiscovered functions of A52. It has been found that the TRAFs have role in regulation of apoptosis, possibly by monitoring a cell survival checkpoint (Lomaga *et al.*, 2000; Arch *et al.*, 1998), so it is feasible that the TRAFs can interact with proteins possessing the structural hallmarks of apoptotic molecules. Thus, the retention of the Bcl-2-like fold might be important in the binding of A52 to the TRAFs or to the modulation of TRAF function.

In addition to the discovery of a Bcl-2-like fold in A52, the structural studies revealed that A52 dimerises (Figure 4.19; Graham *et al.*, 2008). The aromatic side chain of F154 is exposed and lies adjacent to the dimer interface (Figure 4.19, highlighted in red). Since the F154 residue is adjacent to the dimer interface, there could be a role for it in the formation or stabilisation of the dimer. Based on the structural data, it was hypothesised that the inability of F154A to activate MAPK could be due to a loss of dimerisation in the wild-type A52. In this chapter, the dimerisation of wild-type A52 was examined by native PAGE and the results indicated that there could be at least one fast- and one slow-migrating form of A52, which could correspond to monomeric and dimeric A52 (Figure 4.17). However, the results were ambiguous and could not be reproduced with the TRAF6 binding motif mutants F154A and ΔT6BM (data not shown). In addition, the absence of reliable non-denaturing protein standards for native PAGE made it difficult to interpret the results further. To further investigate A52 dimerisation, untagged and GFP-tagged A52 were co-transfected into cells. Co-precipitation of wild-type A52 and F154A with GFP-A52 has been observed, suggesting that A52 forms homodimers. Since F154A was found to associate with GFP-A52, it is unlikely that the loss of the ability to drive MAP kinase activation with this point mutant is due to a loss of dimerisation. The ΔT6BM was also tested for co-immunoprecipitation with GFP-A52. While no interaction between GFP-A52 and ΔT6BM were detected, it

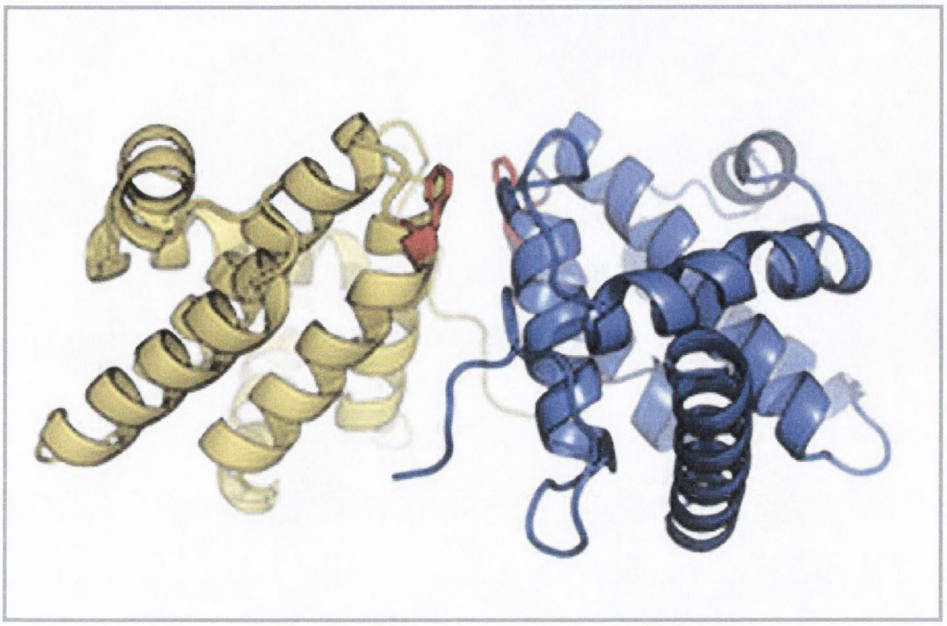

Figure 4.19 A52 forms a homodimer in solution

Structural studies on an N-terminally-truncated construct of A52 found that A52 formed a homodimer. The two monomers are shown in yellow or blue ribbon diagrams. The F154A residue (in red) is adjacent to the dimer interface. This figure was provided by S. Graham, University of Oxford.

could not be concluded that ΔT6BM did not dimerise since the control pull-down of GFP-A52 was not successful in these samples. Nonetheless, the evidence that the F154A mutant retains the ability to dimerise suggests that dimerisation alone is not required for MAPK activation by A52. However, it should be noted that the GFP-tagged A52 present had the wild-type sequence. Mutation of GFP-A52 to F154A and use of the GFP-F154A construct in a similar experiment would be interesting. It could be that mutation of the F154A residue of both interaction partners would abolish dimerisation.

In this chapter, a critical residue required for A52-induced MAPK activation was identified. The mutation of the F154 residue to alanine resulted in a loss of the ability to activate p38, JNK and ERK MAPK. The mutant was still functional in that it was able to inhibit IL-1R/TLR-induced NF-κB activation and to block expression of the NF-κB-dependent cytokine, IL-8. Nonetheless, F154A could still bind to TRAF6, suggesting that the putative TRAF6 binding motif is in fact a TRAF6 activation motif. The mechanism by which A52 can activate MAPK remains to be discovered and the F154A mutant will be used to further explore this function of A52.

Chapter Five: Results III

The effect of wild-type and mutant A52 on TRAF6 auto-ubiquitination

5.1 Introduction

A52 activates p38 MAPK in a TRAF6-dependent manner (Maloney *et al.*, 2005). Mutation of the putative TRAF6 binding motif in A52 at the phenylalanine or deletion of the entire motif prevented p38 activation (Chapter 4). Thus, this TRAF6 binding motif must be required for the mechanism of action of A52.

It is possible that the TRAF6 binding motif is required for more than just binding TRAF6 but for activation as well. Point mutation of the motif is typically insufficient to impair interaction with TRAF6, as observed in the previous chapter. Nonetheless, point mutations of the central glutamine residue have generally resulted in a loss of function of the protein, such as impaired ability to activate NF-κB by mutant IRAK2 (Keating *et al.*, 2007). The TRAF6 binding motif may thus be more important for TRAF6 activation rather than binding. Further, it has been found that RANK-induced osteoclastogenesis can be inhibited by peptides corresponding to the TRAF6 binding motifs of RANK (Poblenz *et al.*, 2007). Peptides containing the other TRAF motifs have been found to mimic TNFR signalling to activate NF-κB and JNK in the absence of ligand stimulation (Sutherland *et al.*, 1999). Thus, the motif could be important for activation of TRAF6 function rather than simply recognition of binding partners.

It has been established that TRAF6-dependent signalling from IL-1R/TLRs to NF-κB and MAPK activation depends on the function of TRAF6 as an E3 ubiquitin ligase (Chen, 2005; Kishida *et al.*, 2005). TRAF6 catalyses K63-linked polyubiquitin chains which are important in activation of proteins for signal transduction rather than for their degradation (Keating and Bowie, 2008; Haglund and Dikic, 2005). For example, TRAF6-mediated K63-linked polyubiquitination is required to activate both TAK1 and the IKK complex (Haglund and Dikic, 2005). The TAK1-binding proteins, TAB2 and TAB3, contain ubiquitin binding domains that are required for the activation of TAK1, possibly by

binding to the K63-linked polyubiquitin chains on the IKK complex (Haglund and Dikic, 2005). The K63-linked polyubiquitination of the IKK subunit, NEMO, is required for NF-κB activation (Haglund and Dikic, 2005). Further, K63-linked ubiquitination of NEMO was shown to be important in the inflammatory response by modulating TLR-induced cytokine production, leading to activation of the IKK complex, JNK and p38 following stimulation with LPS and IL-1 (Ni *et al.*, 2008; Lamothe *et al.*, 2008).

TRAF6 was originally identified as an E3 ligase, working with the E2 enzyme complex Ubc13/UeV1A to conjugate K63-linked polyubiquitin chains onto the IKK complex (Deng *et al.*, 2000). The unique feature of TRAF6-mediated polyubiquitination at the time was that it did not target the IKK complex for proteasomal degradation but rather activated its kinase function (Deng *et al.*, 2000). In addition, it has been shown that TRAF6 is itself ubiquitinated (Kishida *et al.*, 2005). The K124 residue of TRAF6 is the main site of auto-ubiquitination since mutation of this residue to arginine abolishes the ability of TRAF6 to activate TAK1 or the IKK complex (Lamothe *et al.*, 2007a). In addition, wild-type but not K124R TRAF6 can act as an E3 ligase to conjugate K63-linked polyubiquitin chains to NEMO, an essential step in the activation of the IKK complex (Lamothe *et al.*, 2007a). The auto-ubiquitination of TRAF6 is thus critical for signal transduction.

TRAF6 auto-ubiquitination depends upon the presence of an intact RING domain and on association with Ubc13/Uev1A (Deng *et al.*, 2000; Lamothe *et al.*, 2007b). Mutation of residues within the RING domain of TRAF6 (C70A or C85A/H87A) abolished the ability of TRAF6 to activate NF-κB (Deng *et al.*, 2000). The RING domain of an E3 ubiquitin ligase is typically responsible for recruiting the E2 enzyme, followed by the conjugation of ubiquitin to the substrate (Vaux and Silke, 2005). One report found that the TRAF6 RING was responsible for recruiting Ubc13 (Wooff *et al.*, 2004), while another study found that the distal TRAF-N (or coiled-coil) domain interacted with the E2 complex

(Yang *et al.*, 2004). The latter observation is controversial given that numerous studies have indicated the importance of the RING/E2 interaction. Interestingly, structural studies of the RING domain of TRAF6 and Ubc13 by NMR indicated that there was only a weak affinity between them (Mercier *et al.*, 2007). The low affinity could be due to the absence of Uev1A from the structural studies or could suggest that interaction with another region of TRAF6, such as the TRAF-N, is required.

It has been claimed that the ubiquitination status of an E3 is the most sensitive indicator of its *in vitro* activity and may also be of physiological relevance (Fang and Weissman, 2004). Furthermore, substrate association or the interaction with other proteins may regulate the auto-ubiquitination of the E3 (Fang and Weissman, 2004). Since A52 requires an intact TRAF6 binding motif to activate MAPK, together with the fact that TRAF6 auto-ubiquitination is essential for its role in signalling, it was therefore hypothesised that A52 might affect the TRAF6 E3 ligase activity. If A52 could affect TRAF6 auto-ubiquitination, this might regulate substrate recognition and ubiquitination, thus affecting downstream NF-κB and MAPK activation. The inhibition of IL-1R/TLR-induced NF-κB activation by A52 might be due to its inhibition of TRAF6 catalytic activity or auto-ubiquitination, possibly by blocking IRAK2-induced TRAF6 auto-ubiquitination. Since A52 alone can activate MAPK, it was first examined whether A52 could alter TRAF6 auto-ubiquitination in the absence of ligand-stimulation. Subsequently, ligand-induced TRAF6 ubiquitination was examined. The kinetics of IL-1-induced TRAF6 ubiquitination and deubiquitination are rapid, with a peak of ubiquitination at ten minutes post-stimulation (Jensen and Whitehead, 2003; Windheim *et al.*, 2008a). The effect, if any, of A52 on IL-1-induced TRAF6 ubiquitination kinetics was also investigated in this chapter.

5.2 Results

5.2.1 Endogenous ubiquitination of TRAF6 is not detectable

It was hypothesised that A52 may affect TRAF6 ubiquitination or its role as an E3 ligase. In order to test this, it was first necessary to show that TRAF6 was ubiquitinated following stimulation of IL-1R/TLR signalling. Several experiments were performed to detect TRAF6 ubiquitination in HEK 293s or R1s following stimulation with LPS or IL-1, respectively. The samples were immunoprecipitated for TRAF6 and then subsequent blots were incubated with antibody directed against ubiquitin. Initially, an antibody that had been raised against both conjugated and unconjugated ubiquitin chains (Santa Cruz, FL-76) was used in western blotting but no endogenous ubiquitination of TRAF6 was detected (data not shown). Since activated TRAF6 is polyubiquitinated with K63-linked ubiquitin moieties, an antibody directed against poly-ubiquitin chains was obtained (Bio-Mol, clone FK1). FLAG-TRAF6 was over-expressed in R1s and the cells were stimulated with IL-1. No polyubiquitination of FLAG-TRAF6 was visible following IL-1 stimulation (Figure 5.1, top panel). The antibody did not detect much polyubiquitin in the lysates (Figure 5.1, middle panel). The expression of FLAG-TRAF6 was not equal in all samples (Figure 5.1, bottom panel). There is reduced expression in the middle of the blot which is likely due to an uneven transfer (Figure 5.1, middle and bottom panel, lanes 2 and 3). The samples were also resolved on 10-20% gradient gels but, while poly-ubiquitin was detected in the lysates, no poly-ubiquitination of TRAF6 was detected (data not shown). Since the polyubiquitin antibody could not detect much ubiquitin in the lysates, this assay was not further optimised for endogenous ubiquitination of TRAF6 in R1s.

Despite a report that ubiquitination of TRAF6 is observable in HepG2 cells following stimulation with IL-1 (Jensen and Whitehead, 2003), this was not observed when the

experiments were replicated here. No ubiquitinated TRAF6 was observed in HepG2s following IL-1 stimulation for seven minutes (Figure 5.2, top panel, lanes 2-4). The immunoprecipitation of TRAF6 was equal in all samples (Figure 5.2, second panel from top, lanes 1-4) and ubiquitin was detected in the cell lysates (Figure 5.2, second panel from bottom, lanes 1-4). The use of only a single time-point of stimulation may have prevented observation of the onset of TRAF6 ubiquitination. IL-1-induced TRAF6 ubiquitination in HepG2s was reported after 10 minutes and was decreasing by 20 minutes post-stimulation (Jensen and Whitehead, 2003). In order to examine this, other time points following IL-1 stimulation were tested but TRAF6 ubiquitination was not observed (data not shown). No effect of the overexpression of A52 on the ability to detect ubiquitinated TRAF6 was observed.

5.2.2 TRAF6 ubiquitination is detected with over-expressed myc-tagged ubiquitin

Since it was not possible to detect ubiquitination of endogenous or over-expressed TRAF6 in R1s or HepG2s, a myc-tagged construct of ubiquitin was obtained and found to be expressed when transfected into R1s (data not shown). Following over-expression of myc-ubiquitin in R1s, the cells were stimulated with IL-1 for 5, 10 or 15 minutes. The cells were immunoprecipitated for TRAF6 and then immunoblotted for myc (Figure 5.3, top panel). Myc-ubiquitinated TRAF6 was observed following 5 and 10 minutes of IL-1 stimulation (Figure 5.3, top panel, lanes 3 and 4). The apparent increase in myc-ubiquitination of TRAF6 following 10 minutes of IL-1 stimulation could have been due to increased myc-ubiquitin expression in the cells (Figure 5.3, lane 4, compare top and bottom panels). The amount of unmodified TRAF6 precipitated was equal (Figure 5.3, middle panel). In the same samples where myc-ubiquitinated TRAF6 is observed, higher molecular mass forms of TRAF6 were detected in the control blot (Figure 5.3, middle panel, lanes 3 and 4). Other studies have extrapolated from the presence of higher molecular mass forms of TRAF6 in *in vitro* ubiquitination assays to conclude that TRAF6

is ubiquitinated (Yang *et al.*, 2004). Thus, it is likely that the higher molecular mass forms observed are ubiquitinated TRAF6.

Detection of ubiquitinated TRAF6, even when using over-expressed ubiquitin, was found to be variable. One factor that could have impaired detection was the lack of an appropriate inhibitor of the deubiquitinase (DUBs) enzymes in the lysis buffer. The DUBs are typically cysteine proteases (Fang and Weissman, 2004). Iodoacetamide is used to inhibit DUBs (Windheim *et al.*, 2008a) since it alkylates cysteine and methione residues, including those at the active sites of DUBs (Sigma technical data). Therefore, iodoacetamide use was introduced during studies of the IL-1-induced myc-ubiquitination of TRAF6.

In order to determine whether A52 affected TRAF6 E3 ubiquitin ligase activity, a number of experiments were performed to look at the effect, if any, of over-expression of A52 on TRAF6 ubiquitination. When myc-ubiquitin and A52 were co-transfected into R1s, A52 induced the ubiquitination of TRAF6 in the absence of ligand stimulation (Figure 5.4, top panel, lane 4). Following IL-1 stimulation of the cells for 10 minutes, myc-ubiquitination of TRAF6 was observed and this was decreased by A52 (Figure 5.4., top panel, compare lanes 6 and 8). The immunoprecipitation of TRAF6 was reduced in the last two samples and this could account for the apparent reduction in myc-ubiquitination of TRAF6 in the presence of A52 (Figure 5.4., second panel, lanes 7 and 8). Both A52 and myc-ubiquitin were expressed in the cells (Figure 5.4, bottom two panels).The observed increase in TRAF6 ubiquitination in the presence of A52 alone was not reproducible. However, A52 appeared to have an effect on IL-1-induced TRAF6 ubiquitination. A time-course of IL-1 stimulation was planned in order to further elucidate the effects of A52 on TRAF6 ubiquitination.

5.2.3 A52 alters the kinetics of TRAF6 ubiquitination

Preliminary results obtained by over-expression of the myc-ubiquitin construct in R1s suggested that A52 could stimulate TRAF6 ubiquitination in the absence of a ligand (Figure 5.4). Unfortunately, the myc-ubiquitin construct stopped expressing during attempts to study the time-course of IL-1-induced ubiquitination of TRAF6 (data not shown). At this time, a HA-tagged ubiquitin construct became available and was found to be expressed in R1s. The amount of HA-ubiquitin needed to observe IL-1-induced TRAF6 ubiquitination was assessed (Figure 5.5). It was found that 4μg of HA-ubiquitin were needed to observe TRAF6 ubiquitination following IL-1 stimulation (Figure 5.5, top panel, lane 3). The immunoprecipitation of TRAF6 was even in all lanes (Figure 5.5, middle panel). Although the TRAF6 immunoprecipitation control blot was dark, a distinct band of TRAF6 above the heavy chain was observed on the film. Further experiments analysing TRAF6 ubiquitination were performed with the HA-ubiquitin construct. In addition, detection of the HA-ubiquitinated TRAF6 was facilitated by baking the blots at 80°C for one hour prior to blocking.

The effect of A52 on IL-1-induced TRAF6 ubiquitination was assessed following a time-course of IL-1 stimulation (Figure 5.6). A52 enhanced the ubiquitination of TRAF6 following IL-1 stimulation for 5 minutes (Figure 5.6, top panel, compare lanes 5 and 6). Following IL-1 stimulation for 10 minutes, the HA-ubiquitination of TRAF6 was visible in the lane without A52 and was completely absent from the lane with A52 (Figure 5.6, top panel, compare lanes 7 and 8). The immunoprecipitation of TRAF6 was not equal in all lanes, with the amount of precipitation being greater in lanes 3, 4, 6, 7 and 8 than in the other lanes (Figure 5.6, second panel from top). The reduced level of immunoprecipitation of TRAF6 in lane 5 could partially account for the apparent absence of HA-ubiquitination of TRAF6 in this lane (Figure 5.6, top panel). However, the amount of HA-ubiquitination of TRAF6 observed in the sample with A52 was very

intense and it is unlikely that the difference in levels of TRAF6 immunoprecipitation alone could account for all of the increase of TRAF6 ubiquitination observed with A52 (Figure 5.6, top panel, lane 6). The HA-ubiquitin construct and A52 were expressed well (Figure 5.6, bottom two panels).

In order to further elucidate the kinetics of IL-1-induced TRAF6 ubiquitination and the affect of A52 thereon, a more extensive time-course was performed. There was no ubiquitination of TRAF6 in the absence of IL-1 stimulation or in the presence of A52 alone (Figure 5.7, top panel, lanes 1-4). A52 appeared to enhance IL-1-induced TRAF6 ubiquitination at two minutes post-stimulation (Figure 5.7, top panel, compare lane 5 and 6). Similarly, at five minutes post-stimulation, A52 enhanced IL-1-induced TRAF6 ubiquitination (Figure 5.7, top panel, compare lanes 7 and 8). At ten minutes post-stimulation, over-expression of A52 did not alter the level of TRAF6 ubiquitination (Figure 5.7, top panel, lanes 9 and 10). Finally, at twenty minutes post-stimulation, IL-1-induced TRAF6 ubiquitination was decreased but still detectable (Figure 5.7, top panel, lane 11). Remarkably, in the lane containing A52 at twenty minutes post IL-1 stimulation, TRAF6 was fully deubiquitinated (Figure 5.7, top panel, lane 12). Unlike in the previous experiment (Figure 5.6), the immunoprecipitation of TRAF6 was equal in all samples (Figure 5.7, second panel from top). HA-ubiquitin and A52 were well expressed in all the relevant samples (Figure 5.7, bottom two panels). Importantly, A52 enhances TRAF6 ubiquitination at early time points and accelerates deubiquitination of TRAF6 at later time points following IL-1 stimulation. Since this is a stimulatory function of A52 in the acceleration of TRAF6 ubiquitination kinetics, it might correlate with the other known positive role for A52 in MAPK activation. In order to examine this further, the non-functional mutants identified in the previous chapter were analysed in this assay.

5.2.4 The A52 mutants F154A and ΔT6BM do not alter TRAF6 ubiquitination kinetics

Since wild-type A52 accelerated the kinetics of TRAF6 ubiquitination, it was hypothesised that this could account for the ability of A52 to enhance IL-1-induced MAPK activation via TRAF6. If this was the case then the TRAF6 binding motif mutants F154A and ΔT6BM, which do not activate MAPKs, would be expected to be unable to accelerate TRAF6 ubiquitination. In order to test this, the affect of wild-type A52, F154A and ΔT6BM constructs on TRAF6 ubiquitination was compared. During these experiments when ubiquitin was over-expressed, non-specific ubiquitination of TRAF6 was observed in the absence of any stimulus (data not shown). Since this would obscure the results, it was necessary to re-optimise the conditions further before the affect of the TRAF6 binding motif mutants on TRAF6 ubiquitination could be analysed.

Many studies of ubiquitination rely upon over-expressed HA- or myc-tagged ubiquitin. One problem with the use of over-expressed ubiquitin is that it can become associated with the substrate protein in a non-specific manner. Thus it can be necessary to reduce the amount of over-expressed ubiquitin used in order to eliminate non-specific ubiquitination. Initially, it was found that 4μg of HA-ubiquitin was required to observe specific ubiquitination of TRAF6 (Figure 5.6). This quantity was used in numerous ubiquitination experiments and was found to be specific. A new plasmid preparation of the HA-ubiquitin construct was made and found to express better than the previous preparation (data not shown). There was a high level of non-specific ubiquitination of TRAF6 in cells transfected with the new HA-ubiquitin plasmid preparation and in the absence of any stimulus. In order to circumvent this problem, the amount of HA-ubiquitin needed to observe specific ubiquitination of TRAF6 was titrated (Figure 5.8). Without IL-1 stimulation, intense TRAF6 ubiquitination was observed when 1 μg of HA-ubiquitin was transfected into R1s (Figure 5.8, top panel, lane 4). While a faint smear of TRAF6 ubiquitination is detectable in unstimulated cells with 0.5μg HA-ubiquitin, no

ubiquitinated TRAF6 is detectable in the sample containing 0.25µg HA-ubiquitin (Figure 5.8, top panel, lanes 2 and 3). Surprisingly, over-expression of 1 µg of HA-ubiquitin did not result in increased amounts of detectable TRAF6 ubiquitination following IL-1 stimulation (Figure 5.8, top panel, lane 8). In the cells stimulated with IL-1, the over-expression of 0.25µg or 0.5µg of HA-ubiquitin resulted in more ubiquitinated TRAF6 being detected than was found with the over-expression of 1µg of HA-ubiquitin (Figure 5.8, top panel, compare lanes 6 and 7 to lane 8). The immunoprecipitation of TRAF6 was relatively equal in all the samples (Figure 5.8, middle panel). The increasing quantities of the HA-ubiquitin construct transfected were detectable in the lysates (Figure 5.8, bottom panel). It was thus decided that 0.25µg of HA-ubiquitin would be used in future experiments since this quantity produced detectable levels of TRAF6 ubiquitination in response to IL-1 stimulation without any ubiquitinated TRAF6 being detected in unstimulated cells.

The effect of the TRAF6 binding motif mutants on TRAF6 ubiquitination was compared to that of wild-type A52 using the reduced quantity of HA-ubiquitin. Without IL-1 stimulation, ubiquitination of TRAF6 was not observed (Figure 5.9, top panel, lanes 1-4). Following IL-1 stimulation for two minutes, ubiquitinated TRAF6 was observed and this was increased in the sample with A52 transfected (Figure 5.9, top panel, compare lanes 5 and 6). In contrast, neither F154A nor ΔT6BM enhanced IL-1-induced TRAF6 ubiquitination (Figure 5.9, top panel, lanes 7 and 8). After 5 minutes IL-1 stimulaton, A52 enhanced TRAF6 ubiquitination relative to the lane with empty vector (Figure 5.9, lanes 9 and 10). At this time point, neither F154A nor ΔT6BM enhanced IL-1-induced TRAF6 ubiquitination (Figure 5.9, top panel, lanes 11 and 12). Similarly, following 10 minutes IL-1 stimulation, only wild-type A52 and not F154A or ΔT6BM enhanced IL-1 - induced TRAF6 ubiquitination (Figure 5.9, top panel, lanes 14-16). The amount of TRAF6 immunoprecipitated was not equal in all lanes, with reduced precipitate found in

samples containing empty vector and A52 that were either unstimulated of stimulated with IL-1 for five minutes (Figure 5.9, second panel from top, lanes 1, 2, 9 and 10). This may have reduced the amount of IL-1-induced TRAF6 ubiquitination observed in these samples, particularly following five minutes of IL-1 stimulation (Figure 5.9, compare top and second from top panels, lane 9). Co-transfection of ΔT6BM and the HA-ubiquitin construct resulted in a reduced level of expression of the HA-tagged ubiquitin (Figure 5.9, second panel from bottom, lanes 4, 8, 12, and 16). In addition, expression of the ΔT6BM plasmid was much lower than that of wild-type A52 and lower than F154A (Figure 5.9, bottom panel, lanes 4, 8, 12 and 16). Thus, it is difficult to conclude that ΔT6BM does not alter TRAF6 ubiquitination since expression of both the HA-ubiquitin and ΔT6BM are reduced. In contrast, F154A expression was found to be comparable to that of wild-type A52 (Figure 5.9, bottom panel, lanes 3, 7, 11 and 15). In general, co-transfection of F154A and HA-ubiquitin did not impair expression of the HA-tagged ubiquitin, although a slight reduction in expression was observed in the sample stimulated with IL-1 for 10 minutes (Figure 5.9, bottom panel, lane 15). It is thus possible to conclude that IL-1-induced TRAF6 ubiquitination is enhanced by wild-type A52 but not by F154A. However, the use of 0.25μg of HA-ubiquitin made it difficult to discern a difference between the wild-type and the mutants since very little ubiquitinated TRAF6 is detectable.

5.2.5 A52 is itself ubiquitinated

Since A52 was able to shift the kinetics of TRAF6 ubiquitination, it was hypothesised that this could account for the stimulatory effect of A52 on MAPK activation. In contrast, the A52 mutants F154A and ΔT6BM did not appear to shift the kinetics of TRAF6 ubiquitination. One rationale for this was that A52 served as a substrate for ubiquitination by TRAF6 and that mutation of the putative TRAF6 binding motif resulted in a loss of recognition of the mutant A52 as a substrate. Numerous protein post-

translational modification algorithms were used to analyse the A52 amino acid sequence. Unfortunately, there is no direct method to analyse a protein sequence for likelihood of ubiquitination since there is no consensus site for lysines that are to be ubiquitinated (Banerjee and Wade, 2002). A52 has several lysine residues and three of those residues (K4, K41 K75) were found to have a high likelihood of modification with a protein related to ubiquitin, the small ubiquitin-like modifier (SUMO), suggesting that A52 could be sumoylated (data not shown; the algorithm used was SUMOplot^{TM}). Since SUMO is related to ubiquitin, it was considered possible that one or more of the lysine residues in A52 could be ubiquitinated rather than sumoylated. Given that TRAF6 is an E3 ubiquitin ligase, it was examined whether A52 was ubiquitinated by TRAF6.

When myc-ubiquitin and A52 were co-transfected into R1s, A52 was ubiquitinated in unstimulated cells (Figure 5.10, top panel, lane 4). Interestingly, stimulation with IL-1 appeared to enhance the amount of ubiquitin detected in the A52 immunoprecipitates (Figure 5.10, top panel, compare lanes 4 and 8). In addition, the ubiquitination appeared to occur in a step-wise fashion, corresponding to 1-3 ubiquitin moieties being added (Figure 5.10, top panel, lanes 4 and 8). Since ubiquitin is approximately 8kDa, stepwise additions of ubiquitin moieties would increase the molecular mass of A52 by 8kDa at a time. For example, the lowest band of A52 is detected at approximately 30kDa, which is consistent with it being monoubiquitinated (Figure 5.10, top panel, lanes 4 and 8). At molecular masses above the heavy chain, where ubiquitinated TRAF6 is detectable, a typical ubiquitin smear was detected (Figure 5.10, top panel, lanes 4 and 8). It is possible that, while A52 is itself ubiquitinated, it is associating with higher molecular mass proteins that are ubiquitinated, such as TRAF6. One method to distinguish which protein is in fact ubiquitinated has been described and involves boiling the initial immunoprecipitations in SDS to dissociate multi-protein complexes and then re-doing the immunoprecipitation (Windheim et al., 2008a). Since several lower

molecular mass species corresponding to the correct size of A52 with one or more ubiquitin moieties attached were observed, it is possible that A52 is in fact ubiquitinated. The use of the aforementioned method of boiling in SDS, followed by re-extraction, could help confirm whether A52 is ubiquitinated or if it is associating with other ubiquitinated proteins, though this method has not yet been employed to study A52 ubiquitination. The level of myc-ubiquitin expressed was equal in all the samples (Figure 5.10, middle panel, lanes 2, 4, 6 and 8). A52 was expressed and immunoprecipitated itself (Figure 5.10, bottom panel, lanes 3, 4, 7 and 8). There was a slight increase in the amount of A52 precipitated following co-transfection with myc-ubiquitin and stimulation with IL-1 (Figure 5.10, bottom panel, lane 8). This could have accounted for the increased ubiquitination of A52 observed in this sample (Figure 5.10, top panel, lane 8).

To determine if TRAF6 served as the E3 ubiquitin ligase that ubiquitinated A52, ubiquitination of A52 was analysed in wild-type and TRAF6$^{-/-}$ MEFs. Since the amount of the plasmid encoding HA-ubiquitin to transfect into MEFs had not previously been titrated, it was not known how much of the plasmid would be needed in order to be able to detect ubiquitination. Initially, 4μg of HA-ubiquitin was transfected into cells but this resulted in relatively high background ubiquitination (data not shown). Thus, 2 μg of HA-ubiquitin was used in further experiments and appeared to be specific. A52 is ubiquitinated in the wild-type MEFs (Figure 5.11, top panel, lanes 4 and 5). In contrast, no ubiquitination of A52 was detected in the TRAF6$^{-/-}$ MEFs (Figure 5.11, top panel, lanes 9 and 10), although HA-ubiquitin was not expressed as well in these cells. Thus, it is possible that TRAF6 is the E3 ubiquitin ligase that modifies A52. A52 could be a pseudo-substrate for TRAF6 ubiquitination, thereby competing with cellular TRAF6 substrates for ubiquitination. It could also be that A52 needs to be ubiquitinated in

order to be recognised by other, as yet undefined interaction partners since ubiquitin-binding proteins are known to be prevalent in cell signalling.

Since wild-type A52 was ubiquitinated, it was next examined whether the TRAF6 binding motif mutants were also ubiquitinated. The functional mutant E151A and the loss-of-function mutant F154A were analysed for ubiquitination. Both mutants were found to be myc-ubiquitinated (Figure 5.12, top panel, lanes 6 and 8). The ubiquitination of F154A appeared to be less than that of A52 or E151 (Figure 5.12, top panel, compare lanes 4, 6 and 8). However, this was likely due to the lower level of immunoprecipitation of F154A relative to A52 and E151A (Figure 5.12, bottom panel, lanes 5 and 6). The myc-ubiquitin did not express well but was detected in all samples (Figure 5.12, middle panel). Both F154A and E151A were tested separately for ubiquitination. While F154A appeared to be ubiquitinated, the ubiquitination of E151A might have been non-specific due to high background ubiquitination in the absence of E151A (data not shown). Since all of these experiments were done with the myc-ubiquitin construct, the expression problems could reflect the difficulties inherent with using that plasmid as was observed in other myc-ubiquitin experiments. Given that a lot of the parameters have now been optimised for HA-ubiquitination experiments, it would be interesting to repeat the side-by-side comparison of the mutants and A52 to confirm that the mutants are ubiquitinated although this has not yet been attempted.

While A52 was able to accelerate the kinetics of IL-1-induced TRAF6 ubiquitination, A52 was unable to reproducibly induce TRAF6 ubiquitination on its own. Nonetheless, the mutants were unable to accelerate IL-1-induced TRAF6 ubiquitination and this could parallel the inability of the mutants to activate MAPK. In addition, ubiquitination of A52 itself does not correlate with the ability of A52 to activate MAPK since both E151A and F154A appeared to be ubiquitinated. If A52 ubiquitination has a role, it might be in

the inhibition of IL-1R/TLR-induced NF-κB activation although this has not been examined.

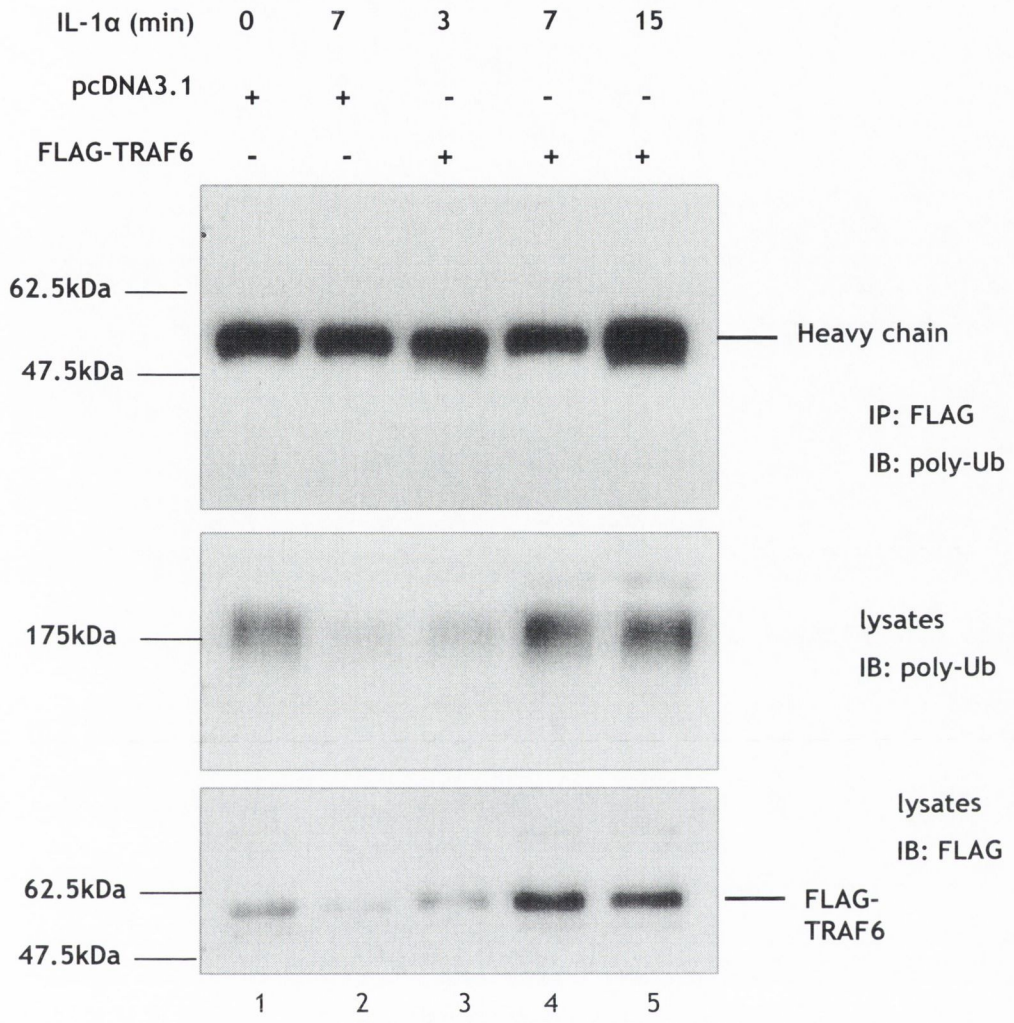

Figure 5.1 Poly-ubiquitinated FLAG-TRAF6 is not detected in R1s following Il-1 stimulation.

R1s were seeded at 1 x 10^5 cells/mL in 100mm dishes. The cells were transfected 24 hours later with 8μg of either pcDNA3.1 or FLAG-TRAF6 as indicated. The following day, the cells were stimulated with IL-1α for 0, 3, 7 or 15 minutes and then were harvested. The cells were lysed and the lysates were immunoprecipitated with either FLAG or TRAF6 (data not shown). The lysates and immunoprecipitates were analysed by SDS-PAGE and were transferred to Immobilon PVDF by a wet transfer system. The blots were incubated with antibodies to poly-ubiquitin or FLAG. This is one of more than three experiments in R1s where poly-uiquitinated endogenous or over-expressed TRAF6 could not be detected following IL-1 stimulation.

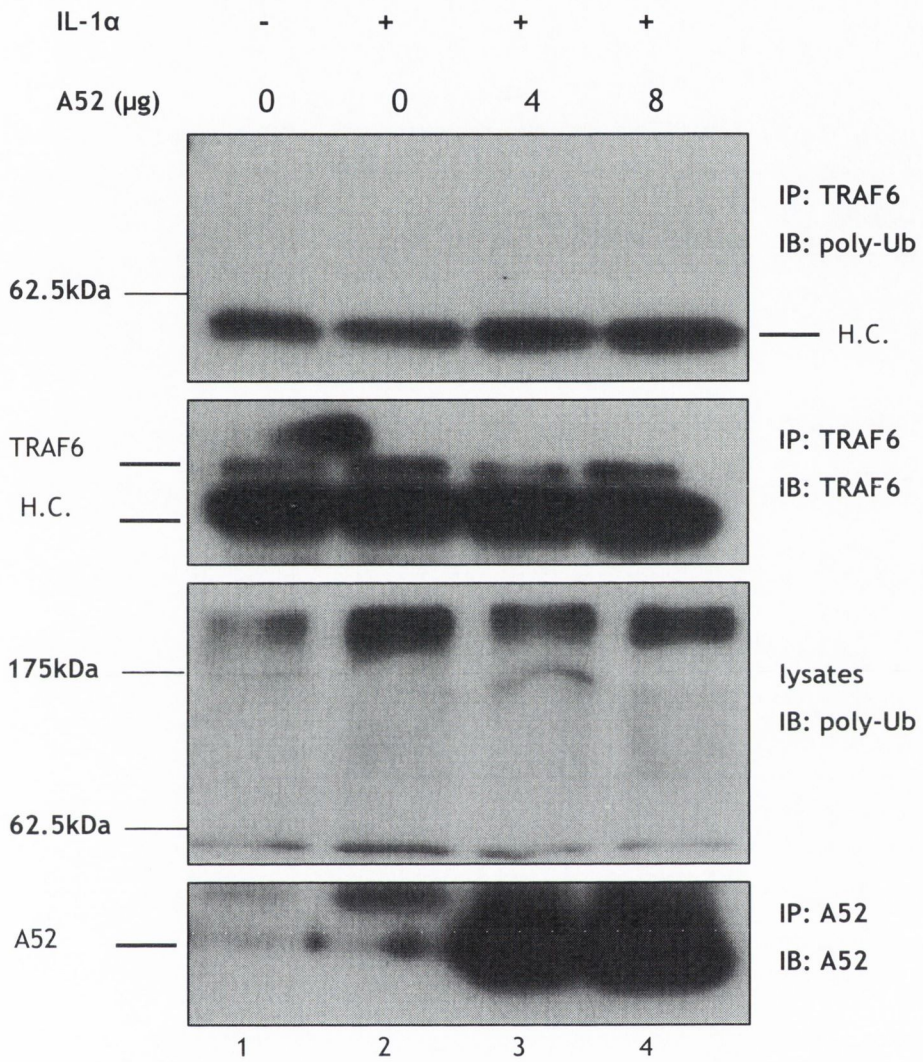

Figure 5.2 Endogenous TRAF6 is not ubiquitinated in HepG2 cells following Il-1 stimulation.

HepG2 cells were seeded at 1 x 10^5 cells/mL in 100mm dishes. The cells were transfected 24 hours later with A52 (4 or 8μg). The following day, the cells were stimulated with IL-1α for 7 minutes and then were harvested. The cells were lysed and the lysates were immunoprecipitated with either TRAF6 or A52. This represents three experiments, with the endogenous TRAF6 being clearly observed in one experiment following modification of the lysis protocol. H.C., antibody heavy chain.

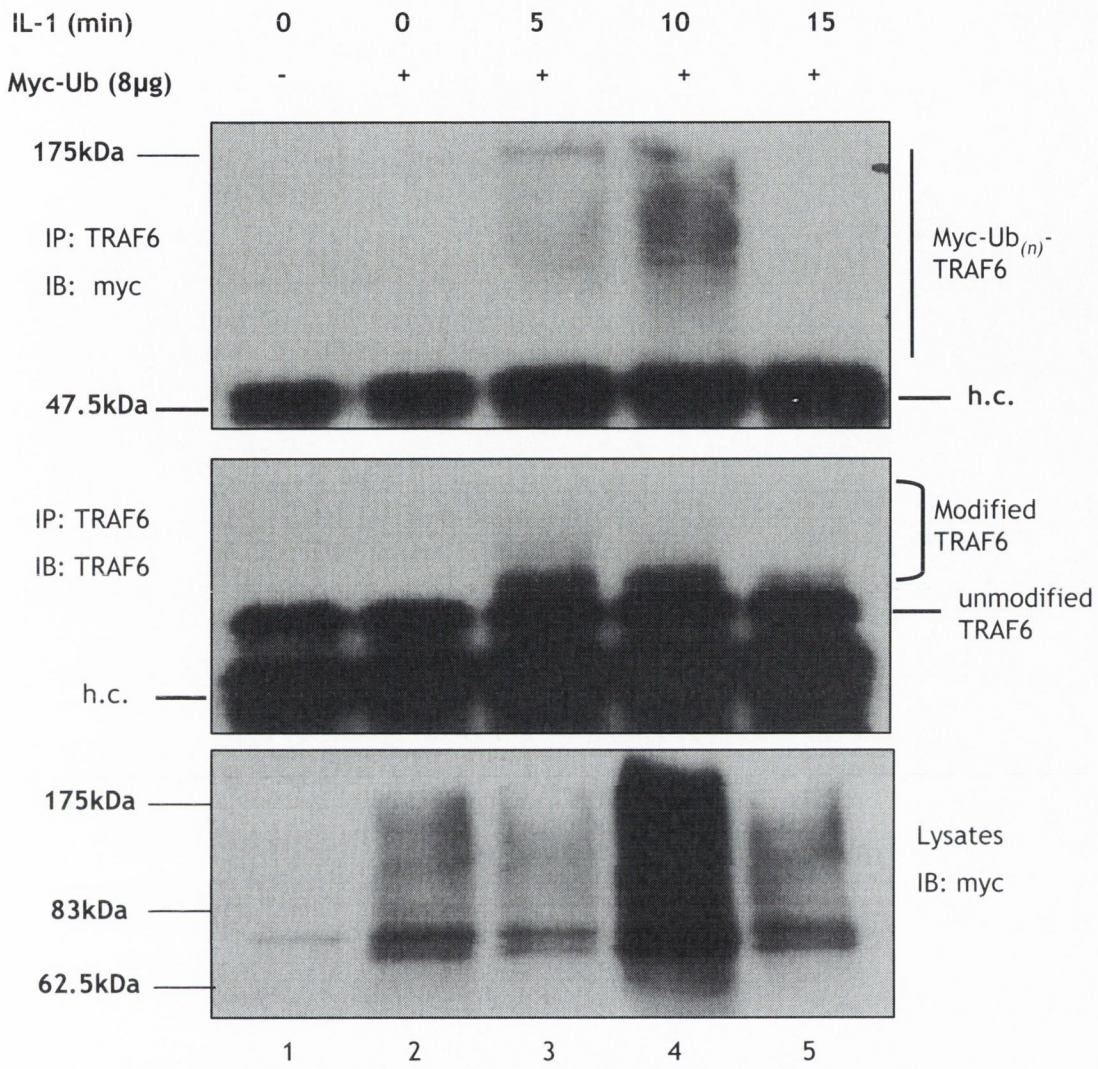

Figure 5.3 Ubiquitinated TRAF6 is detected when myc-ubiquitin is overexpressed.

R1s were seeded at 1.5 x 10^5 cells/mL and transfected the following day with 8 µg of pcDNA3.1 (lane 1) or myc-ubiquitin (lanes 2-5) using GeneJuice™. The cells were stimulated with IL-1β (20ng/mL) for the indicated times and then harvested. The cells were lysed and the lysates immunoprecipitated for TRAF6. The lysates and immunoprecipitates were resolved on a 10% SDS-polyacrylamide gel and transferred to Immobilon PVDF using a wet transfer system. The blots were probed with antibodies to either TRAF6 or myc. This is representative of two experiments. h.c., antibody heavy chain

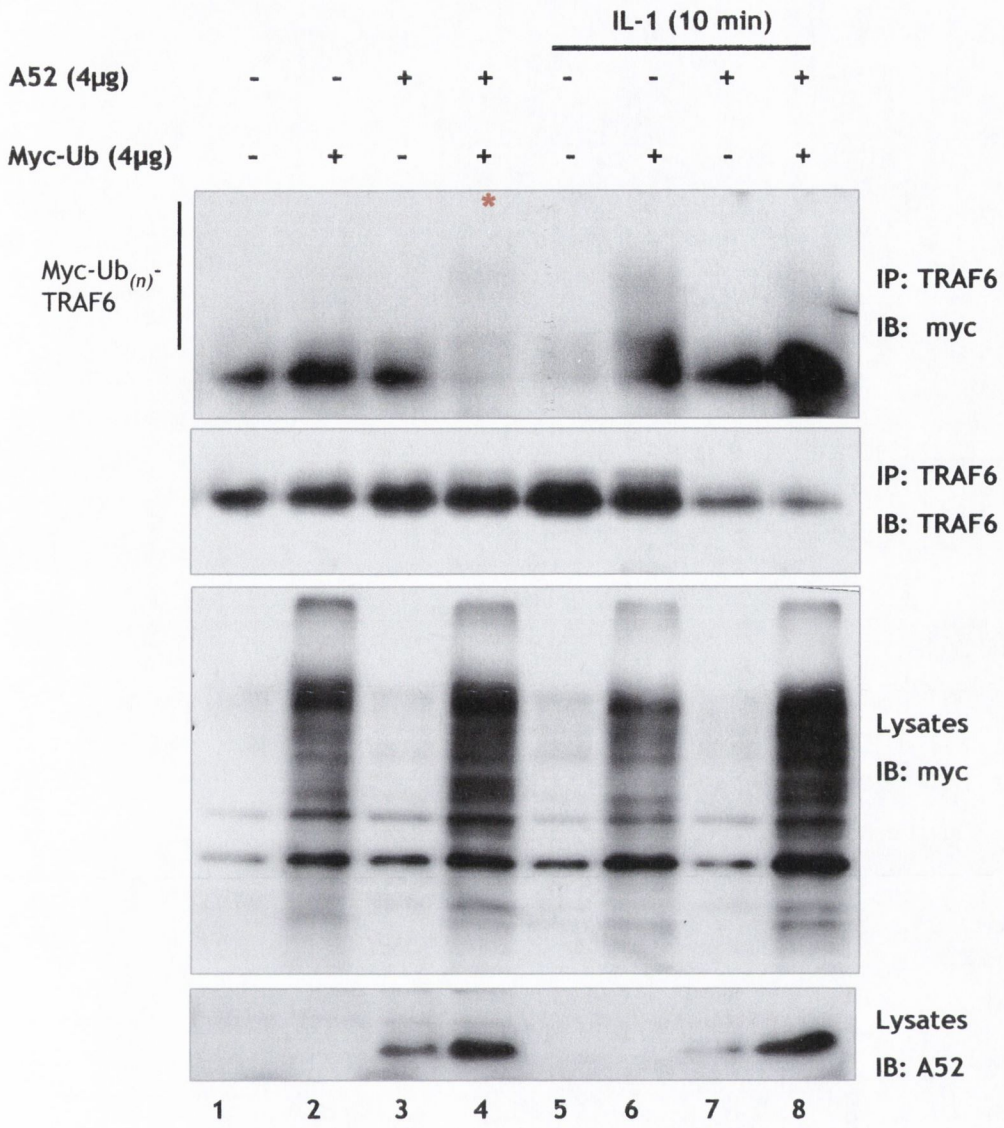

Figure 5.4 TRAF6 ubiquitination is induced by A52 when myc-ubiquitin is overexpressed and in the absence of ligand stimulation.

R1s were seeded at 1.5 x 10^5 cells/mL and transfected the following day with A52 (4 µg) or myc-ubiquitin (4 µg) using GeneJuice™. The cells were stimulated with IL-1β (20ng/mL) for 10 minutes prior to harvesting the cells. The cells were lysed and the lysates immunoprecipitated for TRAF6. The lysates and immunoprecipitates were resolved on a 10% SDS-polyacrylamide gel and transferred to Immobilon PVDF using a wet transfer system. The blots were probed with antibodies to either myc, TRAF6 or A52, as indicated. This is representative of two experiments. Asterisk *, TRAF6 myc-ubiquitination induced by A52.

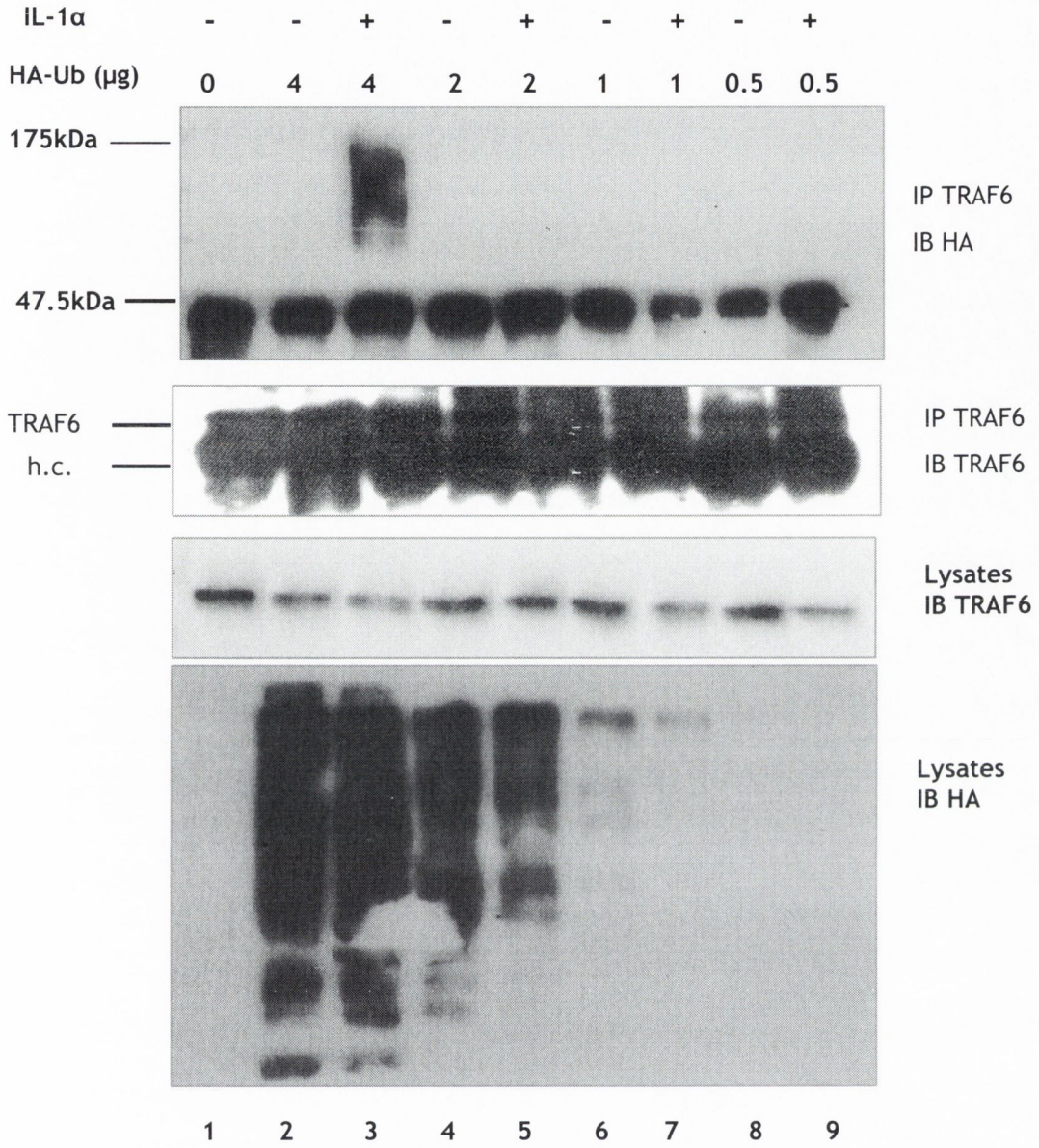

Figure 5.5 Ubiquitinated TRAF6 is detected when HA-ubiquitin is over-expressed.

R1s were seeded at 1.5 x 10^5 cells/mL and transfected the following day with varying amounts of HA-ubiquitin as indicated using GeneJuice™. The cells were stimulated with IL-1α (20ng/mL) for 5 minutes and then harvested. The cells were lysed and the lysates immunoprecipitated for TRAF6. The lysates and immunoprecipitates were resolved on a 10% SDS-polyacrylamide gel and transferred to Immobilon PVDF using a semidry transfer system. The blots were probed with antibodies to either HA or TRAF6. This is one experiment performed to titrate the amount of HA-ubiquitin required in future experiments with A52. h.c., antibody heavy chain

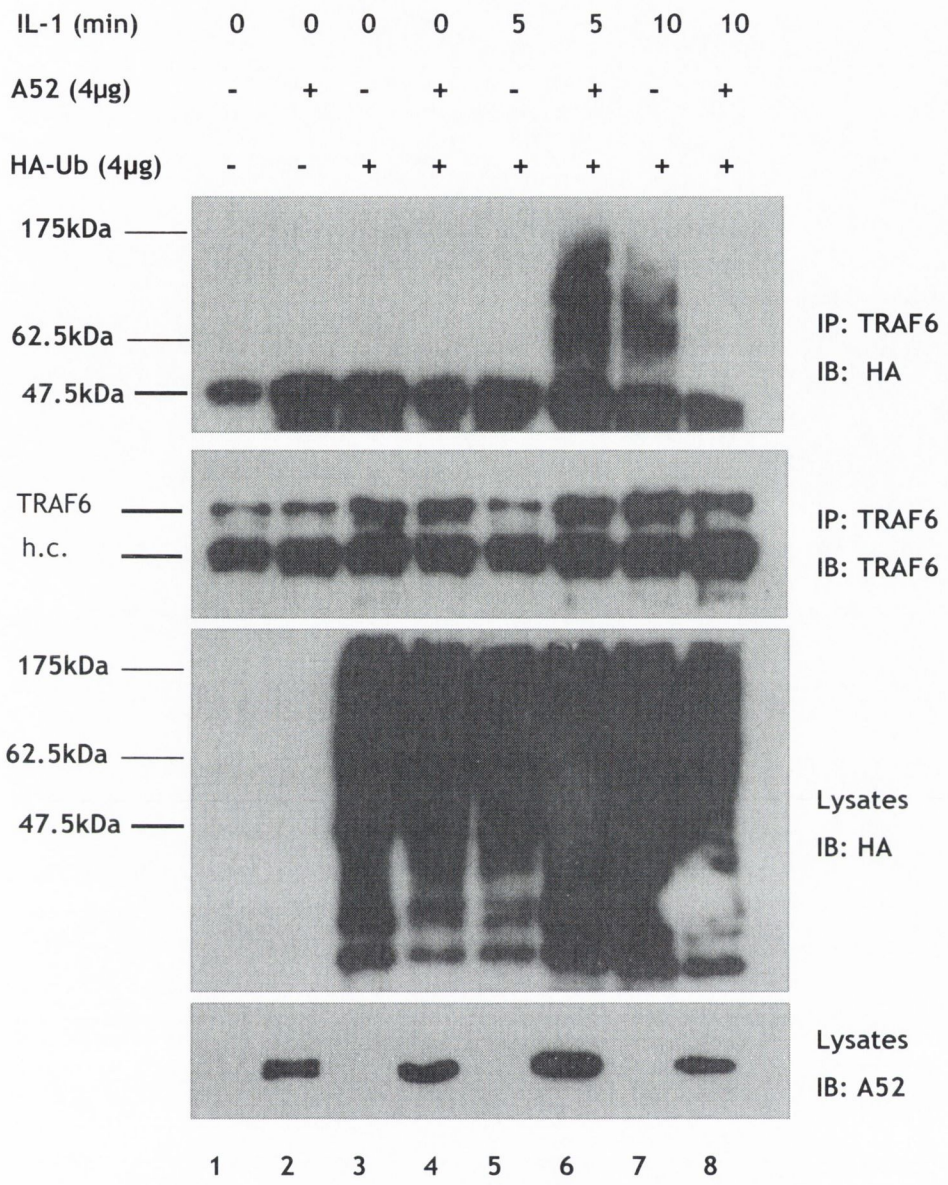

Figure 5.6 A52 enhances TRAF6 ubiquitination at early time-points following IL-1 stimulation.

R1s were seeded at 1.5 x 10^5 cells/mL and transfected the following day with HA-ubiquitin (4μg) and A52 (4μg) as indicated using GeneJuice™. The cells were stimulated with IL-1α (20ng/mL) for the indicated times and then harvested. The cells were lysed and the lysates immunoprecipitated for TRAF6. The lysates and immunoprecipitates were resolved on a 10% SDS-polyacrylamide gel and transferred to Immobilon PVDF using a wet transfer system. The blots were probed with antibodies to either HA, TRAF6 or A52. The modulation of TRAF6 HA-ubiqutination has been observed at least five times, though the kinetics differ slightly amongst individual experiments. h.c., antibody heavy chain.

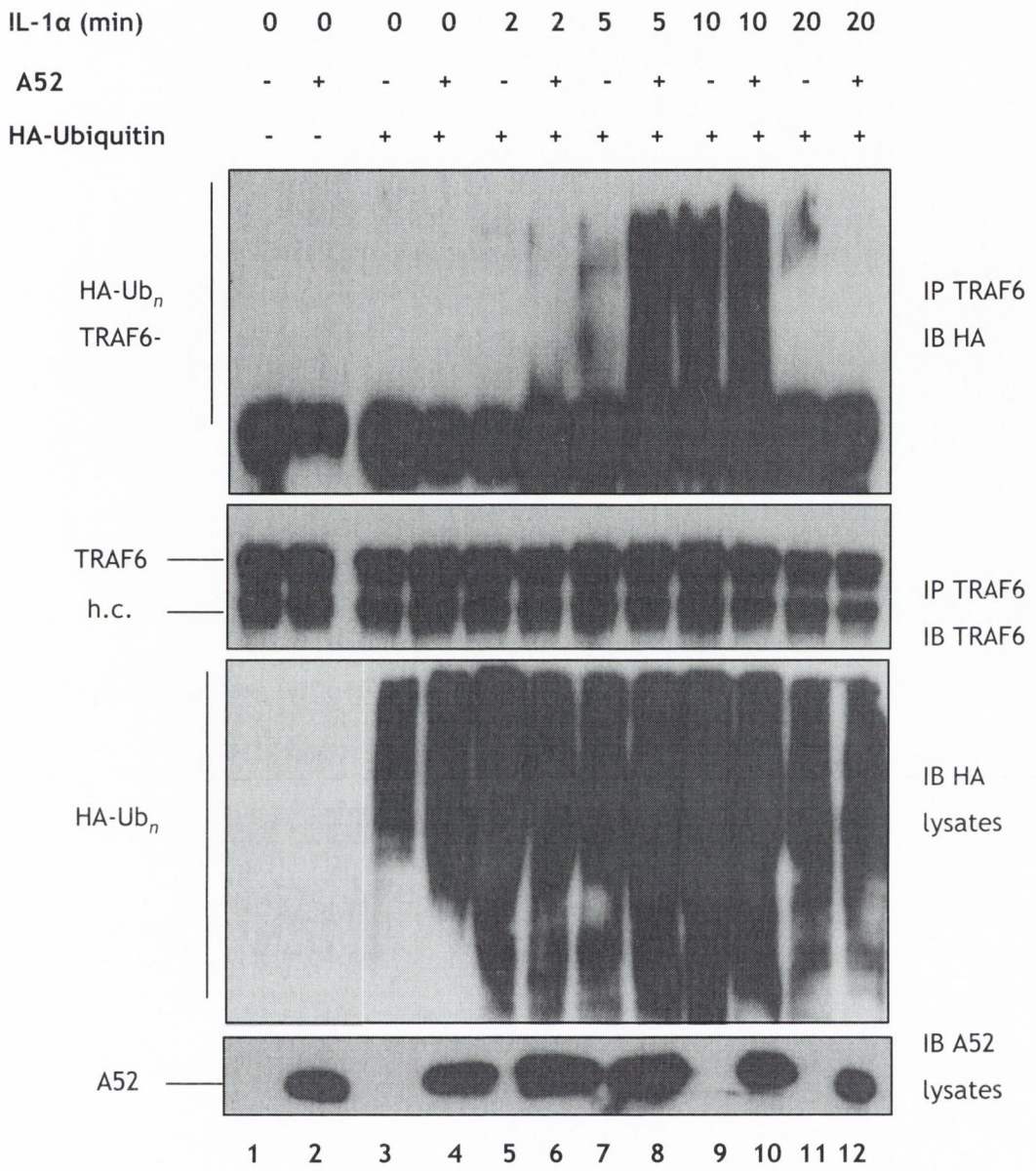

Figure 5.7 A52 enhances TRAF6 ubiquitination at early time-points following IL-1 stimulation.

R1s were seeded at 1.5 x 10^5 cells/mL and transfected the following day with HA-ubiquitin (4μg) and A52 (4μg) as indicated using GeneJuice™. The cells were stimulated with IL-1α (20ng/mL) for the indicated times and then harvested. The cells were lysed and the lysates immunoprecipitated for TRAF6. The lysates and immunoprecipitates were resolved on a 10% SDS-polyacrylamide gel and transferred to Immobilon PVDF using a semidry transfer system. The blots were incubated with antibodies to HA, TRAF6 and A52, as indicated. A similar result was obtained three times. h.c., antibody heavy chain

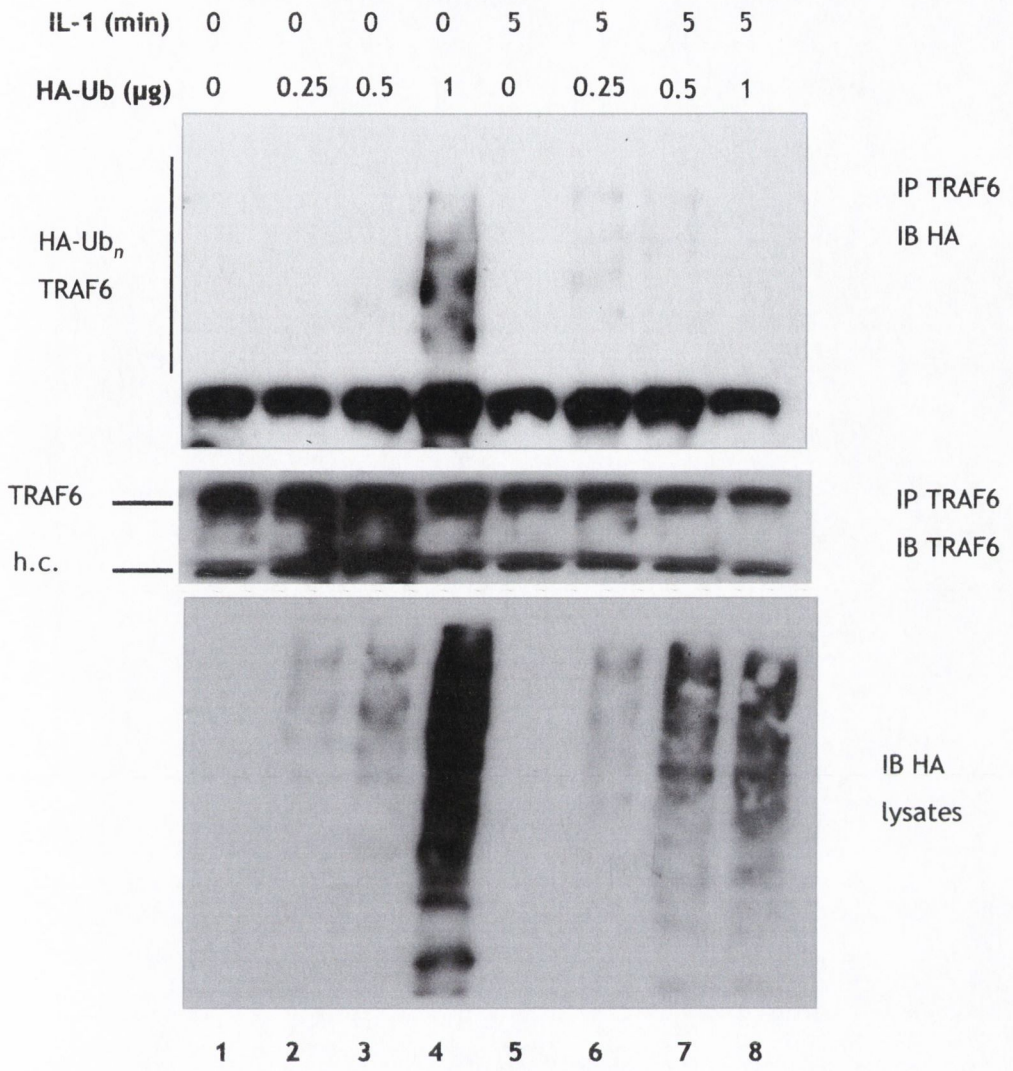

Figure 5.8 Re-titration of the HA-ubiquitin construct.

R1s were seeded at 1.5 x 10^5 cells/mL and transfected the following day with varying amounts of HA-ubiquitin (µg) as indicated using GeneJuice™. The cells were stimulated with IL-1α (20ng/mL) for 5 minutes and then harvested. The cells were lysed and the lysates immunoprecipitated for TRAF6. The lysates and immunoprecipitates were resolved on a 10% SDS-polyacrylamide gel and transferred to Immobilon PVDF using a semidry transfer system. The blots were probed with antibodies to either HA or TRAF6. This is one experiment performed to titrate the amount of HA-ubiquitin required in future experiments with A52 wild-type and mutants. h.c., antibody heavy chain

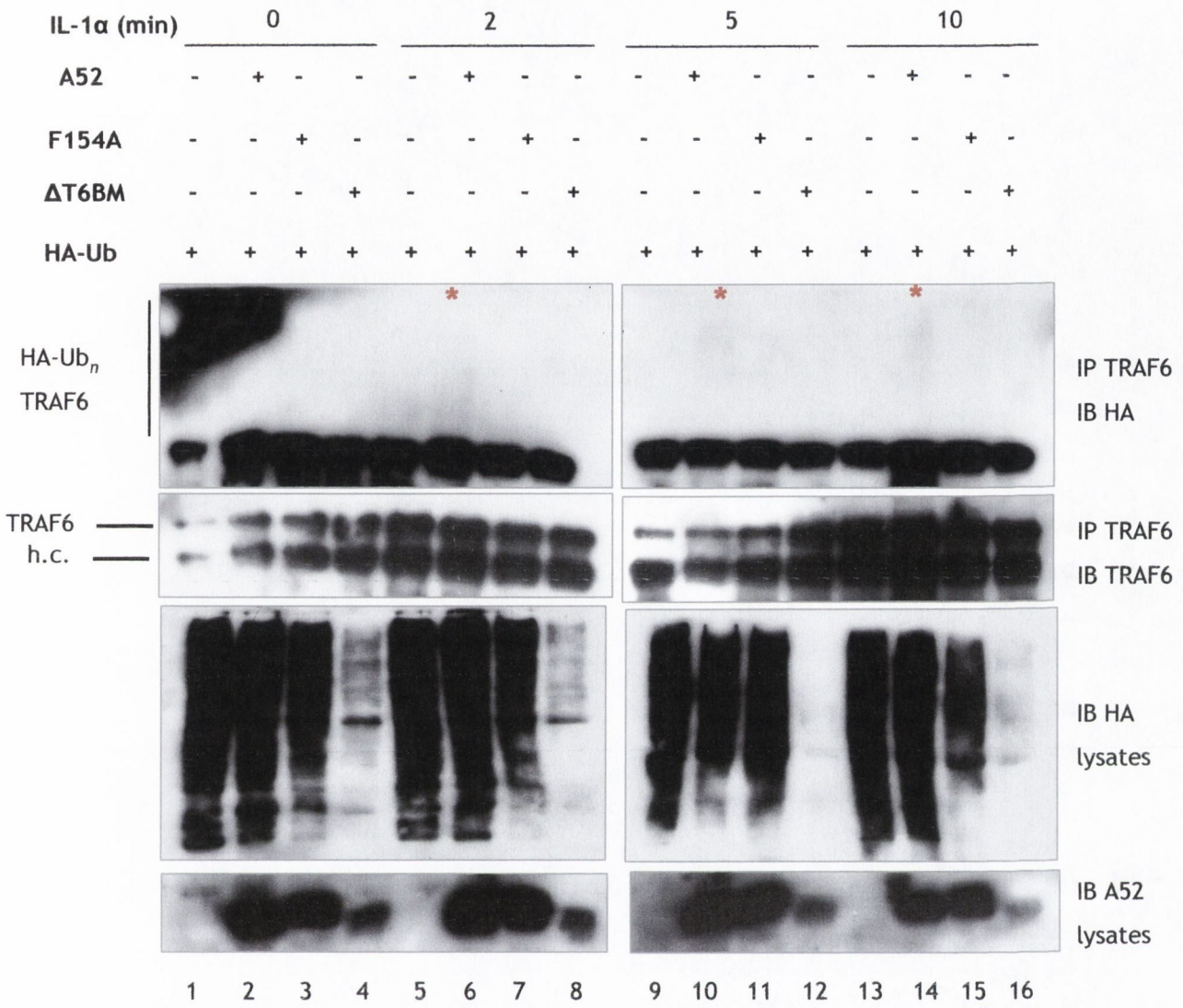

Figure 5.9 F154A and ΔT6BM do not accelerate the kinetics of TRAF6 ubiquitination.

R1s were seeded at 1.5 x 10^5 cells/mL in 100mm dishes and transfected the following day with HA-ubiquitin (0.25μg), A52, F154A or ΔT6BM as indicated using GeneJuice™. The cells were stimulated with IL-1α (20ng/mL) for 0, 2, 5 or 10 minutes and then harvested. The cells were lysed and the lysates immunoprecipitated for TRAF6. The lysates and immunoprecipitates were resolved on a 10% SDS-polyacrylamide gel and transferred to Immobilon PVDF using a semidry transfer system. The blots were probed with antibodies to either HA, TRAF6 or A52. Representative of two experiments with 0.25μg of HA-ubiquitin. The A52-enhanced IL-1-induced ubiquitinated TRAF6 is marked with an asterisk. h.c., antibody heavy chain

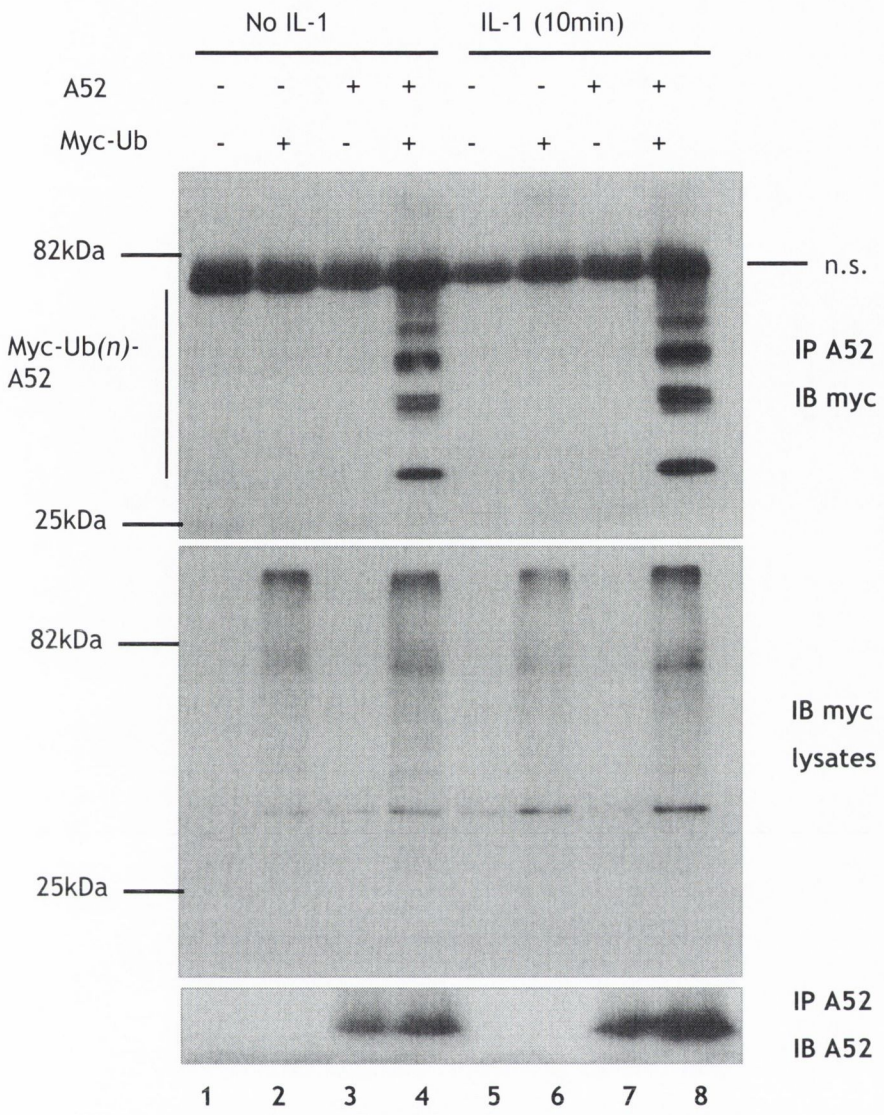

Figure 5.10 A52 is ubiquitinated in R1s

R1s were seeded at $1x10^5$ cells/mL in 100mm dishes 24 hours prior to transfection. The cells were transfected with pRK5, A52, and myc-Ub as indicated using GeneJuice™ according to the manufacturer's directions. Prior to harvesting, the cells in lanes 5-8 were treated with IL-1α (20ng/mL) for 10 minutes. The cells were harvested 24 hours post-transfection and lysed in NP-40 lysis buffer. The lysates were immunoprecipitated for A52. The lysates and immunoprecipitates were resolved by SDS-PAGE and the proteins were transferred to Immobilon PVDF using a wet transfer system. The blots were probed with antibody specific for myc or A52, as indicated. The myc-ubiquitination of A52 was observed five times.

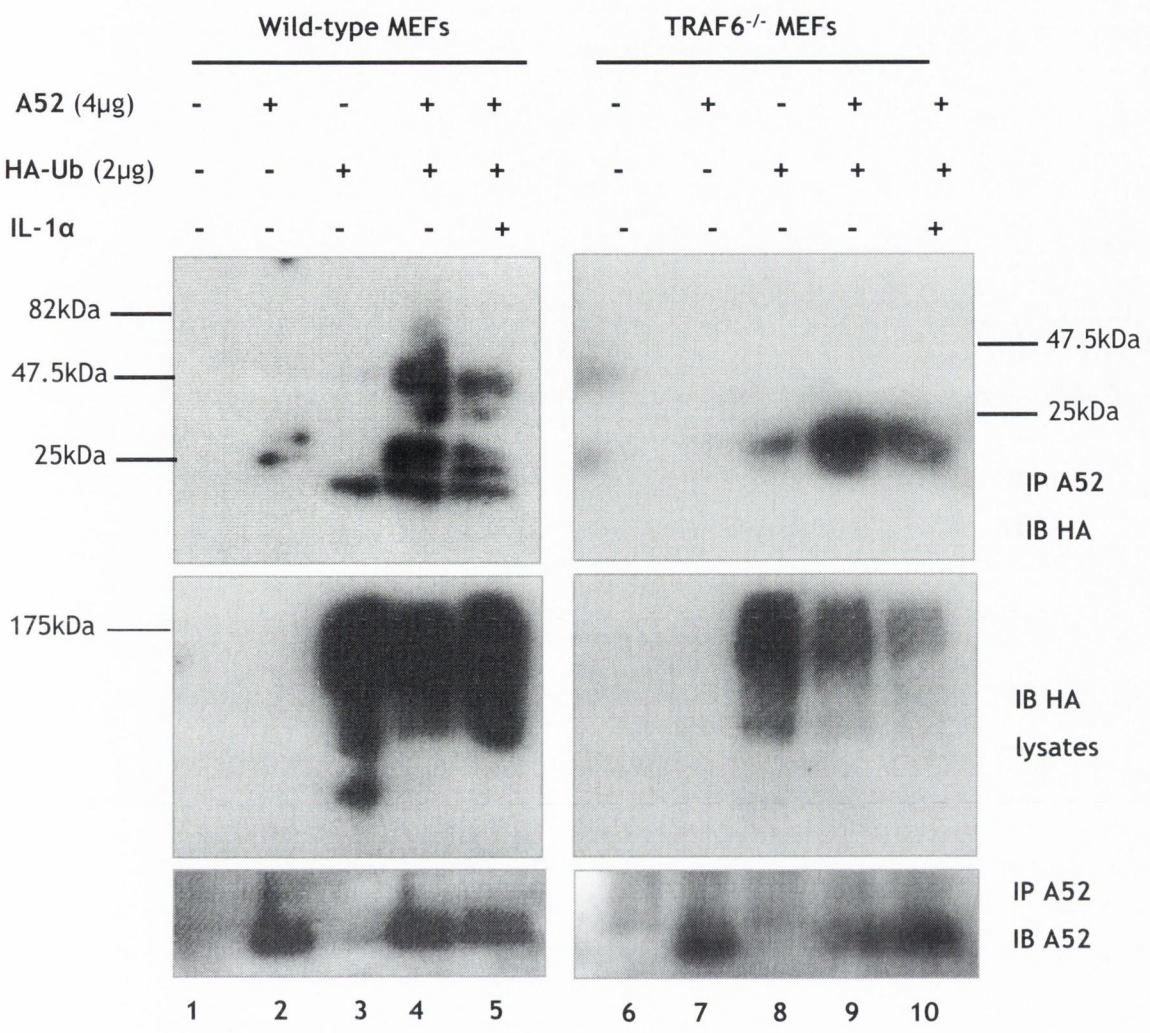

Figure 5.11 A52 is ubiquitinated in wild-type but not *TRAF6*$^{-/-}$ MEFs

Wild-type (A) or *TRAF6*$^{-/-}$ (B) MEFs were seeded into 100mm dishes 24 hours prior to transfection. The cells were transfected with pRK5, A52, and HA-Ub as indicated using GeneJuice™ according to the manufacturer's directions. Prior to harvesting, the cells in lanes 5 and 10 were treated with IL-1α (20ng/mL) for 5 minutes. The cells were harvested 24 hours post-transfection and lysed in NP-40 lysis buffer. The immunoprecipitates and lysates were resolved by SDS-PAGE and the proteins were transferred to Immobilon using a semi-dry transfer system. The blots were probed with antibody specific for HA (top two panels) or A52 (bottom panel). The result was observed four times (wild-type) and three times (TRAF6 null MEFs).

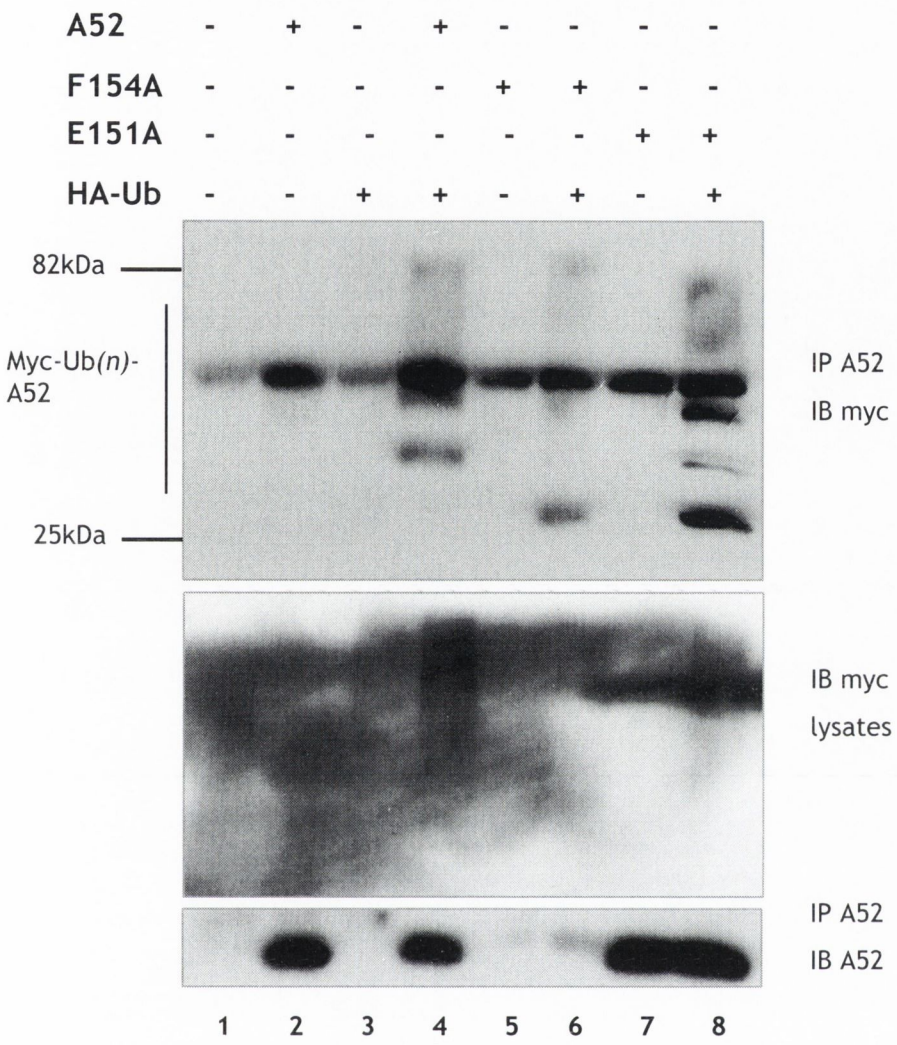

Figure 5.12 The TRAF6 binding motif mutants of A52 are ubiquitinated in R1s.

R1s were seeded at $1x10^5$ cells/mL in 100mm dishes 24 hours prior to transfection. The cells were transfected with pRK5, myc-ubiquitin, and either A52, F154A or E151A using GeneJuice™ according to the manufacturer's directions. The cells were harvested 24 hours post-transfection and lysed in NP-40 lysis buffer. The lysates were immunoprecipitated with A52 antibody pre-coupled to protein A sepharose beads. The immunoprecipitates and lysates were resolved by SDS-PAGE and the proteins were transferred to Immobilon using a wet transfer system. The blots were probed with antibody specific for myc (top two panels) or A52 (bottom panel). This represents one experiment where the mutants were compared side-by-side. In an additional experiment, F154A was found to be ubiquitinated.

5.3 Discussion

TRAF6 is a known E3 ubiquitin ligase that conjugates K63-linked polyubiquitin chains onto substrate proteins, including itself. Ubiquitinated TRAF6 is recognised by the TAB proteins, TAB2 and TAB3, which then recruit TAK1 (Chen, 2005). TAK1 is said to be ubiquitin-activated (Chen, 2005), though it is not clear if it is a substrate for TRAF6-catalysed ubiquitination in this signalling pathway. Once activated, TAK1 can phosphorylate substrates including the IKK complex and other MAP3K, leading to activation of NF-κB and MAPK (Chen, 2005). A necessary step in the process is TRAF6 auto-ubiquitination. It was hypothesised that A52 might alter TRAF6 auto-ubiquitination in order to modulate its function. Therefore, in this chapter, the auto-ubiquitination of TRAF6 and the effect of A52 and the mutants on this were examined.

Initially, it was difficult to detect TRAF6 auto-ubiquitination. This modification of TRAF6 is expected to be transitory. Previous reports have found that IL-1-induced TRAF6 ubiquitination peaked at around 10 minutes post-stimulation and was no longer detectable by 20-minutes post-stimulation (Jensen and Whitehead, 2003; Windheim et al., 2008a). In R1s, endogenous ubiquitination of TRAF6 was not observed. Attempts were made to optimise this assay, such as by using an antibody directed specifically against polyubiquitin chains or over-expressing TRAF6 to enrich the cells for the substrate of ubiquitination (Figure 5.3). When TRAF6 ubiquitination was not observed in R1s following these modifications to the protocol, another cell line was obtained in which TRAF6 auto-ubiquitination had been observed. The majority of TRAF6 in HepG2s is expected to be modified with ubiquitin following IL-1 stimulation (Jensen and Whitehead, 2003), presumably making it easier to detect in this cell line. Although ubiquitin was detected in the lysates, no ubiquitination of endogenous TRAF6 was detected in HepG2s stimulated with IL-1 in the presence of absence of A52 (Figure 5.2).

The technical difficulties of observing TRAF6 auto-ubiquitination have been circumvented by both immunoprecipitating and immunoblotting for TRAF6 (Yang *et al.*, 2004). In this paper, the higher molecular mass forms of TRAF6 that are detected following induction with the E2 enzyme (Ubc13/Uev1A) are claimed to be ubiquitinated TRAF6 (Yang *et al.*, 2004). While it is likely that these higher molecular mass proteins are modified TRAF6, it is not possible to say that they ubiquitinated TRAF6 since the evidence is indirect. In this chapter, higher molecular mass forms of TRAF6 are frequently detected on immunblots following IL-1 stimulation (Figure 5.3). However, since immunoblotting with the anti-ubiquitin antibodies did not detect any ubiquitinated TRAF6, it is difficult to conclude that the bands detected with the TRAF6 antibody represent ubiquitinated TRAF6. Despite the ease of detection of the modified TRAF6 with the TRAF6 antibody, further attempts were made to directly observe ubiquitinated TRAF6.

In order to improve detection of ubiquitinated TRAF6, iodoacetamide was included in the lysis buffer. Most deubiquitinating (DUBs) enzymes are cysteine proteases (Love *et al.*, 2007). Thiol-reacting agents are required to inactivate the DUBs (Mimnaugh and Neckers, 2002). Iodoacetamide acts by transferring the acetamide group to the sulphydryl group of the cysteine residue at the enzyme active site. This is an irreversible modification and renders the enzyme non-functional. Since TRAF6 is known to be deubiquitinated shortly after stimulation, the action of DUBs could have compounded the difficulty in observing TRAF6 auto-ubiquitination. There is also one class of DUBs that are metalloproteases (Love *et al.*, 2007). The EDTA that is included in the lysis buffer chelates metal ions and this should inhibit the action of metalloproteases.

In addition to inhibiting the DUBs, baking the blots at 80°C for one hour proved to be essential for detection of the HA-ubiquitinated TRAF6. It has been stated that the heating of the ubiquitin blots improves detection by making the ubiquitin more immunogenic (Si *et al.*, 2008). There are various methods of heating the blot, including autoclaving (Si *et al.*, 2008) and boiling (Mimnaugh and Necker, 2002). While the baking improved detection of the HA-ubiquitinated TRAF6, the other methods were not attempted and it is thus not known if autoclaving or boiling would give better results than baking the blots. This method was only attempted following introduction of the HA-ubiquitin construct. It was not attempted during the endogenous ubiquitination experiments and thus it is not known if this method would have enabled detection of endogenous ubiquitinated TRAF6. An alternative method that could make ubiquitinated TRAF6 easier to detect is to enhance the elution of the protein from the SDS-PAGE gel by incubating the gel in a solution of SDS and 2-mercaptoethanol prior to transfer to PVDF (Mimnaugh and Neckers, 2002). This method was not attempted in this chapter but it is worth investigating, particularly for endogenous ubiquitination studies.

Over-expression of myc- or HA-tagged ubiquitin made it possible to detect ubiquitinated TRAF6. IL-1-induced TRAF6 myc-ubiquitination appeared at five minutes post-stimulation and was no longer detected at 15 minutes post-stimulation (Figure 5.3). With the HA-tagged ubiquitin plasmid, ubiquitination of TRAF6 typically peaked at 5 or 10 minutes post-stimulation (Figure 5.6 and 5.7). This is consistent with previous reports of the kinetics of TRAF6 ubiquitination. However, there was variability from one experiment to the next with regards to the peak in IL-1-induced TRAF6 ubiquitination (compare Figure 5.5 and Figure 5.6), with the peak in ubiquitination being typically at either five or ten minutes post-stimulation. This variability is likely due to the passage of the cells and the transfection efficiency. The addition of wild-type A52 accelerated the kinetics of IL-1-induced TRAF6 ubiquitination reproducibly.

At early time-points when IL-1-induced TRAF6 ubiquitination was not yet detectable, the addition of A52 resulted in a more intense smear of ubiquitinated TRAF6 (Figures 5.6 and 5.7).

In MAPK studies, A52 enhanced IL-1-induced p38 activation and activated p38 in the absence of a ligand (Maloney *et al.*, 2005). If the affect of A52 on TRAF6 ubiquitination is essential for its role in promoting MAPK activation, it was expected that A52 would activate TRAF6 ubiquitination on its own, without IL-1 stimulation. Although this was observed twice with the myc-ubiquitin construct, it was observed only once or twice when using HA-ubiquitin and thus may not be a reproducible result. This result is in parallel with the result obtained in the study of MAPK phosphorylation in R1s (Chapter 4). In R1s, IL-1 induced phosphorylation of p38 and JNK MAPKs. A52 enhanced IL-1-induced phosphorylation of p38 and JNK but did not activate it in the absence of IL-1 stimulation. It could be that this is a cell specific effect, since A52 can activate MAPKs in the absence of ligand stimulation in wild-type MEFs (Figure 4.1).

The TRAF6 binding motif mutant of A52, F154A, did not accelerate the kinetics of TRAF6 ubiquitination (Figure 5.9). This is consistent with a loss of function of the mutant in that it no longer activates p38 and JNK MAPKs (Chapter 4). Moreover, although a role for TRAF6 in p38 activation has been established, the F154A mutant that no longer activated p38 still co-precipitated with TRAF6 (Chapter 4). It could be that the TRAF6 binding motif is in fact required for recognition of a substrate of TRAF6 for ubiquitination. If the TRAF6 binding motif of A52 is required for TRAF6 E3 ligase activity, then it could be that this motif is an activation switch for TRAF6 enzymatic function. For example, IRF7 has been found to bind directly to TRAF domain of TRAF6 via TRAF6 binding motifs and is activated by TRAF6-dependent ubiquitination (Kawai *et al.*, 2004).

Surprisingly, A52 was found to be ubiquitinated when myc-ubiquitin was over-expressed (Figure 5.10). Furthermore, the ubiquitination of A52 appeared to depend upon TRAF6, since A52 ubiquitination was not observed in TRAF6 null MEFs (Figure 5.11). However, mutation of the TRAF6 binding motif did not abrogate A52 ubquitination (Figure 5.12), suggesting that that motif alone does not determine substrate specificity for TRAF6-mediated ubiquitination. Furthermore, this suggests that A52 ubiquitination is not sufficient for p38 activation yet a role in inhibition of IL-1R/TLR-induced NF-κB activation remains a possibility. Since wild-type and mutant A52 appear to be ubiquitinated, this could correlate with their ability to inhibit NF-κB activation. Endogenous ubiquitination of A52 was not tested.

While A52 has lysine residues that are predicted to be SUMOylated or ubiquitinated, it is not clear if these motifs are recognised by TRAF6. At least one of the potential SUMO or ubiquitin motifs predicted by SUMOplot and ELM, IKPD (40-43), might also be a specific site recognised by TRAF6 for ubiquitination. A recent report described a consensus recognition motif for two proteins ubiquitinated by TRAF6 in complex with the scaffold protein p62 (Jadhav *et al.*, 2008). The motif is [(hydrophobic)-K-(hydrophobic)-X-X-(hydrophobic)-(polar)-(hydrophobic)-(polar)-(hydrophobic)], with X being any amino acid and K being the lysine that gets ubiquitinated (Jadhav *et al.*, 2008). The A52 sequence was scanned to determine if it had a motif that fit this pattern. One site in A52 was found to be quite close to the consensus pattern: IKP DY LE YDD (40-49). While the last three residues are polar instead of being hydrophobic-polar-hydrophobic, the rest of the motif matches the consensus pattern. In addition, A52 residues 40-49 are in the N-terminal coiled region, thereby making it accessible to ubiquitin modification. The acceptor site described above could be unique to TRAF6 signalling in conjunction with p62 and another site could be ubiquitinated by TRAF6 in

other signalling pathways. This is the only TRAF6-specific consensus site described thus far.

At least one other viral protein has been shown to enhance TRAF6 ubiquitination in order to manipulate the innate immune response. The Herpesvirus saimiri protein STP-C interacts with TRAF6 and induces TRAF6 ubiquitination (Chung *et al.*, 2007b). The induction of TRAF6 ubiquitination resulted in activation of NF-κB, which leads to increased IL-8 and ICAM expression (Chung *et al.*, 2007b). Other microbial virulence factors have been known to target TRAF6 ubiquitination as a means of turning off innate immune pathways. For example, the *Yersinia pestis* protein YopJ acts as a deubiquitinase, removing K63-linked polyubiquitin chains from TRAF6 and TRAF3 in order to inhibit NF-κB, MAPK and IRF3 activation (Sweet *et al.*, 2007). No examples of modulation of the kinetics of TRAF6 ubiquitination have been reported.

Modulation of the auto-ubiquitination of TRAF6 is essential to both activation and suppression of innate immune signalling pathways. Protein phosphatase 4 (PP4) has recently been demonstrated to bind to TRAF6 and prevent is ubiquitination, thereby suppressing NF-κB activation (Chen et al., 2008). It is not known if TRAF6 is phosphorylated as part of the mechanism of activation. The primary sequence of TRAF6 was analysed with the algorithm Prosite (Falquet et al., 2002) and found to have several predicted phosphorylation sites (data not shown). Three of these sites, when phosphorylated, are recognition sites for FHA-domain containing proteins: TleD (336-339), TilD (433-436) and TrfD (501-504). At least one interaction partner of TRAF6, TIFA, is a FHA-domain containing protein and its FHA domain is essential for it to activate TRAF6 (Takatsuna et al., 2003). However, the interaction between TRAF6 and TIFA is constitutive and thus may not require phosphorylation of the aforementioned FHA recognition motifs. It has not been demonstrated that activation of TRAF6 involves

phosphorylation or that phosphorylation of TRAF6 is required to induce its auto-ubiquitination. If TRAF6 is phosphorylated for activation, it would clarify the role of PP4 as a suppressor of TRAF6 activation.

The finding that A52 accelerated IL-1-induced TRAF6 ubiquitination is a novel positive role for A52 in its modulation of the innate immune response. Since A52 has another stimulatory function in the activation of MAPK via its interaction with TRAF6, it is possible that there is a correlation between the effect of A52 on TRAF6 ubiquitination and MAPK activation. This was further supported by the subtle difference between A52 and the mutants in their ability to modulate TRAF6 ubiquitination following IL-1 stimulation. While A52 accelerated the kinetics of TRAF6 ubiquitination, neither F154A nor ΔT6BM were able to do so and this correlated the inability of F154A and ΔT6BM to activate MAPK. However, A52 is able to stimulate MAPK activation in the absence of ligand stimulation, while no reproducible effect of A52 on TRAF6 ubiquitination could be detected without IL-1 stimulation. It could be that the level of ubiquitination induced by A52 in the absence of stimulation is too low to be detected by the system used herein. A more sensitive assay, such as *in vitro* ubiquitination, might detect A52-induced TRAF6 ubiquitination that is below detection levels here. While the modulation of IL-1-induced TRAF6 ubiquitination is a key discovery relating to the mechanism of action of A52, it was a subtle effect and it was hypothesised that other signalling molecules might play a role in the activation of MAPK by A52.

Chapter Six: Results IV

Determining the role of the TRAF6 binding / signalling domain in A52-induced p38 MAPK activation

6.1 Introduction

In previous chapters, A52 has been shown to specifically activate p38 MAPK in a TRAF6-dependent manner. Further, A52 was able to modulate IL-1-induced TRAF6 ubiquitination and this correlated with its ability to enhance MAPK activation. It is feasible that other signalling molecules are needed for A52-induced p38 activation and this was examined in this chapter. In addition, the consequences of the effect of A52 on TRAF6 ubiquitination on known TRAF6 pathway components were explored.

Since TRAF6 does not interact directly with IL-1R/TLR family members but is recruited to the receptor/TIR adaptor complex by the IRAKs (Chung *et al.*, 2007a), it was feasible that there could be a role for IRAKs in A52-induced p38 MAPK. A role for the IRAKs in IL-1-induced MAPK activation has been demonstrated, with IRAK1$^{-/-}$ MEFs being defective in MAPK phosphorylation following IL-1 stimulation (Kanakaraj *et al.*, 1998). Following IL-1 stimulation, IRAK1 is polyubiquitinated and interacts with the IKK to mediate NF-κB activation (Windheim et al., 2008a; Conze *et al.*, 2008). Interestingly, IRAK1 polyubiquitination was not required for MAP kinase activation (Conze *et al.*, 2008), suggesting that the pathways to NF-κB and MAP kinase activation bifurcate at IRAK1 or that there is an alternative pathway parallel to IRAK1. IRAK1 thus seems to be important in IL-1-induced NF-κB and MAPK activation but possibly via alternative pathways. In addition, another IRAK family member, IRAK2, was found to specifically ubiquitinate TRAF6 in order to activate NF-κB (Keating *et al.*, 2007). Unlike IRAK1, over-expressed IRAK2 was able to activate p38 MAP kinase (Keating *et al.*, 2007), suggesting that IRAK2-induced TRAF6 ubiquitination could be required for MAPK activation.

Since A52 was found to affect TRAF6 ubiquitination, it was hypothesised that it might also have an effect on oligomerisation of TRAF6. In parallel with other members of the

TRAF family, TRAF6 is hypothesised to oligomerise following stimulation. For example, following CD40L binding to CD40, the receptor forms a higher order oligomer that is required for TRAF6-mediated NF-κB and MAPK activation (Pullen *et al.*, 1999). It has been postulated that TRAF6 needs to be a trimer in order to engage the oligomerised CD40 (Pullen *et al.*, 1999). It is not known if TRAF6 forms a trimer following stimulation or if it exists ready-made as a trimer in the cytosol (Pullen *et al.*, 1999). In the crystal studies of the TRAF domain of TRAF6, trimers were only observed when large concentrations of the protein were used (Chung *et al.*, 2007a). The structure of the crystal showed one TRAF6 domain per unit, suggesting that TRAF6 is a monomer (Chung *et al.*, 2007a). In addition, the crystal structure of the coiled-coil domain precludes trimer formation (Chung *et al.*, 2007a). In one study, the homo-trimerisation of TRAF2 and TRAF6 was forced by fusion of the N-terminal domain of the TRAFs to an immunophilin that can be made to oligomerise (Baud *et al.*, 1999). While oligomerisation was then found to be able to activate JNK, p38 and the IKK complex (Baud *et al.*, 1999), it was an artificial system and might not be physiologically relevant.

There is some evidence that TRAF6 oligomerises in cells following receptor stimulation. Recently, it was found that overexpression of IRAK1 but not MyD88 was able to induce TRAF6 oligomerisation by using over-expressed TRAF6 (Muroi and Tanamoto, 2008). From this, it was concluded that MyD88 and IRAK1 induced NF-κB activation by distinct mechanisms, presumably with only the IRAK1-mediated pathway requiring TRAF6 oligomerisation. Another report showed TRAF6 oligomerisation following IL-1 stimulation by using gel-filtration. The TRAF-interacting protein with a forkhead-associated domain (TIFA) has been found to mediate the interaction of IRAK1 and TRAF6 in the IL-1 signalling cascade (Takatsuna *et al.*, 2003). Furthermore, TIFA induced TRAF6 oligomerisation and this was required for activation of the IKK complex (Ea *et al.*, 2004). In addition, downstream of the T-cell receptor (TCR), oligomerised MALT1

and BCL10 bind to TRAF6 and induce both oligomerisation and E3 ubiquitin ligase activity of TRAF6 (Sun *et al.*, 2004). The mutation of TRAF6 binding motifs (E2A) in MALT1 abrogates the MALT1-TRAF6 interaction, the ability of MALT1 to induce TRAF6 oligomerisation and the activation of the IKK complex (Sun *et al.*, 2004). Crucially, the MALT1-induced oligomerisation of TRAF6 was found to be important for activation of its E3 ligase activity (Sun *et al.*, 2004). The E2A mutants of MALT1 were no longer able to induce TRAF6 ubiquitination (Sun *et al.*, 2004).

The role of downstream effectors of TRAF6 in A52-induced p38 activation was also examined. A critical signalling molecule downstream of TRAF6 is TAK1, a MAP3K that activates MAP2Ks, MKK3/6 and MKK4/7, which subsequently phosphorylate p38 and JNK, respectively (Katsoulidis *et al.*, 2005). Since A52 requires TRAF6 in order to activate MAP kinases, it is feasible that A52 affects the mechanism by which TRAF6 activates TAK1. Following receptor activation, auto-ubiquitinated TRAF6 is thought to be recognised by TAB2 and this recruits TAK1 and TAB1 to form a complex that can also activate the IKK complex via the kinase activity of TAK1 (Windheim et al., 2008a). TAB2 and a related protein, TAB3, are known to bind to polyubiquitinated TRAF6 and this interaction is required for signalling (Kanayama *et al.*, 2004). TAB2 and TAB3 are ubiquitinated and this is required for activation of TAK1 by an as yet unknown mechanism (Ishitani *et al.* 2003). TAB2 translocates from the membrane to the cytosol in an IL-1-dependent manner to stimulate the association of TRAF6 and TAK1, since TAB2 binds to both TRAF6 and TAK1 in an IL-1-dependent manner (Takaesu *et al.*, 2000). Further, TAB2 is required for IL-1-induced TRAF6 auto-ubiquitination (Kishida *et al.*, 2005). TAK1 is required for both MAP kinase and IKK activation by TRAF6 (Wang *et al.*, 2001). TAK1 is a MAP3K which activates the signalling cascade leading to p38 activation (Ashwell, 2006). TAK1 activation involves its ubiquitination since activation of TAK1 is inhibited by the deubiquitiating enzyme, CYLD, following T-cell receptor

(TCR) activation (Reiley *et al.*, 2007). Whether TAK1 is ubiquitinated in other signalling pathways than the TCR is uncertain. Since TRAF6 is an E3 ubiquitin ligase, it is possible that it ubiquitinates other proteins and this may include TAK1 as in the TCR pathway.

In summary then, TRAF6-mediated signal transduction requires many other signalling molecules. Upstream of TRAF6, the IRAKs bridge the interaction between the activated receptor complexes and TRAF6 recruitment. The mechanism of TRAF6 activation is known to involve TRAF6 autoubiquitination and is postulated to require TRAF6 trimerisation. Once ubiquitinated, TRAF6 is thought to recruit TAB2/3 and TAK1, thereby initiating a kinase cascade that leads to MAPK activation. In order to further elucidate the role of A52 in TRAF6-mediated p38 activation, these other signalling molecules, as well as TRAF6 oligomerisation, were studied.

Results

6.2.1 Requirement for IRAK1 or IRAK2 required for A52-mediated p38 activation

A52 has previously been found to interact with IRAK2 (Harte *et al.*, 2003). In addition, a role for IRAK2 in p38 MAP kinase activation has been demonstrated (Keating *et al.*, 2007). To determine if IRAK2 was required for A52-mediated p38 activation, the CHOP assay was performed in wild-type and IRAK2$^{-/-}$ MEFs. However, there was no activation of CHOP observed following IL-1 stimulation or A52 expression in either the wild-type or IRAK2$^{-/-}$ MEFs (Figure 6.1A and B). Furthermore, MKK3 was used as a positive control but was unable to activate CHOP in either wild-type or IRAK2$^{-/-}$ MEFs (Figure 6.1A and B). In order to optimise the assay, varying amounts of the plasmid encoding CHOP-Gal4 fusion protein were tested but this did not improve the activation, nor did changing the transfection reagent from Lipofectamine to GeneJuice™ (data not shown).

Previously, IRAK1 has been found to be required for p38 MAP kinase activation by IL-1 (Kanakaraj *et al.*, 1998). In order to test whether IRAK1 had a role in A52-TRAF6-dependent p38 activation, the CHOP assay was performed in parallel in R1s and in cells deficient in IRAK1 (I1A). While IL-1 activated p38 in R1s, no p38 activation was detected in I1A cells in response to IL-1 stimulation (Figure 6.2). A52 activated p38 weakly in R1s but this was activation was not observed in I1A cells (Figure 6.2). Over-expression of TRAF6 and MKK3 activated p38 in R1s but not in I1A cells (Figure 6.2). Since both of these signalling molecules are expected to be downstream of IRAK1, it was anticipated that they would activate p38 despite the IRAK1 deficiency. The absence of p38 activation in response to TRAF6 and MKK3 overexpression in I1A cells suggests that the assay does not work in this cell type. It was thus not possible to conclude whether A52 needs IRAK1 to activate p38.

6.2.2 An effect of A52 on TRAF6 oligomerisation could not be detected

Although the role of TRAF6 oligomerisation in signalling is still uncertain, it has been found to stabilise effector domains and permit signal transduction to MAPK and NF-κB activation (Baud *et al.*, 1999). It was hypothesised that A52 could alter TRAF6 oligomerisation and that this might correlate with the modulation of IL-1-induced TRAF6 ubiquitination (Chapter 5). Thus, the effect of A52 on TRAF6 oligomerisation was examined. Initially, the ability of IL-1 to induce oligomerisation of endogenous TRAF6 was tested by native PAGE. In the absence of IL-1 stimulation, an intense band at high molecular mass was observed (Figure 6.3, top panel, lane 1). The molecular mass standards were those normally used on SDS-PAGE and their apparent mobility on the native PAGE might not be the same as that observed on denaturing gels. The molecular masses indicated are thus only approximate for native PAGE. On the native gel, the band between the 82kDa and 175kDa standards became slightly more intense following IL-1 stimulation and this could have corresponded to TRAF6 oligomerisation, possibly the

formation of a trimer (Figure 6.3, top panel, lanes 4 and 5). However, the band was present in all lanes and the increase in intensity could have been due to unequal loading of the samples (Figure 6.3, top panel, lanes 4 and 5). The presence of the high molecular mass band in all samples suggested that TRAF6 could exist in a ligand-independent oligomer or that the protein formed aggregates, possibly during the lysis procedure. A band that could correspond to monomeric TRAF6 was visible and appeared to get more intense following IL-1 stimulation (Figure 6.3, top panel, lanes 3-5) but this effect was not reproducible. In the denatured samples, TRAF6 protein levels were equal in all lanes (Figure 6.3, middle panel). To test that the cells were responding to IL-1, IκBα degradation was analysed by western blotting. The amount of IκBα detected was reduced in the sample treated with Il-1 for 5 minutes compared to the control (Figure 6.3, bottom panel, compare lanes 1 and 2). After 10 minutes of IL-1 stimulation, IκBα was barely detectable (Figure 6.3, bottom panel, lane 3). There was no detectable IκBα following 15 and 30 minutes IL-1 stimulation (Figure 6.3, bottom panel, lanes 4 and 5). This is consistent with Il-1-induced IκBα degradation, confirming that the R1s used in this experiment responded to IL-1. Thus, the absence of a detectable change in TRAF6 oligomerisation following IL-1 stimulation was not due to irresponsiveness of the cells.

The effect of over-expressed A52 on endogenous TRAF6 oligomerisation was next examined. As observed in the previous experiment, endogenous TRAF6 was detected as a high molecular mass band when the non-denatured samples were analysed by native PAGE (Figure 6.4, top panel). There was no difference observed between the samples following treatment with IL-1 alone (lanes 3 and 4), A52 alone (lane 5), over-expression of A52 together with Il-1 stimulation (lanes 6 and 7) or increasing amounts of A52 with IL-1 stimulation (lanes 8-10). The band between the approximate 82 and 175Da molecular mass standards described above did not become more intense following IL-1

stimulation or A52 expression. The amount of TRAF6 in the samples was even (Figure 6.4, middle panel). A52 expression was equal in all the relevant samples (Figure 6.4, bottom panel, lanes 5-10), although the transfection efficiency was not known. The absence of a change in the native oligomerisation status of TRAF6 following stimulation suggests that the aggregate of TRAF6 is not sensitive to Il-1-stimulation or that the assay is not sensitive enough to detect any changes that are present. As mentioned above, it could be an aggregate of TRAF6 that is not resolved properly under native conditions. While IL-1 is thought to induce TRAF6 oligomerisation, it is possible that oligomerisation of TRAF6 does not occur in R1s in response to IL-1.

An alternative method was devised whereby over-expressed FLAG-tagged TRAF6 was transfected into cells and the oligomerisation of FLAG-TRAF6 was assayed by native PAGE. Since FLAG-TRAF6 auto-activates following expression in cell culture, it was expected that if TRAF6 oligomerised for activation it would be observed following FLAG-TRAF6 expression. The effect of IL-1 and A52 on the level of auto-oligomerisation of TRAF6 was examined (Figure 6.5). Over-expression of FLAG-TRAF6 resulted in the formation of oligomers or aggregates similar in molecular mass to those observed in the studies of endogenous TRAF6 (Figure 6.5, top panel, lanes 2, 4 and 5). It is possible that the oligomers observed comprise poly-ubiquitinated TRAF6, although this was not determined in this assay. IL-1 stimulation did not enhance the oligomerisation (Figure 6.5, top panel, compare lanes 2 and 4). Similarly, co-transfection of A52 had no effect on FLAG-TRAF6 oligomerisation (Figure 6.5, top panel, lane 5). In addition, the band that appeared in the endogenous TRAF6 blots that appeared to correspond to monomeric TRAF6 was only weakly detected on the FLAG-TRAF6 blots (data not shown). From these experiments, it was not possible to conclude that TRAF6 oligomerised following ligand stimulation since both endogenous and over-expressed TRAF6 formed high molecular mass aggregates on the native gels. The aggregates may be or may

include ubiquitinated TRAF6, though this was not tested and it might be difficult to distinguish between oligomerised and ubiquitinated TRAF6 by this method. Since FLAG-TRAF6 appeared to form aggregates in each sample regardless of stimulation or the presence of A52, it was not possible to discern an effect of A52 on TRAF6 oligomerisation by this method. In conclusion, A52 appeared to have no effect on TRAF6 oligomerisation although the sensitivity of this assay may preclude the observation of an effect.

6.2.3 TAB2 interacts with TRAF6 in the absence of ligand stimulation

Since TAB2 is required for IL-1-induced TRAF6 ubiquitination (Kishida *et al.*, 2005), it was next examined whether A52 affects the TAB2-TRAF6 interaction. Preliminary experiments suggested that endogenous TRAF6 co-precipitated with endogenous and over-expressed TAB2 in the absence of any stimulus. Immunoprecipitation for TAB2, followed by immunoblotting for TRAF6, showed an interaction band in all lanes (Figure 6.6, top panel). Since the immunoprecipitation was for TAB2, endogenous TAB2 was present in all samples. However, it was expected that TAB2 would only immunoprecipitate with TRAF6 following IL-1-stimulation. As can be observed, there is co-immunoprecipitation of TAB2 and TRAF6 in the absence of stimulation with IL-1 or the presence of A52 (Figure 6.6, top panel, lane 1). The co-precipitation was greater in unstimulated samples than it was in the samples stimulated with IL-1 (Figure 6.6, top panel, compare lanes 1-4 to lanes 5-8). In IL-1-stimulated samples, A52 appeared to slightly enhance the co-immunoprecipitation of TAB2 and TRAF6 (Figure 6.6, top panel, compare lanes 5 and 6). The IL-1-induced co-immunoprecipitation of TRAF6-TAB2 was greater when TAB2 was over-expressed than when only endogenous TAB2 was present (Figure 6.6, top panel, compare lanes 5 and 7). The over-expression of A52 reduced the IL-1-induced co-immunoprecipitation of over-expressed TAB2 and endogenous TRAF6 (Figure 6.6, top panel, compare lanes 7 and 8). However, the amount of TAB2

immunoprecipitated was not equal in all samples, since four of the samples had over-expressed TAB2 (Figure 6.6, second panel from top, lanes 3, 4, 7 and 8). The other samples had endogenous TAB2 and this was detected as a faint band at the same level as the over-expressed TAB2 (Figure 6.6, second panel from top, lanes 1, 2, 5 and 6). The amount of TAB2 immunoprecipitated in lane 8 is much less than that in lane 7, despite the fact that both lanes had over-expressed TAB2 (Figure 6.6, second panel from top). Thus, the apparent reduction in IL-1-induced TAB2/TRAF6 co-immunoprecipitation observed in the presence of A52 is likely due to less of the TAB2 protein being precipitated (Figure 6.6, compare lane 8 in the top panel and the second panel from top). Endogenous TRAF6 was equally detected in the samples (Figure 6.6, second panel from bottom). In this experiment, A52 was also immunoprecipitated. No specific co-precipitation of A52 with TAB2 was detected (data not shown). Immunoblotting for A52 showed equal levels in all samples containing over-expressed A52 (Figure 6.6, bottom panel). Importantly, the presence of A52 did not affect the amount of TRAF6 co-immunoprecipitated with TAB2. Thus, A52 did not affect the TRAF6-TAB2 interaction in the presence or absence of IL-1 stimulation.

6.2.4 A role for TAK1 in A52-induced p38 activation

A52 is able to activate p38 in the absence of ligand stimulation and this function of A52 depends upon its interaction with TRAF6 (Maloney *et al.*, 2005). In light of the role for TRAF6 in activating the MAP3K, TAK1, it was next examined if A52 required TAK1 to activate p38 MAPK. Previously, a kinase-inactive form of TAK1 (K63W) was found to function as a dominant-negative, preventing IL-1-induced NF-κB activation (Ninomiya-Tsuji *et al.*, 1999) and MAP kinase activation (Holtmann *et al.*, 2001). In order to assess the role of TAK1 in p38 activation, the CHOP assay was performed and the TAK1 K63W dominant negative (TAK1 DN) construct was added to test for inhibition. Thus, inhibition of p38 activation in the presence of the TAK1 DN would imply that TAK1 is

required for that signalling pathway. The level of IL-1- and A52-induced CHOP activation observed was low. However, the TAK1 DN inhibited the IL-1-induced p38 activation as anticipated (Figure 6.7A). Further, the TAK1 DN inhibited A52-induced p38 activation at both doses of A52 (Figure 6.7B). TAK1 thus mediates the pathway leading to p38 activation following A52 expression.

6.2.5 The association of TRAF6 and TAK1 in the presence of A52

Given that TAK1 potentially had a role in A52-induced p38 activation, the effect of A52 on the TRAF6-TAK1 interaction was examined. The interaction between TRAF6 and TAK1 was initially assessed with endogenous forms of both proteins. While the endogenous proteins could be detected in the control immunoprecipitates, the bands were faint and difficult to observe on the blots (data not shown). Interaction bands were detected following IL-1 stimulation in at least two fully endogenous experiments but this was always a faint band (data not shown). In order to circumvent this problem, both FLAG-TAK1 and myc-TRAF6 were over-expressed. Since A52 has been found to precipitate with the FLAG antibody (Chapter 3), the immunoprecipitation was done only with myc antibody. When the myc-TRAF6 samples were immunoblotted for FLAG, co-precipitation of TRAF6 and TAK1 was observed (Figure 6.8, top panel, lanes 5-8). The co-precipitation of TRAF6 and TAK1 occurred in samples that were not stimulated with IL-1 (Figure 6.8, top panel, lanes 5 and 6). Stimulation with IL-1 decreased the intensity of the co-precipitation band (Figure 6.8, top panel, compare lanes 5 and 7). The presence of A52 with or without IL-1 stimulation did not increase the intensity of TRAF6-TAK1 co-precipitation (Figure 6.8, top panel, lanes 6 and 8). Unfortunately, a band at the same position was also weakly detected in a sample that contained only myc-TRAF6 (Figure 6.8, top panel, lane 3). This suggests that immunoprecipitation with the myc antibody is non-specific under these conditions. Immunoprecipitation of myc-TRAF6 was equal in most lanes, with a slight decrease in lane 7 (Figure 6.8, second

panel from top). Also, there appeared to be a decrease in the amount of heavy chain detected in the lane with A52 and IL-1 stimulation (Figure 6.8, second panel from top, lane 8). There was a detectable smear just above the band for myc-TRAF6 in all lanes that contained myc-TRAF6 (Figure 6.8, second panel from top, lanes 3, 5-8). This could represent TRAF6 auto-ubiquitination since over-expression of TRAF6 is known to auto-activate it. FLAG-TAK1 was detected in the lysates although there were numerous non-specific bands on the blot, including a faint band at the same molecular mass as FLAG-TAK1 (Figure 6.8, second panel from bottom, lanes 4-8). A52 expression was detected in all samples in which it was transfected (Figure 6.8, bottom panel, lanes 2, 6 and 8).

Since an apparent interaction band was detected in sample containing only myc-TRAF6, the immunoprecipitation conditions were likely not sufficiently stringent. In order to increase the stringency, the immunoprecipitation was performed using buffer that had higher salt (250mM) and NP-40 (1%) concentrations than normal lysis buffer (see Materials and Methods). The immunoprecipitation was allowed to proceed for two hours at 4□C and was then washed in the same high salt and NP40 buffer as used for the lysis. Using these conditions resulted in a reduction of the non-specific co-precipitation bands (Figure 6.9, top panel). Importantly, A52 induced the interaction of myc-TRAF6 and FLAG-TAK1 in the absence of IL-1 stimulation (Figure 6.9, top panel, compare lanes 5 and 6). IL-1 stimulation did not induce co-precipitation of FLAG-TAK1 and myc-TRAF6 in either the presence or absence of A52 (Figure 6.9, top panel, lanes 7 and 8). It was possible that the cells were not responding to IL-1 at the time and this was not assessed by another method. The level of myc-TRAF6 detected in the immunoprecipitation was not even, with less myc-TRAF6 precipitated in the samples that were stimulated with IL-1 (Figure 6.9, second panel from top, lanes 7 and 8). The decreased amount of myc-TRAF6 immunoprecipitated in the samples treated with IL-1 could account for the absence of a myc-TRAF6-FLAG-TAK1 interaction in these samples. Furthermore, the

expression of myc-TRAF6 was reduced in the IL-1-stimulated samples, suggesting that there was relatively less protein in these samples to precipitate (Figure 6.9, middle panel, lanes 7 and 8). FLAG-TAK1 was detected in the lysates in equal quantities in all samples (Figure 6.9, second panel from bottom). A52 was expressed equally in all samples in which it was transfected (Figure 6.9, bottom panel, lanes 2, 6 and 8). This was a preliminary experiment using the more stringent lysis conditions. This result has since been observed two more times. Thus, it is possible that A52 could induce the association of TRAF6 and TAK1 in the absence of ligand stimulation and this would correlate with the ability of over-expressed A52 alone to activate MAPK.

6.2.6 A52 interacts with TAK1 in the absence of TRAF6

The interaction of A52 with TAK1 was observed fortuitously when a blot with both TRAF6 and TAK1 immunoprecipitates was immunoblotted with A52 (Figure 6.10). In samples in which A52 was over-expressed, it always co-precipitated with TAK1 (Figure 6.10, top panel, lanes 2, 4, 6 and 8). The co-precipitation band was much more intense following IL-1 stimulation for 5 minutes (Figure 6.10, top panel, lane 6). This did not correlate with greater immunoprecipitation of TAK1 itself (Figure 6.10, second panel from top, lane 6). In fact, immunoprecipitation of endogenous TAK1 was barely detectable in all samples (Figure 6.10, second panel from top). This effect of IL-1 on the TAK1/A52 co-immunoprecipitation was not reproducible since in a repeat experiment the unstimulated sample and the sample stimulated with IL-1 for 10 minutes gave similarly intense bands (data not shown). It is thus possible that the A52-TAK1 co-immunoprecipitation is independent of IL-1 stimulation but can also be intensified by stimulation. Expression of TAK1 was detected in the lysates and was equal in all samples (Figure 6.10, second panel from bottom). A52 was detected in equal quantities in all samples in which it was transfected (Figure 6.10, bottom panel).

A52 reproducibly co-precipitated with endogenous (Figure 6.10) and over-expressed (data not shown) TAK1 in R1s. However, since R1s contain TRAF6, it was feasible that the A52-TAK1 interaction was indirectly mediated by TRAF6. In order to examine this hypothesis, the co-precipitation of A52 and TAK1 was tested in wild-type and TRAF6 null MEFs (Figure 6.11). It was anticipated that if TRAF6 was required for the A52-TAK1 interaction, then no co-precipitation would be observed in TRAF6 null MEFs. A52 co-precipitated with TAK1 in both the wild-type and TRAF6 null MEFs (Figure 6.10, top panels, lanes 2 and 4). As observed in the R1s, the immunoprecipitation of endogenous TAK1 was barely detectable. The predicted molecular mass of murine TAK1 was 64kDa, whereas the human isoform is predicted to be approximately 70kDa. Murine TAK1 was observed just above the heavy chain (Figure 6.11, second panel from top). Interestingly, a smear of higher molecular mass TAK1 was observed in wild-type MEFs but not in TRAF6 null MEFs and only when A52 was present (Figure 6.11, second panel from top, lane 2, marked with an asterisk). This smear could be modified TAK1 or ubiquitinated TRAF6 that is coming down in the same complex.

6.2.7 F154A interacts weakly with TAK1 in the presence or absence of TRAF6

In order to determine if co-precipitation of A52 and TAK1 was important for A52 function, the ability of the TRAF6 binding motif mutant F154A to co-precipitate with TAK1 was examined. Increasing quantities of A52 and F154A were transfected into wild-type and TRAF6 null MEFs. In wild-type MEFs, A52 co-precipitated with TAK1 while F154A did not (data not shown). In TRAF6 null MEFs, A52 co-precipitated with TAK1 in a dose-dependent manner (Figure 6.12, top panel, lanes 2-4). In contrast, no co-precipitation of F154A and TAK1 was detected in the TRAF6 null MEFs at the lower doses of F154A (Figure 6.12, top panel, lanes 5 and 6). At the top dose of F154A, co-precipitation of F154A and TAK1 was detected (Figure 6.12, top panel, lane 7). The intensity of the F154A-TAK1 co-precipitation was of the same intensity as that observed

between A52 and TAK1 at the lowest dose of A52 (Figure 6.12, top panel, compare lanes 2 and 7). This suggests that F154A interacts weakly with TAK1 whereas the A52-TAK1 interaction is robust. However, the ability to detect the interaction is impaired by low expression levels of F154A and thus it is possible that wild-type and mutant A52 interact with TAK1 to the same extent. The F154A mutant could be prepared again in an attempt to obtain better expression levels.

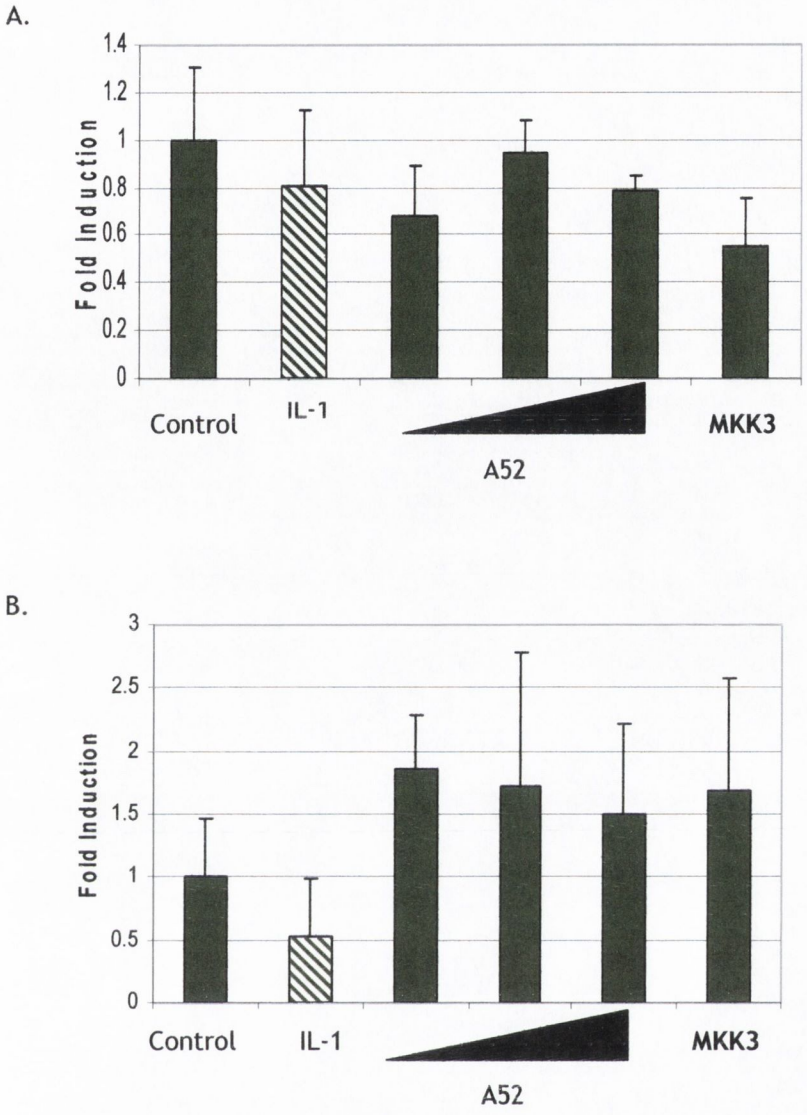

Figure 6.1. A52 does not activate the p38 CHOP assay in wild-type or IRAK2 $^{-/-}$ MEFs.

IRAK2 wild-type (A) and null (B) MEFs were seeded in 96-well plates at a density of 1 x 10^5 cells/mL. The following day, the cells were transfected with pFR-luciferase (60ng), TK-Renilla (20ng), Gal4-CHOP (0.25ng), MKK3 (100ng) and varying amounts of A52 (10, 30 and 100ng) with Lipofectamine. The following day, the cells were stimulated with IL-1α (20ng/ml) and harvested 6 hours later. The cells were lysed and the reporter gene activity was measured. Data is expressed as mean fold induction +/- s.d. for an experiment performed in triplicate. A similar result was obtained twice with Lipofectamine and three times using GeneJuice.

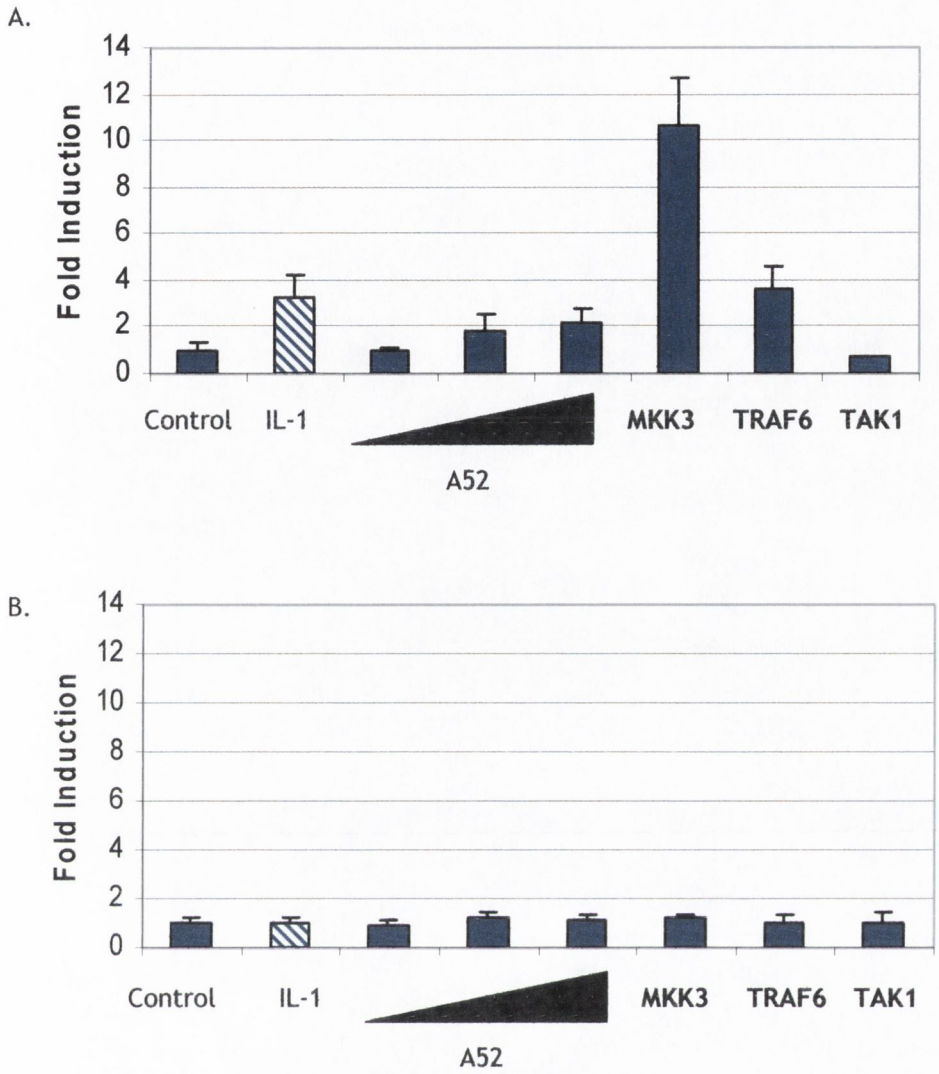

Figure 6.2. A52 activates p38 CHOP in IL-1R cells but not in IRAK1-deficient cells.

R1s (A) and IRAK1-deficient cells (B) were seeded in 96-well plates at a density of 1 x 10^5 cells/mL. The following day, the cells were transfected with pFR luciferase (60ng), TK-Renilla (20ng), CHOP (0.25ng), varying amounts of A52 (10, 30 and 100ng), MKK3 (100ng), TRAF6 (100ng) and TAK1 (100ng). The following day, the cells were stimulated with IL-1α (20ng/mL) and harvested 6 hours later. The cells were lysed and the reporter gene activity was measured. Data is expressed as mean fold induction +/- s.d. for an experiment performed in triplicate. Similar results were obtained three times.

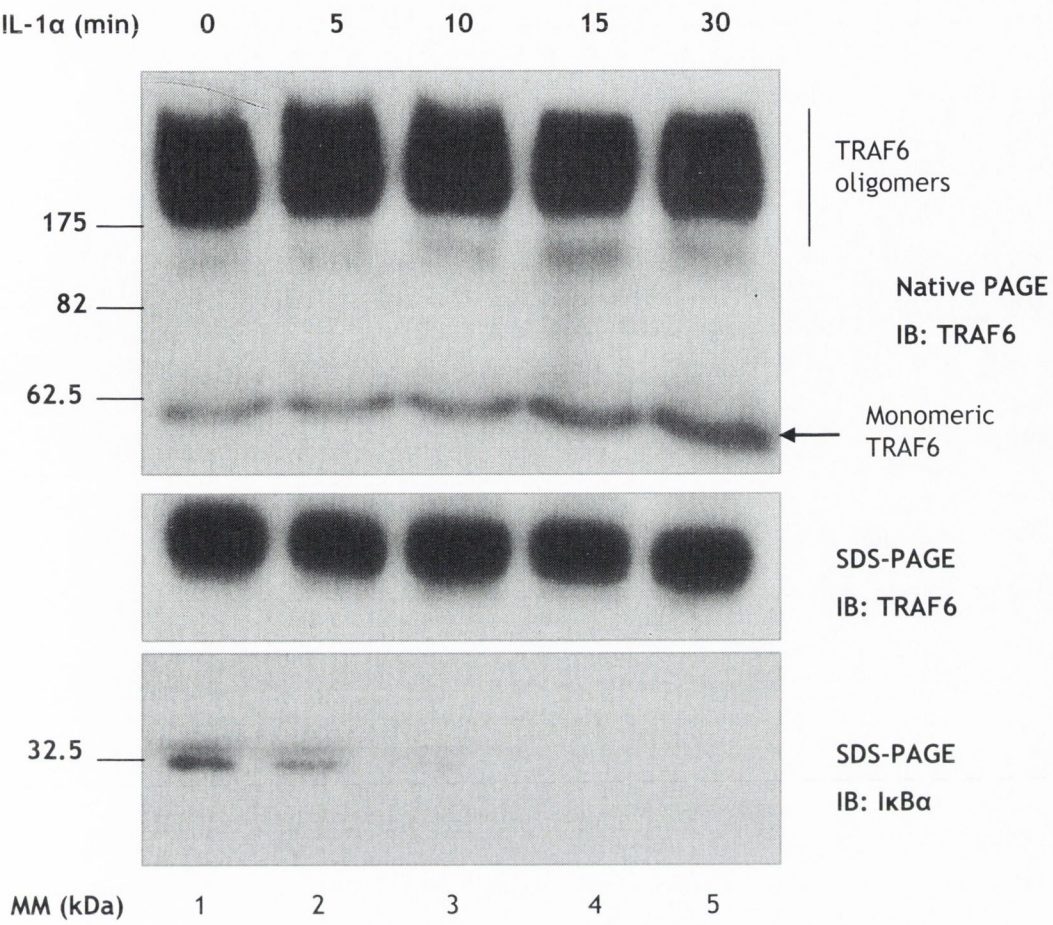

Figure 6.3 Endogenous TRAF6 oligomerisation is observed in the absence of IL-1 stimulation

R1s were seeded at $1x10^5$ cells/mL in 6-well plates 24 hours prior to stimulation. The cells were stimulated with IL-1α (20ng/mL) for 0, 5, 10, 15 or 30 minutes. The cells were harvested and then lysed using NP40 lysis buffer. The lysate was divided into two samples and mixed with either non-denaturing or denaturing sample buffer. Lysates mixed with non-denaturing sample buffer were analysed by native PAGE (top panel). The lysates that were mixed with denaturing sample buffer were analysed by SDS-PAGE (bottom two panels). The gels were transferred to PVDF using a semi-dry transfer system. The blots were incubated with antibodies directed against TRAF6 or IκBα, as indicated. The molecular masses indicated for native PAGE are approximations (see text). The higher molecular mass form of endogenous TRAF6 has been observed at least four times in the absence of IL-1 stimulation. MM, molecular mass standards.

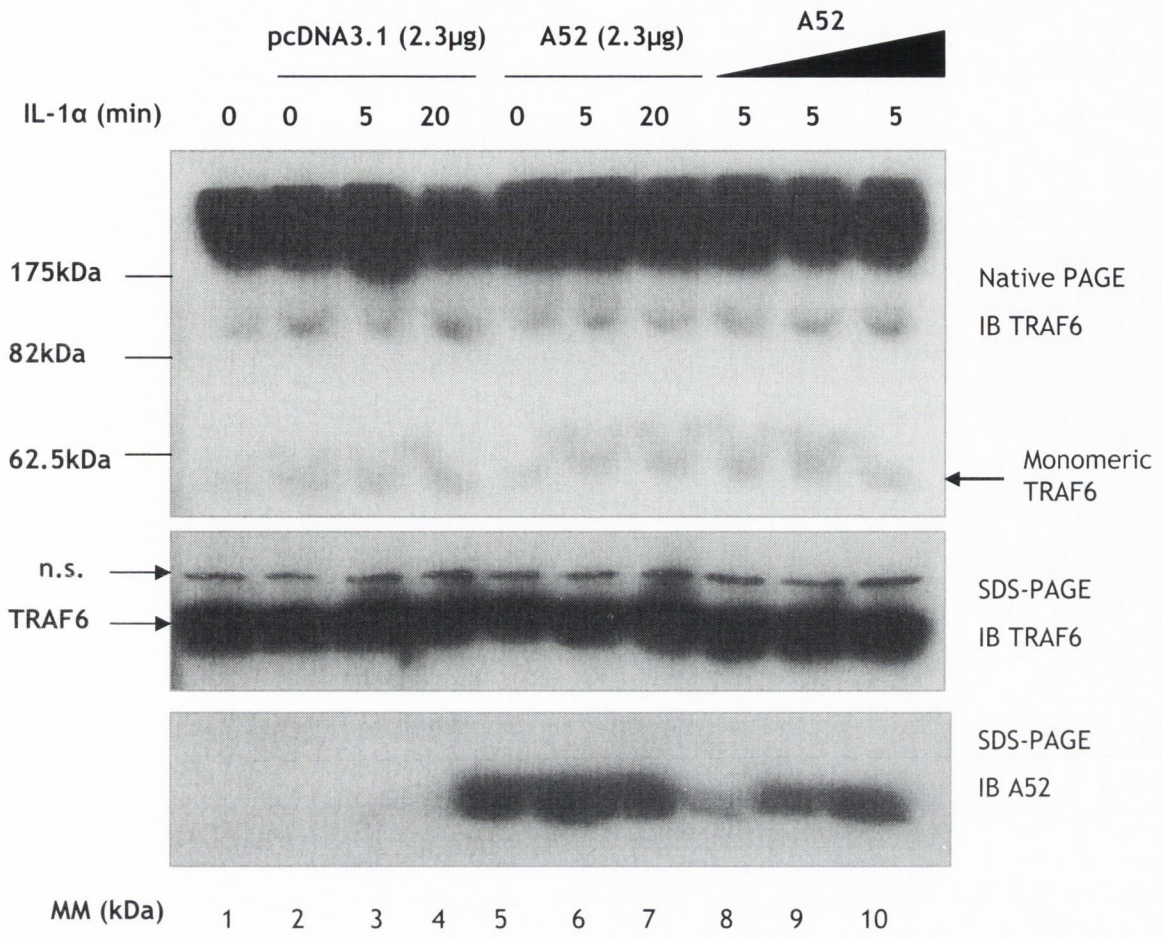

Figure 6.4 Oligomerisation of endogenous TRAF6 is not altered by IL-1 stimulation or A52 expression.

R1s were seeded at $1x10^5$ cells/mL in 6-well plates 24 hours prior to transfection. The cells were transfected with pcDNA3.1 (2.3μg), A52 (2.3μg) or increasing quantities of A52 (0.5, 1 and 1.5μg) using Genejuice TM according to the manufacturer's directions. The cells were lysed using NP40 lysis buffer. The lysates were divided into two samples and mixed with either non-denaturing or denaturing sample buffer. Lysates mixed with non-denaturing sample buffer were analysed by native PAGE (top panel). The lysates that were mixed with denaturing sample buffer were analysed by SDS-PAGE (bottom two panels). The gels were transferred to PVDF using a semi-dry transfer system. The blots were incubated with antibodies directed against TRAF6 or A52, as indicated. A similar result was obtained three times. The molecular masses indicated for native PAGE are approximations. MM, molecular mass standards; n.s., non-specific band.

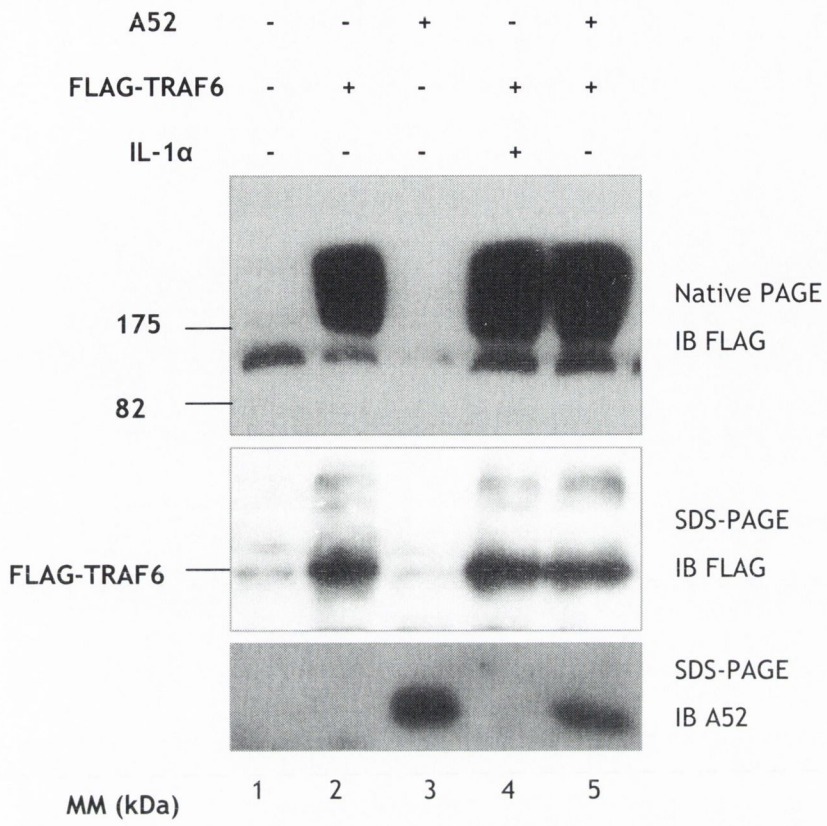

Figure 6.5 Oligomerisation of over-expressed TRAF6

R1s were seeded at $1x10^5$ cells/mL in 6-well plates 24 hours prior to transfection. The cells were transfected with A52 (0.5μg) or FLAG-TRAF6 (0.5μg) using Genejuice TM according to the manufacturer's directions. The cells were lysed using NP40 lysis buffer and then the lysates were divided into two samples. The samples were mixed with either non-denaturing or denaturing sample buffer. Lysates mixed with non-denaturing sample buffer were analysed by native PAGE (top panel). The lysates that were mixed with denaturing sample buffer were analysed by SDS-PAGE (bottom two panels). The gels were transferred to PVDF using a semi-dry transfer system. The blots were incubated with antibodies directed against FLAG or A52, as indicated. The molecular masses indicated for native PAGE are approximations. A similar result has been obtained three times. MM, molecular mass standards.

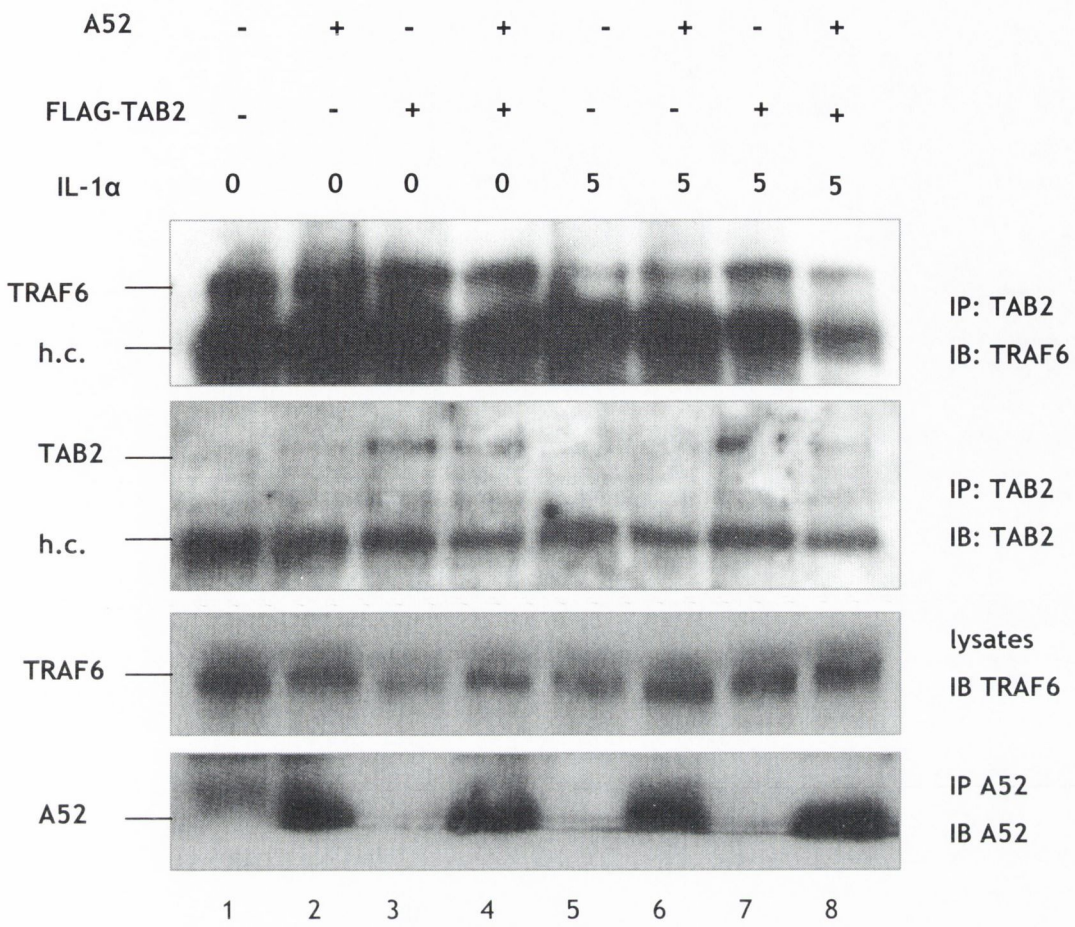

Figure 6.6 TAB2 and TRAF6 co-precipitate in the absence of IL-1 stimulation

R1s were seeded at 1 x 10^5 cells/mL in 100mm dishes. The cells were transfected 24 hours later with FLAG-TAB2 (4μg) or A52(4μg). The following day, the cells were stimulated with IL-1α (20ng/mL) for 5 minutes and then were harvested. The cells were lysed and the lysates were immunoprecipitated with either TAB2 or A52. TRAF6 and TAB2 co-precipitating in the presence and absence of IL-1 stimulation or A52 expression was observed twice. h.c., antibody heavy chain.

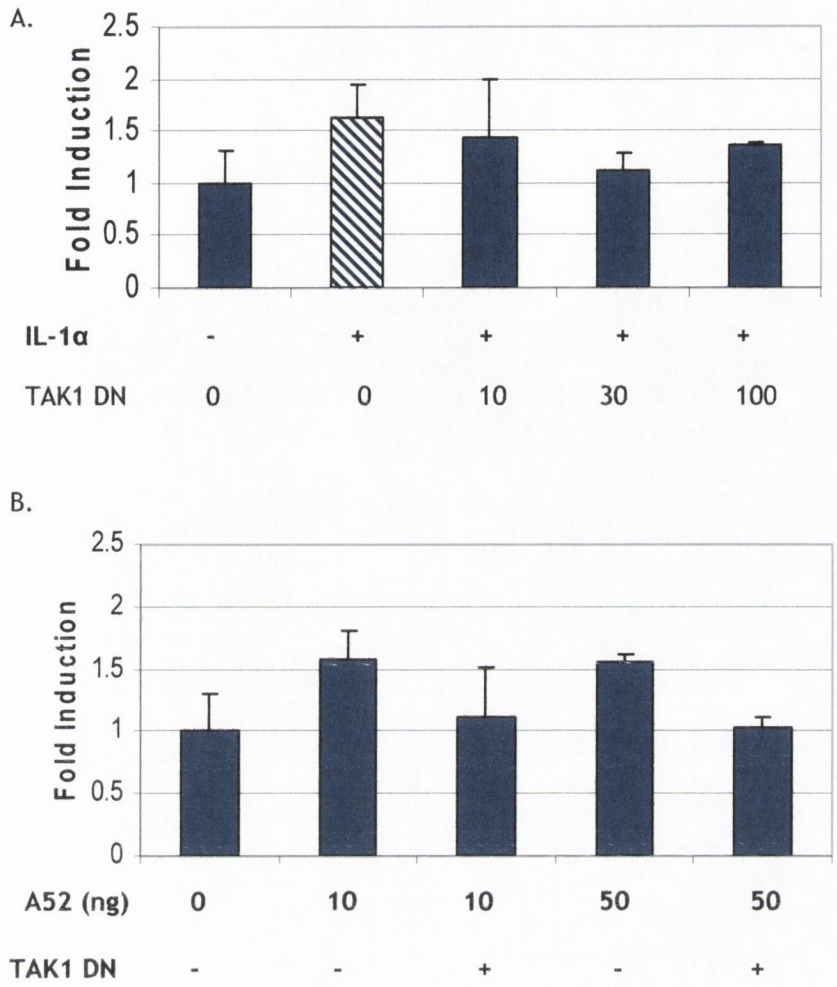

Figure 6.7. TAK1 is involved in A52-induced p38 activation

R1s were seeded in 96-well plates at a density of 1 x 10^5 cells/mL. The following day, the cells were transfected with pFR luciferase (60ng), TK-Renilla (20ng), and CHOP (0.25ng) using GeneJuice™. In addition, the cells were transfected with: (A) varying amounts of TAK1 dominant negative (DN) (10, 30, 100ng) or (B) varying amounts of A52 (10 and 50ng) and TAK1 DN (100ng). The following day, the cells were stimulated with IL-1α (20ng/mL) and harvested 6 hours later. The cells were lysed and the reporter gene activity was measured. Data is expressed as mean fold induction +/- s.d. for an experiment performed in triplicate. This result has been observed twice.

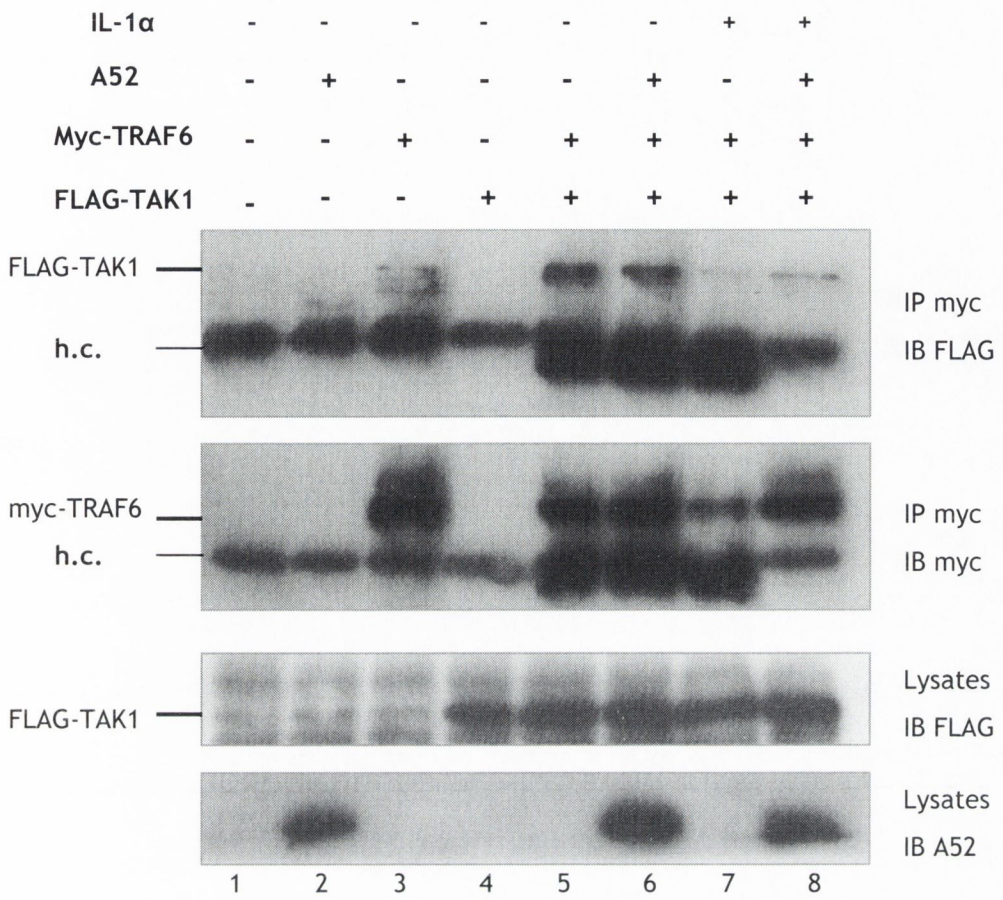

Figure 6.8 TAK1 and TRAF6 co-precipitate in the absence of IL-1 stimulation

R1s were seeded at 1 x 10^5 cells/mL in 100mm dishes. The cells were transfected 24 hours later with FLAG-TAK1 (2μg), myc-TRAF6 (2μg) or A52(4μg). The following day, the cells were stimulated with IL-1α (20ng/mL) for 5 minutes and then were harvested. The cells were lysed and the lysates were immunoprecipitated with antibody to myc that had been pre-coupled to protein A/G sepharose beads. The immunoprecipitates and lysates were analysed by SDS-PAGE, followed by transfer to PVDF using a semi-dry system. The blots were incubated with antibody to FLAG, myc or A52, as indicated on the right. Similar results were obtained in two other experiments. h.c., antibody heavy chain.

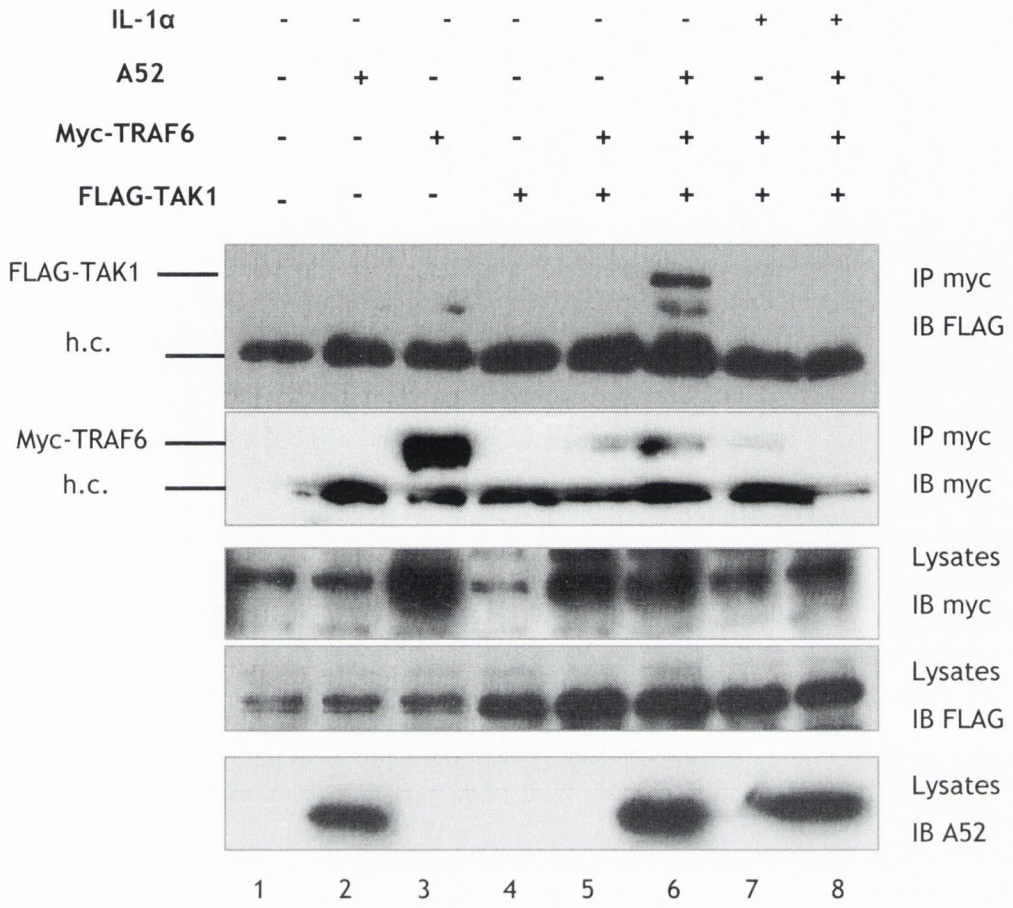

Figure 6.9 A52 induces the interaction of TAK1 and TRAF6

R1s were seeded at 1 x 10^5 cells/mL in 100mm dishes. The cells were transfected 24 hours later with FLAG-TAK1 (2μg), myc-TRAF6 (2μg) or A52(4μg). The following day, the cells were stimulated with IL-1α (20ng/mL) for 5 minutes and then were harvested. The cells were lysed in lysis buffer containing higher NaCl and NP-40 concentrations (50mM HEPES, 250mM NaCl, 1mM EDTA, 10% glycerol, 1% NP-40) than in regular lysis buffer. The lysates were immunoprecipitated for 2 hours at 4℃ with antibody to myc that had been pre-coupled to protein A/G sepharose beads. The immunoprecipitates and lysates were analysed by SDS-PAGE, followed by transfer to PVDF using a semi-dry system. The blots were incubated with antibody to FLAG, myc or A52, as indicated on the right. This result has been observed three times. h.c., antibody heavy chain.

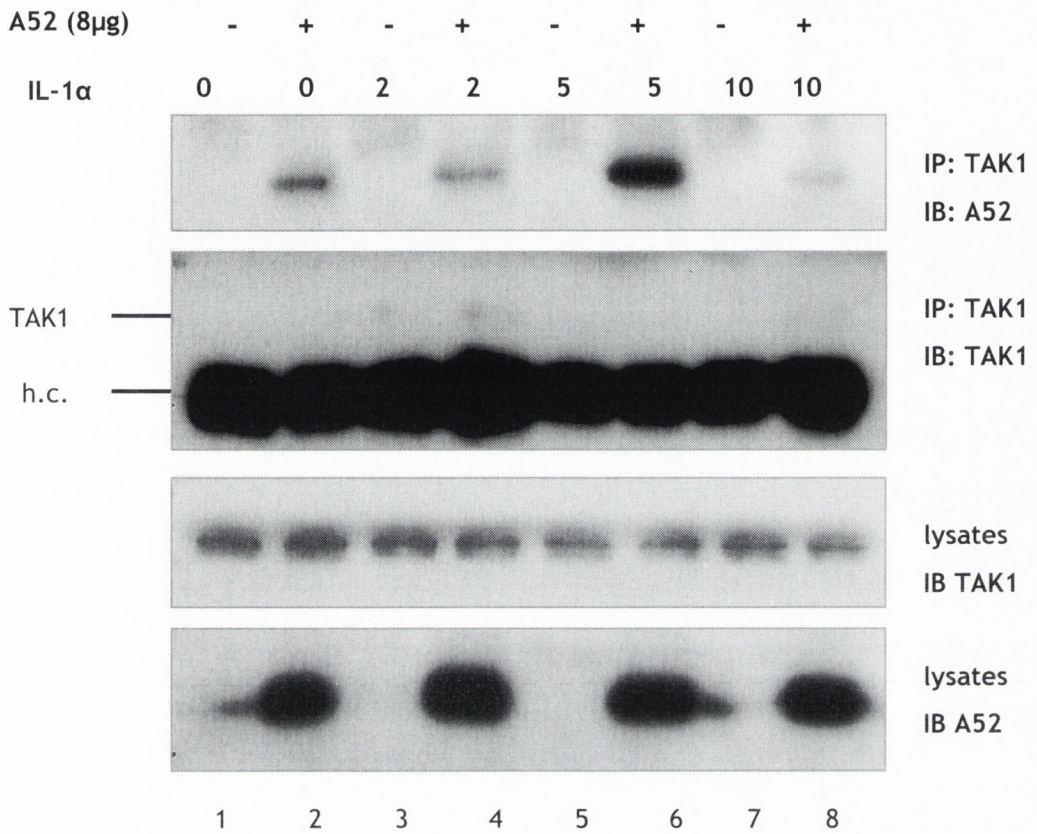

Figure 6.10 A52 co-precipitates with endogenous TAK1 in R1s

R1s were seeded at 1 x 10^5 cells/mL in 100mm dishes. The cells were transfected 24 hours later with pRK5 (8μg) or A52(8μg). The following day, the cells were stimulated with IL-1α (20ng/mL) for 0, 2, 5 or 10 minutes and then were harvested. The cells were lysed in NP-40 lysis buffer (100mM NaCl, 1% NP-40). The lysates were immunoprecipitated with antibody to TAK1 that had been pre-coupled to protein A/G sepharose beads. The co-precipitation of A52 and endogenous TAK1 was observed in three experiments in R1s. H.C., antibody heavy chain.

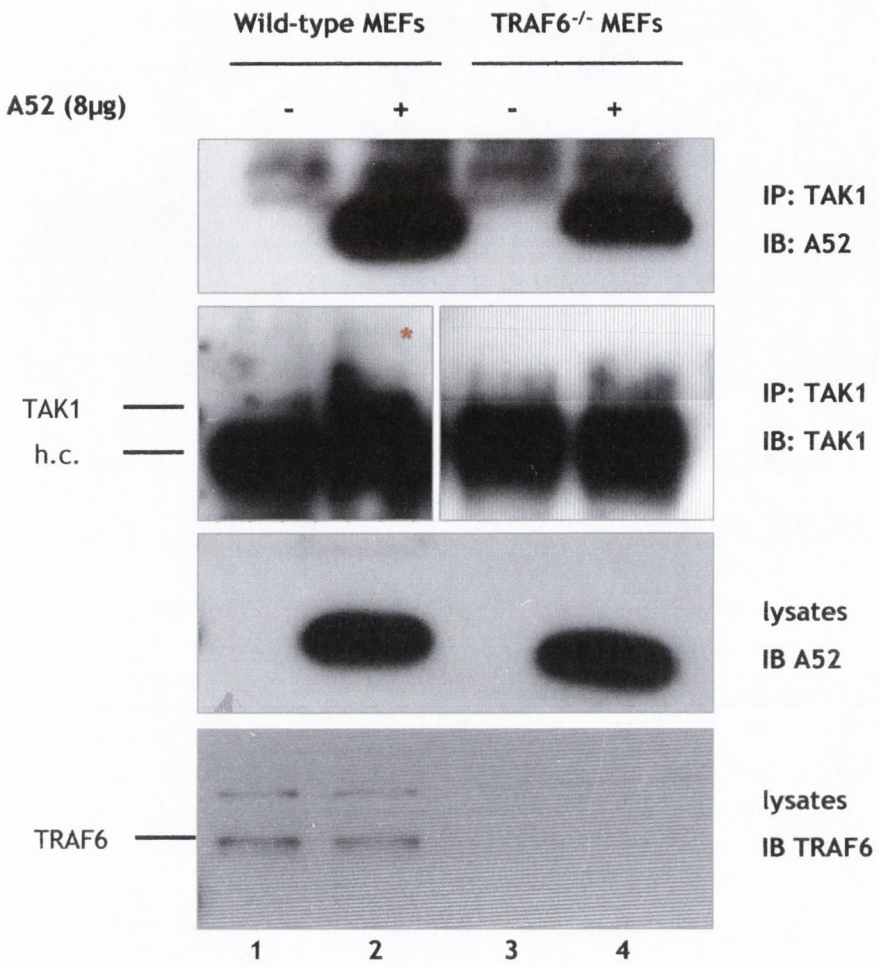

Figure 6.11 A52 co-precipitates with TAK1 in TRAF6$^{-/-}$ MEFs

TRAF6 null MEFs were seeded in 100mm dishes 24 hours prior to transfection. The following day, when the monolayer was approximately 75% confluent, the cells were transfected with pRK5 (8μg) or A52 (8μg). The cells were harvested 24 hours post-transfection and lysed in NP-40 lysis buffer. The lysates were immunoprecipitated with TAK1 antibody that had been pre-coupled to protein A/G sepharose beads. This result was observed twice. h.c., antibody heavy chain.

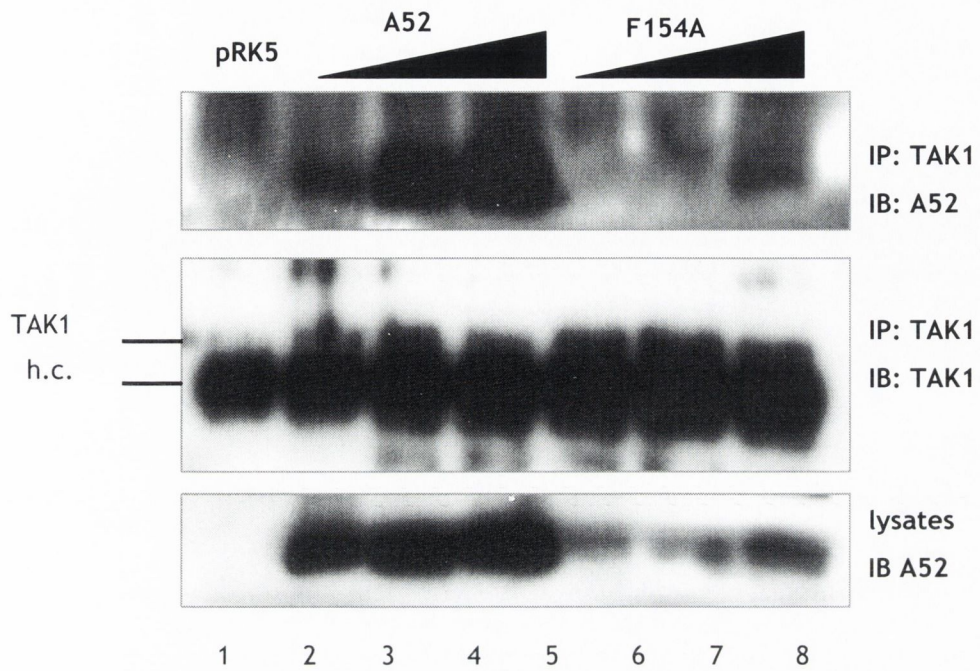

Figure 6.12 A52 and F154A co-precipitate with TAK1 in TRAF6$^{-/-}$ MEFs

TRAF6 null MEFs were seeded into 100mm dishes and then transfected when the monolayer was approximately 75% confluent. The cells were transfected with pRK5 (8μg), or increasing doses of A52 or F154A (2,4, and 8μg). The following day, the cells were harvested and then lysed in NP-40 lysis buffer. The lysates were immunoprecipitated with antibody to TAK1 that had been pre-coupled to protein A/G sepharose beads. The lysates and immunoprecipitates were analysed by SDS-PAGE followed by transfer to PVDF using a semi-dry transfer system. This experiment was done twice in TRAF6$^{-/-}$ MEFs and A52 was found to interact with TAK1 in both experiments. In the second experiment using F154A, the co-precipitation was not observed, likely due to low expression levels. h.c., antibody heavy chain.

6.3 Discussion

The aim of this chapter was to investigate the roles of IRAKs, TRAF6 oligomerisation and downstream effectors in A52-induced MAPK activation. It has previously been reported that A52 does not immunoprecipitate with IRAK1 (Harte *et al.*, 2003). It has been found that the interaction of A52 with TRAF6 was required for A52-induced p38 activation (Maloney *et al.*, 2005) and that the A52-TRAF6 interaction was not affected by the absence of IRAK1 (Chapter 3). Thus, it was likely that IRAK1 was not involved in A52-induced MAPK activation. In order to test this hypothesis, the CHOP assay was performed in IRAK1-deficient cells in parallel with R1s. While IL-1, A52, as well as over-expressed TRAF6 and MKK3, could activate p38 in R1s, no activation of p38 was observed in I1A cells. Instead of confirming that IRAK1 is not required for p38 activation, this result suggested that the CHOP assay did not work in this cell line. In order to show that IRAK1 is not needed for A52-induced MAPK activation, phosphorylation of p38, JNK and ATF2 could be assessed by western blotting. However, the use of HEK 293-derived cell lines in phospho-MAPK detection by western blotting has not been successful and thus the I1A cells are unlikely to be a good system in which to analyse phosphorylation of MAPK. Since phospho-MAPK detection by western blotting works well in MEFs, the use of IRAK1-deficient MEFs could be useful in assessing the need for IRAK1 in A52-induced MAPK activation.

Over-expression of IRAK2 in the CHOP assay in HEK293 cells activated p38, while over-expression of IRAK1 did not (Keating *et al.*, 2007). In order to determine if A52 required IRAK2 to drive p38 activation, the CHOP assay was performed in wild-type and IRAK2$^{-/-}$ MEFs. Unfortunately, the CHOP assay did not work in either the wild-type or IRAK2$^{-/-}$ MEFs. It was thus not possible to determine if there was a role for IRAK2 in A52-induced p38 activation. It has previously been found that an A52 construct that interacts with IRAK2 but not TRAF6 is unable to activate p38 (Maloney *et al.*, 2005). Thus, it is

unlikely that IRAK2 plays a role in A52-induced p38 activation. A52 likely targets IRAK2 solely to inhibit ligand-induced NF-κB activation (Keating *et al.*, 2007).

Other studies have observed that TRAF6 is an oligomer (usually a trimer) and that this self-association is required for signal transduction (Wu and Arron, 2003; Baud *et al.*, 1999). TRAF6 oligomerisation was studied in this chapter using native PAGE. In this method, the non-denatured protein should migrate in monomeric or multimeric forms as found in the cell. However, using this method to analyse TRAF6 found that it migrated as a non-specific high-molecular mass protein. It was not possible to determine the mass of the complex since the molecular mass standards used were in denatured sample buffer and were not designed for use with native PAGE. It is also not possible to conclude that it is TRAF6 alone in the aggregates since it could be in complex with other signalling proteins. Thus, since TRAF6 migrates as an aggregate in non-denatured samples, another method such as gel filtration will need to be employed to determine whether A52 alters the oligomerisation of TRAF6.

TAB2 had been reported to interact with TRAF6 in the absence of stimulation (Takaesu *et al.*, 2000). This interaction was enhanced by IL-1 stimulation, likely due to IL-1-induced redistribution of TAB2 from the cell membrane to the cytosol (Takaesu *et al.*, 2000). In this chapter, endogenous TRAF6 co-precipitated with TAB2 in the absence of ligand stimulation. Stimulation with IL-1 did not enhance the interaction between TRAF6 and TAB2 (Figure 6.6). Moreover, over-expression of A52 did not alter the intensity of the interaction between TRAF6 and TAB2. Preliminary results suggest that A52 does not affect the association of TRAF6 and TAB2. To determine if this is the case, a time course following IL-1 stimulation and varying amounts of A52 need to be tested for their effect on the TAB2-TRAF6 interaction. Further work is needed to rule out a role for TAB2 or other TAB proteins in A52-induced p38 activation.

TAK1 is a MAP3K that activates the MKK3/MKK6 which subsequently phosphorylates p38 (Ashwell, 2006). It was hypothesised that TAK1 is needed for A52-induced p38 activation. Using a TAK1 dominant-negative construct in the CHOP assay resulted in inhibition of both IL-1- and A52-induced p38 activation. Thus, TAK1 is needed for A52 to activate p38.

It was possible based on the TAK1 dominant negative studies that A52 was facilitating the formation of the TAK1/TRAF6 complex. Initial attempts to examine the TAK1-TRAF6 interaction were futile due to the low levels of the endogenous proteins. Once the proper conditions for immunoprecipitation of the over-expressed FLAG-TAK1 and myc-TRAF6 were established, it was found that A52 could enhance the TRAF6-TAK1 interaction in the absence of IL-1 stimulation (Figure 6.9). Unfortunately, the immunoprecipitation in the IL-1 stimulated samples did not work well so it is not possible to tell if A52 affects recruitment of TAK1 to TRAF6 after IL-1 stimulation. This is a preliminary experiment since the conditions were only optimised after three less stringent experiments and there was not time to repeat it. However, it bears further examination since facilitating the TAK1-TRAF6 interaction could be the mechanism of action of A52-induced p38 activation. Further, it could be that the effect of A52 on the TAK1-TRAF6 interaction is direct and does not involve the TAB proteins. TAB2 and TAB3 are known to be essential for the recruitment of TAK1 to polyubiquitinated TRAF6 following IL-1 stimulation (Besse *et al.*, 2007). However, as discussed above, preliminary results suggest that A52 does not affect the TAB2-TRAF6 interaction. It has previously been shown that A52 does not interact with TAB1 (Harte *et al.*, 2003). The interaction between A52 and TAB3 has not been tested. It is thus feasible that the effect of A52 on TAK1 could be due to a direct interaction of A52 with TAK1.

It was previously found that A52 weakly interacted with over-expressed TAK1 (Harte *et al.*, 2003). In the present study, A52 co-precipitated with endogenous TAK1 in R1s (Figure 6.10). TRAF6$^{-/-}$ MEFs were used to determine if the interaction between A52 and TAK1 was indirect and due to the A52-TRAF6 interaction. Surprisingly, A52 co-precipitated with TAK1 in the absence of TRAF6 (Figure 6.11). It is possible that the co-precipitation of TAK1 and A52 is indirect and is mediated by other cell signalling molecules, including the TAB proteins. However, the co-precipitation of TAK1 and A52 in the absence of TRAF6 suggested that the A52-TRAF6 interaction could be independent of the A52-TAK1 interaction. Further, the ability of A52 to interact with both TAK1 and TRAF6 could be necessary for the mechanism of action whereby A52 brings TAK1 and TRAF6 into association. The inactive mutant, F154A, was also found to interact with TAK1 in both wild-type and TRAF6$^{-/-}$ MEFs, though this was only observed at the top dose (Figure 6.12). The low expression levels of F154A likely account for the problems with detecting an F154A-TAK1 interaction at the lower doses. The interaction of F154A with TAK1 might be weaker than that of A52 and TAK1, which would correlate with the inability of F154A to activate p38 (Chapter 4). TRAF6 is known to be required for the activation of p38 by A52 but both A52 and F154A co-immunoprecipitate with TRAF6 (Chapter 4). Binding to TRAF6 alone cannot account for the ability of A52 to activate p38. It was hypothesised that the interaction between A52 and TAK1 could account for the ability of A52 to activate p38, possibly via the recruitment of TAK1 to TRAF6. However, the finding that the inactive mutant F154A was still able to interact with TAK1 suggests that this might not be the case. It could be that the F154A mutant is still able to interact with both TAK1 and TRAF6 but cannot cause them to associate in the absence of IL-1R/TLR stimulation. To test this, the experiment with myc-TRAF6 and FLAG-TAK1 should be repeated with F154A in place of wild-type A52. Since the CHOP assay did not work in the MEFs, it was not possible to determine if A52 could activate p38 in the TRAF6$^{-/-}$ MEFs by this method. However, phosphorylation of MAP kinases

tested by western blotting showed minimal activation of p38 in the TRAF6$^{-/-}$ MEFs, but no phosphorylation of ATF-2 (Figure 4.1). In the absence of TRAF6, A52 could still associate with TAK1 and this might be sufficient to induce phosphorylation of the MAPK. However, TAK1-TRAF6 association might be needed to fully activate p38 such that it is able phosphorylate ATF-2 and other p38-dependent genes. Thus, if TAK1 has a role in A52-induced p38 activation, it is likely to be via the TRAF6-TAK1 interaction. It could be that A52 activates p38 via recruiting TAK1 to TRAF6. Furthermore, there is evidence that TAK1 is ubiquitinated in the TCR signalling pathway (Reiley *et al.*, 2007) and it might be that TAK1 is generally ubiquitinated during signalling. The ubiquitination kinetics of TAK1 could be accelerated in the presence of A52, as observed with TRAF6. A52 could accelerate TRAF6 ubiquitination in order to enhance ubiquitination and activation of TAK1. The affect of A52 on TAK1 ubiquitination, if any, should be examined.

In this chapter, the mechanism by which A52 activates p38 and inhibits IL-1-induced NF-κB activation was examined by looking components of the IL-1 signalling pathway. No role for the IRAKs in A52-induced p38 activation could be discerned since the CHOP assay did not work in the IRAK2$^{-/-}$ MEFs or the IRAK1-deficient cells. Neither could an effect of A52 on TRAF6 oligomerisation be determined due to the non-specific aggregation of TRAF6 in the native PAGE assay. A putative new role for TAK1 in A52-induced p38 activation was described herein. The TAK1 DN construct inhibited A52-induced p38 activation in the CHOP assay, suggesting that TAK1 is part of this pathway. Furthermore, A52 co-precipitates with TAK1 in the absence of TRAF6, suggesting that TAK1 is a cellular target of A52. In addition, it is possible that A52 alters the kinetics of TRAF6-catalysed TAK1 ubiquitination. In conclusion, work in this chapter has shown that A52 interacts with endogenous TAK1 independently of TRAF6 and that A52 can induce the association of TAK1 and TRAF6 in the absence of IL-1 stimulation. The

ability of A52 to bring TAK1 and TRAF6 together into a complex could be part of the mechanism by which A52 induces MAPK activation.

Chapter Seven: Final Discussion

The typical definition of a virus is that it is an obligate intracellular parasite since it must infect permissive cells in order to replicate. Once within the host cell, the virus faces the obstacle of replication amidst numerous cellular defence mechanisms. The innate immune system is a complex array of pathogen-detecting receptors and intracellular signalling pathways that has evolved to quell microbial infection. The study of innate immunity to viruses has progressed dramatically over the last few years and it is now clear that there are numerous mechanisms to sense viral infection. The mechanism of detection of viral nucleic acids has been clarified to some extent by the discovery of the 5'-triphosphate as the PAMP recognised by RIG-I. Detection of viral infection by TLRs or cytosolic PRRs, like RIG-I, is important for the activation of antiviral signalling pathways leading to the induction of pro-inflammatory cytokines and interferons.

Although viruses are considered to be parasites, there is considerable interplay between viral replication and immune evasion strategies and the host defences against them. Coexistence with the host is necessary for the virus since excessive virulence and viremia would destroy its life support system. The benefit to the host of coexistence is not as obvious since productive viral infections are usually harmful and can be lethal. However, at least one study has found that latent herpesviruses are protective against bacterial infections since the latent viruses prime the immune response (Barton et al., 2007). Further evidence for the co-existence and co-evolution of viruses and cells can be found in the immunomodulatory proteins of large DNA viruses like VACV, many of which were originally captured from cells and have since become adapted to serve viral immune evasion. For example, VACV secretes a soluble homologue of the IFNγ receptor that binds to extracellular IFNγ and prevents activation of the cellular receptor. Another strategy employed by VACV is the expression of proteins that target innate immune signalling pathways yet bear no obvious homology to host cell proteins.

Recently, the structures of VACV immunomodulatory proteins N1, A52 and B14 were solved and found to possess a Bcl-2-like fold despite the lack of sequence homology to cellular proteins (Cooray et al., 2007; Graham et al., 2008). The modulation of innate immune signalling pathways by VACV proteins is complex, since related signalling pathways are both inhibited and activated by the virus. The complexities of VACV immune modulation are exemplified by the VACV protein A52.

A52 has at least two distinct functions in VACV immunomodulation: it inhibits TLR- and IL-1-induced NF-κB activation (Harte et al., 2003) and stimulates p38 and JNK MAPK activation (Maloney et al., 2005). The mechanism of A52 function is difficult to discern since the apparent contradictory effects of A52 are exerted upon common signalling pathways. A52 has been found to interact with over-expressed (Harte et al., 2003) and endogenous (Chapter 3) TRAF6 and IRAK2. The distinct function of A52 could be mediated via differential interactions with either TRAF6 or IRAK2.

A role for IRAK2 in NF-κB activation has recently been described (Keating et al., 2007). IRAK2 interacted with either the TIR adaptors Mal and MyD88 or directly to TLR3 and, following stimulation, dissociated from the receptor/adapter complex in order to activate TRAF6 (Keating et al., 2007). Further, IRAK2 induced ubiquitination of TRAF6 and this correlated with the activation of NF-κB by over-expressed IRAK2 (Keating et al., 2007). As previously described, deletion of the C-terminus of A52 (ΔA52) resulted in a loss of interaction with TRAF6 (Maloney et al., 2005). ΔA52 was still able to co-immunoprecipitate with IRAK2 and to inhibit IL-1R/TLR-induced NF-κB (Maloney et al., 2005). Thus, the inhibition of NF-κB by A52 is likely mediated by its interaction with IRAK2 (Maloney et al., 2005).

The stimulatory role of A52 on MAPK activation depends upon its ability to interact with TRAF6 (Maloney et al., 2005). In this thesis, a putative TRAF6 binding motif was identified in A52 and this motif was mutated. All of the mutants generated were able to inhibit NF-κB activation, consistent with an unaltered interaction with IRAK2. In contrast, one point mutant (F154A) and the deletion construct (ΔT6BM) were unable to activate MAPK. This highlighted the dual functionality of A52, since the NF-κB inhibitory function was maintained when the MAPK stimulatory role was abolished. Further, these studies identified a key residue involved in activation of MAPK by A52. Intriguingly, the A52 mutants were still able to co-immunoprecipitate with TRAF6, suggesting that the putative TRAF6 binding motif of A52 was not solely required for interaction with TRAF6. It is feasible that other residues of TRAF6 facilitate the interaction between TRAF6 and its binding partners (Zapata et al., 2007a). Thus, mutation of one (F154A) or a few (ΔT6BM) amino acids in the TRAF6 binding motif would be unlikely to be sufficient to impair the TRAF6-A52 interaction. However, the putative TRAF6 binding motif of A52, and particularly the F154 residue, appears to function as a switch to activate TRAF6-mediated MAPK activation. The A52-induced p38 activation correlates with induction of the anti-inflammatory cytokine IL-10 (Maloney et al., 2005). Since A52 induces MAPK in a TRAF6-dependent manner, it is likely that A52 modulates TRAF6 function to suppress the antiviral immune response. In addition to TRAF6, data presented herein showed that A52 co-immunoprecipitated with endogenous TRAF2 and TRAF3, thereby having the potential to exert a broader effect on TRAF-mediated innate immune signalling.

The need for TRAF6 in both the NF-κB and MAPK pathways makes it difficult to reconcile the contradictory effects of A52. While both functions of A52 lead to immune suppression, it is hard to see how A52 could both inhibit and activate TRAF6 to achieve this same objective. There are three possible solutions to this quandary. In the first, the temporal usage of TRAF6 may be targeted. Since A52 appeared to enhance TRAF6

auto-ubiquitination at early time points following stimulation, it is feasible that early TRAF6 auto-ubiquitination results in activation of pathways leading to MAPK activation. At later time points following IL-1 stimulation, A52 seemed to enhance the deubiquitination of TRAF6, possibly blocking NF-κB activation in the process. As mentioned above, over-expression of IRAK2 is known to induce TRAF6 ubiquitination and there is a correlation between IRAK2-induced TRAF6 ubiquitination and NF-κB activation (Keating et al., 2007). However, since the study investigated the function of an over-expressed protein, it was not possible to correlate kinetics of IRAK2-induced TRAF6 ubiquitination and NF-κB activation. Data presented in this thesis showed a subtle difference in the ability of wild-type A52 and of the loss-of-function mutants of A52 (F154A and ΔT6BM) to modulate TRAF6 ubiquitination. While the wild-type A52 shifted the kinetics of TRAF6 ubiquitination, this was not observed when the mutants were analysed in the same assay. The inability of the mutants to enhance early TRAF6 ubiquitination could correlate with their inability to drive MAPK activation. Thus it remains a possibility that the early induction of TRAF6 ubiquitination by A52 is required for MAPK activation. The interpretation of these results is impaired by the low level of ubiquitinated TRAF6 observed on the western blot. Although the same effect was observed a few times, it was difficult to detect TRAF6 ubiquitination when using only 0.25μg of the HA-ubiquitin construct and thus the assay might not be robust enough to support the above conclusion.

The second possible explanation for the contradictory roles of A52 has to do with the differential usage of the domains of TRAF6. Distinct signalling pathways from different stimuli (LPS and IL-1) and to different effects (NF-κB and MAPK activation) have been mapped to particular domains of TRAF6 (Kobayashi et al., 2001). LPS induced NF-κB activation required the second and third zinc fingers, while IL-1-induced NF-κB activation required the fourth and fifth zinc fingers (Kobayashi et al., 2001). Activation

of NF-κB by both LPS and IL-1 did not require the RING domain or first zinc finger of TRAF6 (Kobayashi et al., 2001). In contrast, full activation of p38 and JNK MAPK required both the RING domain and all of the zinc fingers of TRAF6 (Kobayashi et al., 2001). The TRAF domain was present intact in all of the constructs tested (Kobayashi et al., 2001) and thus the need for the TRAF domain in both protein-protein interactions (Zapata et al., 2006) and in auto-ubiquitination (Yang et al., 2004) was not examined. Since the RING domain of TRAF6 was required for TAK1 activation, it is tempting to speculate that TAK1 is need for MAPK and not NF-κB activation (see below). Given the role for the RING and zinc fingers in MAPK activation, it is possible that A52 could be acting on these domains of TRAF6 in order to activate MAPK. While previous work showed that the TRAF domain of TRAF6 had a dominant-negative effect on A52-induced MAPK activation (Maloney et al., 2005), it is possible that the negative effect is due to competitive inhibition of A52 binding to full-length TRAF6. While interaction with binding partners is mediated by the TRAF domain, the other domains of TRAF6 are required for signalling and thus any A52 bound to the TRAF domain alone would be unable to induce TRAF6-mediated signalling. It is feasible that that the inhibitory effect of A52 on IRAK2-induced NF-κB activation could be due to A52 blocking access to the specific zinc fingers of TRAF6 required to activate this pathway. It is worth noting that another group using similar methods have found that the RING and the first zinc finger were needed for IKK activation (Lamothe et al., 2008). There is confusion among different reports as to the functionality of the different domains of TRAF6 and the resolution of this matter would help with dissecting the effect of A52 on TRAF6.

The third potential resolution of the opposing effects of A52 on TRAF6 function has to do with recruitment of signalling molecules to TRAF6. There is substantial confusion in the literature with regards to the signalling molecules that are recruited to TRAF6 and required for activation of MAPK versus NF-κB. It has been found that TRAF6 is auto-

ubiquitinated and that this requires its RING domain and the E2 enzyme (Ubc13/UeV1A) (Wooff et al., 2004; Lamothe et al., 2007b). However, the interaction between the TRAF6 RING domain and Ubc13 was found to be weak, possibly due to the study of the RING domain in isolation from the rest of the TRAF6 protein (Mercier et al., 2007). However, it is possible that Ub13 is recruited to TRAF6 for K48-linked ubiquitination and degradation, not for signalling (Mercier et al., 2007). It is unknown what effect, if any, A52 has on the recruitment of E1 and E2 enzymes to TRAF6. Since A52 enhances IL-1-induced TRAF6 ubiquitination, it is possible that it recruits the E1 and E2 enzymes to TRAF6.

It is usually agreed that TRAF6 is ubiquitinated through K63-linked ubiquitin moieties for signal transduction and that it functions as an E3 ubiquitin ligase (Deng et al., 2000). Although there might be other substrates, TRAF6 has been found to ubiquitinate the regulatory IKKγ (or NEMO), thus highlighting the importance of TRAF6 E3 ligase activity in NF-κB activation (Chen, 2005). The ubiquitinated TRAF6 is recognised by proteins with ubiquitin binding domains, the TAK1 adaptor proteins (TABs). The TABs then recruit other signalling molecules including TAK1, which then mediate downstream signalling. TAK1 itself might be a substrate of TRAF6-catalysed ubiquitination (Wang et al., 2001). The confusion here is which TAB (TAB1, 2 or 3) is required in which signalling pathway, if at all. While a role for an interaction between TAK1 and TAB2/3 has been found to be required for TAK1-dependent activation of IKK and MAPK (Besse et al., 2007), other studies have found that it is TAK1 and not TAB1/2 that is required for signalling (Shim et al., 2005). While TAB2 was identified in one study as a critical adaptor molecule, linking TAK1 and TRAF6 association following IL-1 stimulation (Takaesu et al., 2000), another studied suggested that TAB2 was not required for IL-1-induced NF-κB or MAPK activation (Sanjo et al., 2003). If TAB2 is required as an adaptor linking ubiquitinated TRAF6 and TAK1, it likely functions by binding to the poly-ubiquitin

chains on TRAF6 via ubiquitin-binding CUE and zinc finger domains (Kanayama et al., 2004). TAB3 has been identified as a TAB2 homologue and the two are reported to be functionally redundant in TAK1 and NF-κB activation (Ishitani et al., 2003).

The activation of p38 activation can be modulated by different upstream activators and the formation of distinct signalling complexes (Lu et al., 2006). For example, TAB1 mediated MKK-independent p38 MAPK activation while it also inhibited MKK-dependent p38 activity (Lu et al., 2006). It was hypothesised that A52 could regulate the activation of p38 by recruiting downstream signalling molecules, such as TAB1. However, it was previously found that A52 does not interact with over-expressed TAB1 (Harte et al., 2003). Moreover, A52 disrupted the TRAF6/TAB1 complex (Harte et al., 2003). A weak interaction between A52 and over-expressed TAK1 had been found (Harte et al., 2003). Data presented in this thesis showed that A52 co-immunoprecipitated with endogenous TAK1 (Chapter 6). Furthermore, A52 co-immunoprecipitated with TAK1 in the absence of TRAF6, suggesting that TAK1 is another interaction partner of A52. Preliminary data suggests that A52 can bridge the interaction between TAK1 and TRAF6, thereby activating TAK1 in the absence of ligand stimulation. In this thesis, data has been presented to show a novel role for TAK1 in A52-induced p38 activation since this was inhibited by over-expression of a TAK1 dominant negative (K63W) construct. Thus, it is possible that A52 acts as an adaptor that recruits TAK1 to TRAF6 in order to activate p38, possibly without using the TAB proteins (Figure 7.1), and without stimulating NF-κB.

Finally, it is possible that there are distinct TAK1-dependent and TAK1-independent signalling pathways downstream of the IL-1R (Yao et al., 2007). The TAK1-dependent pathway involves IKKα/β phosphorylation and IKKβ activation, resulting in IκBα phosphorylation and degradation (Yao et al., 2007). In contrast, TAK1-independent NF-

κB activation involves MEKK3-dependent IKKγ phosphorylation and IKKα activation, leading to IκBα phosphorylation but not degradation (Yao et al., 2007). While the TAK1-dependent pathway involved the recruitment of the TAB proteins, the TAK1-independent pathway did not require the TABs (Yao et al., 2007). This is supported by another study that showed that TAK1 was an upstream kinase activating IKKβ and JNK but not IKKα in response to TNF, IL-1 and TLR stimulation in MEFs (Shim et al., 2005). Although A52 has been found to interact with TAK1, whether this interaction is required for one of the functions of A52 is not known. It could be that A52 interacts with TAK1 in order to more effectively inhibit NF-κB. The role for the other MAP3K, MEKK3, in A52-induced MAPK activation was not examined.

Interestingly, there is one example of a cellular protein with similar effects on signalling to A52: under conditions of osmotic stress, TAO2 inhibits TAK1-induced NF-κB and activates MAPK (Huangfu et al., 2006). This suggests that modulation of TAK1 signalling by endogenous signalling molecules can turn off one pathway (NF-κB activation) while turning on another one (JNK activation). If distinct complexes of signalling molecules are involved in NF-κB and MAPK signalling downstream of IL-1R/TLRs, then A52 could modulate recruitment of the molecules in order activate MAPK whilst inhibiting NF-κB activation at the level of IRAK2.

In addition to examining how A52 modulates TRAF6 function, A52 itself was studied. A52 was found to oligomerise and it is possible that oligomerisation is required for function. The F154A mutant of A52 also appeared to dimerise, suggesting that F154 is not a critical residue for dimerisation. It would be interesting to mutate residues at the dimer interface and determine if A52 can still function in its monomeric form. It was hypothesised that since TRAF6 is an E3 ubiquitin ligase, association of A52 with TRAF6 would result in A52 ubiquitination. Indeed, over-expressed A52 was found to be

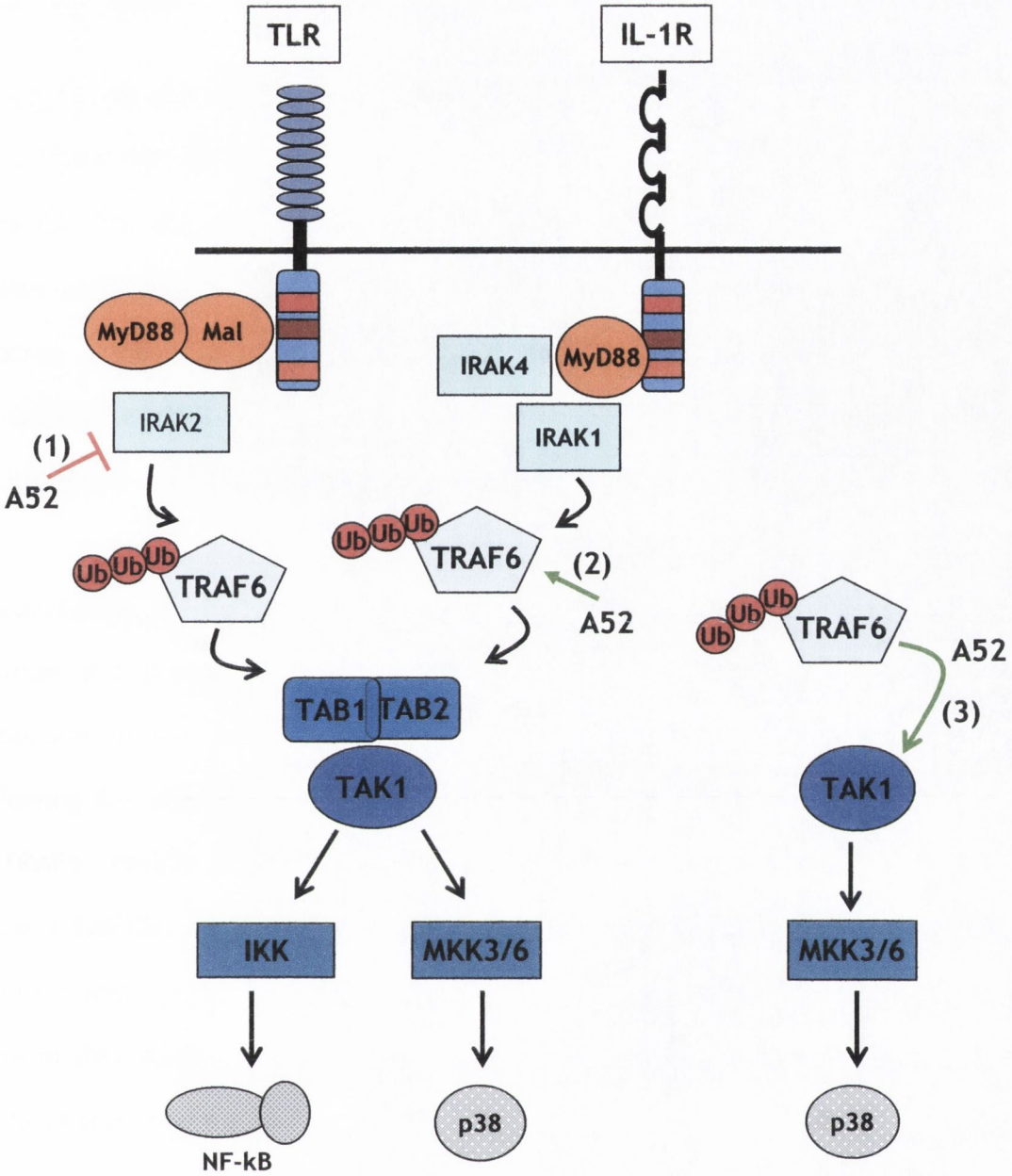

Figure 7.1 Model of A52-mediated MAPK activation and NF-κB inhibition

TLR-induced NF-κB activation occurs via recruitment of IRAK2 and subsequent ubiquitination and activation of TRAF6. Activated TRAF6 recruits the TAB1/2 and TAK1 complex, which then activates IKK and MKK3/6, leading to activation of NF-κB and p38, respectively. The same pathway is likely used by IL-1R. A52 inhibits IL-1R/TLR-induced NF-κB (1) and enhances IL-1-induced p38 activation (2). A52 also stimulates p38 activation in the absence of ligand stimulation, possibly by uncoupling regulation of TRAF6/TAK1 association from the IL-1R/TLR and the IRAKs (3).

ubiquitinated and this was not observed in TRAF6 deficient MEFs. This suggests that A52 is ubiquitinated by TRAF6 but the function of this modification is not yet known. It is possible that A52 acts as a pseudo-substrate for TRAF6 ubiquitination since this would presumably prevent ubiquitination of normal substrates and thereby block TRAF6 function. This idea does not fit with a model of A52 binding to IRAK2 to mediate its inhibitory function. However, it could be that A52 ubiquitination has a positive role in facilitating the TRAF6/TAK1 interaction, though this remains to be tested.

In conclusion, the stimulatory effect of A52 on MAPK activation was mapped to the F154 residue of a putative TRAF6 binding motif in A52. This motif was also found to be important in the ability of A52 to accelerate the kinetics of TRAF6 ubiquitination following IL-1 stimulation since the F154A mutant did not alter the ubiquitination status of TRAF6. Finally, a novel role for TAK1 in A52-induced MAPK activation was identified since a TAK1DN construct was able to inhibit A52-induced MAPK. Further, A52 could interact with TAK1 and might induce the association of TAK1 and TRAF6. Thus, the work in this thesis has provided insight into the mechanism by which A52 can activate MAPK in the absence of ligand stimulation. Research presented herein has suggested a number of other questions that could be addressed in the future:

1. TRAF6 oligomerisation

The role for TRAF6 oligomerisation in signalling is not clear. Although there are reports of TRAF6 being ubiquitinated, they are usually based on chimeric proteins that are artificially induced to oligomerise (Wang et al., 2001; Baud et al., 1999). Attempts to investigate TRAF6 oligomerisation by native PAGE were not successful (Chapter 6). Gel filtration could be used to analyse TRAF6 oligomerisation following IL-1 stimulation or A52 over-expression. In addition, it would be interesting to confirm whether oligomerisation is required for ubiquitination of TRAF6.

2. A52-induced ubiquitination of TRAF6

Since A52 has been found to enhance TRAF6 ubiquitination at early time points following IL-1 stimulation, it is feasible that A52 induces TRAF6 ubiquitination on its own. Given the technical difficulties inherent in the studies of ubiquitination, it could be that this is below detection levels. Detection of endogenous ubiquitination has not been successful (Chapter 4) but could be more fruitful with better ubiquitin antibodies. Another method that could be attempted is the *in vitro* ubiquitination of TRAF6 in the presence or absence of A52. In addition, although it has been shown that ubiquitination of TRAF6 is typically through K63 linkages (Wang et al., 2001), it is not known if A52 induces K63- or K48-linked TRAF6 ubiquitination. HA-ubiquitin with mutated lysine residues (K63R, K48R) could be used in immunoprecipitation experiments in order to determine which linkage is present. Alternatively, antibodies that were raised against either K48- or K63-linked ubiquitination could be used if they become commercially available (Newton et al., 2008).

3. Ubiquitination of A52

The ubiquitination of A52 was not observed in TRAF6$^{-/-}$ MEFs, suggesting that TRAF6 is responsible for conjugating ubiquitin chains onto A52. However, the result is indirect and *in vitro* ubiquitination assays could be used to determine that it is TRAF6 that conjugates the ubiquitin chains onto A52. Since there is no evidence of A52 degradation following ubiquitination, it is likely that the ubiquitination of A52 is K63-linked. This could be examined as described above for TRAF6.

4. TAK1 recruitment and activation

Although TAK1 is presumed to be recruited to ubiquitinated TRAF6 by the adaptor proteins TAB1, TAB2 and TAB3, there is considerable confusion about which proteins are

recruited to TRAF6 following ligand stimulation. The evidence of many different studies suggests that there are cell-type and ligand specific differences in the complex that is formed. In order to determine if TAB1, TAB2 and TAB3 are needed for A52 to recruit TAK1 to TRAF6, the co-immunoprecipitation could be performed in MEFs lacking one or all of the TABs, if these cells exist. Alternatively, siRNA to the TABs could be used. Preliminary data presented in this thesis suggested that A52 might be able to act as an adaptor, bringing TAK1 and TRAF6 together in the absence of ligand stimulation (Chapter 6). The model in Figure 7.1 suggests that A52 can act directly on TRAF6 and TAK1 to bring them into association, like a TAB protein uncoupled to ligand stimulation. To determine if inducing this association is important in A52-induced MAPK activation, the assay will be repeated with both wild-type and mutant A52. The role for TRAF6 ubiquitination in this process is unclear since it is not known if A52 can induce TRAF6 ubiquitination in the absence of IL-1 stimulation. If so, then A52 could bring TAK1 into association with TRAF6 in order for TAK1 to be ubiquitinated. In order to investigate this, TAK1 ubiquitination in response to A52 over-expression in $TRAF6^{+/+}$ and $TRAF6^{-/-}$ MEFs could be examined. These further studies should help elucidate the mechanism by which TRAF6 can activate MAPK by clarifying the signalling molecules involved in the pathway and also provide more insight into the mechanism of action of A52 on TRAF6-mediated MAPK activation.

Chapter Eight: References

Akira, S., K. Takeda, et al. (2001). Toll-like receptors: critical proteins linking innate and acquired immunity. Nat. Immunol. **2**(8): 675-680.

Akira, S. and Takeda, K. (2004) Toll-like receptor signalling. Nat. Rev. Immunol., **4**: 499-511.

Akira, S., Uematsu, S. and Takeuchi, O. (2006) Pathogen Recognition and Innate Immunity. Cell, **124**: 783-801.

Alexopoulou, L., A. C. Holt, et al. (2001). Recognition of double-stranded RNA and activation of NF-κB by Toll-like receptor 3. Nature **413** (6857): 732-738.

Alff, P. J., I. N. Gavrilovskaya, et al. (2006). The Pathogenic NY-1 Hantavirus G1 Cytoplasmic Tail Inhibits RIG-I- and TBK-1-Directed Interferon Responses. J. Virol. **80** (19): 9676-9686.

Arch, R.H., Gedrich, R.W. and Thompson, C.B. (1998) Tumor necrosis factor receptor-associated factors (TRAFs)--a family of adapter proteins that regulates life and death. Genes. Dev. **12**: 2821-2830.

Arch, R.H., Gedrich, R.W. and Thompson, C.B. (2000) Translocation of TRAF proteins regulates apoptotic threshold of cells. Biochem. Biophys. Res. Commun. **272**: 936-945.

Ardila-Osorio, H., C. Pioche-Durieu, et al. (2005). TRAF interactions with raft-like buoyant complexes, better than TRAF rates of degradation, differentiate signaling by CD40 and EBV latent membrane protein 1. Int. J. Cancer **113**(2): 267-75.

Ashwell, J. D. (2006). The many paths to p38 mitogen-activated protein kinase activation in the immune system. Nat. Rev. Immunol. **6**(7): 532-40.

Assarsson, E., J. A. Greenbaum, et al. (2008). Kinetic analysis of a complete poxvirus transcriptome reveals an immediate-early class of genes. Proc. Natl. Acad. Sci. U.S.A. **105** (6): 2140-5.

Banerjee, A. and R. C. Wade (2002). Elusive recognition determinants for ubiquitination. J. Mol. Recognit. **15** (1): 3-5.

Banerjee, A., Gugasyan, R., McMahon, M. and Gerondakis, S. (2006) Diverse Toll-like receptors utilize Tpl2 to activate extracellular signal-regulated kinase (ERK) in hemopoietic cells. Proc. Natl. Acad. Sci. U.S.A. **103**: 3274-3279.

Bartlett, N., Symons, J.A., Tscharke, D.C. and Smith, G.L. (2002) The vaccinia virus N1L protein is an intracellular homodimer that promotes virulence. J. Gen. Virol. **83**: 1965-1976.

Bartlett, N.W., Dumoutier, L., Renauld, J.C., Kotenko, S.V., McVey, C.E., Lee, H.J. and Smith, G.L. (2004) A new member of the interleukin 10-related cytokine family encoded by a poxvirus. J. Gen. Virol. **85**: 1401-1412.

Barton, E. S., D. W. White, et al. (2007). Herpesvirus latency confers symbiotic protection from bacterial infection. Nature **447**(7142): 326-9.

Baud, V. r., Z.-G. Liu, et al. (1999). Signaling by proinflammatory cytokines: oligomerization of TRAF2 and TRAF6 is sufficient for JNK and IKK activation and target gene induction via an amino-terminal effector domain. Genes & Development **13**(10): 1297-1308.

Beignon, A. S., K. McKenna, et al. (2005). Endocytosis of HIV-1 activates plasmacytoid dendritic cells via Toll-like receptor-viral RNA interactions. J. Clin. Invest., **115** (11): 3265-75.

Bell, J. K., J. Askins, et al. (2006). The dsRNA binding site of human Toll-like receptor 3. Proceedings of the National Academy of Sciences **103**(23): 8792-8797.

Besse, A., B. Lamothe, et al. (2007). TAK1-dependent signaling requires functional interaction with TAB2/TAB3. J. Biol. Chem. **282** (6): 3918-28.

Beutler, B. (2004) Inferences, questions and possibilities in Toll-like receptor signalling. Nature, **430**: 257-263.

Bidère, N., A. L. Snow, et al. (2006). Caspase-8 Regulation by Direct Interaction with TRAF6 in T Cell Receptor-Induced NF-κB Activation. Current Biology **16**(16): 1666-1671.

Bisht, H., A. S. Weisberg, et al. (2008). Vaccinia virus l1 protein is required for cell entry and membrane fusion. J. Virol. **82**(17): 8687-94.

Boehme, K.W. and Compton, T. (2004) Innate sensing of viruses by toll-like receptors. J. Virol. **78**: 7867-7873.

Borden, K.L. (2000) RING domains: master builders of molecular scaffolds? J. Mol. Biol., **295**: 1103-1112.

Bowie, A., Kiss-Toth, E., Symons, J.A., Smith, G.L., Dower, S.K. and O'Neill, L.A. (2000) A46R and A52R from vaccinia virus are antagonists of host IL-1 and toll-like receptor signaling. Proc. Natl. Acad. Sci. U.S.A. **97**: 10162-10167.

Bowie, A.G. and Haga, I.R. (2005) The role of Toll-like receptors in the host response to viruses. Mol. Immunol. **42**: 859-867.

Bradley, J. R. and J. S. Pober (2001). Tumor necrosis factor receptor-associated factors (TRAFs). Oncogene **20**(44): 6482-91.

Broyles, S.S. (2003) Vaccinia virus transcription. J. Gen. Virol. **84**: 2293-2303.

Bryson, K., L. J. McGuffin, et al. (2005). Protein structure prediction servers at University College London. Nucl. Acids Res. **33**(suppl_2): W36-38.

Burns, K., S. Janssens, et al. (2003). Inhibition of Interleukin 1 Receptor/Toll-like Receptor Signaling through the Alternatively Spliced, Short Form of MyD88 Is Due to Its Failure to Recruit IRAK-4. J. Exp. Med. **197**(2): 263-268.

Butler, M.P. Hanly, J.A. and Moynagh, P.N. (2007) Kinase-active interleukin-1 receptor associated kinases promote polyubiquitination and degradation of the pellino family: direct evidence for pellino proteins being ubiquitin-protein isopeptide ligases. J. Biol. Chem. **282**: 29729-29737.

Buwitt-Beckmann, U., H. Heine, et al. (2006). TLR1- and TLR6-independent Recognition of Bacterial Lipopeptides. J. Biol. Chem. **281**(14): 9049-9057.

Carter, G.C., Law, M., Hollinshead, M. and Smith, G.L. (2005) Entry of the vaccinia virus intracellular mature virion and its interactions with glycosaminoglycans. J. Gen. Virol. 86, 1279-1290.

Carty, M., R. Goodbody, et al. (2006). The human adaptor SARM negatively regulates adaptor protein TRIF-dependent Toll-like receptor signaling. Nat. Immunol. **7**(10): 1074-1081.

Cao, Z., J. Xiong, et al. (1996). TRAF6 is a signal transducer for interleukin-1. Nature **383**(6599): 443-446.

Chen, Z.J. (2005) Ubiquitin signalling in the NF-kappaB pathway. Nat. Cell Biol. 7, 758-765.

Chen, L., W. Dong, et al. (2008). Protein phosphatase 4 negatively regulates LPS cascade by inhibiting ubiquitination of TRAF6. FEBS Lett. **582**(19): 2843-9.

Choe, J., M. S. Kelker, et al. (2005). Crystal Structure of Human Toll-Like Receptor 3 (TLR3) Ectodomain. Science 309(5734): 581-585.

Chuang, T.-H. and R. J. Ulevitch (2004). Triad3A, an E3 ubiquitin-protein ligase regulating Toll-like receptors. Nat. Immunol. **5** (5): 495-502.

Chung, J.Y., Park, Y.C., Ye, H. and Wu, H. (2002) All TRAFs are not created equal: common and distinct molecular mechanisms of TRAF-mediated signal transduction. J. Cell Sci. 115, 679-688.

Chung, Y.-H., N.-h. Cho, et al. (2004). Activation of Stat3 Transcription Factor by Herpesvirus Saimiri STP-A Oncoprotein. J. Virol. **78**(12): 6489-6497.

Chung, J. Y., M. Lu, et al. (2007a). Molecular basis for the unique specificity of TRAF6. Adv. Exp. Med. Biol. **597**: 122-30.

Chung, Y. H., B. H. Jhun, et al. (2007b). STP-C, an oncoprotein of herpesvirus saimiri augments the activation of NF-κB through ubiquitination of TRAF6. J. Biochem. Mol. Biol. **40**(3): 341-8.

Claros, M.G. and von Heijne, G. (1994) TopPred II: an improved software for membrane protein structure predictions. Comput. Appl. Biosci. 10, 685-686.

Conze, D. B., C.-J. Wu, et al. (2008). Lys63-Linked Polyubiquitination of IRAK-1 Is Required for Interleukin-1 Receptor- and Toll-Like Receptor-Mediated NF-κB Activation. Mol. Cell. Biol. **28**(10): 3538-3547.

Cooray, S., M. W. Bahar, et al. (2007). Functional and structural studies of the vaccinia virus virulence factor N1 reveal a Bcl-2-like anti-apoptotic protein. J. Gen. Virol. **88** (Pt 6): 1656-66.

Dadgostar, H. and G. Cheng (2000). Membrane localization of TRAF 3 enables JNK activation. J. Biol. Chem. **275**(4): 2539-44.

Darnay, B.G., Ni, J., Moore, P.A. and Aggarwal, B.B. (1999) Activation of NF-kappaB by RANK requires tumor necrosis factor receptor-associated factor (TRAF) 6 and NF-kappaB-inducing kinase. Identification of a novel TRAF6 interaction motif. J. Biol. Chem. **274**: 7724-7731.

Darnay, B. G., A. Besse, et al. (2007). TRAFs in RANK signaling. Adv. Exp. Med. Biol. **597**: 152-9.

Davidson, D. J., A. J. Currie, et al. (2006). IRAK-4 Mutation (Q293X): Rapid Detection and Characterization of Defective Post-Transcriptional TLR/IL-1R Responses in Human Myeloid and Non-Myeloid Cells. J. Immunol. **177**(11): 8202-8211.

Davies, C.C., Mak, T.W., Young, L.S. and Eliopoulos, A.G. (2005) TRAF6 is required for TRAF2-dependent CD40 signal transduction in nonhemopoietic cells. Mol. Cell Biol. **25**: 9806-9819.

de Bouteiller, O., E. Merck, et al. (2005). Recognition of Double-stranded RNA by Human Toll-like Receptor 3 and Downstream Receptor Signaling Requires Multimerization and an Acidic pH. J. Biol. Chem. **280**(46): 38133-38145.

Deng, L., Wang, C., Spencer, E., Yang, L., Braun, A., You, J., Slaughter, C., Pickart, C. and Chen, Z.J. (2000) Activation of the IκB kinase complex by TRAF6 requires a dimeric ubiquitin-conjugating enzyme complex and a unique polyubiquitin chain. Cell **103**: 351-361.

Deng, L., P. Dai, et al. (2008). Vaccinia virus subverts a mitochondrial antiviral signaling protein-dependent innate immune response in keratinocytes through its double-stranded RNA binding protein, E3. J. Virol. **82**(21): 10735-46.

Di Fiore, P. P., S. Polo, et al. (2003). When ubiquitin meets ubiquitin receptors: a signalling connection. Nat. Rev. Mol. Cell Biol. **4**(6): 491-497.

DiPerna, G., Stack, J., Bowie, A.G., Boyd, A., Kotwal, G., Zhang, Z., Arvikar, S., Latz, E., Fitzgerald, K.A. and Marshall, W.L. (2004) Poxvirus protein N1L targets the I-kappaB kinase complex, inhibits signaling to NF-κB by the tumor necrosis factor superfamily of receptors, and inhibits NF-κB and IRF3 signaling by toll-like receptors. J. Biol. Chem. **279**: 36570-36578.

Doyle S, Vaidya S, O'Connell R, Dadgostar H, Dempsey P, Wu T, Rao G, Sun R, Haberland M, Modlin R, Cheng G. (2002). IRF3 mediates a TLR3/TLR4-specific antiviral gene program. Immunity **17**(3):251-63.

Ea, C. K., L. Sun, et al. (2004). TIFA activates IκB kinase (IKK) by promoting oligomerization and ubiquitination of TRAF6. Proc. Natl. Acad. Sci. U.S.A. **101**(43): 15318-23.

Eliopoulos, A.G., Wang, C.C., Dumitru, C.D. and Tsichlis, P.N. (2003) Tpl2 transduces CD40 and TNF signals that activate ERK and regulates IgE induction by CD40. Embo J. **22**: 3855-3864.

Equils, O., E. Faure, et al. (2001). Bacterial Lipopolysaccharide Activates HIV Long Terminal Repeat Through Toll-Like Receptor 4. J Immunol. **166**(4): 2342-2347.

Equils, O., M. L. Schito, et al. (2003). Toll-Like Receptor 2 (TLR2) and TLR9 Signaling Results in HIV-Long Terminal Repeat Trans-Activation and HIV Replication in HIV-1 Transgenic Mouse Spleen Cells: Implications of Simultaneous Activation of TLRs on HIV Replication. J. Immunol. **170**(10): 5159-5164.

Ermolaeva, M. A., M.-C. Michallet, et al. (2008). Function of TRADD in tumor necrosis factor receptor 1 signaling and in TRIF-dependent inflammatory responses. Nat. Immunol. 9(9): 1037-1046.

Falquet, L., Pagni, M., Bucher, P., Hulo, N., Sigrist, C.J., Hofmann, K. and Bairoch, A. (2002) The PROSITE database, its status in 2002. Nucleic Acids Res. **30**: 235-238.

Fang, S. and A. M. Weissman (2004). A field guide to ubiquitylation. Cell Mol. Life Sci. **61**(13): 1546-61.

Finlay, B.B. and McFadden, G. (2006) Anti-immunology: evasion of the host immune system by bacterial and viral pathogens. Cell **124**: 767-782.

Fitzgerald, K.A., Palsson-McDermott, E.M., Bowie, A.G., Jefferies, C.A., Mansell, A.S., Brady, G., Brint, E., Dunne, A., Gray, P., Harte, M.T., McMurray, D., Smith, D.E., Sims, J.E., Bird, T.A. and O'Neill, L.A. (2001) Mal (MyD88-adapter-like) is required for Toll-like receptor-4 signal transduction. Nature **413**: 78-83.

Fitzgerald, K. A., D. C. Rowe, et al. (2003). LPS-TLR4 Signaling to IRF-3/7 and NF-κB Involves the Toll Adapters TRAM and TRIF. J. Exp. Med. **198**(7): 1043-1055.

Fukushima, T., S. Matsuzawa, et al. (2007). Ubiquitin-conjugating enzyme Ubc13 is a critical component of TNF receptor-associated factor (TRAF)-mediated inflammatory responses. Proc. Natl. Acad. Sci. U.S.A. **104**(15): 6371-6.

Garcia, M. I., J. Kaserman, et al. (2007). Herpesvirus Saimiri STP-A Oncoprotein Utilizes Src Family Protein Tyrosine Kinase and Tumor Necrosis Factor Receptor-Associated Factors To Elicit Cellular Signal Transduction. J. Virol. **81**(6): 2663-2674.

Gasteiger, E., Gattiker, A., Hoogland, C., Ivanyi, I., Appel, R.D. and Bairoch, A. (2003) ExPASy: The proteomics server for in-depth protein knowledge and analysis. Nucleic Acids Res. **31**: 3784-3788.

Gedey, R., X. L. Jin, et al. (2006). Poxviral regulation of the host NF-κB response: the vaccinia virus M2L protein inhibits induction of NF-κB activation via an ERK2 pathway in virus-infected human embryonic kidney cells. J. Virol. **80**(17): 8676-85.

Gee, K., J. B. Angel, et al. (2007). IL-10 regulation by HIV-Tat in primary human monocytic cells: involvement of calmodulin/calmodulin-dependent protein kinase-activated p38 MAPK and Sp-1 and CREB-1 transcription factors. J. Immunol. **178**(2): 798-807.

Geetha, T. and Wooten, M.W. (2002) Structure and functional properties of the ubiquitin binding protein p62. FEBS Lett. 512, 19-24.

Geetha, T., Kenchappa, R.S., Wooten, M.W. and Carter, B.D. (2005) TRAF6-mediated ubiquitination regulates nuclear translocation of NRIF, the p75 receptor interactor. Embo J. **24**: 3859-3868.

Gilliet, M., W. Cao, et al. (2008). Plasmacytoid dendritic cells: sensing nucleic acids in viral infection and autoimmune diseases. Nat. Rev. Immunol. **8**(8): 594-606.

Girgis, N. M., B. C. Dehaven, et al. (2008). Cell surface expression of the vaccinia virus complement control protein is mediated by interaction with the viral A56 protein and protects infected cells from complement attack. J. Virol. **82**(9): 4205-14.

Gohda, J., Matsumura, T. and Inoue, J. (2004) Cutting edge: TNFR-associated factor (TRAF) 6 is essential for MyD88-dependent pathway but not toll/IL-1 receptor domain-containing adaptor-inducing IFN-beta (TRIF)-dependent pathway in TLR signaling. J. Immunol. **173**: 2913-2917.

Gottipati, P., T. N. Cassel, et al. (2008). Transcription-Associated Recombination Is Dependent on Replication in Mammalian Cells. Mol. Cell. Biol. **28**(1): 154-164.

Graham, S. C., M. W. Bahar, et al. (2008). Vaccinia virus proteins A52 and B14 Share a Bcl-2-like fold but have evolved to inhibit NF-κB rather than apoptosis. PLoS Pathog. **4** (8): e1000128.

Gray, P., A. Dunne, et al. (2006). MyD88 Adapter-like (Mal) Is Phosphorylated by Bruton's Tyrosine Kinase during TLR2 and TLR4 Signal Transduction. J. Biol. Chem. **281**(15): 10489-10495.

Guasparri, I., Wu, H. and Cesarman, E. (2006) The KSHV oncoprotein vFLIP contains a TRAF-interacting motif and requires TRAF2 and TRAF3 for signalling. EMBO Rep. **7**: 114-119.

Gubser, C., D. Bergamaschi, et al. (2007). A new inhibitor of apoptosis from vaccinia virus and eukaryotes. PLoS Pathog. **3** (2): e17.

Haas, T., J. Metzger, et al. (2008). The DNA Sugar Backbone 2' Deoxyribose Determines Toll-like Receptor 9 Activation. Immunity **28**(3): 315-323.

Habelhah, H., Takahashi, S., Cho, S.G., Kadoya, T., Watanabe, T. and Ronai, Z. (2004) Ubiquitination and translocation of TRAF2 is required for activation of JNK but not of p38 or NF-kappaB. Embo J. **23**: 322-332.

Habjan, M., I. Andersson, et al. (2008). Processing of genome 5' termini as a strategy of negative-strand RNA viruses to avoid RIG-I-dependent interferon induction. PLoS ONE **3** (4): e2032.

Hacker, H., Redecke, V., Blagoev, B., Kratchmarova, I., Hsu, L.C., Wang, G.G., Kamps, M.P., Raz, E., Wagner, H., Hacker, G., Mann, M. and Karin, M. (2006) Specificity in Toll-like receptor signalling through distinct effector functions of TRAF3 and TRAF6. Nature, 439: 204-207.

Haglund, K. and I. Dikic (2005). Ubiquitylation and cell signaling. Embo J. **24** (19): 3353-9.

Harte, M.T., Haga, I.R., Maloney, G., Gray, P., Reading, P.C., Bartlett, N.W., Smith, G.L., Bowie, A. and O'Neill, L.A. (2003) The poxvirus protein A52R targets Toll-like receptor signaling complexes to suppress host defense. J. Exp. Med. **197**: 343-351.

Hauer, J., Puschner, S., Ramakrishnan, P., Simon, U., Bongers, M., Federle, C. and Engelmann, H. (2005) TNF receptor (TNFR)-associated factor (TRAF) 3 serves as an inhibitor of TRAF2/5-mediated activation of the noncanonical NF-κB pathway by TRAF-binding TNFRs. Proc. Natl. Acad. Sci. U.S.A. **102**: 2874-2879.

Hasan, U., C. Chaffois, et al. (2005). Human TLR10 Is a Functional Receptor, Expressed by B Cells and Plasmacytoid Dendritic Cells, Which Activates Gene Transcription through MyD88. J. Immunol. **174**(5): 2942-2950.

Heinemann, S., B. Biesinger, et al. (2006). NF-κB signaling is induced by the oncoprotein Tio through direct interaction with TRAF6. J. Biol. Chem. **281**(13): 8565-72.

Hemmi, H., O. Takeuchi, et al. (2004). The Roles of Two IκB Kinase-related Kinases in Lipopolysaccharide and Double Stranded RNA Signaling and Viral Infection. J. Exp. Med. **199**(12): 1641-1650.

Heuser, J. (2005) Deep-etch EM reveals that the early poxvirus envelope is a single membrane bilayer stabilized by a geodetic "honeycomb" surface coat. J. Cell Biol. **169**: 269-283.

Hiscott, J., Lin, R., Nakhaei, P. and Paz, S. (2006) MasterCARD: a priceless link to innate immunity. Trends Mol. Med. **12**: 53-56.

Hoebe, K., Janssen, E. and Beutler, B. (2004) The interface between innate and adaptive immunity. Nat. Immunol. **5**: 971-974.

Hofmann, K. and Stoffel, W. (1993) TMbase - A database of membrane-spanning protein segments. Bio. Chem. Hoppe-Seyler, 34, 166.

Honda, K., Yanai, H., Mizutani, T., Negishi, H., Shimada, N., Suzuki, N., Ohba, Y., Takaoka, A., Yeh, W.C. and Taniguchi, T. (2004) Role of a transductional-transcriptional processor complex involving MyD88 and IRF-7 in Toll-like receptor signaling. Proc. Natl. Acad. Sci. U.S.A. **101**: 15416-15421.

Honda, K., Ohba, Y., Yanai, H., Negishi, H., Mizutani, T., Takaoka, A., Taya, C. and Taniguchi, T. (2005) Spatiotemporal regulation of MyD88-IRF-7 signalling for robust type-I interferon induction. Nature **434**: 1035-1040.

Horng, T., Barton, G.M. and Medzhitov, R. (2001) TIRAP: an adapter molecule in the Toll signaling pathway. Nat. Immunol. **2**: 835-841.

Hornung, V., J. Ellegast, et al. (2006). 5'-Triphosphate RNA is the ligand for RIG-I. Science **314** (5801): 994-7.

Howell, M. D., R. L. Gallo, et al. (2006). Cytokine milieu of atopic dermatitis skin subverts the innate immune response to vaccinia virus. Immunity **24**(3): 341-8.

Hu, H.M., O'Rourke, K., Boguski, M.S. and Dixit, V.M. (1994) A novel RING finger protein interacts with the cytoplasmic domain of CD40. J. Biol. Chem. **269**:30069-30072.

Huangfu, W. C., E. Omori, et al. (2006). Osmotic stress activates the TAK1-JNK pathway while blocking TAK1-mediated NF-κB activation: TAO2 regulates TAK1 pathways. J. Biol. Chem. **281**(39): 28802-10.

Hutchens, M. A., K. E. Luker, et al. (2008). Protective effect of Toll-like receptor 4 in pulmonary vaccinia infection. PLoS Pathog. **4** (9): e1000153.

Inoue, J., T. Ishida, et al. (2000). "Tumor necrosis factor receptor-associated factor (TRAF) family: adapter proteins that mediate cytokine signaling." Exp. Cell. Res., **254** (1): 14-24.

Ishida, T., Mizushima, S., Azuma, S., Kobayashi, N., Tojo, T., Suzuki, K., Aizawa, S., Watanabe, T., Mosialos, G., Kieff, E., Yamamoto, T. and Inoue, J. (1996) Identification of TRAF6, a novel tumor necrosis factor receptor-associated factor protein that mediates signaling from an amino-terminal domain of the CD40 cytoplasmic region. J. Biol. Chem. **271**: 28745-28748.

Ishii, K.J., Coban, C. and Akira, S. (2005) Manifold mechanisms of toll-like receptor-ligand recognition. J. Clin. Immunol. **25**: 511-521.

Ishii, K. J., C. Coban, et al. (2006). A Toll-like receptor-independent antiviral response induced by double-stranded B-form DNA. Nat. Immunol., **7**(1): 40-8.

Ishii, K. J. and S. Akira (2008). Potential link between the immune system and metabolism of nucleic acids. Curr. Opin. Immunol. **20**(5): 524-9.

Ishitani, T., G. Takaesu, et al. (2003). Role of the TAB2-related protein TAB3 in IL-1 and TNF signaling. Embo J. **22**(23): 6277-88.

Iwamura, T., Yoneyama, M., Yamaguchi, K., et al., (2001). Induction of IRF-3/-7 kinase and NF-κB in response to double-stranded RNA and virus infection: common and unique pathways. Genes to Cells **6**(4): 375-388.

Jackson, R. J., A. J. Ramsay, et al. (2001). Expression of mouse interleukin-4 by a recombinant ectromelia virus suppresses cytolytic lymphocyte responses and overcomes genetic resistance to mousepox. J. Virol. **75**(3): 1205-10.

Jackson, S.S., Ilyinskii, P., Philippon, V., Gritz, L., Yafal, A.G., Zinnack, K., Beaudry, K.R., Manson, K.H., Lifton, M.A., Kuroda, M.J., Letvin, N.L., Mazzara, G.P. and Panicali, D.L. (2005) Role of genes that modulate host immune responses in the immunogenicity and pathogenicity of vaccinia virus. **J. Virol. 79**: 6554-6559.

Jadhav, T., T. Geetha, et al. (2008). Identification of a consensus site for TRAF6/p62 polyubiquitination. Biochem. Biophys. Res. Commun. **371**(3): 521-4.

Janssens, S., K. Burns, et al. (2002). Regulation of Interleukin-1- and Lipopolysaccharide-Induced NF-κB Activation by Alternative Splicing of MyD88. Current Biology **12**(6): 467-471.

Janssens, S. and Beyaert, R. (2003). Functional diversity and regulation of different interleukin-1 receptor-associated kinase (IRAK) family members. Mol. Cell. **11** (2): 293-302.

Jefferies, C.A. and Fitzgerald, K.A. (2005) Interferon gene regulation: not all roads lead to Tolls. Trends Mol. Med. **11**: 403-411.

Jensen, L.E. and Whitehead, A.S. (2003) Ubiquitin activated tumor necrosis factor receptor associated factor-6 (TRAF6) is recycled via deubiquitination. FEBS Lett. 553: 190-194.

Jiang, Z., M. Zamanian-Daryoush, et al. (2003a). Poly(dI:dC)-induced Toll-like Receptor 3 (TLR3)-mediated Activation of NF-κB and MAP Kinase Is through an Interleukin-1 Receptor-associated Kinase (IRAK)-independent Pathway Employing the Signaling Components TLR3-TRAF6-TAK1-TAB2-PKR. J. Biol. Chem. **278**(19): 16713-16719.

Jiang, Z., Johnson, H.J., Nie, H., Qin, J., Bird, T.A. and Li, X. (2003b).Pellino 1 is required for interleukin-1-mediated signalling through its interaction with the IL-1 receptor-associated kinase 4 (IRAK4)-IRAK-tumour necrosis factor receptor-associated factor 6 (TRAF6) complex. J. Biol. Chem. 278 (13): 10952-10956.

Jin, H. and R. M. Elliott (1993). Non-viral sequences at the 5' ends of Dugbe nairovirus S mRNAs. J. Gen. Virol. **74**(10): 2293-2297.

Jin, M. S., S. E. Kim, et al. (2007). Crystal Structure of the TLR1-TLR2 Heterodimer Induced by Binding of a Tri-Acylated Lipopeptide. Cell **130**(6): 1071-1082.

Johnson, C.L. and Gale, M., Jr. (2006) CARD games between virus and host get a new player. Trends Immunol. **27**: 1-4.

Johnston, J.B. and McFadden, G. (2005) Immunomodulation by poxviruses. Chapter 8 in Modulation of Host Gene Expression and Innate Immunity by Viruses, Ed. Peter Palese. Springer: Dordrecht, The Netherlands.

Kagan, J. C. and R. Medzhitov (2006). Phosphoinositide-Mediated Adaptor Recruitment Controls Toll-like Receptor Signaling. Cell **125**(5): 943-955.

Kajita, E., T. Nishiya, et al. (2006). The transmembrane domain directs TLR9 to intracellular compartments that contain TLR3. Biochemical and Biophysical Research Communications **343**(2): 578-584.

Kanakaraj, P., P. H. Schafer, et al. (1998). Interleukin (IL)-1 receptor-associated kinase (IRAK) requirement for optimal induction of multiple IL-1 signaling pathways and IL-6 production. J. Exp. Med. **187**(12): 2073-9.

Kanayama, A., R. B. Seth, et al. (2004). TAB2 and TAB3 activate the NF-κB pathway through binding to polyubiquitin chains. Mol. Cell **15**(4): 535-48.

Karikó K., Bhuyan P., Capodici J., Ni H., Lubinski J., Friedman H., Weissman D. (2004) Exogenous siRNA Mediates Sequence-Independent Gene Suppression by Signaling through Toll-Like Receptor *3*. Cells Tissues Organs **177**: 132-138.

Kato, H., S. Sato, et al. (2005). Cell type-specific involvement of RIG-I in antiviral response. Immunity **23**(1): 19-28.

Kato, H., O. Takeuchi, et al. (2006). Differential roles of MDA5 and RIG-I helicases in the recognition of RNA viruses. Nature **441**(7089): 101-5.

Kato, H., O. Takeuchi, et al. (2008). Length-dependent recognition of double-stranded ribonucleic acids by retinoic acid-inducible gene-I and melanoma differentiation-associated gene 5. J. Exp. Med. **205**(7): 1601-10.

Katsoulidis, E., Y. Li, et al. (2005). The p38 Mitogen-Activated Protein Kinase Pathway in Interferon Signal Transduction. Journal of Interferon & Cytokine Research **25**(12): 749-756.

Kawagoe, T., S. Sato, et al. (2008). Sequential control of Toll-like receptor-dependent responses by IRAK1 and IRAK2. Nat. Immunol. **9**(6): 684-691.

Kawai, T., Sato, S., Ishii, K.J., Coban, C., Hemmi, H., Yamamoto, M., Terai, K., Matsuda, M., Inoue, J., Uematsu, S., Takeuchi, O. and Akira, S. (2004) Interferon-alpha induction through Toll-like receptors involves a direct interaction of IRF7 with MyD88 and TRAF6. Nat. Immunol. **5**: 1061-1068.

Kawai, T., K. Takahashi, et al. (2005). IPS-1, an adaptor triggering RIG-I- and Mda5-mediated type I interferon induction. Nat. Immunol. 6(10): 981-8.

Kawai, T. and Akira, S. (2006a) Innate immune recognition of viral infection. 7, 131-137.

Kawai, T. and Akira, S. (2006b) TLR signaling. Cell Death Differ. **13** (5): 816-825.

Kawai, T. and S. Akira (2007). TLR signaling. Semin. Immunol. **19** (1): 24-32.

Keating, S. E., G. M. Maloney, et al. (2007). IRAK-2 participates in multiple toll-like receptor signaling pathways to NFkappaB via activation of TRAF6 ubiquitination. J. Biol. Chem. **282**(46): 33435-43.

Keating, S. E. and A. G. Bowie (2008). The role of non-degradative ubiquitination in interleukin-1 and Toll-like receptor signalling. J. Biol. Chem.: R800038200.

Kerr, P. J., H. D. Perkins, et al. (2004). Expression of rabbit IL-4 by recombinant myxoma viruses enhances virulence and overcomes genetic resistance to myxomatosis. Virology **324** (1): 117-28.

Khan, J. A., E. K. Brint, et al. (2004). Crystal Structure of the Toll/Interleukin-1 Receptor Domain of Human IL-1RAPL. J. Biol. Chem. **279** (30): 31664-31670.

Khor, C. C., S. J. Chapman, et al. (2007). A Mal functional variant is associated with protection against invasive pneumococcal disease, bacteremia, malaria and tuberculosis. Nat. Genet. **39** (4): 523-528.

Kim, M., Ahn, J.W., Song, K., Paek, K.H. and Pai, H.S. (2002) Forkhead-associated domains of the tobacco NtFHA1 transcription activator and the yeast Fhl1 forkhead transcription factor are functionally conserved. J. Biol. Chem. **277**: 38781-38790.

Kim, H. M., B. S. Park, et al. (2007). Crystal Structure of the TLR4-MD-2 Complex with Bound Endotoxin Antagonist Eritoran. Cell **130**(5): 906-917.

Kishida, S., Sanjo, H., Akira, S., Matsumoto, K. and Ninomiya-Tsuji, J. (2005) TAK1-binding protein 2 facilitates ubiquitination of TRAF6 and assembly of TRAF6 with IKK in the IL-1 signaling pathway. Genes Cells 10: 447-454.

Kobayashi, N., Y. Kadono, et al. (2001). Segregation of TRAF6-mediated signaling pathways clarifies its role in osteoclastogenesis. Embo J. **20**(6): 1271-80.

Kobayashi, K., L. D. Hernandez, et al. (2002). IRAK-M Is a Negative Regulator of Toll-like Receptor Signaling. Cell **110**(2): 191-202.

Kobayashi, T., Walsh, M.C. and Choi, Y. (2004) The role of TRAF6 in signal transduction and the immune response. Microbes Infect. 6: 1333-1338.

Komuro, A. and C. M. Horvath (2006). RNA- and virus-independent inhibition of antiviral signaling by RNA helicase LGP2. J. Virol. **80**(24): 12332-42.

Kopecky-Bromberg, S. A., L. Martinez-Sobrido, et al. (2006). 7a Protein of Severe Acute Respiratory Syndrome Coronavirus Inhibits Cellular Protein Synthesis and Activates p38 Mitogen-Activated Protein Kinase. J. Virol. **80**(2): 785-793.

Koyama, S., K. J. Ishii, et al. (2008). Innate immune response to viral infection. Cytokine **43**(3): 336-41.

Kumar, H., T. Kawai, et al. (2006). Essential role of IPS-1 in innate immune responses against RNA viruses. J. Exp. Med. **203** (7): 1795-803.

Kyte, J. and Doolittle, R.F. (1982) A simple method for displaying the hydropathic character of a protein. J. Mol. Biol. **157**, 105-132.

Lad, S. P., G. Yang, et al. (2008). Identification of MAVS splicing variants that interfere with RIGI/MAVS pathway signaling. Mol. Immunol., **45**(8): 2277-87.

Lakshmanan, U. and A. G. Porter (2007). Caspase-4 Interacts with TNF Receptor-Associated Factor 6 and Mediates Lipopolysaccharide-Induced NF-κB-Dependent Production of IL-8 and CC Chemokine Ligand 4 (Macrophage-Inflammatory Protein-1). J. Immunol. **179** (12): 8480-8490.

Lamothe, B., A. Besse, et al. (2007a). Site-specific Lys-63-linked tumor necrosis factor receptor-associated factor 6 auto-ubiquitination is a critical determinant of IκB kinase activation. J. Biol. Chem. **282** (6): 4102-12.

Lamothe, B., W. K. Webster, et al. (2007b). TRAF6 ubiquitin ligase is essential for RANKL signaling and osteoclast differentiation. Biochem. Biophys. Res. Commun. **359**(4): 1044-9.

Lamothe, B., A. D. Campos, et al. (2008). The RING Domain and First Zinc Finger of TRAF6 Coordinate Signaling by Interleukin-1, Lipopolysaccharide, and RANKL. J. Biol. Chem. **283**(36): 24871-24880.

Langland, J. O. and B. L. Jacobs (2002). The Role of the PKR-Inhibitory Genes, E3L and K3L, in Determining Vaccinia Virus Host Range. Virology **299**(1): 133-141.

Langland, J. O., J. C. Kash, et al. (2006). Suppression of proinflammatory signal transduction and gene expression by the dual nucleic acid binding domains of the vaccinia virus E3L proteins. J Virol **80**(20): 10083-95.

Li, X. D., L. Sun, et al. (2005). Hepatitis C virus protease NS3/4A cleaves mitochondrial antiviral signaling protein off the mitochondria to evade innate immunity. Proc. Natl. Acad. Sci. U.S.A., **102** (49): 17717-22.

Li, Q., Harraz, M.M., Zhou, W., Zhang, L.N., Ding, W., Zhang, Y., Eggleston, T., Yeaman, C., Banfi, B. and Engelhardt, J.F. (2006) Nox2 and Rac1 regulate H2O2-dependent recruitment of TRAF6 to endosomal interleukin-1 receptor complexes. Mol. Cell. Biol., **26**: 140-154.

Li, J. C. and A. S. Lau (2007). A role for mitogen-activated protein kinase and Ets-1 in the induction of interleukin-10 transcription by human immunodeficiency virus-1 Tat. Immunology **121**(3): 337-48.

Liu, Y.C. (2004) Ubiquitin ligases and the immune response. Annu. Rev. Immunol., **22**: 81-127.

Liu, Y.C., Penninger, J. and Karin, M. (2005) Immunity by ubiquitylation: a reversible process of modification. Nat. Rev. Immunol., 5: 941-952.

Liu, X., K. Fitzgerald, et al. (2008). Herpesvirus tegument protein activates NF-kappaB signaling through the TRAF6 adaptor protein. Proc. Natl. Acad. Sci. U.S.A., **105**(32): 11335-9.

Lomaga, M.A., Yeh, W.C., Sarosi, I., Duncan, G.S., Furlonger, C., Ho, A., Morony, S., Capparelli, C., Van, G., Kaufman, S., van der Heiden, A., Itie, A., Wakeham, A., Khoo, W., Sasaki, T., Cao, Z., Penninger, J.M., Paige, C.J., Lacey, D.L., Dunstan, C.R., Boyle, W.J., Goeddel, D.V. and Mak, T.W. (1999) TRAF6 deficiency results in osteopetrosis and defective interleukin-1, CD40, and LPS signaling. Genes Dev., **13**: 1015-1024.

Love, K. R., A. Catic, et al. (2007). Mechanisms, biology and inhibitors of deubiquitinating enzymes. Nat Chem Biol **3**(11): 697-705.

Lu, G., Y. J. Kang, et al. (2006). TAB-1 modulates intracellular localization of p38 MAP kinase and downstream signaling. J. Biol. Chem., **281**(9): 6087-95.

Luftig, M. A., E. Cahir-McFarland, et al. (2001). Effects of the NIK aly mutation on NF-kappaB activation by the Epstein-Barr virus latent infection membrane protein, lymphotoxin beta receptor, and CD40. J. Biol Chem **276**(18): 14602-6.

Luftig, M., Prinarakis, E., Yasui, T., Tsichritzis, T., Cahir-McFarland, E., Inoue, J., Nakano, H., Mak, T.W., Yeh, W.C., Li, X., Akira, S., Suzuki, N., Suzuki, S., Mosialos, G. and Kieff, E. (2003) Epstein-Barr virus latent membrane protein 1 activation of NF-kappaB through IRAK1 and TRAF6. Proc. Natl. Acad. Sci. U.S.A., **100**: 15595-15600.

Lund, J. M., L. Alexopoulou, et al. (2004). Recognition of single-stranded RNA viruses by Toll-like receptor 7. Proceedings of the National Academy of Sciences of the United States of America **101**(15): 5598-5603.

Ma, W., Lim, W., Gee, K., Aucoin, S., Nandan, D., Kozlowski, M., Diaz-Mitoma, F. and Kumar, A. (2001) The p38 mitogen-activated kinase pathway regulates the human interleukin-10 promoter via the activation of Sp1 transcription factor in lipopolysaccharide-stimulated human macrophages. J. Biol. Chem., **276**: 13664-13674.

Mahy, B. W. (2003). An overview on the use of a viral pathogen as a bioterrorism agent: why smallpox? Antiviral Res., 57(1-2): 1-5.

Maloney, G., Schroder, M. and Bowie, A.G. (2005) Vaccinia virus protein A52R activates p38 mitogen-activated protein kinase and potentiates lipopolysaccharide-induced interleukin-10. J. Biol. Chem., **280**: 30838-30844.

Manna, S. K. and G. T. Ramesh (2005). Interleukin-8 Induces Nuclear Transcription Factor-κB through a TRAF6-dependent Pathway. J. Biol. Chem. **280**(8): 7010-7021.

Mansell, A., Brint, E., Gould, J.A., O'Neill, L.A. and Hertzog, P.J. (2004) Mal interacts with tumor necrosis factor receptor-associated factor (TRAF)-6 to mediate NF-kappaB activation by toll-like receptor (TLR)-2 and TLR4. J Biol Chem, 279, 37227-37230.

Marshall-Clarke, S., J. E. Downes, et al. (2007). Polyinosinic acid is a ligand for toll-like receptor 3. J Biol Chem 282(34): 24759-66.

Mayr, A. (2003). Smallpox vaccination and bioterrorism with pox viruses. Comp Immunol Microbiol Infect Dis 26(5-6): 423-30.

McCoy, S.L., Kurtz, S.E., Macarthur, C.J., Trune, D.R. and Hefeneider, S.H. (2005) Identification of a peptide derived from vaccinia virus A52R protein that inhibits cytokine secretion in response to TLR-dependent signaling and reduces in vivo bacterial-induced inflammation. J Immunol., **174**: 3006-3014.

McFadden, G. (2005) Poxvirus tropism. Nat Rev Microbiol, 3, 201-213.

McGettrick, A. F., E. K. Brint, et al. (2006). Trif-related adapter molecule is phosphorylated by PKCÎµ during Toll-like receptor 4 signaling. Proceedings of the National Academy of Sciences **103**(24): 9196-9201.

McGuffin, L.J., Bryson, K. and Jones, D.T. (2000) The PSIPRED protein structure prediction server. Bioinformatics, 16, 404-405.

McLennan, A. G. (2007). Decapitation: poxvirus makes RNA lose its head. Trends Biochem Sci 32(7): 297-9.

Medvedev, A. E., K. Thomas, et al. (2005). Cutting Edge: Expression of IL-1 Receptor-Associated Kinase-4 (IRAK-4) Proteins with Mutations Identified in a Patient with Recurrent Bacterial Infections Alters Normal IRAK-4 Interaction with Components of the IL-1 Receptor Complex. J. Immunol., **174**(11): 6587-6591.

Medzhitov, R., P. Preston-Hurlburt, et al. (1997). A human homologue of the Drosophila Toll protein signals activation of adaptive immunity. Nature, **388**(6640): 394-397.

Melchjorsen, J., S. B. Jensen, et al. (2005). Activation of innate defense against a paramyxovirus is mediated by RIG-I and TLR7 and TLR8 in a cell-type-specific manner. J. Virol., **79** (20): 12944-51.

Mercier, P., M. J. Lewis, et al. (2007). Structure, interactions, and dynamics of the RING domain from human TRAF6. Protein Sci., **16**(4): 602-14.

Meylan, E., J. Curran, et al. (2005). Cardif is an adaptor protein in the RIG-I antiviral pathway and is targeted by hepatitis C virus. Nature **437** (7062): 1167-72.

Michallet, M.-C., E. Meylan, et al. (2008). TRADD Protein Is an Essential Component of the RIG-like Helicase Antiviral Pathway. Immunity **28**(5): 651-661.

Miggin, S. M. and O'Neill, L.A.J. (2006). New Insights into the regulation of TLR signalling. Journal of Leukocyte Biology. J. Leukoc. Biol. **80**(2): 220-6.

Miggin, S. M., E. Pålsson-McDermott, et al. (2007). NF-κB activation by the Toll-IL-1 receptor domain protein MyD88 adapter-like is regulated by caspase-1. Proceedings of the National Academy of Sciences 104(9): 3372-3377.

Mimnaugh, E. G. and L. M. Neckers (2002). Immunoblotting methods for the study of protein ubiquitination. Methods Mol Biol **194**: 179-203.

Mogensen, T.H. and Paludan, S.R. (2005). Reading the viral signature by Toll-like receptors and other pattern recognition receptors. Journal of Molecular Medicine 83 (3): 180-192.

Morgenstern, B. (2004) DIALIGN: multiple DNA and protein sequence alignment at BiBiServ10.1093/nar/gkh373. Nucl. Acids Res., 32, W33-36.

Moss, B. (2006) Poxvirus entry and membrane fusion. Virology, 344, 48-54.

Mukundan, L., Bishop, G.A., Head, K.Z., Zhang, L., Wahl, L.M. and Suttles, J. (2005) TNF receptor-associated factor 6 is an essential mediator of CD40-activated proinflammatory pathways in monocytes and macrophages. J Immunol, 174, 1081-1090.

Muller, S., Hoege, C., Pyrowolakis, G. and Jentsch, S. (2001) SUMO, ubiquitin's mysterious cousin. Nat. Rev. Mol. Cell Biol., **2**: 202-210.

Muroi, M. and K. Tanamoto (2008). TRAF6 distinctively mediates MyD88- and IRAK-1-induced activation of NF-kappaB. J. Leukoc. Biol. **83**(3): 702-7.

Muzio, M., Ni, J., Feng, P. and Dixit, V.M. (1997) IRAK (Pelle) family member IRAK-2 and MyD88 as proximal mediators of IL-1 signaling. Science, 278, 1612-1615.

Muzio, M., G. Natoli, et al. (1998). The Human Toll Signaling Pathway: Divergence of Nuclear Factor kappa B and JNK/SAPK Activation Upstream of Tumor Necrosis Factor Receptor-associated Factor 6 (TRAF6). J. Exp. Med. **187**(12): 2097-2101.

Myskiw, C., Y. Deschambault, et al. (2007). Aurintricarboxylic acid inhibits the early stage of vaccinia virus replication by targeting both cellular and viral factors. J. Virol. 81(6): 3027-32.

Nerenberg, B.T., Taylor, J., Bartee, E., Gouveia, K., Barry, M. and Fruh, K. (2005) The poxviral RING protein p28 is a ubiquitin ligase that targets ubiquitin to viral replication factories. J Virol, 79, 597-601.

Netea, M.G., Van der Meer, J.W. and Kullberg, B.J. (2004) Toll-like receptors as an escape mechanism from the host defense. Trends Microbiol, 12, 484-488.

Ni, C. Y., Z. H. Wu, et al. (2008). Cutting edge: K63-linked polyubiquitination of NEMO modulates TLR signaling and inflammation in vivo. J Immunol **180**(11): 7107-11.

Nishiya, T., E. Kajita, et al. (2007). Distinct roles of TIR and non-TIR regions in the subcellular localization and signaling properties of MyD88. FEBS Letters **581**(17): 3223-3229.

Noels, H., G. van Loo, et al. (2007). A Novel TRAF6 Binding Site in MALT1 Defines Distinct Mechanisms of NF-κB Activation by API2.MALT1 Fusions. J. Biol. Chem. **282**(14): 10180-10189.

Nyman, T., P. Stenmark, et al. (2008). The Crystal Structure of the Human Toll-like Receptor 10 Cytoplasmic Domain Reveals a Putative Signaling Dimer. J. Biol. Chem. **283**(18): 11861-11865.

O'Neill, L.A., Fitzgerald, K.A. and Bowie, A.G. (2003) The Toll-IL-1 receptor adaptor family grows to five members. Trends Immunol, 24, 286-290.

O'Neill, L.A. (2006) How Toll-like receptors signal: what we know and what we don't know. Curr Opin Immunol, 18, 3-9.

O'Neill, L. A. and A. G. Bowie (2007). The family of five: TIR-domain-containing adaptors in Toll-like receptor signalling. Nat Rev Immunol 7(5): 353-64.

Oganesyan, G., S. K. Saha, et al. (2006). Critical role of TRAF3 in the Toll-like receptor-dependent and -independent antiviral response. Nature 439(7073): 208-211.

Piao, W., C. Song, et al. (2008). Tyrosine Phosphorylation of MyD88 Adapter-like (Mal) Is Critical for Signal Transduction and Blocked in Endotoxin Tolerance. J. Biol. Chem. **283**(6): 3109-3119.

Pichlmair, A., O. Schulz, et al. (2006). RIG-I-mediated antiviral responses to single-stranded RNA bearing 5'-phosphates. Science 314(5801): 997-1001.

Pichlmair, A. and C. Reis e Sousa (2007). Innate recognition of viruses. Immunity 27(3): 370-83.

Pickart, C. M. and D. Fushman (2004). Polyubiquitin chains: polymeric protein signals. Current Opinion in Chemical Biology **8**(6): 610-616.

Poblenz, A. T., J. J. Jacoby, et al. (2007). Inhibition of RANKL-mediated osteoclast differentiation by selective TRAF6 decoy peptides. Biochemical and Biophysical Research Communications **359**(3): 510-515.

Poltorak, A., X. He, et al. (1998). Defective LPS Signaling in C3H/HeJ and C57BL/10ScCr Mice: Mutations in Tlr4 Gene. Science **282**(5396): 2085-2088.

Poole, E., C. A. King, et al. (2006). The UL144 gene product of human cytomegalovirus activates NFkappaB via a TRAF6-dependent mechanism. Embo J. **25**(18): 4390-9.

Pullen, S. S., T. T. Dang, et al. (1999). CD40 signaling through tumor necrosis factor receptor-associated factors (TRAFs). Binding site specificity and activation of downstream pathways by distinct TRAFs. J. Biol. Chem., **274**(20): 14246-54.

Puntervoll, P., Linding, R., Gemund, C., Chabanis-Davidson, S., Mattingsdal, M., Cameron, S., Martin, D.M.A., Ausiello, G., Brannetti, B., Costantini, A., Ferre, F., Maselli, V., Via, A., Cesareni, G., Diella, F., Superti-Furga, G., Wyrwicz, L., Ramu, C., McGuigan, C., Gudavalli, R., Letunic, I., Bork, P., Rychlewski, L., Kuster, B., Helmer-Citterich, M., Hunter, W.N., Aasland, R. and Gibson, T.J. (2003) ELM server: a new resource for investigating short functional sites in modular eukaryotic proteins. Nucl. Acids Res., 31, 3625-3630.

Purkerson, J.M., Smith, R.S., Pollock, S.J. and Phipps, R.P. (2005) The TRAF6, but not the TRAF2/3, binding domain of CD40 is required for cytokine production in human lung fibroblasts. Eur J Immunol, 35, 2920-2928.

Rahaus, M., N. Desloges, et al. (2004). Replication of varicella-zoster virus is influenced by the levels of JNK/SAPK and p38/MAPK activation. J. Gen. Virol. **85**(12): 3529-3540.

Randall, R. E. and S. Goodbourn (2008). Interferons and viruses: an interplay between induction, signalling, antiviral responses and virus countermeasures. J. Gen. Virol. **89**(1): 1-47.

Rassa, J.C. and Ross, S.R. (2003) Viruses and Toll-like receptors. Microbes Infect, 5, 961-968.

Ravid, T. and Hochstrasser, M. (2004) NF-κB signaling: flipping the switch with polyubiquitin chains. Curr. Biol. **14**: R898-900.

Regnier, C.H., Tomasetto, C., Moog-Lutz, C., Chenard, M.P., Wendling, C., Basset, P. and Rio, M.C. (1995) Presence of a new conserved domain in CART1, a novel member of the tumor necrosis factor receptor-associated protein family, which is expressed in breast carcinoma. J. Biol. Chem. **270**: 25715-25721.

Reiley, W. W., W. Jin, et al. (2007). Deubiquitinating enzyme CYLD negatively regulates the ubiquitin-dependent kinase Tak1 and prevents abnormal T cell responses. J. Exp. Med. **204**(6): 1475-85.

Rivera, R., M. Hutchens, et al. (2007). Murine alveolar macrophages limit replication of vaccinia virus. Virology **363**(1): 48-58.

Roff, M., J. Thompson, et al. (1996). Role of IkappaBalpha Ubiquitination in Signal-induced Activation of NF-κB in Vivo. J. Biol. Chem. **271**(13): 7844-7850.

Rothe, M., S. C. Wong, et al. (1994). A novel family of putative signal transducers associated with the cytoplasmic domain of the 75 kDa tumor necrosis factor receptor. Cell **78**(4): 681-92.

Rowe, D. C., A. F. McGettrick, et al. (2006). The myristoylation of TRIF-related adaptor molecule is essential for Toll-like receptor 4 signal transduction. **103**(16): 6299-6304.

Saha, S. K., E. M. Pietras, et al. (2006). Regulation of antiviral responses by a direct and specific interaction between TRAF3 and Cardif. Embo J. **25**(14): 3257-63.

Samuelsson, C., J. Hausmann, et al. (2008). Survival of lethal poxvirus infection in mice depends on TLR9, and therapeutic vaccination provides protection. J. Clin. Invest. 118(5): 1776-84.

Sanjo, H., K. Takeda, et al. (2003). TAB2 is essential for prevention of apoptosis in fetal liver but not for interleukin-1 signaling. Mol. Cell Biol. **23**(4): 1231-8.

Sarkar, S. N., H. L. Smith, et al. (2003). Double-stranded RNA Signaling by Toll-like Receptor 3 Requires Specific Tyrosine Residues in Its Cytoplasmic Domain. J. Biol. Chem. **278**(7): 4393-4396.

Sato, S., Sugiyama, M., Yamamoto, M., Watanabe, Y., Kawai, T., Takeda, K. and Akira, S. (2003) Toll/IL-1 receptor domain-containing adaptor inducing IFN-beta (TRIF) associates with TNF receptor-associated factor 6 and TANK-binding kinase 1, and activates two distinct transcription factors, NF-κB and IFN-regulatory factor-3, in the Toll-like receptor signaling. J. Immunol. **171**: 4304-4310.

Schlee, M., V. Hornung, et al. (2006). siRNA and isRNA: two edges of one sword. Mol. Ther. **14** (4): 463-70.

Schlender, J., V. Hornung, et al. (2005). Inhibition of toll-like receptor 7- and 9-mediated alpha/beta interferon production in human plasmacytoid dendritic cells by respiratory syncytial virus and measles virus. J. Virol. **79**(9): 5507-15.

Schneider, K., Benedict, C.A. and Ware, C.F. (2006) A TRAFfic cop for host defense. Nat. Immunol. **7**: 15-16.

Schnell, J.D. and Hicke, L. (2003) Non-traditional functions of ubiquitin and ubiquitin-binding proteins. J. Biol. Chem. **278**: 35857-35860.

Schramm, B. and Locker, J.K. (2005) Cytoplasmic organization of POXvirus DNA replication. Traffic, **6**: 839-846.

Schroder, M., M. Baran, et al. (2008). Viral targeting of DEAD box protein 3 reveals its role in TBK1/IKKepsilon-mediated IRF activation. Embo J., **27**(15): 2147-57.

Schultheiss, U., Puschner, S., Kremmer, E., Mak, T.W., Engelmann, H., Hammerschmidt, W. and Kieser, A. (2001) TRAF6 is a critical mediator of signal transduction by the viral oncogene latent membrane protein 1. Embo J., **20**: 5678-5691.

Schulz, O., S. S. Diebold, et al. (2005). Toll-like receptor 3 promotes cross-priming to virus-infected cells. Nature, **433** (7028): 887-892.

Schwandner, R., Yamaguchi, K. and Cao, Z. (2000) Requirement of tumor necrosis factor receptor-associated factor (TRAF)6 in interleukin 17 signal transduction. J. Exp. Med., **191**: 1233-1240.

Seet, B.T., Johnston, J.B., Brunetti, C.R., Barrett, J.W., Everett, H., Cameron, C., Sypula, J., Nazarian, S.H., Lucas, A. and McFadden, G. (2003) Poxviruses and immune evasion. Annu. Rev. Immunol., **21**: 377-423.

Seibenhener, M.L., Babu, J.R., Geetha, T., Wong, H.C., Krishna, N.R. and Wooten, M.W. (2004) Sequestosome 1/p62 is a polyubiquitin chain binding protein involved in ubiquitin proteasome degradation. Mol. Cell Biol., **24**: 8055-8068.

Servant, M. J., N. Grandvaux, et al. (2002). Multiple signaling pathways leading to the activation of interferon regulatory factor 3. Biochemical Pharmacology **64**(5-6): 985-992.

Seth, R. B., L. Sun, et al. (2005). Identification and characterization of MAVS, a mitochondrial antiviral signaling protein that activates NF-kappaB and IRF 3. Cell 122(5): 669-82.

Shen-Ying Zhang, E. J., Vanessa Sancho-Shimizu, Horst von Bernuth, Kun Yang, Laurent Abel, Capucine Picard, Anne Puel, Jean-Laurent Casanova, (2007). Human Toll-like receptor-dependent induction of interferons in protective immunity to viruses. Immunological Reviews 220(1): 225-236.

Shim, J. H., C. Xiao, et al. (2005). TAK1, but not TAB1 or TAB2, plays an essential role in multiple signaling pathways in vivo. Genes Dev **19**(22): 2668-81.

Shirakata, M., Imadome, K.I., Okazaki, K. and Hirai, K. (2001) Activation of TRAF5 and TRAF6 signal cascades negatively regulates the latent replication origin of Epstein-Barr virus through p38 mitogen-activated protein kinase. J. Virol., **75**: 5059-5068.

Shisler, J. L. and X. L. Jin (2004). The vaccinia virus K1L gene product inhibits host NF-kappaB activation by preventing IκBα degradation. J. Virol., **78**(7): 3553-60.

Si, X., G. Gao, et al. (2008). Ubiquitination is required for effective replication of coxsackievirus B3. PLoS ONE **3**(7): e2585.

Simard, S., É. Maurais, et al. (2008). LPS reduces HIV-1 replication in primary human macrophages partly through an endogenous production of type I interferons. Clinical Immunology, **127**(2): 198-205.

Smiley, J. R. (2004). Herpes simplex virus virion host shutoff protein: immune evasion mediated by a viral RNase? J. Virol., **78**(3): 1063-8.

Smith, G.L. and Law, M. (2004) The exit of vaccinia virus from infected cells. Virus Res., **106**: 189-197.

Smith, G.L. and McFadden, G. (2002) Smallpox: anything to declare? Nat. Rev. Immunol., **2**: 521-527.

Song, H.Y., Regnier, C.H., Kirschning, C.J., Goeddel, D.V. and Rothe, M. (1997) Tumor necrosis factor (TNF)-mediated kinase cascades: bifurcation of nuclear factor-kappaB and c-jun N-terminal kinase (JNK/SAPK) pathways at TNF receptor-associated factor 2. Proc Natl Acad Sci U S A, 94, 9792-9796.

Stack, J., Haga, I.R., Schroder, M., Bartlett, N.W., Maloney, G., Reading, P.C., Fitzgerald, K.A., Smith, G.L. and Bowie, A.G. (2005) Vaccinia virus protein A46R

targets multiple Toll-like-interleukin-1 receptor adaptors and contributes to virulence. J. Exp. Med., **201**: 1007-1018.

Stanford, M.M. and McFadden, G. (2005) The 'supervirus'? Lessons from IL-4-expressing poxviruses. Trends Immunol., **26**: 339-345.

Staros, E.B. (2005) Innate immunity: New approaches to understanding its clinical significance. Am J Clin Pathol, **123**: 305-312.

Sun, L., L. Deng, et al. (2004). The TRAF6 ubiquitin ligase and TAK1 kinase mediate IKK activation by BCL10 and MALT1 in T lymphocytes. Mol. Cell, **14**(3): 289-301.

Suzuki, N., S. Suzuki, et al. (2002). Severe impairment of interleukin-1 and Toll-like receptor signalling in mice lacking IRAK-4. Nature **416**(6882): 750-756.

Sweet, C. R., J. Conlon, et al. (2007). YopJ targets TRAF proteins to inhibit TLR-mediated NF-κB, MAPK and IRF3 signal transduction. Cell Microbiol., **9**(11): 2700-15.

Symons, J. A., D. C. Tscharke, et al. (2002). A study of the vaccinia virus interferon-gamma receptor and its contribution to virus virulence. J. Gen. Virol., **83**(Pt 8): 1953-64.

Symons, A., Beinke, S. and Ley, S.C. (2006) MAP kinase kinase kinases and innate immunity. Trends in Immunology, **27**: 40-48.

Tabeta, K., Georgel, P., Janssen, E., Du, X., Hoebe, K., Crozat, K., Mudd, S., Shamel, L., Sovath, S., Goode, J., Alexopoulou, L., Flavell, R.A. and Beutler, B. (2004) Toll-like receptors 9 and 3 as essential components of innate immune defense against mouse cytomegalovirus infection. Proc Natl Acad Sci U S A, 101, 3516-3521.

Takaoka, A., Yanai, H., Kondo, S., Duncan, G., Negishi, H., Mizutani, T., Kano, S., Honda, K., Ohba, Y., Mak, T.W. and Taniguchi, T. (2005) Integral role of IRF-5 in the gene induction programme activated by Toll-like receptors. Nature, 434 (7030), 243-249.

Takaoka, A. and Yanai, H. (2006). Interferon signalling network in innate defence. Cellular Microbiology, **8**(6): 907-922.

Takaoka, A., Z. Wang, et al. (2007). "DAI (DLM-1/ZBP1) is a cytosolic DNA sensor and an activator of innate immune response." Nature 448(7152): 501-505.

Takatsuna, H., H. Kato, et al. (2003). "Identification of TIFA as an adapter protein that links tumor necrosis factor receptor-associated factor 6 (TRAF6) to interleukin-1 (IL-1) receptor-associated kinase-1 (IRAK-1) in IL-1 receptor signaling." J Biol Chem **278**(14): 12144-50.

Takeda, K. and Akira, S. (2005) Toll-like receptors in innate immunity. Int. Immunol., 17, 1-14.

Takeshita, F., K. J. Ishii, et al. (2005). TRAF4 acts as a silencer in TLR-mediated signaling through the association with TRAF6 and TRIF. Eur. J. Immunol., **35**(8): 2477-85.

Takeuchi, M., Rothe, M. and Goeddel, D.V. (1996) Anatomy of TRAF2. Distinct domains for nuclear factor-kappaB activation and association with tumor necrosis factor signaling proteins. J Biol Chem, 271, 19935-19942.

Taylor, J. M. and M. Barry (2006). "Near death experiences: Poxvirus regulation of apoptotic death." Virology **344**(1): 139-150.

Tenno, T., Fujiwara, K., Tochio, H., Iwai, K., E. Morita, H., Hayashi, H., Murata, S., Hiroaki, H., Sato, M., Tanaka, K., Shirakawa, M. (2004). "Structural basis for distinct roles of Lys63- and Lys48-linked polyubiquitin chains." Genes to Cells **9**(10): 865-875.

Thomas, D., G. Blakqori, et al. (2004). "Inhibition of RNA polymerase II phosphorylation by a viral interferon antagonist." J Biol Chem 279(30): 31471-7.

Thompson, J.D., Higgins, D.G. and Gibson, T.J. (1994) CLUSTAL W: improving the sensitivity of progressive multiple sequence alignment through sequence weighting, position-specific gap penalties and weight matrix choice. Nucleic Acids Res, 22, 4673-4680.

Thompson, J. M. and A. Iwasaki (2008). "Toll-like receptors regulation of viral infection and disease." Advanced Drug Delivery Reviews **60**(7): 786-794.

Townsley, A. C., A. S. Weisberg, et al. (2006). "Vaccinia virus entry into cells via a low-pH-dependent endosomal pathway." J Virol **80**(18): 8899-908.

Treier, M., Staszewski, L.M. and Bohmann, D. (1994) Ubiquitin-dependent cJun degradation in vivo is mediated by the delta domain. Cell 78, 787-798.

Trompier, D., M. Alibert, et al. (2006). "Transition from Dimers to Higher Oligomeric Forms Occurs during the ATPase Cycle of the ABCA1 Transporter." J. Biol. Chem. **281**(29): 20283-20290.

Tsan, M.F. and Gao, B. (2004) Endogenous ligands of Toll-like receptors. J Leukoc Biol, 76, 514-519.

Tscharke, D. C., W.-P. Woo, et al. (2006). "Poxvirus CD8+ T-Cell Determinants and Cross-Reactivity in BALB/c Mice." J. Virol. **80**(13): 6318-6323.

Tsung A, McCoy SL, Klune JR, Geller DA, Billiar TR, Hefeneider SH. (2007) A novel inhibitory peptide of Toll-like receptor signaling limits lipopolysaccharide-

induced production of inflammatory mediators and enhances survival in mice. Shock **27**(4):364-9.

Tusnády, G.E. and Simon, I. (2001) The HMMTOP transmembrane topology prediction server. Bioinformatics **17**: 849-850.

Uematsu, S. and S. Akira (2006). "The role of Toll-like receptors in immune disorders." Expert Opinion on Biological Therapy **6**(3): 203-214.

Unterholzner, L. and A. G. Bowie (2008). "The interplay between viruses and innate immune signalling: recent insights and therapeutic opportunities." Biochem. Pharmacol. **75**(3): 589-602.

Vaux, D. L. and J. Silke (2005). IAPs, RINGs and ubiquitylation. Nat. Rev. Mol. Cell Biol. **6**(4): 287-97.

Vercammen, E., J. Staal, et al. (2008). Sensing of Viral Infection and Activation of Innate Immunity by Toll-Like Receptor 3. Clin. Microbiol. Rev. **21**(1): 13-25.

von Bernuth, H., C. Picard, et al. (2008). Pyogenic Bacterial Infections in Humans with MyD88 Deficiency. Science **321**(5889): 691-696.

von Heijne, G. (1992) Membrane protein structure prediction. Hydrophobicity analysis and the positive-inside rule. J Mol Biol, 225, 487-494.

Wajant, H., Henkler, F. and Scheurich, P. (2001) The TNF-receptor-associated factor family: scaffold molecules for cytokine receptors, kinases and their regulators. Cell Signal. **13**: 389-400.

Wan, J., W. Zhang, et al. (2006). BS69, a specific adaptor in the latent membrane protein 1-mediated c-Jun N-terminal kinase pathway. Mol. Cell Biol. **26**(2): 448-56.

Wang, C., L. Deng, et al. (2001). TAK1 is a ubiquitin-dependent kinase of MKK and IKK. Nature **412**(6844): 346-351.

Wang, T., T. Town, et al. (2004). Toll-like receptor 3 mediates West Nile virus entry into the brain causing lethal encephalitis. Nat. Med. **10**(12): 1366-1373.

Wang, Y., Tang, Y., Teng, L., Wu, Y., Zhao, X. and Pei, G. (2006) Association of beta-arrestin and TRAF6 negatively regulates Toll-like receptor-interleukin 1 receptor signaling. Nat. Immunol. **7**: 139-147.

Wang, R.-P., M. Zhang, et al. (2008). Differential regulation of IKKα-mediated activation of IRF3/7 by NIK. Molecular Immunology **45** (7): 1926-1934.

Wietek, C., S. M. Miggin, et al. (2003). Interferon Regulatory Factor-3-mediated Activation of the Interferon-sensitive Response Element by Toll-like receptor (TLR) 4 but Not TLR3 Requires the p65 Subunit of NF-κB. J. Biol. Chem. **278**(51): 50923-50931.

Windheim, M., M. Stafford, et al. (2008a). Interleukin-1 (IL-1) induces the Lys63-linked polyubiquitination of IL-1 receptor-associated kinase 1 to facilitate NEMO binding and the activation of IκBα kinase. Mol. Cell Biol. **28**(5): 1783-91.

Windheim, M., M. Peggie, et al. (2008b). Two different classes of E2 ubiquitin-conjugating enzymes are required for the mono-ubiquitination of proteins and elongation by polyubiquitin chains with a specific topology. Biochem. J. **409** (3): 723-729.

Wooff, J., Pastushok, L., Hanna, M., Fu, Y. and Xiao, W. (2004) The TRAF6 RING finger domain mediates physical interaction with Ubc13. FEBS Letters, **566**: 229-233.

Wooten, M.W., Geetha, T., Seibenhener, M.L., Babu, J.R., Diaz-Meco, M.T. and Moscat, J. (2005) The p62 scaffold regulates nerve growth factor-induced NF-kappaB activation by influencing TRAF6 polyubiquitination. J. Biol. Chem. **280**: 35625-35629.

Wu, H. and Arron, J.R. (2003) TRAF6, a molecular bridge spanning adaptive immunity, innate immunity and osteoimmunology. Bioessays **25**: 1096-1105.

Xiang, T., N. Zong, et al. (2008). Pseudomonas syringae effector AvrPto blocks innate immunity by targeting receptor kinases. Curr. Biol. **18** (1): 74-80.

Xu, Y., X. Tao, et al. (2000). Structural basis for signal transduction by the Toll/interleukin-1 receptor domains. Nature **408** (6808): 111-115.

Xu, L. G., L. Y. Li, et al. (2004). TRAF7 potentiates MEKK3-induced AP1 and CHOP activation and induces apoptosis. J. Biol. Chem. **279**(17): 17278-82.

Xu, L. G., Y. Y. Wang, et al. (2005). VISA is an adapter protein required for virus-triggered IFN-beta signaling. Mol Cell. **19** (6): 727-40.

Yamamoto, M., Sato, S., Mori, K., Hoshino, K., Takeuchi, O., Takeda, K. and Akira, S. (2002) Cutting edge: a novel Toll/IL-1 receptor domain-containing adapter that preferentially activates the IFN-beta promoter in the Toll-like receptor signaling. J. Immunol. **169**: 6668-6672.

Yamamoto, M., Sato, S., Hemmi, H., Hoshino, K., Kaisho, T., Sanjo, H., Takeuchi, O., Sugiyama, M., Okabe, M., Takeda, K. and Akira, S. (2003) Role of adaptor TRIF in the MyD88-independent toll-like receptor signaling pathway. Science **301**: 640-643.

Yang, K., Zhu, J., Sun, S., Tang, Y., Zhang, B., Diao, L. and Wang, C. (2004) The coiled-coil domain of TRAF6 is essential for its auto-ubiquitination. Biochem. Biophys. Res. Commun. **324**: 432-439.

Yao, J., T. W. Kim, et al. (2007). Interleukin-1 (IL-1)-induced TAK1-dependent Versus MEKK3-dependent NF-κB activation pathways bifurcate at IL-1 receptor-associated kinase modification. J. Biol. Chem. **282**(9): 6075-89.

Ye, H., Arron, J.R., Lamothe, B., Cirilli, M., Kobayashi, T., Shevde, N.K., Segal, D., Dzivenu, O.K., Vologodskaia, M., Yim, M., Du, K., Singh, S., Pike, J.W., Darnay, B.G., Choi, Y. and Wu, H. (2002). Distinct molecular mechanism for initiating TRAF6 signalling. Nature, **418**: 443-447.

Yoneyama, M., M. Kikuchi, et al. (2004). The RNA helicase RIG-I has an essential function in double-stranded RNA-induced innate antiviral responses. Nat. Immunol., **5** (7): 730-7.

Yoneyama, M., M. Kikuchi, et al. (2005). Shared and unique functions of the DExD/H-box helicases RIG-I, MDA5, and LGP2 in antiviral innate immunity. J. Immunol., **175** (5): 2851-8.

Yoneyama, M. and T. Fujita (2007). Function of RIG-I-like Receptors in Antiviral Innate Immunity. J. Biol. Chem., **282** (21): 15315-15318.

Yoneyama, M. and T. Fujita (2008). Structural Mechanism of RNA Recognition by the RIG-I-like Receptors. Immunity **29**(2): 178-181.

Yoneyama, M., K. Onomoto, et al. (2008). Cytoplasmic recognition of RNA. Adv. Drug Deliv. Rev. **60** (7): 841-6.

Yoshida, H., H. Jono, et al. (2005). The tumor suppressor cylindromatosis (CYLD) acts as a negative regulator for toll-like receptor 2 signaling via negative cross-talk with TRAF6 AND TRAF7. J. Biol. Chem. **280**(49): 41111-21.

Zapata, J. M., K. Pawlowski, et al. (2001). A diverse family of proteins containing tumor necrosis factor receptor-associated factor domains. J. Biol. Chem. **276** (26): 24242-52.

Zapata, J. M., S. Lefebvre, et al. (2007a). Targeting TRAFs for therapeutic intervention. Adv. Exp. Med. Biol. **597**: 188-201.

Zapata, J. M., V. Martinez-Garcia, et al. (2007b). Phylogeny of the TRAF/MATH domain. Adv. Exp. Med. Biol. **597**: 1-24.

Zhang D, Facchinetti V, Wang X, Huang Q, Qin J, Su B. (2006). Identification of MEKK2/3 serine phosphorylation site targeted by the Toll-like receptor and stress pathways. EMBO J. **25** (1):97-107

Zhang, S.-Y., E. Jouanguy, et al. (2007). TLR3 Deficiency in Patients with Herpes Simplex Encephalitis. Science **317** (5844): 1522-1527.

Zhong, J. and J. M. Kyriakis (2004). Germinal center kinase is required for optimal Jun N-terminal kinase activation by Toll-like receptor agonists and is regulated by

the ubiquitin proteasome system and agonist-induced, TRAF6-dependent stabilization. Mol. Cell. Biol. **24**(20): 9165-75.

Zhu, J., J. Martinez, et al. (2007). Innate immunity against vaccinia virus is mediated by TLR2 and requires TLR-independent production of IFN-beta. Blood **109** (2): 619-25.

Zou, W., A. Amcheslavsky, et al. (2003). CpG Oligodeoxynucleotides Modulate the Osteoclastogenic Activity of Osteoblasts via Toll-like Receptor 9. J. Biol. Chem. **278**(19): 16732-16740.

Appendices

Protein	Molecular Mass (kDa)
A52	22
GST-A52	46
GFP-A52	49
TRAF1	46
TRAF2	56
TRAF3	64.5
TRAF4	53.5
TRAF5	64
TRAF6	60
TAK1*	67
TAB2	77
Ubiquitin	8.5
HA-ubiquitin	10
p38	40-43
JNK1	54-56
JNK2	43-46
ERK1 (p44)	44
ERK2 (p42)	45
ATF2*	65 to 75
IκBα	35-41
B-actin	43
FLAG tag (DYKDDDDK)	1
Myc tag (EQKLISEEDL)	1.2
HA tag (YPYDVPDYA)	1.1

Table A1.1 The predicted molecular masses of the proteins studied in this thesis. *There are known splice variants of these proteins and thus it may be possible to detect proteins of molecular masses that differ from the prediction.

Dilution	Rabbit L114	Rabbit L116
PBS	0.0366	0.0369
Preimmune serum 1:1000	0.0702	0.0519
Preliminary serum 1:1000	0.2414	0.3103
Final serum 1:1000	0.3273	0.5258
Final serum 1:10 000	0.1933	0.2009
Final serum 1:100 000	0.0853	0.0594

Table A2.1 ELISA data for antiserum raised to GST-A52 protein in rabbits. The GST-A52 was made as described in Chapter Three. Data provided by Inbiolabs.

Serum Dilution	Rabbit SG-4607	
	Pre-immune Serum	Test Bleed 1
1:1000	0.133	0.417
1:5000	0.061	0.246
1:25 000	0.029	0.131
1:125 000		0.087
1:625 000		0.044

Table A2.2 ELISA data for antiserum raised to A52 peptide in rabbit SG-4607. The titre was found to be 1:25 000, where the titre represents the dilution of the antiserum hat gives values approaching background levels. The peptide used was described in Chaıter Three. Data provided by Sigma Genosys.

Serum Dilution	Rabbit SG-4608	
	Pre-immune Serum	Test Bleed 1
1:1000	0.128	0.311
1:5000	0.056	0.155
1:25 000	0.027	0.071
1:125 000		0.049
1:625 000		0.027

Table A2.3 ELISA data for antiserum raised to A52 peptide in rabbit SG-4608. The titre was found to be 1:5000, where the titre represents the dilution of the antiserum that gives values approaching background levels. The peptide used was described in Chapter Three. Data provided by Sigma Genosys.